انجمن مهندسان مکانیک ایران

نشریه علمی
ماشین های کشاورزی

دانشگاه فردوسی مشهد

جلد ۱۱ شماره ۱
سال ۱۴۰۰
(شماره پیاپی: ۲۱)

شاپا: ۶۸۲۹-۲۲۲۸

عنوان مقالات

مقالات علمی-پژوهشی

مقالات کوتاه پژوهشی

Journal of Agricultural Machinery

Vol. 11 **No. 1** **2021**

Published by: Ferdowsi University of Mashhad, (College of Agriculture), Iran

Publisher: Ferdowsi University of Mashhad Press

Address: College of agriculture, Ferdowsi University of Mashhad, Iran

P.O. BOX: 91775-1163

Fax: +98-05138787430

E-Mail: Jame@um.ac.ir

Web Site: http://jame.um.ac.ir

Contents

Full Research Papers

Short Papers

Journal of Agricultural Machinery
Vol. 11, No. 1, Spring- Summer 2021, p. 1-15

نشریه ماشین‌های کشاورزی
جلد ۱۱، شماره ۱، نیمسال اول ۱۴۰۰، ص ۱۵-۱

Full Research Paper

Greenhouse Mobile Robot Navigation Using Wheel Revolution Encoding and Learning Algorithm

A. Heidari[1], J. Amiri Parian[2*]

Received: 15-05-2019
Accepted: 12-10-2019

Abstract

Repetitive and dangerous tasks such as harvesting and spraying have made robots usable in the greenhouses. The mechanical structure and navigation algorithm are two important parameters in the design and fabrication of mobile greenhouse robots. In this study, a four- wheel differential steering mobile robot was designed and constructed to act as a greenhouse robot. Then, the navigation of the robot at different levels and actual greenhouses was evaluated. The robot navigation algorithm was based on the path learning, so that the route was stored in the robot memory using a remote control based on the pulses transmitted from the wheels encoders; then, the robot automatically traversed the path. Robot navigation accuracy was tested at different surfaces (ceramics, concrete, dense soil and loose soil) in a straight path 20 meters long and a square path, 4×4 m. Then, robot navigation accuracy was investigated in a greenhouse. Robot movement deviation value was calculated using root mean square error (RMSE) and standard deviation (SD). The results showed that the RMSE of deviation of autonomous method from manual control method in the straight path to the length of 20 meters in ceramic, concrete, dense soil and loose soil were 4.3, 2.8, 4.6 and 8 cm, and in the 4×4 m square route were 6.6, 5.5, 13.1 and 47.1 cm, respectively.

Keywords: Agricultural robot, Encoder sensor, Vehicle navigation, Wheeled mobile robot

Introduction

Productivity in agriculture is obtained by increasing the quality and yield of the product, for which technology plays a crucial role. Greenhouses are expanding in order to use soil and water and other agricultural inputs better, resulting in high production efficiency and better quality of agricultural products. Hard and harmful tasks such as harvesting, spraying and pruning are needed in the greenhouse environment. Working in such an environment reduces the usefulness and damages operator's health (Nuyttens *et al*., 2004). Working in such an environment with a high temperature and humidity is a tough task. In a closed environment with low air flow, it is harmful for workers to act especially when toxic chemicals are used (Sánchez-Hermosilla *et al*., 2013). In recent years, the advancements in robotics have made mobile robots be used in the greenhouse, which can reduce operator fatigue and heavy work, and also increase the operator's productivity and health. The application of a robot in a greenhouse is successful if two issues are considered: 1- Designing vehicles appropriate to the greenhouse structure, 2- Implementing navigation techniques that permit the vehicle to move through the corridors between the rows of plants (González *et al*., 2009). Designing suitable navigation techniques for autonomous vehicles that travel in closed construction environments such as greenhouses is an important issue (Kondo *et al*., 2011). Various navigation technologies have been used to apply robots in the greenhouse. Manipulator robots have been used successfully in the industry. Therefore, these types of robots were examined in the greenhouse environment, too. These robots, usually being controlled by vision systems, have had an acceptable performance in the

1- PhD Student, Biosystems Engineering Department, Faculty of Agriculture, Bu-Ali Sina University, Hamedan, Iran
2- Assistant Professor, Biosystems Engineering Department, Faculty of Agriculture, Bu-Ali Sina University, Hamedan, Iran
(*- Corresponding Author Email: amiriparian@basu.ac.ir)
DOI: 10.22067/jam.v11i1.80722

greenhouse environment (Dario *et al*., 1994; Kondo and Ting, 1998; Sandini *et al*., 1990). Several researchers investigated automated guided vehicle (AGV) in the greenhouse. An automated guided vehicle or automatic guided vehicle is a portable robot that follows along marked long lines or wires on the floor, or uses radio waves, vision cameras, magnets, or lasers for navigation. They are most often used in industrial applications to transport heavy materials around a large industrial building, such as a factory or a warehouse. Sammons *et al*. (2005) describes an autonomous spraying robot whose navigation control relies on inductive sensors which detect metallic pipes buried in the soil. Van Henten *et al*. (2002) presents a robot for harvesting cucumbers in the greenhouse, and its guidance system was based on sensing heating steel pipes. Sulakhe and Karanjkar (2013) made and tested an autonomous robot for greenhouse spraying, and the navigation experiment was conducted by tracking a signal wire on the ground. Similarly, a rail type traveling robot was described by Rajendra *et al*. (2009) for strawberry harvesting with a vision algorithm in a table top culture greenhouse. Successful use of AGV in agricultural fields has been reported by Comba *et al*. (2012). One of disadvantages of using these devices in the greenhouse is necessity of installation of rails or metal tubes leading to a high cost for the use of these types of robots in the greenhouse. Sánchez-Hermosilla *et al*. (2013) reported the successful use of AGV in the greenhouse without any changes in the plant or greenhouse structure. Distance measuring sensors such as ultrasonic, laser, etc., have been tested by many researchers to robot navigation. Ultrasonic sensors have been used in many studies to identify the plant, as well as navigation in the greenhouse and agricultural environments because of the low cost and ease of use. In these types of sensors, the time interval between transmitting and receiving waves is measured, and according to the speed of sound in that environment, the distance to object is estimated. Singh *et al*. (2005) developed a robotic vehicle with the six-wheel differential steering for greenhouse spraying. It was tested on sand and concrete surfaces through simulated greenhouse corridors using ultrasonic sensors. Iida and Burks (2002) conducted the tractor autonomous navigation in horticulture using ultrasonic sensors. Mandow *et al*. (1996) applied ultrasonic sensors in greenhouse sprayer for navigation. Ultrasonic sensors were used to detect the plant to guide the robot across the row crops (Celen *et al*., 2015). Masoudi *et al*. (2012) developed an automatic guidance system for sprayer robot by using ultrasonic sensors. Ultrasonic sensors have been introduced in some studies for obstacle detection (Borenstein and Koren, 1989; Harper and McKerrow, 1999; Veelaert and Bogaerts, 1999). Borenstein and Koren (1989) listed three reasons why ultrasonic sensors are poor sensors when accuracy is required. These reasons are: (i) Poor directionality that limits accuracy in determining the spatial position of an obstacle to 10-50 cm, depending on the distance to the obstacle and the angle between the obstacles surface and the acoustic beam. (ii) Frequent misreading caused by either ultrasonic noise from external sources or stray reflections from neighboring sensors (crosstalk). Misreading cannot always be filtered out and they cause the algorithm to see nonexistent obstacles. (iii) Specular reflections that occur when the angles between the wave front and the normal to a smooth surface is too large. In this case, the surface reflects the incoming ultra sound waves away from the sensor, and the obstacle is either not detected at all, or (since only part of the surface is detected) is seen much smaller than it is in reality. However, despite all the limitations of ultrasonic sensors, the technique can still be put to good use as a safety net sensor. The use of optical sensors, especially, has been reported in open environments for plant detection and navigation. Machine vision is another method for greenhouse robot navigation. Mehta *et al*., (2008) used machine vision to guide the robot among the corridors. Xue *et al*. (2017) developed a vision-based algorithm for navigation and operations of row

planting crops, taking operations of spraying water and weeding by machine as examples. Dario *et al*. (1994) developed an AGOBOT platform with stereo vision and a manipulator arm equipped with a gripper and six degrees freedom for greenhouse cultivation of tomatoes, whose vision system controlled the moving direction and kept the vehicle at the center of the free path. Vision systems are most commonly used in outdoor agricultural environments for navigation and obstacle avoidance. The disadvantage of this method includes the effects of ambient light conditions on vision sensors performance, especially in outdoor environments. Another method of navigation of mobile robots is odometry. This method, in addition to being easy to use, is inexpensive. Odometry uses motion sensor data to estimate position changes in time. Mobile robots are used to estimate the relative position to the starting location. The inequality of wheels, wheel slippage, bump and tracks are factors that cause errors in this method. Due to these limitations, many researchers have used this method along with other methods to navigate mobile robots (Cox, 1991; Byrne *et al*., 1992; Chenavier and Crowley; 1992). A number of researchers have used complementary sensors (for example accelerometers, magnetic compass, gyroscope, machine vision, etc.) with odometry to increase navigational accuracy (Borenstein *et al*., 1996; Younse and Burks, 2007; Cho and Ki, 1999; Kleeman, 1992; Tsai, 1998; Piedrahita and Guayacundo, 2006). Goli *et al.* (2014) in a research compared four different positioning methods in order to evaluate their accuracy, using a remotely controlled robot on a specific route. These methods included: using a single GPS module, combining the data from three GPS modules, using an Inertial Measurement Unit (IMU), and GPS/IMU data fusion. The comparison of these four methods showed that GPS/IMU data fusion along with a Kalman filter was the most precise method, having a root mean square error of 23.4 cm.

Considering that in previous researches, different navigation systems have been used for greenhouse robots that sometimes have disadvantages and advantages and are relatively complex mechanism with high cost. So, in this project, a new navigation mechanism using wheel rotation coding as well as learning algorithm was designed, which, in addition to its simplicity and low cost, has an acceptable performance in robot routing in known environments such as greenhouses.

Materials and Methods

Mechanical structure

The width and length of the robot are two important parameters in designing of a greenhouse robot. The width of the greenhouse corridor and corridor's end space to turn, as well as the devices which mount on the robot chassis (Including battery, engine, power transmission system and sprayer) are the basis for determining the length and width of the robot. Commercial greenhouse corridors in Iran have a width of 70 to 120 cm. There is also a length of 2 meters at the end of the corridor to turn. By considering these factors, the width and the length of the robot were considered 55 and 110 cm, respectively. A four-wheel drive system was designed for the robot to minimize wheel slippage and more stability (Figure 1). Two electrical motors (24 V, 200 W) were equipped with a snail gearbox that were mounted in left and right sides and were connected to driver wheels by chain and sprocket. The electrical power which was required for motors, as well as the electrical circuit, was supplied by two batteries (12V, 45 Ah). Due to low speed (0.35 m s^{-1}) and the path of the robot in the greenhouse corridors which was fairly uniform, a suspension system was not designed for the device.

Fig.1. Robot platform

Turning mechanism

Differential drive was used to drive the robot. Differential drive is the simplest mechanical drive since it does not need rotation of a driven axis. The robot included a four-wheel drive, with a two-wheel drive on the right and two wheels on the left side of the robot platform. In this case, the two sides of the vehicle are independently powered. The velocity of right and left wheels was equal. If the wheels rotate at the same speed, the robot moves straight forward or backward. If both wheels are rotating at the same velocity in opposite directions, the robot turns about the midpoint of the two driving wheels (Figure 2). This mechanism was used to steer the robot due to the similar speed of the right and left wheels.

Fig.2. Turning mechanism

Navigation algorithm and robot learning

This robot is able to operate in every environment such as greenhouses and the path can be taught to the robot (Figure 3). But, because of using 3 paths: straight, square shape and move through the greenhouse corridors in this study, training process was done in these paths. Therefore, the learning algorithm was used in this robot. At first, the robot traveled the path with the operator's guidance and was trained during the course of the journey. After learning, the robot traveled autonomously. The learning process was carried out with the help of an advanced electronic system. The block diagram of the advanced electronic circuit is presented in Figure 4.

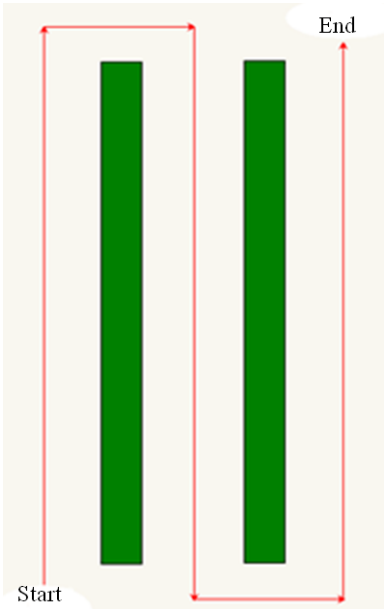

Fig.3. Rows of plants in a greenhouse and robot moving route

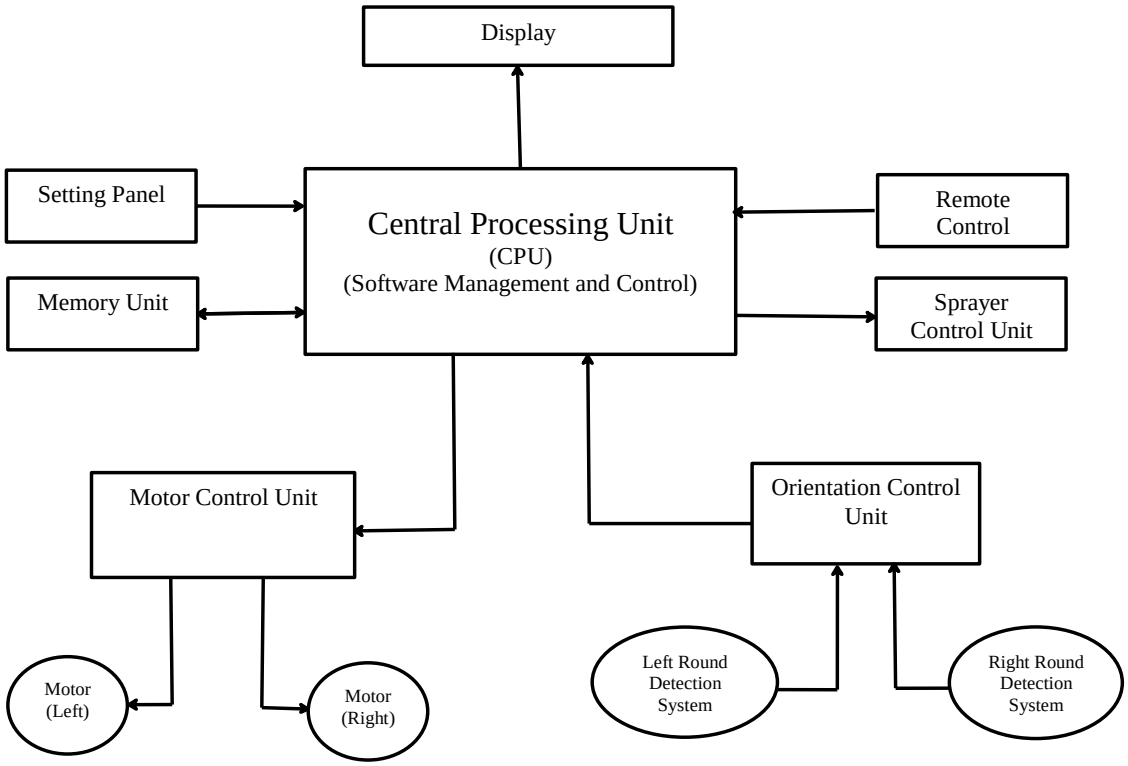

Fig.4. Flow Chart of the robot electronic circuit

Wheel revolution encoding

The motion control unit was designed to measure the angular rotation of the wheel. The two rotary encoders (E40H12-1024-3-T-24, Autonics, South Korea) with the specifications presented in Table 1 were mounted on the right and left rotating shafts to measure their position by converting axis rotation into electronics pulse (Figure 5).

Fig.5. Rotary encoder mounted on rotating shaft

Table 1- Encoder specifications

Sensor	Mark	Model	Resolution	Signal output	Power supply	Shaft type	Encoder diameter
Incremental	Autonics	E40H12-1024-3-T-24	1024	Pulse	12-24	Hallow shaft	40
			Pulse/rev		volt		mm

Software unit

Software program of the robot includes three main parts: 1) Learning unit, 2) Arithmetic logic unit (ALU) and 3) Algorithm execution unit.

The learning unit was designed to follow the path by the robot; by operator guidance appropriate pulses were sent to this unit and robot followed them into the specified path. In the ALU, the trained path was stored in the robot's memory after correction and reduction of noises. Finally, algorithm execution unit leads the robot to move into the preset path.

Robot navigation estimation

Considering that greenhouse corridors are usually earthy or concrete (Figure 6), robot navigation accuracy was tested on various surfaces including ceramics (in Lab), concrete, dense soil and loose soil (Figure 7) in straight path (20 m in length) (Fig. 8) and a square path 4×4 m (Borenstein *et al*., 1996) (Figure 9). A test with five replications was used. The test procedure was carried out using the following method:

At first by sending the appropriate pulses, the robot was traveling in the right direction and was learning the path from beginning to end. Then, the traveled path was stored in the robot memory unit by ALU. Learned path was traversed again exactly from the starting point independently by the robot and eventually stopped at pseudo-end point algorithm execution unit. The difference between this pseudo-end point and the end point of the real path was measured as the total deviation value.

To determine the robot's lateral deviation from the target line, the robot was tested in a straight line of 20 meters long. On the route at intervals of 4 meters (5 points), the horizontal distance of the robot was measured from the central line in two modes of manual and autonomous control (Figure 10).

(a)

(b)

Fig.6. Greenhouse (a- Earthy surface; b- Concrete surface)

(a) (b) (c)

Fig.7. Various surfaces (a- Ceramic; b- Concrete; c- Soil)

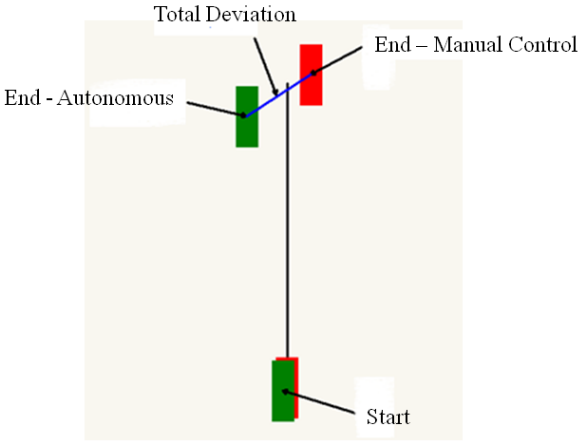

Fig.8. Robot testing in the straight line, 20 m long

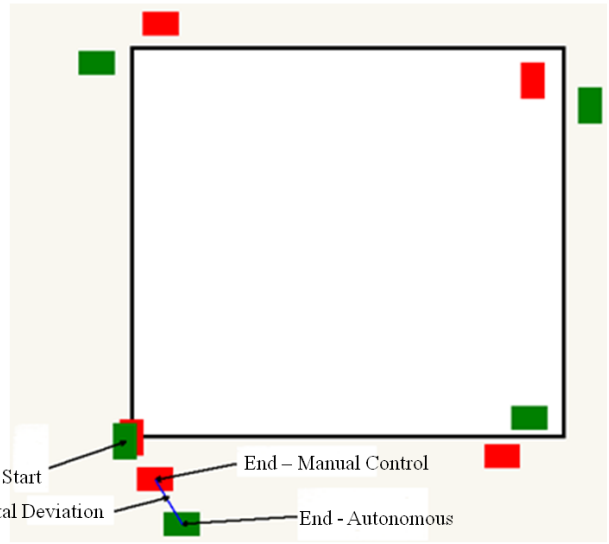

Fig.9. Robot testing in the 4×4 m square path

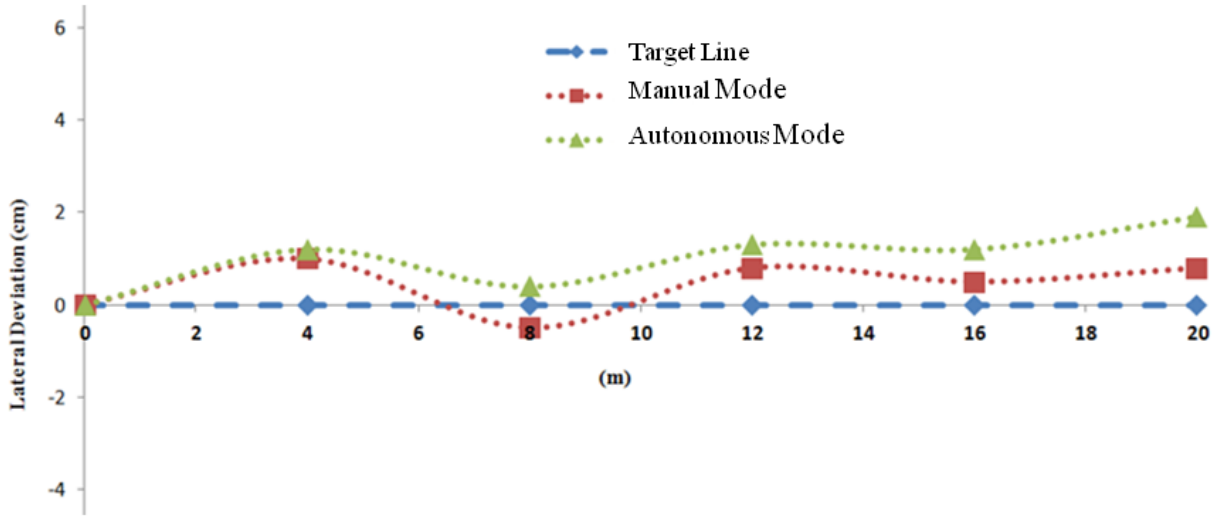

Fig.10. Determining the lateral deviation of the robot from the target line

Robot navigation accuracy tested in greenhouse environment

A sprayer have been installed on the robot chassis (Figure 11), and sprayer robot was tested in a greenhouse with a concrete surface. The area of the greenhouse was about 250 square meters. First, the robot was guided by manual control from the initial point to the end point (Figure 12). Then, the robot automatically traversed the path, and at the end the robot error rate was calculated. This experiment was repeated five times.

Fig.11. Sprayer robot

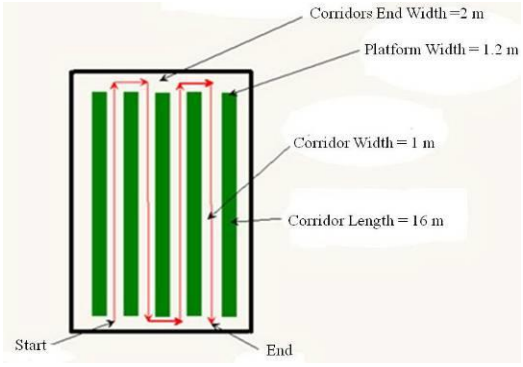

Fig.12. Greenhouse specifications

Data analysis

The statistical indices including RMSE and SD were used to measure the precision of the robot navigation (Wang *et al*., 2019). The following equations were used to calculate RMSE and SD.

$$RMSE=\sqrt{\frac{\sum e^2}{n}} \quad (1)$$

$$SD=\sqrt{\frac{\sum(e-\bar{e})^2}{n-1}} \quad (2)$$

Where e and ē are total deviation (cm) and average deviation (cm), respectively and n is the number of collected data during the robot task.

Results and Discussion

Robot lateral deviation from central line in straight path

The average deviation of the robot from the center line in the direct path test in two manual and autonomous modes at different levels is presented in Table 2 and Figure 13. In both manual and autonomous states, the robot deviated from the central line. In manual control mode, if there are no systematic and non-systematic errors (Borenstein *et al*., 1996) and also no operator error, the robot must move in the straight line without any lateral deviation. However, in practice, due to systematic and non-systematic errors and operator error, there is always an error. But, in manual mode, this ability was available to allow the robot to move in a path with a minimum deviation of the target line. In an autonomous state, it was expected to follow the specified path with manual control by the robot but in practice, it did not happen, and there was always some errors, which was probably due to the wheel's slippage and probably due to a delay in the electric motors responding to commands issued by the central processing unit (It should be noted that two atmega8 microcontrollers were used to control the motors and increase the speed of execution of the commands in the control system). Also considering that the right and left sides of the robot have separate power systems (Includes motor and gearbox, wheel and chain system and wheels). As a result, there may be differences in the execution of the commands of the two systems in a fraction of the time, which can also affect the overall system error. Operator error can be in time to train the robot and also place the robot at the starting point in autonomous mode. During training, due to operator error, the robot's lateral deviation from target line is too high. As a result, lateral deviation from the target line also increases in autonomous mode. Any slight difference in the starting point in the autonomous state

compared to training state causes an error in the autonomous state. As the results indicate, the robot deviations from the specified path decreased in loose soil, dense soil, ceramic and concrete, respectively. On the other words, the accuracy of the robot's navigation and compliance with the path specified in the rigid levels was higher. The least deviation was observed in the concrete surface, which is probably due to less slipping of the wheels. The reason for the increase in error at the ceramic surface relative to the concrete surface, despite its relatively uniform stiffness, may be due to the smoothness of the ceramic surface, which causes the wheels to slide. Celen *et al*. (2015) reported the precision of row guide using ultrasonic sensors is ±7cm at the velocity of 1 m s^{-1}. González *et al*. (2009) using sensors including of encoder, ultrasonic and magnetic compass reported the mean deviation of robot from the desired path (middle of the greenhouse aisles) was less than 15 cm. Xue *et al*. (2017), using the machine vision, showed that maximum deviation of the robot from the central lines of row crop was 4.7 cm. A study based on laid cable detection was carried out by Aghkhani and Abbaspoure-Fard (2009) for automatic off-road vehicle steering system. The system included a cable-spreading unit with a slim steel cable, a fifth or ground wheel with some cable-positioning sensors, a control unit and processor along with an electro-mechanical steering wheel driver. It was reported that, the overall offset deviation (error) on a longitudinal path from the desired path was 26 mm m^{-1} and 27.4 mm m^{-1}, on soil and asphalt surfaces, respectively.

Another factor that can affect the robot error is encoder resolution. Encoder resolution is commonly measured in pulses per revolution (PPR) for incremental encoders. Therefore, using a high-resolution encoder reduces the robot error. The use of high-resolution encoders can reduce the error of the robot, but it also increases costs.

Robot total deviation in straight and square paths

The values of mean deviation, SD and RMSE of autonomous mode from manual mode in a straight and a square path with 4×4 m dimensions on various surfaces are presented in Table 3. RMSE of autonomous mode from manual mode in a straight path (20 m long) on ceramic, concrete, dense soil and loose soil were 4.3, 2.8, 4.6 and 8 cm, respectively, whereas these values were 6.6, 5.5, 13.1 and 47.1 cm for the square path, respectively. Results show that robot deviation is smaller in straight path than the square-shaped path at various surfaces that was a predictable result because of increasing the error in the corners for turning. Also, it can be concluded that robot deviation is less on firm surfaces. The results are inconsistent with reports by Younse and Burks (2007). They used visual odometer for greenhouse robot navigation. The average robot error (difference in distance between the measured position and the position estimated by the visual odometer) in a straight path with a length of 154 cm on the concrete, sand, gravel and land laboratory surfaces have been 12.4, 4.75, 8.75, and 6.05 cm, respectively. The high robot error on concrete surfaces was due to the low efficiency of the camera in detecting these levels. Masoudi *et al*. (2012) applied ultrasonic sensors for robot navigation in a greenhouse which had been equipped with conductor lines. The root mean square errors (RMSE) of robot from the desired path at various velocities were 4.93 to 6.51cm. In a 60 cm wide corridor, the RMSE of robot from central line was 2.5 cm (Singh *et al*., 2005). Also, in the square path, especially in the loose soils, the amount of deviation was high. This amount of deviation has occurred in square corners to turn due to the sinking of the robot wheels into the soil; as a result, this parameter increases the slip of the wheels (Fig. 14). According to the results of the other studies, the robot navigation on concrete, ceramic and dense surfaces is acceptable. Therefore, it is suggested, to minimize the robot deviation from specified path in the greenhouse, especially those with a soil surface, the path of the robot movement should be compressed (Figure 15).

Table 2- The maximum deviation of the robot from central lines in two modes (manual and autonomous control) in the 20 meters long straight path test at different levels

Surface type	Maximum lateral deviation in manual control mode (cm)	Maximum lateral deviation in autonomous control mode (cm)
Ceramic	1.6	3.6
Concrete	1.4	2.1
Dense soil	2.2	5.2
Loose soil (Soft soil)	2.5	7.8

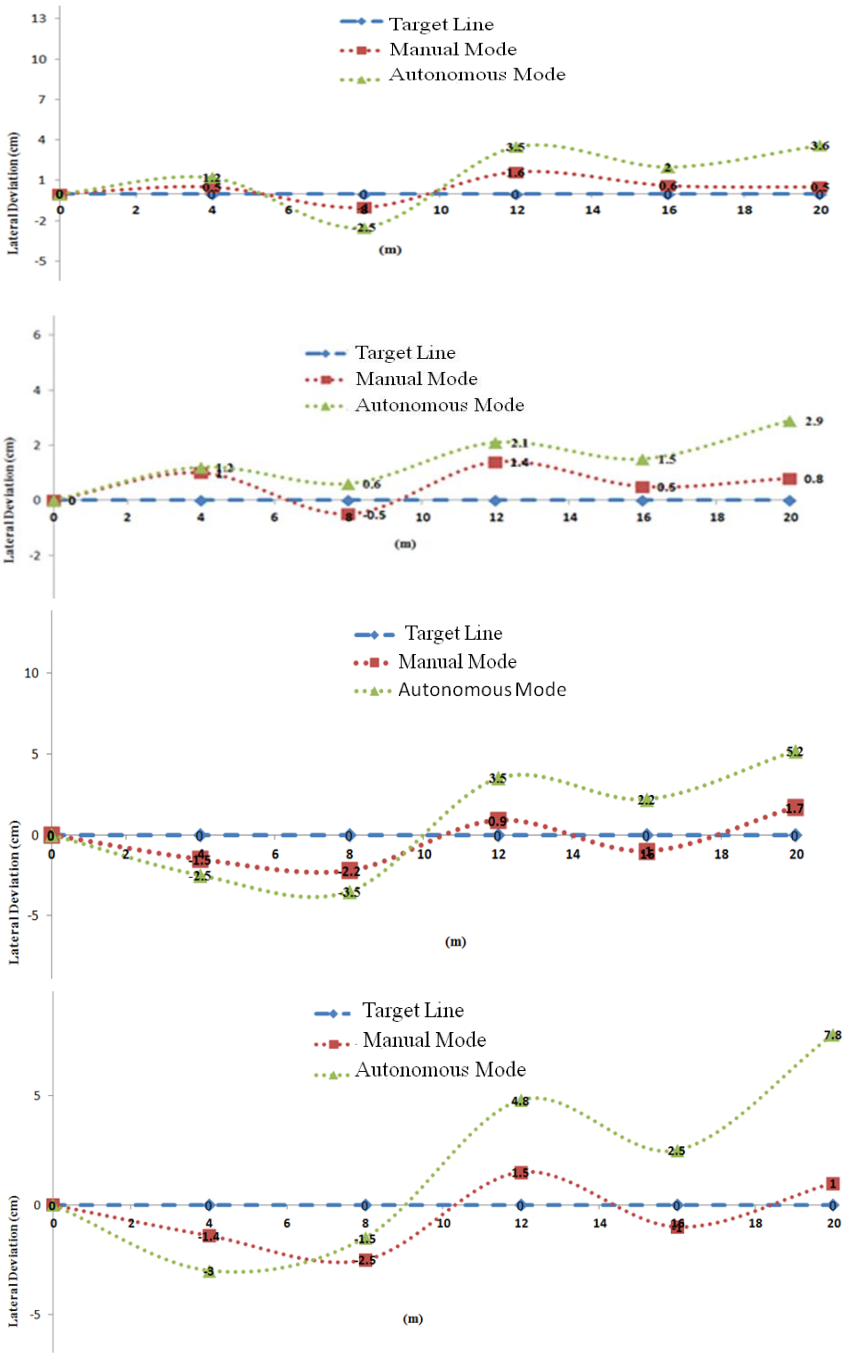

Fig.13. Robot lateral deviation from the central line in two modes (manual and autonomous control) at the different levels (a- Ceramic, b- Concrete, c- Dense soil and d- Soft soil)

Table 3- Comparison of automatic method error from manual control method at different levels and paths

Rep.	Error (cm) Straight path (20 meters long)				Error (cm) 4×4 m square path			
	Ceramic	Concrete	Dens soil	Loose soil	Ceramic	Concrete	Dens soil	Loose soil
1	3.5	2	5.4	8.4	8.2	4.9	13.8	46.5
2	6.4	2.5	4.5	7.5	7.4	5.2	14.1	42
3	4.5	3.4	4.8	8.8	7	5.8	11.5	50.4
4	3	2	5.7	7.9	6.8	6.1	12.2	47.8
5	3.2	2.7	5.2	7.3	8.4	5.4	13.5	48.4
Mean	4.1	2.8	5.1	8	7.6	5.5	13	47
RMSE	4.3	2.8	4.6	8	6.6	5.5	13.1	47.1
SD	1.4	0.58	0.47	0.62	0.71	0.47	1.1	3.1

Fig.14. Turning in loose soil

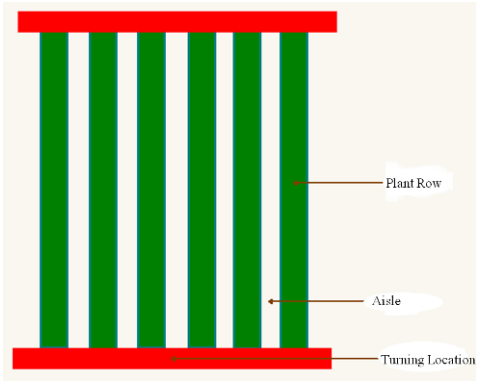

Fig.15. Plan view of the greenhouse

Accurate robot navigation in the greenhouse

Values of mean deviation, RMSE and SD of autonomous mode from manual mode in actual greenhouse are presented in Table 4. Mean deviation, RMSE and SD of autonomous mode from manual mode were 15.8, 15.85 and 1.75 cm, respectively. It can be concluded that robot efficiency in small greenhouses is acceptable. In large greenhouses, it is suggested that the greenhouse be divided into smaller parts or using complementary sensors along with this mechanism to enhance robot navigation accuracy.

Table 4- Total deviation of autonomous mode from manual mode at greenhouse

Rep.	Total deviation(cm)
1	15.5
2	13.8
3	16.8
4	18.2
5	14.6
Mean	15.8
RMSE	15.85
SD	1.75

Conclusions

In this study, the design and fabrication of an appropriate mobile wheel robot for the greenhouse environment were described. This robot has two important characteristics: 1) Simple mechanism, 2) Low cost of construction. Then, robot navigation accuracy was studied at different levels in a straight path and a square path. Robot navigation performance was acceptable at rigid surfaces

such as concrete and compacted soil. In greenhouses with a soft soil, it is recommended to increase the accuracy of the robot's navigation, the path of the robot movement should be compressed. It is also suggested the robot navigation be investigated at various velocities.

References

1. Aghkhani, M. H., and M. H. Abbaspour-Fard. 2009. Automatic off-road vehicle steering system with a surface laid cable: Concept and preliminary tests. Biosystems Engineering 103: 265-270.
2. Borenstein, J., H. Everett, and L. Feng. 1996. Navigating mobile robots: Systems and techniques: AK Peters Wellesley, MA.
3. Borenstein, J., H. R. Everett, L. Feng, and D. Wehe. 1997. Mobile robot positioning: Sensors and techniques. Journal of Robotic Systems 14 (4): 231-249.
4. Borenstein, J., and Y. Koren. 1989. Real-time obstacle avoidance for fast mobile robots. IEEE Transactions on systems, Man, and Cybernetics 19 (5): 1179-1187.
5. Byrne, R., P. Klarer, and J. Pletta. 1992. Techniques for autonomous navigation. Sandia Report SAND92-0457, Sandia National Laboratories, Albuquerque, NM, March.
6. Celen, I., E. Onler, and E. Kilic. 2015. A Design of an Autonomous Agricultural Robot to Navigate between Rows. Paper presented at the 2015 International Conference on Electrical, Automation and Mechanical Engineering; Atlantis Press: Phuket, Thailand.
7. Chenavier, F., and J. L. Crowley. 1992. Position estimation for a mobile robot using vision and odometry. Paper presented at the Robotics and Automation, 1992. Proceedings., 1992 IEEE International Conference on.
8. Cho, S., and N. Ki. 1999. Autonomous speed sprayer guidance using machine vision and fuzzy logic. Transactions of the ASAE 42 (4): 1137-1143.
9. Comba, L., S. Martínez, P. Gay, and D. Aimonino. 2012. Reliable low cost sensors and systems for the navigation of autonomous robots in pot crop nurseries. Paper presented at the Proceedings of the First International Conference on Robotics and Associated High-technologies and Equipment for Agriculture. Applications of automated systems and robotics for crop protection in sustainable precision agriculture, (RHEA-2012) Pisa, Italy-September 19-21, 2012.
10. Cox, I. J. 1991. Blanche-an experiment in guidance and navigation of an autonomous robot vehicle. IEEE transactions on Robotics and Automation 7 (2): 193-204.
11. Dario, P., G. Sandini, B. Allotta, A. Bucci, F. Buemi, M. Massa, F. Ferrari, M. Magrassi, L. Bosio, R. Valleggi, E. Gallo, A. Bologna, F. Cantatore, G. Torrielli, and A. Mannucci. 1994. The Agrobot project for greenhouse automation. Acta Horticulturae 361: 85-92. DOI: 10.17660/ActaHortic.1994.361.7
12. González, R., F. Rodríguez, J. Sánchez-Hermosilla, and J. Donaire.2009. Navigation techniques for mobile robots in greenhouses. Applied Engineering in Agriculture 25 (2): 153-165.
13. Harper, N., and P. McKerrow. 1999. Detecting plants for landmarks with ultrasonic sensing. Paper presented at the Proceedings of the International Conference on Field and Service Robotics.
14. Iida, M., and T. Burks. 2002. Ultrasonic sensor development for automatic steering control of orchard tractor, Proceedings of the Automation Technology for Off-Road Equipment Chicago, Illinois, p. 221- 229.
15. Kleeman, L. 1992. Optimal estimation of position and heading for mobile robots using ultrasonic beacons and dead-reckoning. Paper presented at the Robotics and Automation, 1992.

Proceedings., 1992 IEEE International Conference on Robotics and Automation.12-24 May. Nice. France.
16. Kondo, N., M. Monta, and N. Noguchi. 2011. Agricultural Robots: Mechanisms and Practice: Apollo Books.
17. Kondo, N., and K. Ting. 1998. Robotics for plant production. artificial intelligence Review 12 (1-3): 227-243.
18. Mandow, A., J. Gomez-de-Gabriel, J. L. Martinez, V. F. Munoz, A. Ollero, and A. Garcia-Cerezo. 1996. The autonomous mobile robot AURORA for greenhouse operation. IEEE Robotics & Automation Magazine 3 (4): 18-28.
19. Masoudi, H., R. Alimardani, M. Omid, S. S. Mohtasebi, and N. Noguchi.2012. Determination of ultrasonic sensor ability for use as guidance sensors of mobile robots. Sensors and Materials 24 (3): 115-126.
20. Mehta, S., T. Burks, and W. Dixon. 2008. Vision-based localization of a wheeled mobile robot for greenhouse applications: A daisy-chaining approach. Computers and Electronics in Agriculture 63 (1): 28-37.
21. Goli, H., S. Minaee, A. Jafari, A. R. Keyhani, A. Hajiahmad, H. Abdolmaleki, and A. M. Borghaei. 2014. Comparision of foure different methods for agricultural positioning using GPS and IMU. Journal of Agicultural Machinery 4 (2): 285-295. (In Farsi).
22. Nuyttens, D., S. Windey, and B. Sonck. 2004. Comparison of operator exposure for five different greenhouse spraying applications. Journal of Agricultural Safety and Health 10 (3): 187.
23. Piedrahita, G. A., and D. M. Guayacundo. 2006. Evaluation of accelerometers as inertial navigation system for mobile robots. Paper presented at the IEEE 3rd Latin American Robotics Symposium. Santiago. Chile.
24. Rajendra, P., N. Kondo, K. Ninomiya, J. Kamata, M. Kurita, T. Shiigi, and Y. Kohno. 2009. Machine vision algorithm for robots to harvest strawberries in tabletop culture greenhouses. Engineering in Agriculture, Environment and Food 2 (1): 24-30.
25. Sammons, P. J., T. Furukawa, and A. Bulgin. 2005. Autonomous pesticide spraying robot for use in a greenhouse. Paper presented at the Australian Conference on Robotics and Automation. Canberra Australia.
26. Sánchez-Hermosilla, J., R. González, F. Rodríguez, and J. G. Donaire. 2013. Mechatronic description of a laser autoguided vehicle for greenhouse operations. Sensors 13 (1): 769-784.
27. Sandini, G., F. Buemi, M. Massa, and M. Zucchini. 1990. Visually guided operations in green-houses. Paper presented at the IEEE International Workshop on Intelligent Robots and Systems. Towards a New Frontier of Application. Ibaraki. Japan.
28. Singh, S., T. Burks, and W. Lee. 2005. Autonomous robotic vehicle development for greenhouse spraying. Transactions of the ASAE 48 (6): 2355-2361.
29. Sulakhe, A., and M. N. Karanjkar. 2013. Design and operation of agricultural based pesticide spraying robot. International Journal of Science and Research 4: 1286-1289.
30. Tsai, C. C. 1998. A localization system of a mobile robot by fusing dead-reckoning and ultrasonic measurements. IEEE Transactions on Instrumentation and Measurement, 47 (5): 1399-1404.
31. Van Henten, E. J., J. Hemming, B. Van Tuijl, J. Kornet, J. Meuleman, J. Bontsema, and E. Van Os. 2002. An autonomous robot for harvesting cucumbers in greenhouses. Autonomous Robots 13 (3): 241-258.
32. Veelaert, P., and W. Bogaerts. 1999. Ultrasonic potential field sensor for obstacle avoidance. IEEE transactions on Robotics and Automation 15 (4): 774-779.
33. Wang, H., J. Li, W. Cui, X. Lu, Z. Zhange, C. Sheng, and Q. Liu. 2019. Mobile robot indoor positioning system base on K-ELM. Journal of Sensors.http:\\doi.org\10.1155\2019\7547648.

34. Xue, J. l., B. W. Fan, X. X. Zhang, and F. Yong. 2017. An Agricultural Robot for Multipurpose Operations in a Greenhouse. DEStech Transactions on Engineering and Technology Research (icmme).
35. Younse, P., and T. Burks. 2007. Greenhouse robot navigation using KLT feature tracking for visual odometry. Agricultural Engineering International: CIGR Journal.

نشریه ماشین‌های کشاورزی
جلد ۱۱، شماره ۱، نیمسال اول ۱۴۰۰، ص ۱۵-۱

Journal of Agricultural Machinery
Vol. 11, No. 1, Spring- Summer 2021, p. 1-15

مقاله علمی-پژوهشی

ناوبری ربات متحرک گلخانه با استفاده از کدگذاری چرخش چرخ و الگوریتم یادگیری

احمد حیدری[۱]، جعفر امیری پریان[۲*]

تاریخ دریافت: ۱۳۹۸/۰۲/۲۵
تاریخ پذیرش: ۱۳۹۸/۰۷/۲۰

چکیده

وجود کارهای تکراری، سخت و طاقت‌فرسا و بعضاً خطرناک در محیط گلخانه هم‌چون سم‌پاشی و برداشت، استفاده از ربات را در گلخانه ضروری نموده است. ساختار مکانیکی و الگوریتم ناوبری دو فاکتور مهم در طراحی و ساخت ربات‌های گلخانه می‌باشند. در این پروژه یک ربات متحرک گلخانه چهار چرخ محرک با فرمان‌گیری دیفرانسیلی طراحی و ساخته شد. سپس ناوبری ربات در سطوح با جنس‌های مختلف و نیز محیط گلخانه واقعی مورد ارزیابی قرار گرفت. الگوریتم ناوبری ربات بر اساس یادگیری مسیر بود بدین صورت که ابتدا مسیر مورد نظر با استفاده از کنترل راه دور بر اساس پالس ارسالی از اینکودرهای چرخ، در حافظه ربات ذخیره می‌شد سپس ربات به‌صورت خودکار این مسیر را طی می‌کرد. دقت ناوبری ربات در سطوح با جنس‌های مختلف (سرامیک، بتون، خاک متراکم و خاک نرم) در مسیر مستقیم به طول ۲۰ متر و مسیر مربع شکل ۴×۴ متر مورد آزمایش قرار گرفت. هم‌چنین دقت ناوبری ربات در محیط گلخانه ارزیابی شد. مقدار انحراف ربات با استفاده از شاخص‌های آماری ریشه میانگین مربعات خطا (RMSE) و انحراف معیار (SD) محاسبه شدند. نتایج نشان داد که ریشه میانگین مربعات خطای انحراف ربات در حالت خودکار نسبت به روش دستی در مسیر مستقیم به طول ۲۰ متر در سطوح سرامیکی، سیمانی، خاک متراکم و خاک نرم به‌ترتیب ۴/۳، ۲/۸، ۴/۶ و ۸ سانتی‌متر و در مسیر مربع شکل۴×۴ متر، ۶/۶، ۵/۵، ۱۳/۱ و ۴۷/۱ سانتی‌متر به‌دست آمد.

واژه‌های کلیدی: حسگر اینکودر، ربات کشاورزی، ربات متحرک چرخ‌دار، ناوبری

۱- دانشجوی دکتری، گروه مهندسی بیوسیستم، دانشکده کشاورزی، دانشگاه بوعلی سینا، همدان
۲- استادیار، گروه مهندسی بیوسیستم، دانشکده کشاورزی، دانشگاه بوعلی سینا، همدان
(*- نویسنده مسئول: Email: amiriparian@basu.ac.ir)

DOI: 10.22067/jam.v11i1.80722

Journal of Agricultural Machinery
Vol. 11, No. 1, Spring- Summer 2021, p. 17-27

نشریه ماشین‌های کشاورزی
جلد ۱۱، شماره ۱، نیمسال اول ۱۴۰۰، ص ۲۷-۱۷

Full Research Paper

Prediction of Seed Flow Rate of a Multi-Slot Rotor Feeding Device of a Corn Planter

H. Balanian[1], S. H. Karparvarfard[2*], A. Mousavi Khaneghah[3], M. H. Raoufat[4], H. Azimi-Nejadian[5]

Received: 10-04-2019
Accepted: 09-11-2019

Abstract

In this study, a model was developed for predicting the seeding rate of corn seeds of a typical row-crop planter equipped with a multi-slot feeding device. To this, nine multi-slot rotors (with 4, 5 and 6 slots in three angles of mouth including 23°, 25° and 27°) were designed and manufactured. Tests were carried out at four levels of angular velocity of 40, 52, 62 and 78 rpm on grease belt moving at constant speed of 3.5 km h^{-1}. Tests were completed in three replications. Discharge flow rate was measured and recorded for each treatment. The data were used to develop a model which can be used for predicting the seeding rate under various numbers of slot, mouth angle and rotor angular velocity. According to the results, angle mouth of slots, number of slots, angular velocity and the dual interaction between them showed increasing effects on weight flow rate of seeds (*P-value*<0.01). In the next step, raw data were used to develop the two desired models: based on the dimensional analysis technique and response surface methodology (RSM). The models outputs were compared to experimental data. The standard error of estimate for flow rate for dimensional analysis and response surface methodology (RSM) were 68.13 mm^3 s^{-1} and 475.59 mm^3 s^{-1}, respectively. The dimensional analysis model was closer to experimental data rather than the RSM method. Thus, to predict the volume flow rate of seed, the dimensional analysis model is recommended.

Keywords: Corn, Dimensional analysis, Response surface methodology, Row planting

Notation

Vertical intersept	C	Solids volumetric Flowrate (mm^3 s^{-1})	Q
Effective diameter of seed (mm)	d	Number of rotor	R
Effective diameter of Rotor (mm)	D_e	Rotor thikness (mm)	t
Casing inside diameter(mm)	D	The mean width of slots (mm)	W
Acceleration of gravity (=9806)	g	Solid mass flow rate (g min^{-1})	$\dot{W}$
Depth of the slot (mm)	h	Angle of repose (degree)	θ
Slope of logarithmic line	K	Angle mouth of slot (degree)	β
Mean seed longitude (mm)	l	Density of solid particles (g min^{-1})	ρ_s
Rotating speed of rotor (rps)	n	Loose bulk density (g min^{-1})	γ
Slots number	N	Function of ….	φ

Introduction

Some of the seeds planted per unit area cannot survive through germination and emergence stages. Hence, the seeds number must be greater than the desired plant stand (Raheman and Singh, 2003; Srivastava, 2006). Therefore, a planter must meter seeds at proper rate and also must control the horizontal placement of seeds in the desired pattern.

The seed metering mechanism is one of the main components of a planter that affects directly on yield efficiency (Ani *et al*., 2016). Seed metering devices are categorized as either precision or dune flow metering based on planting pattern result (Murray *et al*., 2006). Single-seed metering devices have been developed to provide precision for seed spacing planters which can provide exact and unique placement of single seeds at equal intervals within each rows. However, in this

1- MSc student, Department of Biosystem Engineering, College of Agriculture, Shiraz University, Shiraz, Iran
2- Associate Professor, Department of Biosystem Engineering, College of Agriculture, Shiraz University, Shiraz, Iran
3- Assistant Professor, Department of Food Science, Faculty of Food Engineering, State University of Campinas (UNICAMP), 13083-862 Campinas, São Paulo, Brazil
4- Professor, Department of Biosystem Engineering, College of Agriculture, Shiraz University, Shiraz, Iran
5- PhD student, Department of Biosystem Engineering, College of Agriculture, Shiraz University, Shiraz, Iran
(*- Corresponding Author Email: Karparvr@shirazu.ac.ir)
DOI: 10.22067/jam.v11i1.79992

technique, less attention has been given to the physical properties of seeds (Khan, 2008).

Precision meters attempt to meter single seeds. While there is a large range of precision metering devices, most of them can be broadly classified as 'plate', 'belt', 'disc', 'drum' or 'finger' types. The classification largely depends on the design and/or shape of the principle moving element that enables seed simulation (i.e. the selection of single seeds from the seed lot) (Gray and Maclntyre, 2012). Plate metering devices consist of a driving disk with indents on its periphery, and their efficiency depends on the seeds size (Ani *et al*., 2016). They can be sub-categorized as horizontal and vertical plate types (Murray *et al*., 2006). In this context, the multi-slot rotors are classified among the vertical sheet metal metering devices.

Among the agricultural crops, corn has great importance as food, livestock and poultry feed, industrial and medicinal consumptions and as a rich source of carbohydrates, protein, iron, and vitamin B (Al-Mallahi and Kataoka, 2013; Ani *et al*., 2016). It is necessary to cultivate corn seeds in a row. Therefore, the distance between consecutive seeds should be kept constant to minimize damage to them. This distance depends on the correct forward speed of the planter, rotational speed of the metering device and the space of the metering device cells (Anantachar *et al*., 2011).

Rebati and Zareian (2003) fabricated a metering device for hill-planting with parallel slots on its roller surface which was used for hill-planting of roof rice in laboratory conditions. In order to evaluate the performance of the unit, forward velocity and diameter of the seed metering device were considered. According to their findings, the seeding speed of 3 km h^{-1} was considered as the optimum speed for minimum seeds' damage. In another investigation, Jafari (1991) considered main characteristics of a fluted-roller metering device of a grain drill and developed a model equation for predicting discharge volume flow rate.

A new methodology to estimate the mass of grain seeds, which flow in the shape of clumps, was suggested in a study. The methodology used an off-the-shelf digital fiber sensor to detect the behavior of the clumps and multiple linear regression modeling to estimate the mass by the parameters detected by the sensor which were the length and the density of the clumps. An indoor apparatus was used for modeling which resembled the sowing process using the grain drill. A fluted roller was installed in the apparatus to regulate the flow of seeds. Results showed that the digital fiber sensor could be used for estimating mass flow of seeds at variable sowing rates within the speed limits of the grain drill (Al-Mallahi and Kataoka, 2013).

In the absence of any characteristic relationship for predicting volume flow rate of a multi-slot rotors in row-crop planting, the current investigation was aimed to fabricate a test rig and establish a model for estimating the volume flow rate of corn seeds.

Materials and Methods

Laboratory tests were conducted to measure the discharge flow rate of feeding device for a number of treatments. Treatments were three rotors having different slots (4, 5 and 6), each rotor having three angle of mouth (23°, 25° and 27°) at four angular velocity (40, 52, 63 and 78 rpm). Tests were replicated three times.

Development of the required test-rig

A test rig was assembled to measure the discharge flow rate for each settings (Figure 1), the rig consists following parts:

1- Metering device: In the design of the metering device, the shape and number of slots are important factors. The dimensions of each slot are associated with the seed size and the number of seeds cells. Three fundamental design variables including the effective diameter of the metering devices (D_e), the slot depth (h) and the angled mouth of slots (β), as shown in Figure 2 (Rebati and Zareian, 2003). Considering the shape and size of the corn seeds, three angles of 23°, 25° and 27° were calculated and defined as the angles mouth of slots. Angles have direct effect on the depth of the slots and the effective diameter of the metering devices. In order to provide different distance between consecutive seeds on the

ground, the fluted rotors with 4, 5 and 6 slots were used. Therefore, the nine rotors were designed in SolidWorks software (SP 3.0, Dassault Systèmes, Vélizy-Villacoublay, France, 2016) and were fabricated from Polytetrafluoroethylene material (Figure 3).

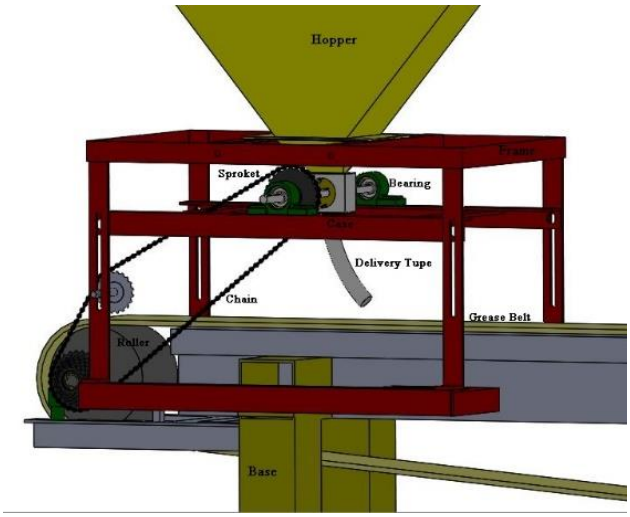

Fig.1. The layout of the test apparatus

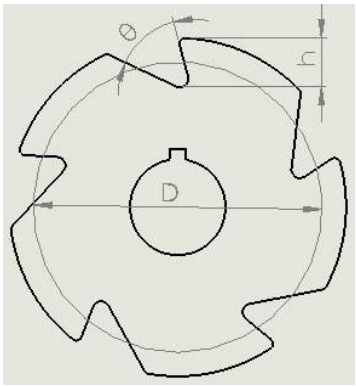

Fig.2. Variables related to design of the metering devices

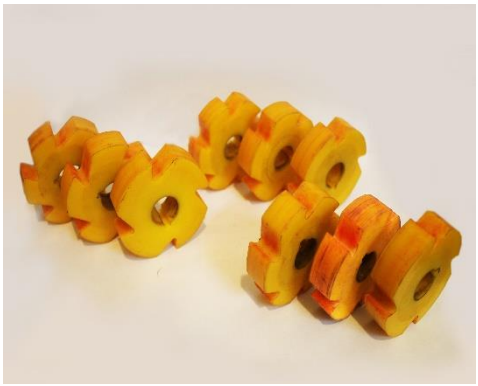

Fig.3. Metering devices used in this study

2- Metering device Case: The metering device case was fabricated from polyethylene material with dimensions of 50 mm×100 mm×75 mm. This case has a 50 mm×25 mm

intake gate and 50 mm×13 mm outlet opening, and a ball bearing (B17-99) was used to accommodate the shaft of the metering device in the center of the case.

3- Power transmission system: In order to facilitate the movement of the metering device and control the spacing of seeds along the row of the grease belt, a chain, and sprocket system was used to provide the desired rotational speeds of 40, 52, 63 and 78 rpm.

Experimental Design

The volumetric flow rate of seed discharge from a planter feeding device depends on the following groups of parameters (Jafari, 1991):

1. Metering device parameters, which include the effective diameter of the metering devices, the number of slots, the angled mouth of slots, the depth of slots and the rotational speed of the metering device.

2. Seed parameters including mean length and the effective diameter of seeds, the density of solid particle, surface characteristics, and seed shape factor.

3. Flow parameters including solids flow rate, gravitational acceleration, and friction between solids and wall.

The dimensional analysis and response surface methodology (RSM) approaches were considered to express the relationship between the selected parameters. In summary, the bulk volume flow rate of solids (depended variable) was considered as a function of nine independent variables as follow:

$$Q = \varphi(n, t, g, h, N, D_e, \beta, l, d) \quad (1)$$

Thus, based on π- Buckingham theorem (Murphy, 1950), the selected model has the formula for the linear form:

$$nt^3Q^{-1} = C\left[\varphi_1\left(e^{n\sqrt{tg^{-1}}}\right) \times \varphi_2\left(e^{n\sqrt{tg^{-1}}}\right) \times \varphi_3(th^{-1}) \times \varphi_4(NtD_e^{-1}) \times \varphi_5(\beta) \times \varphi_6(D_e l^{-1}) \times \varphi_7(D_e d^{-1})\right]^K \quad (2)$$

The Response Surface Methodology (RSM) consists of a group of mathematical and statistical techniques used in the development of an adequate functional relationship between a response of dependent and some independent variables denoted (Maged *et al*., 2018; Khuri, 2017; Salar and Karparvarfard, 2017). The miss index, multiple index, quality of feed index and precision in spacing were considered as dependent variables as details mentioned in Balanian *et al.* (2018). The angle mouth of slots (β), number of slots (N) and the rotational speed of the rotor (n) are used as independent and changeable variables, and the volume flow rate of solids (Q) was considered as the dependent variable. The RSM model was recommended as below:

$$Q = C_1 \times \beta + C_2 \times N + C_3 \times n + C_4 \times \beta \times N + C_5 \times \beta \times n + C_6 \times N \times n + C_7 \times \beta^2 + C_8 \times N^2 + C_8 \times n^2 + C \quad (3)$$

Where C_1, C_2, …, C_8 are constants.

Considering the proposed models, the parameters in the study were selected. The average particle diameter and the length of scorn seeds were calculated according to a previously published method (Mohsenin, 1970). Besides, the loose bulk density was calculated by using the equation (4):

$$\gamma = \frac{M}{V} \quad (4)$$

Where M is the weight of the sample and V is the volume of the particle samples. The loose bulk density as obtained to be 0.81 $g.L^{-1}$ which was used to calculate the volume flow rate of particles. The thickness and outside diameter of each rotor were considered to be constant and equal to 15 mm and 60 mm, respectively.

The number of slots, the depth of slots, the angled mouth of slots and the effective diameter of the rotors could be varied. By changing the values of the slot's mouth angle, the quantities of h and D_e were defined by using SolidWorks® software. The specification and the weight flow rate of solid for all rotors are given in Table 1. Based on the size of the rotor case chamber, the rotor thickness was considered as 18 mm. At different times, the average values for weight flow rate ($\dot{W}$) were obtained in three replications for each run. The forward speed of the grease belt was considered to be constant and adjusted as 3.5 km h^{-1}. Particles damage within the range for this test run were found approximately 5.6%.

Table 1- The specification and weight flow rate of Corn seed for each rotor used

Rotor Number	N	β (degree)	h (mm)	D_e (mm)	n (rpm)	Ẇ (g min^{-1})
R_1	4	23	7.72	52.22	40	88
					52	108.55
					63	122.83
					78	124.53
R_2	5	23	7.72	52.22	40	93.55
					52	116.17
					63	121.36
					78	136.40
R_3	6	23	7.72	52.22	40	138.37
					52	180.94
					63	186.55
					78	211.32
R_4	4	25	8.72	51.22	40	97.43
					52	124.90
					63	141.07
					78	143.85
R_5	5	25	8.72	51.22	40	125.46
					52	163.41
					63	181.60
					78	202.96
R_6	6	25	8.72	51.22	40	157.43
					52	187
					63	225.85
					78	253.11
R_7	4	27	9.72	50.19	40	120.85
					52	149.82
					63	180.98
					78	194.97
R_8	5	27	9.72	50.19	40	148.79
					52	184.09
					63	214.66
					78	233.89
R_9	6	27	9.72	50.19	40	191.81
					52	251.53
					63	284.70
					78	328.91

The regression equation allows us to make predictions, while no indication of the accuracy of the prediction was detected. Thus, the standard error of the estimate as the measure of the accuracy of prediction was calculated by the following equation:

$$\text{The standard error of estimate} = \sqrt{\frac{\sum(\text{measured value} - \text{predicted value})^2}{\text{the number of pairs of scores}}} \quad (5)$$

Results and Discussion

The Experimental Results

By increasing the rotational speed of rotors, the weight of solids would be increased. This increase showed a descending slope which may be correlated with further increasing the centrifugal force and decreasing the seed entrance rate to the intake gate (Figure 4a). According to Table 1, by increasing the angled mouth of slots, the number of slots and the rotational speed of rotors, the weight of solids, would be increased (Figure 4b). In other words, the factors chosen in Equations (2) and (3) could be verified. Additionally, the effect of each treatment and the dual interaction between them were significantly higher for the weight flow rate of solids (Table 2), and the coefficient of estimate of each factor was

shown in Table 3. According to Table 3, since the coefficient of estimate of single effects was greater than dual effects, the results were presented based on the single effects. Then, the effect of those factors would be examined by the RSM method simultaneously while the corn seed specifications were examined by the dimensional analysis.

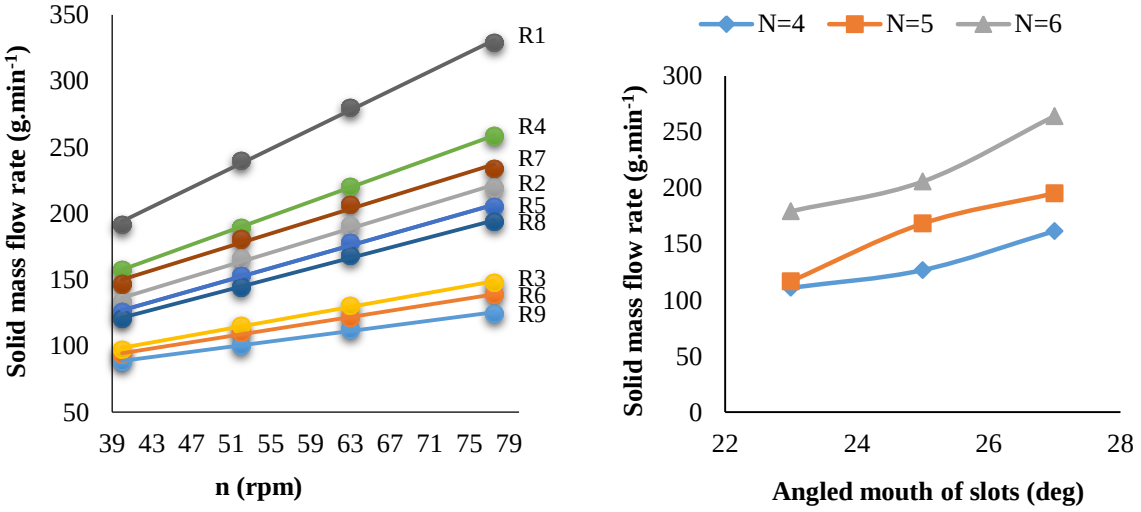

(a) (b)

Fig.4. Weight of solids versus (a) Rotational speed of rotors and (b) Angle mouth of slots

Table 2- Analysis of variance of the effect of the treatment on weight flow rate of solids

Treatments	df	Mean Square	F-Value
Angle mouth of the slot (β)	2	46075.9910	786.41**
Number of slot (N)	2	65024.2958	1109.81**
Rotor Speed (n)	3	27279.9565	465.6**
N × β	4	1865.9782	31.85**
β × n	6	1084.8282	18.52**
N × n	6	1032.1254	17.62**
β × N × n	12	106.6767	1.82ns
Model	35		158.72
Total	108		
cv	4.504		

**= P-value ≤ 0.01 , ns = not-significant

Table 3- Coefficient of estimate of each factor

Factor	Coefficient of estimate
Angle mouth of the slot (β)	742.48
Number of slots (N)	865.11
Rotor Speed (n)	758.26
N × β	176.26
β × n	258.83
N × n	246.05
β^2	90.39
N^2	300.6
n^2	-230.43
Intercept	3386.48

Development of model, dimensional analysis approach

In the first step, 80 percent of the data was randomly selected to develop the desired equation. As mentioned, the data collected were categorized based on dimensional analysis according to Equation (2). Initially, logarithms of both sides of Equation (2) were used to have linear correlation, and then equation groups were correlated as previously worked by Jafari (1991).

$$\begin{aligned}&\mathrm{Log}(\mathrm{nt}^3\mathrm{Q}^{-1})\\&=\mathrm{LogC}\\&+\mathrm{K}\left[\mathrm{Log}\varphi_1\left(e^{\mathrm{n}\sqrt{\mathrm{tg}^{-1}}}\right)+\mathrm{Log}\varphi_2\left(e^{\mathrm{n}\sqrt{\mathrm{tg}^{-1}}}\right)+\mathrm{Log}\varphi_3(\mathrm{th}^{-1})\right.\\&\left.+\mathrm{Log}\varphi_4\left(\mathrm{NtD_e}^{-1}\right)+\mathrm{Log}\varphi_5(\beta)+\mathrm{Log}\varphi_6(\mathrm{D_el}^{-1})\right.\\&\left.++\mathrm{Log}\varphi_7(\mathrm{D_ed}^{-1})\right]\end{aligned}\quad(6)$$

In Equation (6), C and K represent the intercept and the slope of the logarithmic line, which can be calculated after founding all functional correlations of the above equation. Therefore, for convenience, log C and K were considered to be 0 and 1, respectively (Karparvarfard and Rahmanian-Koushkaki, 2015).

$$\begin{aligned}&\mathrm{Log}(\mathrm{nt}^3\mathrm{Q}^{-1})\\&=\mathrm{Log}\varphi_1\left(e^{\mathrm{n}\sqrt{\mathrm{tg}^{-1}}}\right)+\mathrm{Log}\varphi_2\left(e^{\mathrm{n}\sqrt{\mathrm{tg}^{-1}}}\right)+\mathrm{Log}\varphi_3(\mathrm{th}^{-1})\\&+\mathrm{Log}\varphi_4\left(\mathrm{NtD_e}^{-1}\right)+\mathrm{Log}\varphi_5(\beta)+\mathrm{Log}\varphi_6(\mathrm{D_el}^{-1})\\&++\mathrm{Log}\varphi_7(\mathrm{D_ed}^{-1})\end{aligned}\quad(7)$$

The functional φ_1 through φ_7 would be analyzed in the same order based on the first residuals to sixth residuals definitions. For example, the first residuals, as an independent term, represent the values of $\mathrm{Log}\varphi_1\left(e^{\mathrm{n}\sqrt{\mathrm{tg}^{-1}}}\right)$ (Equation 8) (Jafari, 1991) which has been subtracted from the corresponding value of the left-hand side, as dependent term, of equation (6) to remove the effect of this function (φ_1) and prepare to set up the next function.

Then the first residual ($\mathrm{Log}\varphi_2\left(e^{\mathrm{n}\sqrt{\mathrm{tg}^{-1}}}\right)$) would be plotted versus their corresponding values of $\exp(\mathrm{n}\sqrt{\mathrm{tg}^{-1}})$ in this effect, and $\mathrm{Log}\varphi_2\left(e^{\mathrm{n}\sqrt{\mathrm{tg}^{-1}}}\right)$ would be obtained (Equation 9). This order would be repeated for second residuals ($(\log\varphi_3(\mathrm{th}^{-1})$) that means subtracting the values of $\mathrm{Log}\varphi_2\left(e^{\mathrm{n}\sqrt{\mathrm{tg}^{-1}}}\right)$ from the corresponding values of the first residuals in order to remove its effect and would be plotted versus their corresponding values of the $\log(\mathrm{th}^{-1})$, and the $\log\varphi_3(\mathrm{th}^{-1})$ would be obtained (Equation 10).

Functional relationships for φ_1 through φ_7, have been already obtained by (Karparvarfard and Rahmanian-Koushkaki, 2015) and were recorded here as below:

$$\begin{aligned}&\log\varphi_1\left(e^{\mathrm{n}\sqrt{\mathrm{tg}^{-1}}}\right)\\&=\left[19.902\log(\mathrm{th}^{-1})\right.\\&\left.+27.093\log\left(\mathrm{NtD_e}^{-1}\right)\right]\exp\left(\mathrm{n}\sqrt{\mathrm{tg}^{-1}}\right)\end{aligned}\quad(8)$$

$$\log\varphi_2(e^{\mathrm{n}\sqrt{\mathrm{tg}^{-1}}})=-6.728\exp(\mathrm{n}\sqrt{\mathrm{tg}^{-1}})\quad(9)$$

$$\log\varphi_3(\mathrm{th}^{-1})=-14.092\log(\mathrm{th}^{-1})\quad(10)$$

$$\log\varphi_4\left(\mathrm{NtD_e}^{-1}\right)=5.2324\log\left(\mathrm{NtD_e}^{-1}\right)\quad(11)$$

$$\log\varphi_5(\beta)=8.6585\log(\beta)\quad(12)$$

$$\log\varphi_6(\mathrm{D_el}^{-1})=-34.996\log(\mathrm{D_el}^{-1})\quad(13)$$

$$\log\varphi_7(\mathrm{D_ed}^{-1})=34.752\log(\mathrm{D_ed}^{-1})\quad(14)$$

At this stage, equations (8) to (14) could be combined with Equation (2) as follow:

$$\begin{aligned}\log(\mathrm{nt}^3\mathrm{Q}^{-1})=\log\mathrm{C}&+\mathrm{K}\left\{[19.901\log(\mathrm{th}^{-1})\right.\\&+27.093\log(\mathrm{NtD}^{-1})\\&-6.728]\mathrm{e}^{\mathrm{n}\sqrt{\mathrm{tg}^{-1}}}\\&-14.092\log(\mathrm{th}^{-1})\\&+5.2324\log\left(\mathrm{NtD_e}^{-1}\right)\\&+8.6586\log(\theta)\\&-34.996\log(\mathrm{D_el}^{-1})\\&\left.+34.752\log(\mathrm{D_ed}^{-1})\right\}\end{aligned}\quad(15)$$

The final value of K and log C were obtained by plotting the corresponding value of $\log(nt^3Q^{-1})$ against the numerical values of the expressions inside bracket of equations (14) (Figure 4).

$\mathrm{K}=-0.0352$ and $\log\mathrm{C}=0.6593$

The final equation was concluded:

$$\begin{aligned}&\mathrm{nt}^3\mathrm{Q}^{-1}\\&=4.564\left\{\left[(\mathrm{th}^{-1})^{19.902}\left(\mathrm{NtD_e}^{-1}\right)^{27.093}(1.87\right.\right.\\&\times10^{-7})\Big]^{\exp\left[\mathrm{n}\sqrt{\mathrm{tg}^{-1}}\right]}\times\left(\frac{\mathrm{h}}{\mathrm{t}}\right)^{14.092}\times(\mathrm{NtD_e})^{5.2324}\\&\times(\beta)^{8.6585}\times(\mathrm{D_el}^{-1})^{34.993}\\&\left.\left.\times(\mathrm{D_ed}^{-1})^{34.752}\right\}^{-0.0352}\end{aligned}\quad(16)$$

It should be noted that the present study was carried out within the limits of the values in Table 4. Therefore above equation can be used for predicting weight flow rate discharge of a multi-slots feeding device of a row-crop planter within the limits mentioned in Table 4.

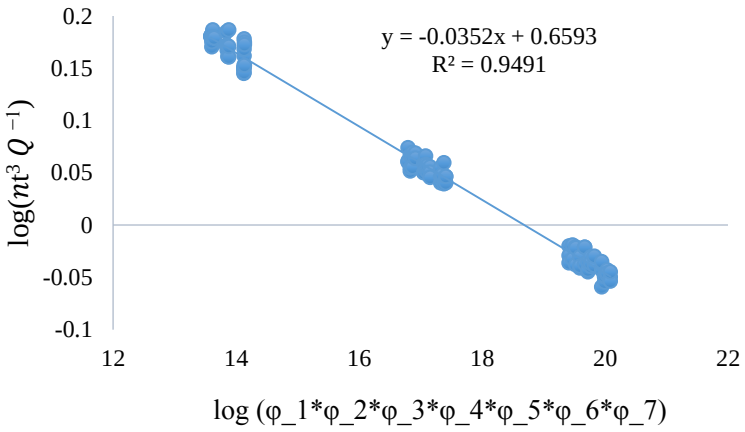

Fig. 5. Plot of $log(nt^3Q\text{^}(-1))$ versus $log(\varphi_1.\varphi_2.\varphi_3.\varphi_4.\varphi_5.\varphi_6.\varphi_7)$

Table 4- Considered a range of dimensionless groups in the present study

Variable groups	Range of variations
th^{-1}	1.646 – 2.073
$NtD_e{}^{-1}$	1.226 – 1.913
$n\sqrt{tg^{-1}}$	0.0269 – 0.0525
β	23 - 27
D_el^{-1}	5.004 – 5.206
D_ed^{-1}	6.460 – 6.721

Development of model, response surface methodology approach

The purposing of modeling performance for the single-seed metering device is crucial to establish the correlations between the requested inputs (for instance: angle mouth of slots, number of slots and the rotational speed of rotor) and outputs (bulk volume flow rate of solids). The RSM as a statistical model was applied for each performance parameter of the planting device using Design-Expert software (Version 11.0.1). Table 5 shows the maximum and minimum of data which were used in the RSM modeling. The result was the following equation which can be used to predict the bulk volume flow rate of solids.

$$\begin{aligned} Q = 31790.1 &- 1604.92 \times \beta - 5115.55 \times N - 7245.58 \times n \\ &+ 88.1321 \times \beta \times N + 414.431 \times \beta \times n \\ &+ 787.949 \times N \times n + 22.5983 \times \beta^2 + 300.6 \\ &+\times N^2 - 2363.13 \times n^2 \end{aligned} \quad (17)$$

$R^2 = 0.96$

The ANOVA table of the RSM model is presented in Table 6.

Table 5- The maximum and minimum of data sets used for RSM modeling

Variable	Maximum	Minimum
B (Degree)	25	23
N	6	4
n (rps)	1.29	0.67
Q ($mm^3.s^{-1}$)	7025.029	1639.235

Table 6- Anova Table of RSM model

Source	Sum of square	df	Mean square	F-Value
Model	3.558E+6	3	1.186E+6	26.57**

**= P-value ≤ 0.01

Accuracy analysis of the RSM and dimensional analysis models

In order to assess the validity and accuracy of estimating the volume flow rate of seeds by the two proposed models, 20 percent of the data was set aside to be used for verifying the two models. The volume flow rate as predicted by dimensional analysis and the RSM model were plotted against the measured volume flow rate (Figure 6). The plot shows that the values predicted by the dimensional analysis are closer to the measured values as compared to values predicted by with the RSM values.

The standard error of estimate was 68.13 mm^3 s^{-1} and 475.59 mm^3 s^{-1} for the dimensional analysis and the RSM method, respectively.

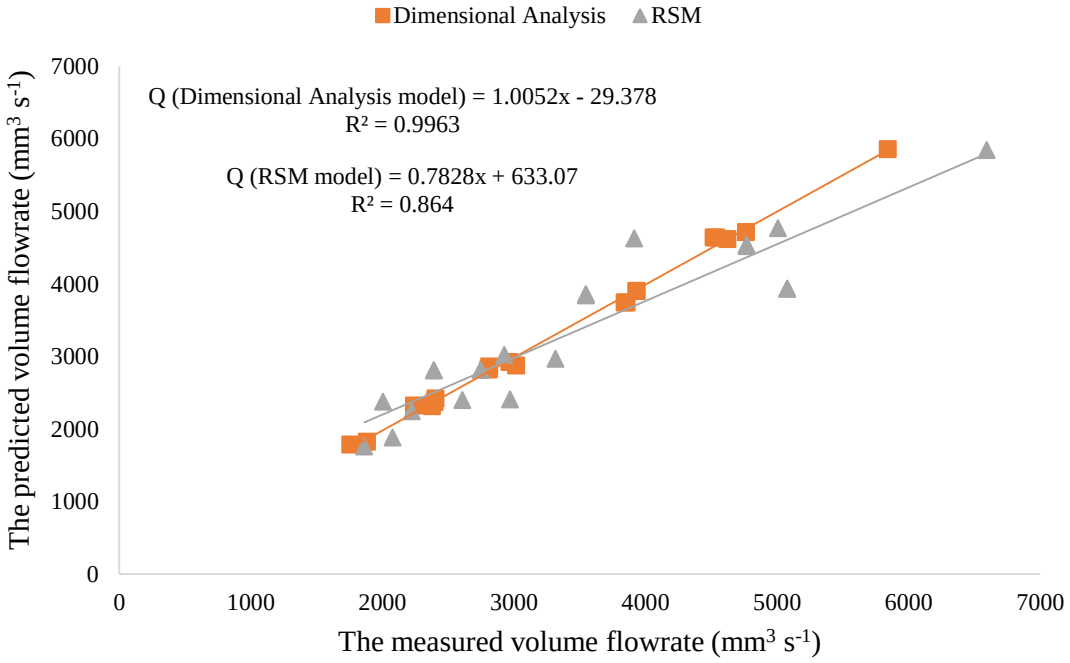

Fig.6. Plot of predicted volume flow rate versus measured volume flow rate

Conclusions

In this study, two equations were developed which can be used to predict the volume flow rate discharge of corn seeds from a new type of planter metering device the following conclusions were also made:

1. The increase in rate for a bulk volume flow rate of solids showed a descending slope by increasing the rotational speed of rotors.

2. More effective performance for bulk volume flow rate of solids can be achieved at lower rotor speeds.

3. Predictions by dimensional analysis approach is more accurate as compared to prediction by the RSM model. The standard error of estimate for dimensional analysis approach and the RSM method were 68.13 mm^3 s^{-1} and 475.59 mm^3 s^{-1}, respectively.

Acknowledgement

The Authors would like to thank the Shiraz University Research Council for supporting and financing this project.

References

1. Al-Mallahi, A. A., and T. Kataoka. 2013. Estimation of mass flow of seeds using fibre sensor and multiple linear regression modelling. Computers and Electronic in Agriculture 99: 116-122.

2. Anantachar, M., G. V. Prasanna Kumar, and T. Guruswany. 2011. Development of artificial neural network models for the performance prediction of an inclined plate seed metering device. Applied Soft Computing 11: 3753-3763.
3. Ani, O. A., B. B. Uzoejinwa, and N. F. Anochili. 2016. Design, construction and evaluation of a vertical plate maize seed planter for gardens and small holder farmers. Nigerian Journal of Technology 35 (3): 647-655.
4. Balanian, H., S. H. Karparvarfard, and H. Azimi-Nejadian. 2018. Investigation for Laboratory Performance of Grooved Roller Metering Device for Corn Planting Effects on Seeds Distance. Iranian Journal of Biosystem Engineering: in press. (In Farsi).
5. Dolati, M., and S. H. Karparvarfard. 2006. Design, Development and Evaluation of a Penumatic Punch Planter for Corn Planting. Iranian Journal of Agriculture Science 37: 193-204. (In Farsi).
6. Gray A. G., and D. Maclntyre. 2012. Soil penetration by disc coulters of direct drills. The Agriculture Engineer 38 (4): 106-109.
7. Grift, T. T., and C. M. Crespi. 2008. Estimation of the flow rate of free falling granular particles using a Poisson model in time. Biosystem Engineering 101: 36-41.
8. Jafari Far, J. 1991. A study of the metering of free flowing particulate solids using multi-flight screws. Journal of Process Mechanical Engineering 205: 113-121.
9. Karparvarfard, S. H., and H. Rahmanian-Koushkaki. 2015. Development of a fuel consumption equation: test case for a tractor chisel-ploughing in a clay loam soil. Biosystem Engineering 130 (1): 23-33.
10. Khan, A. A. 2008. Preplant physiological seed conditioning. Department of Horticultural Sciences, Geneva, New York.
11. Khuri, A. I. 2017. Response Surface Methodology and Its Applications In Agricultural and Food Science. Biometrics and Biostatistics International Journal 5 (5): 00141.
12. Maged, A., S. Haridy, M. Shamsuzzaman, I. Alsyouf, and R. Zaeid. 2018. Statistical Monitoring and Optimization of Electrochemical Machining using Shewhart Charts and Response Surface Methodology. International Journal of Engineering Materials and Manufacture 3 (2): 68-77.
13. Mohsenin, N. N. 1983. Physical Properties of Plant and Animal Materials. Gordon and Breach Science Publishers, New York.
14. Murphy, G. C. 1950. Similitude in engineering. Ronald Press Company, New York.
15. Murray, J. R., J. Tulberg, and B. B. Basnet. 2006. Planting and their components; types, attributes, functional requirements, classification and description. Australian Center for International Agricultural Research Monograph 121.
16. Raheman, H., and U. Singh. 2003. A sensor for seed slow from seed metering mechanisms. IE (I) Journal AG 84: 6-8.
17. Rebati, J., and S. Zareian. 2003. Design Construction and Labotaroty Evaluation of A Roller Metering Device For Hill Dropping. Journal of Agriculture Science 13: 75-85. (In Farsi).
18. Salar, M. R., and S. H. Karparvarfard. 2017. Modeling and Optimization of Wing Geometry Effect on Draft and Vertical Forces of Winged Chisel Plow. Journal of Agricultural Machinery 7 (2): 468-479. (In Farsi).
19. Srivastava, A. K., C. Goering, R. Rohrbach, and D. Buckmaster. 2006. Engineering Principles of Agricultural Machines. American Society of Agriculture and Biological Engineers, Michigan.

نشریه ماشین‌های کشاورزی
جلد ۱۱، شماره ۱، نیمسال اول ۱۴۰۰، ص ۲۷-۱۷

Journal of Agricultural Machinery
Vol. 11, No. 1, Spring- Summer 2021, p. 17-27

مقاله علمی-پژوهشی

تبیین معادله عددی به‌منظور پیش‌بینی دبی خروجی بذر ذرت در موزع‌های غلتکی شیاردار

حسین بلانیان[۱]، سید حسین کارپرورفرد[۲*]، امین موسوی خانقاه[۳]، محمدحسین رئوفت[۴]، هادی عظیمی نژادیان[۵]

تاریخ دریافت: ۱۳۹۸/۰۱/۲۱
تاریخ پذیرش: ۱۳۹۸/۰۸/۱۸

چکیده

در این پژوهش از یک روش جدید به‌منظور پیش‌بینی دبی خروجی بذر ذرت در دقیق‌کارها استفاده شد. بدین منظور ۹ عدد موزع با سه سطح تعداد شیار (۴، ۵ و ۶ شیار) و سه سطح زاویه دهانه شیار (۲۳، ۲۵ و ۲۷ درجه) در چهار سطح سرعت دورانی (۴۰، ۵۲، ۶۳ و ۷۸ دور بر دقیقه) مورد استفاده قرار گرفتند. سرعت پیشروی تسمه آغشته به گریس به‌طور مداوم ۳/۵ کیلومتر برساعت در نظر گرفته شد. تمامی آزمایش‌ها در سه تکرار انجام شدند. ذرت به‌عنوان یک ماده ریزدانه دارای اندازه‌های نزدیک به یکدیگر بودند. میانگین دبی خروجی بذور در مقابل سرعت دورانی محاسبه گردید. بر اساس نتایج حاصله، تغییر زاویه دهانه شیار، تعداد دهانه شیار، سرعت دورانی و اثر دوگانه آن‌ها در سطح احتمال یک درصد بر میزان دبی خروجی بذور تأثیر معنی‌داری داشت. بر اساس روش مدل‌سازی آنالیز ابعادی و سطح پاسخ، داده‌ها مورد ارزیابی قرار گرفتند. میزان خطای استاندارد برای روش آنالیز ابعادی و سطح پاسخ به‌ترتیب برابر با ($mm^3.s^{-1}$) ۱۳/۶۸ و ($mm^3.s^{-1}$) ۵۹/۴۷۵ محاسبه گردید. مدل حاصل از آنالیز ابعادی نسبت به مدل حاصل از روش سطح پاسخ به مقادیر به‌دست آمده از آزمایش‌ها نزدیک‌تر بود، بنابراین به‌منظور پیش‌بینی دبی خروجی بذور، مدل به‌دست آمده از روش آنالیز ابعادی پیشنهاد شد.

واژه‌های کلیدی: آنالیز ابعادی، ذرت، ردیف‌کار، روش سطح پاسخ

۱- دانشجوی کارشناسی ارشد، بخش مهندسی مکانیک بیوسیستم، دانشکده کشاورزی، دانشگاه شیراز، شیراز، ایران
۲- دانشیار، بخش مهندسی مکانیک بیوسیستم، دانشکده کشاورزی، دانشگاه شیراز، شیراز، ایران
۳- استادیار، گروه صنایع غذایی، دانشکده مهندسی مواد غذایی، دانشگاه کمپیناس، کمپیناس، برزیل
۴- استاد، بخش مهندسی مکانیک بیوسیستم، دانشکده کشاورزی، دانشگاه شیراز، شیراز، ایران
۵- دانشجوی دکتری، بخش مهندسی مکانیک بیوسیستم، دانشکده کشاورزی، دانشگاه شیراز، شیراز، ایران
(*- نویسنده مسئول: Email: Karparvr@shirazu.ac.ir)

DOI: 10.22067/jam.v11i1.79992

Journal of Agricultural Machinery
Vol. 11, No. 1, Spring- Summer 2021, p. 29-42

نشریه ماشین‌های کشاورزی
جلد ۱۱، شماره ۱، نیمسال اول ۱۴۰۰، ص ۴۲-۲۹

Full Research Paper

Evaluating Histogram Equalization and Thresholding Methods for Segmentation of *Rosa Damascena* Flowers in Color Images

A. Kohan[1*], S. Minaei[2]

Received: 07-08-2019
Accepted: 31-08-2020

Abstract

Several histogram equalization methods for enhancing the color images of *Rosa Damascena* flowers and some thresholding methods for segmentation of the flowers were examined. Images were taken outdoors at different times of day and light conditions. A factorial experiment in the form of a Completely Randomized Design with two factors of histogram equalization method at 8 levels and thresholding method at 15 levels, was implemented. Histogram equalization methods included: CHE, BBHE, BHEPL-D, DQHEPL, DSIHE, RMSHE, RSIHE, and no histogram equalization (NHE) as the control. Thresholding method levels were: Huang, Intermodes, Isodata, Li, maximum entropy, mean, minimum, moments, Otsu, percentile, Renyi's entropy, Shanbhag, Yen, constant, and global basic thresholding method. The effect of these factors on the properties of the segmented images such as the Percentage of Incorrectly Segmented Area (*PISA*), Percentage of Overlapping Area (*POA*), Percentage of Undetected Area (*PUA*), and Percentage of Detected Flowers (*PDF*) was investigated. Results of histogram equalization analysis showed that DQHEPL and NHE have the statistically significant lowest *PUA* (11.13% and 8.32%, respectively), highest *POA* (89.35% and 92.07%, respectively), and highest *PDF* (61.88% and 64.94%, respectively). Thresholding methods had a significant effect on *PISA*, *PUA*, *POA*, and *PDF*. The highest *PDF* belonged to constant, minimum, and Intermodes (75.07%, 73.08% and 74.30%, respectively) They also had the lowest *PISA* (0.35%, 1.29%, and 1.85%, respectively) and *PUA* (33.72%, 23.09%, and 15.56%, respectively). These methods had the highest *POA* (80.73%, 76.70%, and 84.67%, respectively). Hence, they are suitable methods for segmentation of *Rosa Damascena* flowers in color images.

Keywords: Histogram equalization, Image processing, Image segmentation, *Rosa Damascena*, Thresholding

Introduction

Rosa Damascena is a small plant with aromatic, light pink flowers, from *Rosaceae* family, which appears in spring and is highly cultivated all over the world, including Iran, for medicinal purposes and producing fragrances (Hajhashemi *et al.*, 2010).

Detection of the flowers in the canopy could be applied for yield estimation. It is important for farmers to estimate the quantity of a flower on the bushes at different stages of their growth so that they can make proper arrangement for harvesting labor and its distribution to specific locations in their fields. Early yield estimation can also be used to provide feedback on how crops respond to certain soil and crop management practices and to determine recommendation rates for many crop production inputs (Li *et al.*, 2014). In addition, to harvest the flowers robotically, it is imperative to detect them in the canopy (Kohan *et al.*, 2011). Accordingly, different image processing methods have been developed to detect favorite objects in agriculture, which some of them are mentioned below.

Ramos *et al.* (2017) reported a non-destructive method for counting the number of fruits on a coffee branch using image processing methods. To detect the coffee fruits, homogeneous regions were segmented base on a Canny edge detector with a dynamic

1- Assistant Professor, Department of Biosystems Engineering, College of Agriculture, Shoushtar Branch, Islamic Azad University, Shoushtar, Iran
2- Professor, Department of Biosystems Engineering, College of Agriculture, Tarbiat Modares University, Tehran, Iran
(*- Corresponding Author Email: kohan.armin@gmail.com)
DOI: 10.22067/jam.v11i1.82330

character. Then the generated outlines were analyzed to determine whether they belonged to a coffee fruit arc or not. The points found in the previous step were adjusted into an ellipse which was evaluated for the possibility of belonging to coffee fruits. The final step consisted of placing the adjusted ellipse in the classified image for each vegetative structure, detecting a single fruit per ellipse, and counting the detected fruits according to their maturation stage.

A fast and accurate automatic segmenting method of sea cucumbers was presented by Qiao *et al.* (2017). Image fusion based on the RGB color space and the contrast limited adaptive histogram equalization method was used to increase the contrast of the sea cucumber thorns and body, respectively. An edge detection algorithm was then implemented to extract the edge of the sea cucumber thorns, as an initial contour for thorn segmentation. A rectangular contour based on the edge information was built, as the initial contour for the body segmentation. Finally, the results of the thorn and body were fused. Results showed that the mean values of Euclidean distance, sensitivity, specificity, and accuracy were 12.7, 84.51, 96.97, and 96.54, respectively. Jidong *et al.* (2016) developed a recognition method for apple fruits in a natural environment. After comparing different color spaces, I2color component in the I1I2I3color space with Otsu dynamic threshold segmentation method was chosen. Image perfection and noise removal were carried out and apple fruit contour model was established. The apple fruits were recognized by edge detection and the improved RHT transformation method, the overlapped apples and severely occluded apples by the branches and leaves were respectively separated and restored before they were recognized.

Li *et al.* (2014) reported a blueberry yield mapping system. A stepwise algorithm, termed 'color component analysis based detection' method was developed to identify blueberry fruit at different growth stages using outdoor color images. A dataset was built using manually cropped pixels from training images. Three color components, red, blue and hue, were selected using the forward feature selection algorithm and used to separate all fruits of different maturity stages from the background using different classifiers. The KNN classifier yielded the highest classification accuracy (85-98%), and the developed 'CCAD' method for blueberry was proved to be efficient.

Yamamoto *et al.* (2014) proposed an image-processing method to accurately detect individual intact tomato fruits, including mature, immature and young fruits on the plant using a conventional RGB digital camera in conjunction with machine learning approaches. In the first step, the pixel-based segmentation was conducted to roughly segment the pixels of the images into classes composed of fruits, leaves, stems, and backgrounds. The Blob-based segmentation was then conducted to eliminate misclassifications generated at the first step. At the third step, the *X*-means clustering was applied to detect individual fruits in a fruit cluster. The image segmentation was conducted based on classification models generated by machine learning approaches.

Mohamadi Monavar *et al.* (2013) considered three color spaces including RGB, HSI and YCbCr and three algorithms including threshold recognition, curvature of the image and red/green ratio in order to identify the ripe tomatoes from background under natural illumination. The average error of threshold recognition, red/green ratio and curvature of the image algorithms were 11.82%, 10.03% and 7.95% in HSI, RGB and YCbCr color spaces, respectively. Therefore, they proposed the YCbCr color space and curvature of the image algorithm as the most suitable method for recognizing fruits under natural illumination condition. Okamoto and Lee (2009) presented an image processing method to detect green citrus fruit in individual trees. The objective of the method was estimating the crop yield at the earlier stage of growth. A hyperspectral camera of 369-1042 nm was used. The algorithm was separated into two parts, i.e., pixel spectral

processing and spatial processing. First, spectral processing was applied to each pixel individually for pixel segmentation, and then spatial processing was applied for green citrus fruit detection. A computer vision based method for citrus yield estimation represented by Dorj *et al.* (2017). This citrus recognition and counting algorithm was utilized the color features to detect citrus fruit on the tree. The corresponding models were developed to provide an early estimation of the citrus yield. The citrus counting algorithm consisted of converting the RGB image to HSV, thresholding, orange color detection, noise removal, watershed segmentation, and counting. The mean of the absolute error of the algorithm was determined to be 5.76% for all input images, and the main reasons for obtaining errors was due to the nearly complete occlusion, noise, shadowing, sunlight reflection on the leaves, etc. A cherry-harvesting robot was manufactured by Tanigaki *et al.* (2008). The 3-D vision sensor was equipped with red and infrared laser diodes. Both laser beams scan the object simultaneously. By processing the images from the 3-D vision sensor, the locations of the fruits and obstacles were recognized. Kohan *et al.* (2011) designed and developed a robotic harvester for *Rosa Damascena*. Flowers, which had a different color from canopy, were detected by thresholding H component of HSI color space and stereoscopic machine vision technology was implemented for locating them.

Although histogram equalization is a popular method for image enhancement and theresholding is an accepted method for segmentation, there is no comprehensive research which compare different algorithms of these methods and underline the most efficient one for agricultural use under natural light condition. In this research, several histogram equalization methods for color image enhancement and some thresholding methods for image segmentation using color information was evaluated to recognize the most precise method for detecting *Rosa Damascena*.

Material and Methods

Figure 1 shows the schematic diagram of the process. Imaging was done outdoors, in various light condition, using an A4TECH webcam with resolution of 480×640. All images were in the YCbCr color space. Each image had 3 channels (i.e. Y, Cb, and Cr) and each channel was an 8-bit grey scale image, including 256 levels from 0 to 255. First, the images were transferred to RGB color space and to enhance the color images, the same method of histogram equalization was applied to each component of RGB images individually (Rong *et al*., 2015). The images were transferred to the HSI color space and segmentation was performed by thresholding the H component. The H component is not affected by the intensity and saturation. In addition, different color of pink flowers and the green background of foliage made thresholding the H component more efficient for segmentation.

To understand the accuracy of each method, some features of the segmented images were examined. These features included: Percentage of Incorrectly Segmented Area (*PISA*), Percentage of Undetected Area (*PUDA*), Percentage of Overlapping Area (*POA*) and Percentage of Detected Flowers (*PDF*). The incorrectly segmented area included the area of the regions that were wrongly segmented and did not represent flowers. The undetected area contained parts of a flower or flowers that were not segmented. The overlapping area included the area of segmented regions that overlapped with the flowers. To normalize and calculate the percentage of the mentioned quantities, each was divided by the total area of the flowers in the image. PDF is the number of the obviously detected flowers by the algorithm, divided by the number of all the flowers in the image. Equation (1) to (4) show how these quantities calculated.

$$PISA = \frac{SNF}{AF} \times 100 \quad (1)$$

$$PUDA = \frac{ANS}{AF} \times 100 \quad (2)$$

$$POA = \frac{SOF}{AF} \times 100 \quad (3)$$

$$PDF = \frac{NS}{NF} \times 100 \quad (4)$$

In which:
AF: area covered by flowers
SNF: area of segmented regions that do not belong to flowers
ANS: area of flowers that is not segmented
SOF: area of segmented regions which overlap with flowers in the image
NF: number of flowers in the image
NS: number of segmented flowers

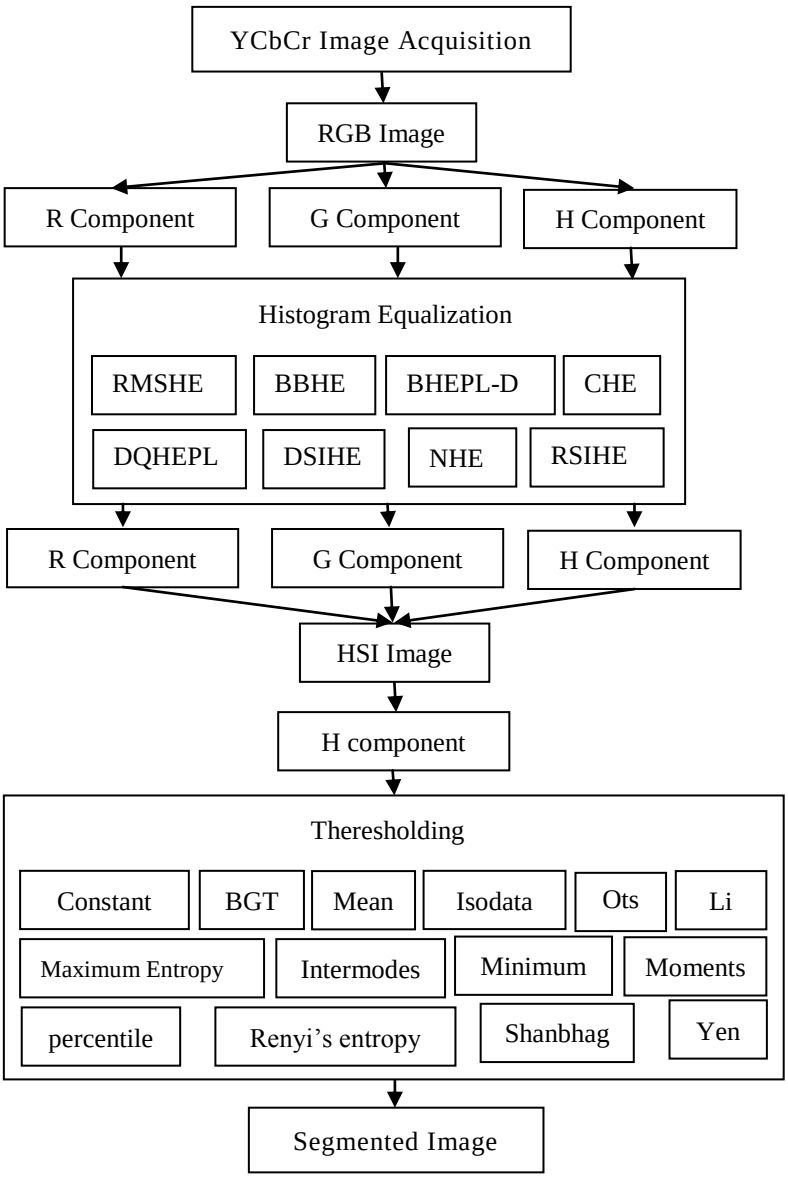

Fig.1. Schematic diagram of the process

Histogram equalization

Histogram equalization methods which examined for enhancing the components of the RGB color images included: Conventional Histogram Equalization (CHE), Brightness Preserving Bi-Histogram Equalization (BBHE), Dualistic Sub-Image Histogram Equalization (DSIHE), Recursive Sub-Image Histogram Equalization (RSIHE), Bi-Histogram Equalization Median Plateau Limit (BHEPL-D), and Dynamic Quadrants

Histogram Equalization Plateau Limit (DQHEPL).

The CHE method uses the Cumulative Distribution Function (CDF) as a transformation function, which maps the input intensity level to a new intensity level. The downside is that CHE shifts the mean intensity value, in the middle grey level of the intensity range (Farhan Khan *et al.*, 2015). To overcome this, other methods have been proposed. BBHE method divides the image histogram into two parts. In this method, the separation intensity is represented by the input mean brightness value, which is the average intensity of all the pixels that construct the input image. After this separation process, these two histograms are independently equalized. Thus the mean brightness of the resultant image will lie between the input mean and the middle grey level (Kim, 1997). DSIHE technique also decomposes the image into two equal-area sub-images based on its grey level probability density function. Then the two sub-images are equalized. The final result is obtained after the processed sub-images are composed into one image (Wang *et al*., 1999).

The extension of BBHE is RMSHE which recursively performs a separation of the input image histogram based on the mean value of the input histogram to the satisfactory number of recursion levels. Each new sub-histogram is separated based on the respective mean. As the number of recursion level increases, the mean brightness of the output image becomes closer to the input image mean brightness (Patel, 2013). Another method to preserve the brightness and natural appearance of the input images, by partitioning the histogram into more than two segments, is RSIHE (Sim and Tso, 2007) which is the extension of DSIHE method and decomposes the image into equal-area sub-images.

The Dynamic Histogram Equalization (DHE) method expands the sub-histograms to a new dynamic range by using a function depending on the number of pixels in the corresponding sub-histogram. This means that sub-histograms constituting a higher number of pixels occupy a larger range compared to other sub-histograms. However, DHE method under low light conditions suffers from intensity saturation problems and produces undesirable visual artifacts (Ibrahim and Kong, 2007). In order to avoid the intensity saturation problem, plateau-based methods have been suggested in the literature. These methods clip the peak of the histogram to some extent so that the intensity levels having high values can be prevented from expanding to a high range. By performing the clipping process, high probability regions of the histogram may be prevented from dominating over its low probability regions. Some of the plateau-based methods, are bi-histogram equalization plateau limit (BHEPL) (Ooi *et al.*, 2009), bi-histogram equalization median plateau limit (BHEPL-D) (Ooi, 2010 a), dynamic quadrants histogram equalization plateau limit (DQHEPL) (Ooi and Isa, 2010 a), and quadrants dynamic histogram equalization (QDHE) (Ooi and Isa, 2010 b).

The plateau-based methods that preserve the brightness and natural appearance of the images, are based on the assumption that the processed histograms having an intensity saturation problem are the main reason for the appearance of visual artifacts in the output images (Ooi and Isa, 2010 b).

Thresholding

Thresholding methods which were evaluated for image segmentation, included: basic global thresholding method, Huang, Intermodes, Isodata, Li, maximum entropy, mean, minimum, moments, Otsu, percentile, Renyi's entropy, Shanbhag, Yen, and constant thresholding.

In the Basic Global Thresholding (BGT) method first, the image is divided into object and background by taking an initial threshold, in the second step, the average values of the pixels at or below the threshold and pixels above it are computed. In the third step, the threshold is set to the average of the two values found in the last step. Finally, the second and third steps are repeated until the difference of threshold in successive iterations is smaller than a predefined level (Gonzalez and Woods, 1992). "Isodata" method is a

variation of the basic global thresholding except that the final step is repeated until the threshold is larger than the average brightness of the two regions (Ridler and Calvard, 1978).

Prewitt and Mendelsohn (1966) supposed that each object to be segmented creates a clear peak around the most frequent grey level value. The histogram is iteratively smoothed until only two peaks remain. In the "Intermodes" thresholding method, the midpoint of the two peaks is taken as the threshold while in the "minimum" thresholding method, the threshold is the minimum point between the peaks. The "Otsu" method searches for the threshold that minimizes intra-class variance (Otsu, 1979). Kapur *et al.* (1985) implemented the "maximum entropy" method which chooses a threshold such that the entropies of distributions above and below the threshold are maximized. This is one of the several entropy-based approaches. "Moments" method (Tsai, 1985) estimates the threshold in a way that the moments of the input image are preserved in an output image. Shanbhag (1994) considered the image as a compositum of two fuzzy sets corresponding to the two classes with membership coefficient associated with each grey level a function of its frequency of occurrence as well as its distance from the intermediate threshold selected.

"Huang's fuzzy thresholding" uses Shannon's entropy function (Huang and Wang, 1995). The measure of fuzziness represents the difference between the original image and its binary version. For a given threshold level, the fuzzy membership function for a pixel is defined by the absolute difference between the pixel grey level and the average grey level of the region to which it belongs, with a larger difference leading to a smaller membership value. The optimal threshold is the value that minimizes the fuzziness, as defined by Shannon's entropy function, applied to the fuzzy membership functions.

Yen *et al.* (1995) proposed a new criterion for multilevel thresholding. The criterion is based on the consideration of two factors. The first one is the discrepancy between the thresholded and original images and the second one is the number of bits required to represent the thresholded image. Based on a new maximum correlation criterion for bi-level thresholding, the discrepancy is defined and then a cost function that takes both factors into account is proposed for multilevel thresholding. By minimizing the cost function, the classification number that the grey-levels should be classified and the threshold values can be determined automatically. In addition, the cost function is proven to possess a unique minimum under very mild conditions.

Similar to the maximum entropy method, Sahoo *et al.* (1997) proposed a new thresholding technique using Renyi's entropy. Their entropic thresholding method uses two probability distributions (object and background) derived from the original grey-level distribution of an image and includes the maximum entropy sum method and the entropic correlation method. The Li thresholding technique was based on an iterative method for minimization of cross-entropy between segmented and original image (Li and Tam, 1998). The percentile method assumes the fraction of foreground pixels to be a specific value which is 0.5 in the current research (Doyle, 1962). The "mean" method uses the mean of grey levels as the threshold. For the constant thresholding method, the color levels of the flowers in several H-component of the images were investigated and the average of 204 was selected as the constant threshold.

Statistical Design

To investigate the effect of different methods of histogram equalization and thresholding, a factorial experiment in the form of a Completely Randomized Design was implemented. The factors involved in the experiment included thresholding method and histogram equalization method at 15 and 8 levels, respectively with 20 replications. As previously mentioned, thresholding method levels included: Huang, Intermodes, Isodata, Li, maximum entropy, mean, minimum, moments, Otsu, percentile, Renyi's entropy, Shanbhag, Yen, Basic Global Thresholding

(BGT), and thresholding with a constant value. The histogram equalization levels were CHE, BBHE, BHEPL-D, DQHEPL, DSIHE, RMSHE, RSIHE and No Histogram Equalization (NHE) as the control. The factorial experiment was performed on ten images that were selected arbitrarily. The images applied to determine the value of the constant threshold were not used in the factorial experiment.

Results and Discussion

As described in the previous sections, after taking image, the histogram of each component of the RGB image was processed individualy. Afterward the components joined together to form a color image with a higher quality. Figures 2, 3 and 4 show the histogram equalization results using different methods under different light conditions.

After applying histogram equalization to each component and corporating them again, the color space of the image transformed to HSI. Figure 5 shows the result of This transformation and extracting the H component. Figure 5a is the original image, which, as can be seen, does not have a good quality because of poor lighting situation. Figure 5b is the same image, which quality is improved by the CHE method. In this image, flowers are easily visible.

Fig.2. Contrast equalization using different methods on an 8-bit image with the mean intensity of 89.68 and Standard Deviation of 68.60; a) NHE, b) BBHE, c) BHEPL-D, d) CHE, e) DQHEPL, f) DSIHE, g) RMSHE and h) RSIHE

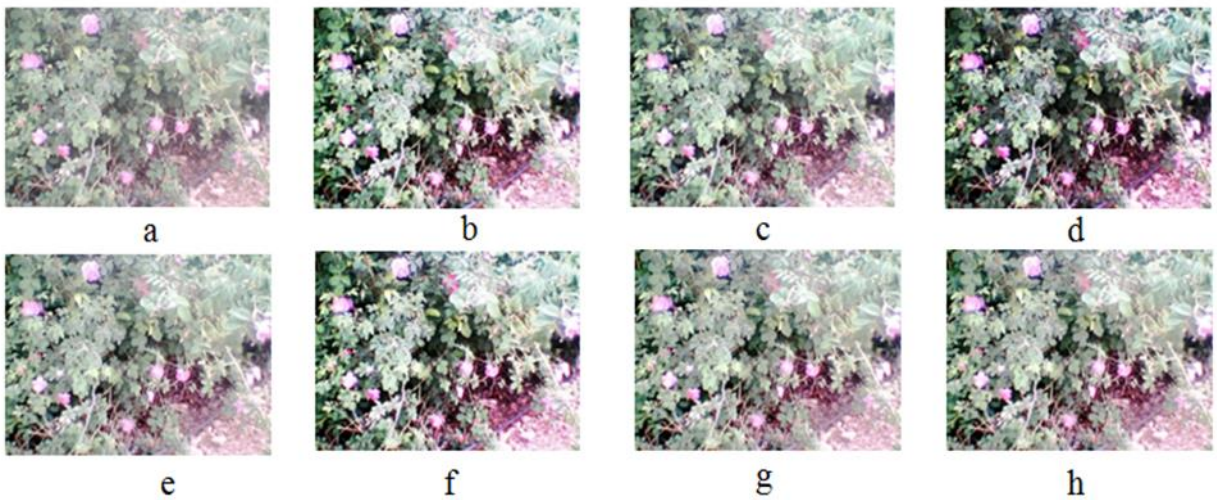

Fig.3. Contrast equalization using different methods on an 8-bit image with the mean intensity of 176.2 and Standard Deviation of 40.99; a) NHE, b) BBHE, c) BHEPL-D; d) CHE; e) DQHEPL, f) DSIHE, g) RMSHE and h) RSIHE

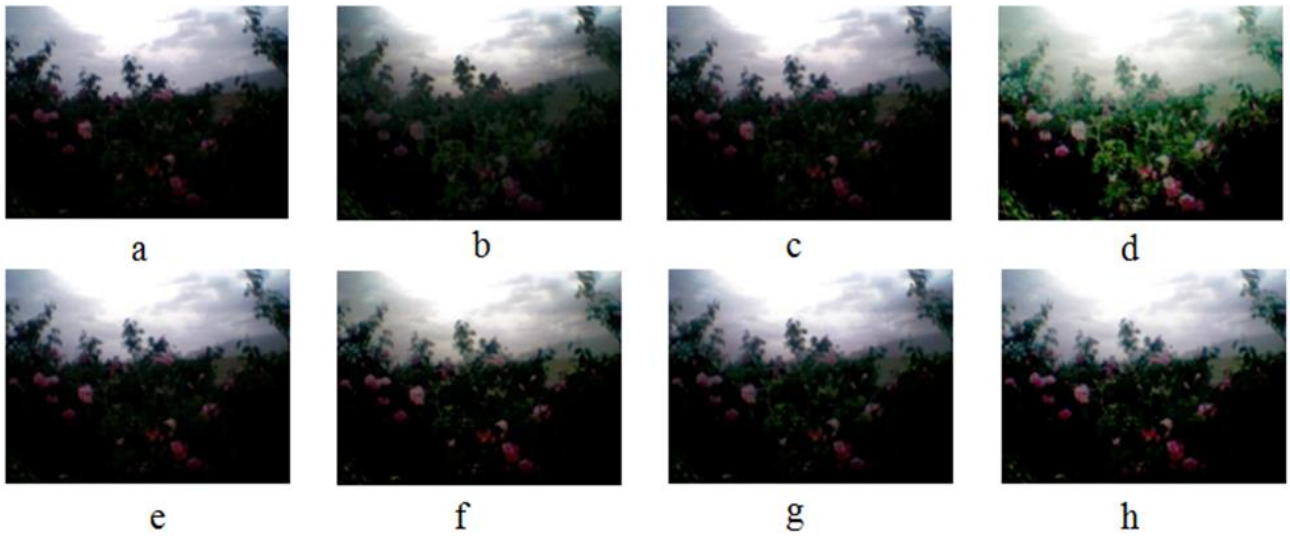

Fig.4. Contrast equalization using different methods on an 8-bit image with the mean intensity of 61.42 and Standard Deviation of 82.71; a) NHE, b) BBHE, c) BHEPL-D, d) CHE, e) DQHEPL, f) DSIHE, g) RMSHE and h) RSIHE

Figure 5c is the H component of Figure 5a which is obtained after transforming this image from RGB to HSI color space. As seen, saturation and intensity do not affect the H component, and the position of the flowers is clearly evident because the H component only contains color information.

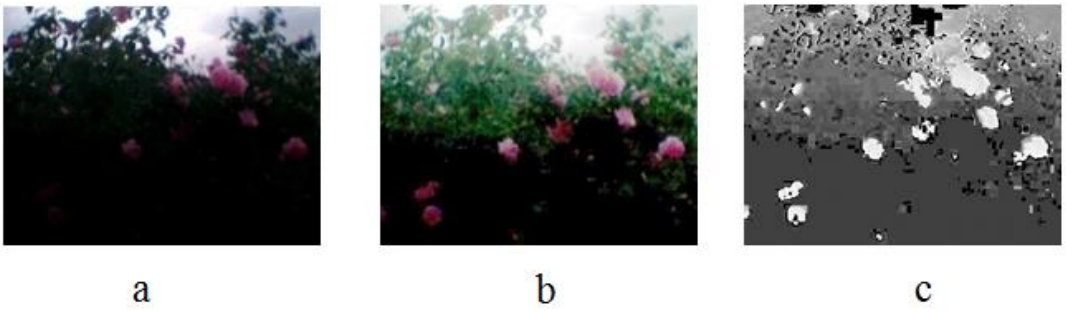

Fig. 5. a) RGB image with poor light condition, b) Image **a** after histogram equalization using CHE method and c) H component of image **a** after conversion from RGB to HSI color space

The final step was theresholding. Figure 6 shows the results of thresholding using different methods. No histogram equalization has been applied to this image.

Figure 7 illustrates the properties of the segmented image visually. Figure 7a, is the reference image and the regions of the flowers are manually specified. Figure 7b shows the result of the segmentation by the software. Figure 7c shows incorrectly segmented areas that do not belong to the flowers, Figure 7d shows undetected areas and Figure 7e shows the areas that are both segmented by the software and belong to the flowers

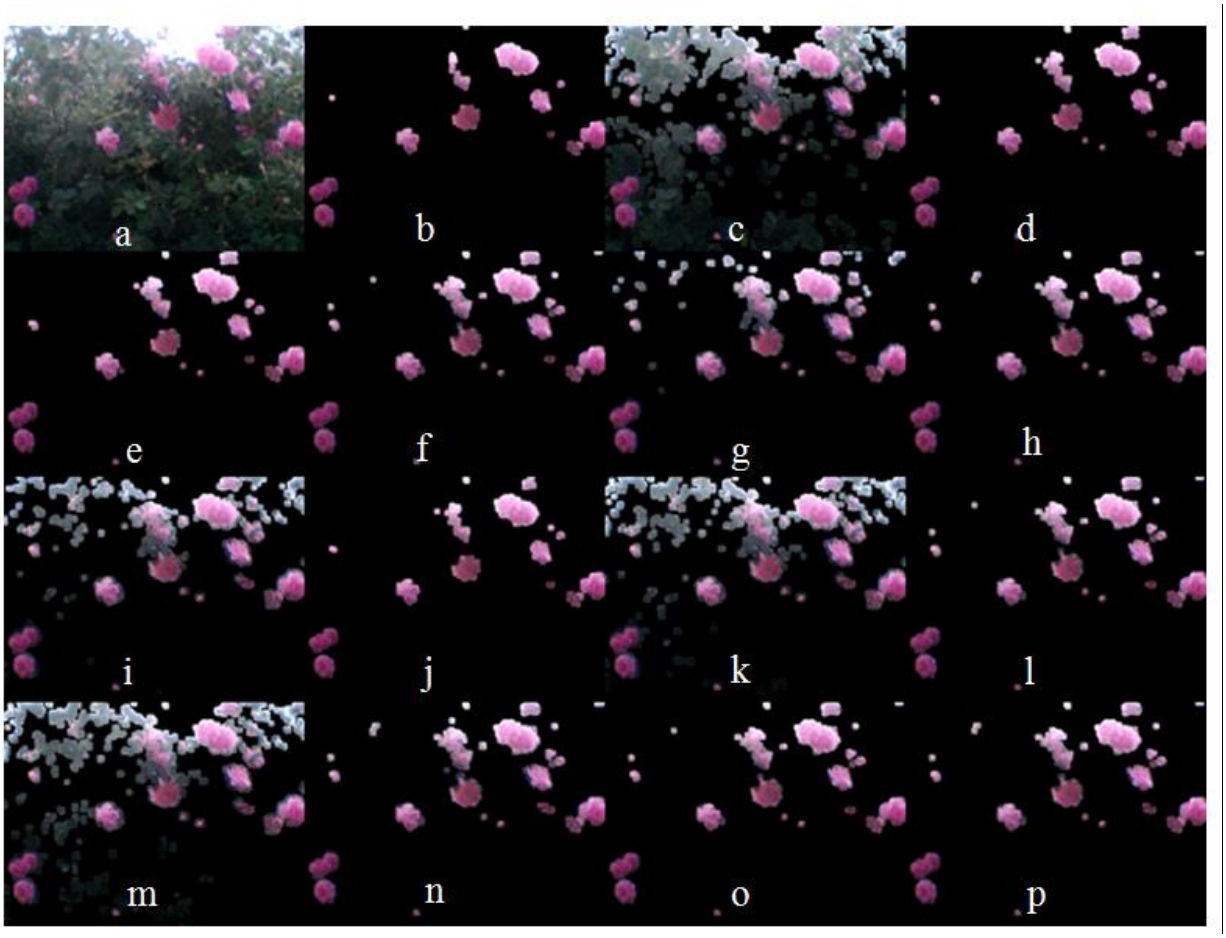

Fig.6. The result of thresholding using different methods: a) Original image with no histogram equalization, b) Constant, c) BGT, d) Huang, e) Intermodes, f) Isodata, g) Li, h) Maximum entropy, i) Mean, j) Minimum, k) Moments, l) Otsu, m) Percentile, n) Renyi's entropy, o) Shanbhag and p) Yen

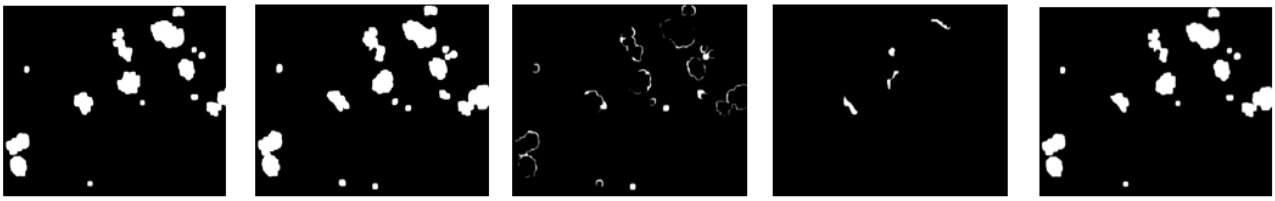

Fig.7. Properties of the segmented image in comparison with the reference image: a) Reference Image, b) Segmented image, c) Incorrectly segmented area, d) Undetected area and e) Overlapping area

Statistical methods applied to determine the best method of histogram equalization and theresholding. Table 1 shows the results of ANOVA for the effect of thresholding method and contrast equalization method on different properties. In cases where analysis of variance showed a significant difference, Duncan's Multiple Range Test at the 5% level was used. The results are shown in Table 2 and Table 3.

Table 1- ANOVA results for the effect of thresholding method and contrast equalization method on different properties

Source	PISA		PUA		POA		PDF	
	F	Sig.	F	Sig.	F	Sig.	F	Sig.
CE	0.838^{ns}	0.555	18.622*	0.000	17.947*	0.000	25.170*	0.000
T	13.317*	0.000	15.281*	0.000	6.427*	0.000	27.871*	0.000
CE*T	0.127^{ns}	1.000	0.086^{ns}	1.000	0.069^{ns}	1.000	0.510^{ns}	1.000

ns: No significant difference, * Significantly different at the 99% confidence interval

According to Table 1, the histogram equalization methods did not have a significant effect on the *PISA*. As shown in Table 2, NHE and DQHEPL had the lowest *PUA*. This is while NHE, DQHEPL, and BHEPL-D showed the highest *POA*. NHE, BHEPL-D, RSIHE, DQHEPL, and RMSHE showed the highest *PDF*. Therefore, NHE and DQHEPL, which had the lowest *PUA*, the highest *POA*, and the highest *PDF*, are appropriate methods for equalizing the histogram.

According to Table 3, the constant and minimum thresholding methods had the lowest *PISA*, but constant thresholding yielded the most *PUA*. The *PUA* of the minimum thresholding method was lower than constant thresholding one level, so it also had a relatively high value. The Li method had the least *PUA* and did not have a significant difference with Huang, Intermodes, Isodata, maximum entropy, mean, moments, Otsu, percentile, Renyi's entropy, Yen, and BGT.

Table 2- Comparison of the means for the effects of histogram equalization method on the studied factors

Method	PUA	POA	PDF
BBHE	20.99c	79.67a	50.58b
BHEPL_D	11.84b	88.84bc	64.87d
CHE	20.56c	80.29a	41.48a
DQHEPL	11.13ab	89.35bc	61.88d
DSIHE	20.34c	80.23a	55.79c
NHE	8.32a*	92.07c	64.94d
RMSHE	12.73b	88.02b	61.58d
RSIHE	12.43b	88.27b	64.12d

*Same lowercase letters show no significant difference between factors in each column at the 5% level using Duncan's Multiple Range Test.

Table 3- Comparison of the Means for the effects of Thresholding Method on the studied factors

Method	PISA	PUA	POA	PDF
BGT	4.31efg	11.52ab	88.47de	53.21d
Constant	0.35a	33.72e	80.73ab	75.07e
Huang	3.63def	14.63abc	85.14bcde	62.94efg
Intermodes	1.85bc	15.56bc	84.67bcd	74.30he
Isodata	4.11efg	11.71ab	88.32de	57.00de
Li	5.89h	9.77a	90.22e	43.51ab
Maximum entropy	2.54bcd	13.17abc	88.33de	65.50g
Mean	5.18gh	10.78ab	89.21de	42.01ab
Minimum	1.29ab	23.09d	76.70a	73.08he
Moments	4.45fg	11.38ab	80.44ab	46.25bc
Otsu	3.96efg	11.80ab	88.23de	57.98def
Percentile	5.87h	10.74ab	89.25de	38.33a
Renyi's entropy	2.46bcd	12.97abc	88.89de	63.93fg
Shanbhag	2.98cde	17.66c	82.37bc	51.59cd
Yen	2.24bc	13.36abc	86.69cde	67.64gh

Same lowercase letters show no significant difference between factors in each column at the 5% level using Duncan's Multiple Range Test.

Observing the *POA* column in Table 3, it is obvious that the Li method had the highest value of *POA* and did not have a significant difference with mean, percentile, Renyi's entropy, Isodata, maximum entropy, Yen, Otsu, Huang and BGT method. But these methods yielded a very high *PISA*, which has caused many regions other than flowers to be segmented incorrectly and the position of the flowers could not be detected well enough. The highest *PDF* was achieved by the constant thresholding method and did not show a significant difference with Intermodes and minimum methods. Although *PUA* is high, and *POA* is low in recently mentioned methods, it should be considered that properly segmented regions are higher and the position of the flowers is well defined. Therefore, the best methods for thresholding are constant, Intermodes and minimum.

It can be seen in Table 4 that the highest detection success rate was 85.66 belonging to constant thresholding method and original images without histogram equalization.

Table 4- Average of PDFs in different methods

Thresholding method	Histogram equalization method							
	BBHE	**BHEPL-D**	**CHE**	**DQHEPL**	**DSIHE**	**NHE**	**RMSHE**	**RSIHE**
Constant	69.24	81.19	63.70	80.52	72.06	85.66	73.67	74.53
BGT	40.28	63.08	39.40	63.85	50.97	52.28	59.79	56.02
Huang	58.05	64.98	42.38	61.13	57.51	76.03	70.57	72.88
Intermode	72.23	78.57	48.57	83.00	69.99	87.31	77.20	77.56
IsoData	50.31	61.57	38.67	63.57	51.33	60.49	62.07	68.01
Li	32.56	50.39	24.34	51.98	43.69	52.66	42.32	50.15
MaxEntropy	52.79	76.71	46.74	71.71	61.87	66.60	72.60	74.99
Mean	36.06	47.15	33.66	39.84	40.22	50.64	43.30	45.17
Minimum	73.50	81.58	51.32	71.73	76.80	80.32	71.66	77.76
Moments	43.72	53.51	34.75	56.39	39.45	48.32	45.93	47.91
Otsu	46.08	64.75	39.58	63.54	54.50	69.37	62.65	63.41
Percentile	37.19	40.82	29.40	36.45	38.80	45.68	37.47	40.80
RenyiEntropy	43.56	75.83	43.35	69.84	62.38	68.95	73.05	74.46
Shanbhag	41.36	61.42	35.81	48.01	50.10	58.44	53.07	64.48
Yen	61.79	71.57	50.50	66.67	67.21	71.31	78.37	73.69

Kohan *et al.* (2011) reported a 98% success rate. The higher detection rate was because of the optimum light condition and imaging conditions there, and the complementary image processing which had been performed.

Ramos *et al*. (2017) reported 80.99% average visibility percentage for counted fruits in images of coffee branches. The method developed by Jidong *et al.* (2016) for recognizing apple fruits in the natural environment resulted in detection percentages of 100%, 100%, and 86%, respectively, for nonoccluded fruit, overlapping fruit and fruit occluded by branches and leaves. The image-processing method proposed by Yamamoto *et al.* (2014) detected 80% of all tomato fruits in the test images. The detection success rate of the image processing method presented by Okamoto and Lee (2009) for detecting green citrus fruit was 70-85%, depending on citrus varieties. The fruit detection tests revealed that 80-89% of the fruits in the foreground of the validation set were identified correctly, though many occluded or highly contrasted fruits were identified incorrectly. The percentage of cherry fruit visibility with the 3-D vision sensor reported by Tanigaki *et al.* (2008) was 59%. Different detection rates, of the mentioned investigations, were due to the use of different image processing methods on crops.

Conclusions

Several methods of histograms equalization for increasing the quality of color images and some thresholding methods for segmentation of *Rosa Damascena* flowers were evaluated. After examining various histogram processing methods, it was found that the statically significant lowest percentage of undetected

area (*PUA*=11.13%) and the highest percentage of overlapping area (*POA*=89.35%) as well as the highest percentage of detected flowers (*PDF*=61.88%) belonged to the DQHEPL method, and did not show a significant difference with images without histogram equalization or NHE (PUA=8.32%, POA=92.07%, PDF=64.94%). The constant thresholding method shows the highest number of correctly segmented which was 75.07% and did not have a significant difference with minimum (PDF=73.08%) and Intermode methods (PDF=74.30%). Therefore, these methods are suitable for segmentation of the images. But due to the fact that one of the most important issues, with machine vision is reduction of computation time, in order to increase the processing speed, it is recommended that histogram equalization should not be performed and the constant thresholding of the H component of HSI color space be used for segmentation of *Rosa Damascena* flowers.

References

1. Bachche S. 2015. Deliberation on Design Strategies of Automatic Harvesting Systems: A Survey. Robotics 4: 194-222.
2. Dorj U. O., M. Lee, and S. S. Yun 2017. A Yield Estimation in Citrus Orchards via Fruit Detection and Counting Using Image Processing. Computers and Electronics in Agriculture 140: 103-112.
3. Doyle, W. 1962. Operation Useful for Similarity-Invariant Pattern Recognition. Journal of the Association for Computing Machinery 9: 259-267.
4. Farhan Khan, M., E. Khan, and Z. A. Abbasi. 2015. Image Contrast Enhancement Using Normalized Histogram Equalization. Optik-International Journal for Light and Electron Optics 126: 4868 4875.
5. Gonzalez, R. C., and R. E. Woods. 1992. Digital Image Processing. Pearson Prentice Hall. Delhi.
6. Hajhashemi, V., A. Ghannadi, and M. Hajiloo. 2010. Analgesic and Anti-inflammatory Effects of Rosa damascenaHydroalcoholic Extract and its Essential Oil in Animal Models. Iranian Journal of Pharmaceutical Research 9 (2): 163-168.
7. Huang, L. K., and M. J. J. Wang. 1995. Image Thresholding by Minimizing the Measures of Fuzziness. Pattern Recognition 28 (1): 41-51.
8. Ibrahim, H., and N. S. P. Kong. 2007. Brightness Preserving Dynamic Histogram Equalization for Image Contrast Enhancement. IEEE Transactions on Consumer Electronics 53: 1752-1758.
9. Jahanbakhshi, A., and K. Kheiralipour. 2018. Carrot Sorting Based on Shape using Image Processing, Artificial Neural Network, and Support Vector Machine. Journal of Agricultural Machinery 9 (2): 295-307.
10. Jidong, L., L. De-An, J. Wei, and D. Shihong. 2016. Recognition of Apple Fruit in Natural Environment. Optik-International Journal for Light and Electron Optics 127: 1354-1362.
11. Kapur N., P. K. Sahoo, and A. K. C. Wong. 1985. A New Method for Gray-Level Picture Thresholding Using the Entropy of the Histogram. Computer Vision, Graphics, and Image Processing 29 (3): 273-285.
12. Kim, Y. T. 1997. Contrast Enhancement Using Brightness Preserving Bi-Histogram Equalization. IEEE Transactions on Consumer Electronics 43 (1): 1-8.
13. Kohan, A., A. M. Borghaee, M. Yazdi, S. Minaei, and M. J. Sheykhdavudi. 2011. Robotic Harvesting of *Rosa Damascena* Using Stereoscopic Machine Vision. World Applied Sciences Journal 12 (2): 231-237.
14. Li C. H., and P. K. S. Tam. 1998. An Iterative Algorithm for Minimum Cross Entropy Thresholding. Pattern Recognition Letters 19: 771-776.

15. Li H., W. S. Lee, and K. Wang. 2014. Identifying Blueberry Fruit of Different Growth Stages Using Natural Outdoor Color Images. Computers and Electronics in Agriculture 106: 91-101.
16. Mohamadi Monavar, H., R. Alimardani, and M. Omid. 2013. Computer Vision Utilization for Detection of Green House Tomato under Natural Illumination. Journal of Agricultural Machinery 3 (1): 9-15. (In Farsi).
17. Okamoto, H., and W. S. Lee. 2009. Green Citrus Detection Using Hyperspectral Imaging. Computers and Electronics in Agriculture 66: 201-208.
18. Ooi, C. H., N. S. P. Kong, and H. Ibrahim. 2009. Bi-Histogram Equalization with a Plateau limit for Digital Image Enhancement. IEEE Transactions on Consumer Electronics 55: 2072-2080.
19. Ooi, C. H., and N. A. M. Isa. 2010a. Adaptive Contrast Enhancement Methods with Brightness Preserving. IEEE Transactions on Consumer Electronics 56: 2543-2551.
20. Ooi, C. H., and N. A. M. Isa. 2010b. Quadrants Dynamic Histogram Equalization for Contrast Enhancement. IEEE Transactions on Consumer Electronics 56: 2552-2559.
21. Otsu, N. 1979. A Threshold Selection Method from Gray Level Histograms. IEEE Transaction on Systems, Man and Cybernetics 9 (1): 62-66.
22. Patel, O., P. S. Yogendra, M. Sharma, and S. Sharma. 2013. A Comparative Study of Histogram Equalization Based Image Enhancement Techniques for Brightness Preservation and Contrast Enhancement. Signal & Image Processing: An International Journal 4 (5): 11-25.
23. Prewitt, J. M. S., and M. L. Mendelsohn. 1966. The Analysis of Cell Images. Annals of the New York Academy of Sciences 128: 1035-1053.
24. Qiao, X., J. Bao, L. Zeng, J. Zou, and D. Li. 2017. An Automatic Active Contour Method for Sea Cucumber Segmentation in Natural Underwater Environments. Computers and Electronics in Agriculture 135: 134-142.
25. Ramos, P. J., F. A. Prieto, E. C. Montoya, and C. E. Oliveros. 2017. Automatic Fruit Count on Coffee Branches Using Computer Vision. Computers and Electronics in Agriculture 137: 9-22.
26. Ridler, T. W., and S. Calvard. 1978. Picture Thresholding Using an Iterative Selection Method. IEEE Transactions on Systems, Man and Cybernetics 8 (8): 630-632.
27. Rong, Z., Z. Li, and L. I. Dong-nan. 2015. Studyof Color Heritage Image Enhancement Algorithms Based on Histogram Equalization. Optik- International Journal for Light and Electron Optics 126 (24): 5665-5667.
28. Sahoo, P., C. Wilkins, and J. Yeager. 1997. Threshold Selection Using Renyi's Entropy. Pattern Recognition 30 (1): 71-84.
29. Shanbhag, A. G. 1994. Utilization of Information Measure as a Means of Image Thresholding. CVGIP: Graphical Models and Image Processing 56 (5): 414-419.
30. Sim, K. S., C. P. Tso, and Y. Y. Tan. 2007. Recursive Sub-Image Histogram Equalization Applied to Gray Scale Images. Pattern Recognition Letters 28: 1209-1221.
31. Tanigaki, K., T. Fujiura, A. Akase, and J. Imagawa. 2008. Cherry-Harvesting Robot. Computers and Electronics in Agriculture 63: 65-72.
32. Tsai, W. 1985. Moment-Preserving Thresholding: a New Approach. Computer Vision, Graphics, and Image Processing 29: 377-393.
33. Wang, Y., Q. Chen, and B. Zhang. 1999. Image Enhancement Based On Equal Area Dualistic Sub Image Histogram Equalization Method. IEEE Transactions on Consumer Electronics 45 (1): 68-75.
34. Yamamoto, K., W. Guo, Y. Yoshioka, and S. Ninomiya. 2014. On Plant Detection of Intact Tomato Fruits Using Image Analysis and Machine Learning Methods. Sensors 14: 12191-12206.
35. Yen, J. C., F. J. Chang, and S. Chang. 1995. A New Criterion for Automatic Multilevel Thresholding. IEEE Transaction on Image Processing 4 (3): 370-378.

نشریه ماشین‌های کشاورزی
جلد ۱۱، شماره ۱، نیمسال اول ۱۴۰۰، ص ۴۲-۲۹

Journal of Agricultural Machinery
Vol. 11, No. 1, Spring- Summer 2021, p. 29-42

مقاله علمی-پژوهشی

بررسی روش‌های متعادل‌سازی هیستوگرام و آستانه‌گیری برای بخش‌بندی گل محمدی در تصاویر رنگی

آرمین کهن[1*]، سعید مینایی[2]

تاریخ دریافت: ۱۳۹۸/۰۵/۱۶
تاریخ پذیرش: ۱۳۹۹/۰۶/۱۰

چکیده

به‌منظور افزایش دقت بخش‌بندی تصاویر گل محمدی، چند روش متعادل‌سازی هیستوگرام برای بهبود کیفیت تصاویر رنگی این گل‌ها و چند روش آستانه‌گیری برای بخش‌بندی گل‌های مذکور در تصویر، مورد بررسی قرار گرفت. قابل ذکر است که تصویربرداری در فضای باز و ساعات مختلف روز و شرایط متفاوتی از شدت نور انجام گرفت. برای بررسی دقیق‌تر، یک آزمایش فاکتوریل در قالب یک طرح کاملاً تصادفی با دو عامل روش متعادل‌سازی هیستوگرام، در ۸ سطح و روش آستانه‌گیری، در ۱۵ سطح به‌کار گرفته شد. روش‌های متعادل‌سازی هیستوگرام عبارت بودند از: CHE, BBHE, BHEPL-D, DQHEPL, DSIHE, RMSHE, RSIHE و تیمار شاهد بدون متعادل‌سازی هیستوگرام (NHE). همچنین روش‌های آستانه‌گیری عبارت بودند از: Huang, Intermodes, Isodata, Li, maximum entropy, mean, minimum, moments, Otsu, percentile, Renyi's entropy, Shanbhag, Yen, constant و global basic thresholding method. تاثیر این دو عامل بر خصوصیات تصویر بخش‌بندی شده از قبیل: درصد سطوحی که به اشتباه بخش‌بندی شده‌اند (PISA)، درصد هم‌پوشانی سطوح (POA)، درصد سطوحی که تشخیص داده نشده‌اند (PUA) و درصد سطوح تشخیص داده شده گل‌ها (PDF) مورد بررسی قرار گرفت. نتیجه روش‌های متعادل‌سازی هیستوگرام نشان داد که DQHEPL و NHE پایین‌ترین میزان PUA (به‌ترتیب ۱۱/۱۳٪ و ۸/۳۲٪)، بالاترین POA (به‌ترتیب ۸۹/۳۵٪ و ۹۲/۰۷٪) و بالاترین PDF (به‌ترتیب ۶۱/۸۸٪ و ۶۴/۹۴٪) را از لحاظ آماری دارا می‌باشند. روش‌های آستانه‌گیری تاثیر معنی‌داری بر PISA, PUA, POA و PDF داشتند. بزرگ‌ترین مقادیر PDF به روش آستانه‌گیری constant، minimum و Intremodes (به‌ترتیب ۷۵/۰۷٪، ۷۳/۰۸٪ و ۷۴/۳۰٪)، همچنین کمترین مقدار PISA مربوط به این موارد بود (به‌ترتیب ۰/۳۵٪، ۱/۲۹٪ و ۰/۳۵٪) و PUA (به‌ترتیب ۳۳/۷۲٪، ۲۳/۰۹٪ و ۱۵/۵۶٪). این روش‌ها بزرگ‌ترین مقدار POA را نشان دادند (به‌ترتیب ۸۰/۷۳٪، ۷۶/۷۰٪ و ۸۴/۶۷٪). لذا روش‌های مناسبی برای بخش‌بندی گل محمدی در تصویر رنگی محسوب می‌گردند.

واژه‌های کلیدی: آستانه‌گیری، بخش‌بندی تصویر، پردازش تصویر، تعدیل هیستوگرام، گل محمدی

۱- استادیار، گروه مهندسی بیوسیستم، دانشکده کشاورزی، واحد شوشتر، دانشگاه آزاد اسلامی، شوشتر، ایران
۲- استاد، گروه مهندسی بیوسیستم، دانشکده کشاورزی، دانشگاه تربیت مدرس، تهران، ایران
(*- نویسنده مسئول: Email: kohan.armin@gmail.com)

DOI: 10.22067/jam.v11i1.82330

Journal of Agricultural Machinery
Vol. 11, No. 1, Spring- Summer 2021, p. 43-53

نشریه ماشین‌های کشاورزی
جلد ۱۱، شماره ۱، نیمسال اول ۱۴۰۰، ص ۵۳-۴۳

Full Research Paper

Effect of Fragmentation of Land on Agricultural Mechanization Development using AHP Technique

M. Sabati Gavgani[1], D. Mohammad Zamani[2*], M. Gholami Par-Shokohi[2]

Received: 09-11-2019
Accepted: 20-07-2020

Abstract

The agricultural sector is in need of a rapid transition from traditional and livelihoods to the stage of advanced production and commercialization, in order to provide food security for the community and to play an effective role in strengthening national independence. Mechanization is an approach that allows the agricultural sector to achieve the stage of commercial production. Without mechanization, there is no clear vision of a dynamic and sustainable agriculture that can rectify the food needs sensibly. The development of mechanization in agricultural societies, especially in the rural areas, has been accompanied by problems that the identification of the factors affecting it can help plan to eliminate them. Therefore, in the present study, the effect of the fragmentation of land on the development of agricultural mechanization in the rural districts has been investigated. The research type is applied and descriptive-analytic, survey method has been used and information has been collected through a questionnaire from 420 users in Jiroft city. The data were analyzed using a hierarchical analytical process technique using Expert Choice11 software. The research findings show that the family-social factor in the city of Jiroft was the main deterrent to the lack of development of mechanization and the cultural-communication, educational-technical, lawful-legal, and economic-financial factors were placed in the next priorities. It is proposed to implement the development of mechanization, the modernization of modern technology, education and promotion, building trust, credit and financial facilities for the modernization of agricultural implements.

Keywords: Analytical hierarchy process, Development of agricultural mechanization, Fragmentation of land

Introduction

Land scattering is one of the consequences of the traditional agricultural structure of country (TurkiBoldaji and Ghanbari, 2013). Such an arrangement in the land system is not exclusively for Iran and also exists in most countries with more or less proportions (Rezvani Alvarand Rachel, 2011). Today, researchers, agricultural experts and policy makers, considering the changes that have taken place in the land utilization system, believe that the dispersal and widespread use of agricultural land is one of the main problems of agricultural mechanization development (Rezvani Alvarand Rachel, 2014). Lack of economic justification for the use of technology in the production stage, the low incentive to invest in this area, the low production efficiency and the low economic profit are among the problems caused by the small-peasant farming systems (Mahdavi and Kiani, 2017).

In spite of the extensive efforts taken during the five-year development plans of Iran from 1990 to 2005 with aim of reforming the structure of the agricultural exploitation systems and the establishment and institutionalization of all types of optimum, efficient and appropriate operating system in accordance with socio-economic conditions and agricultural capacities in different regions of the country, agricultural sector continues to face this challenge in its development direction (Bagheri, 2016).

Fragmentation of agricultural lands is one of the major obstacles to sustainable agriculture development and is an obstacle to

1- PhD, Student, Department of Biosystems Engineering, Islamic Azad University, Takestan Branch, Takestan, Iran
2- Department of Biosystems Engineering, Islamic Azad University, Takestan Branch, Takestan, Iran
(*- Corresponding Author Email: Dr.dmzamani@gmail.com)
DOI: 10.22067/jam.v11i1.82910

optimal and eligible use of land, water, manpower, inputs, mechanization, creation of new ideas, precision agriculture and other factors affecting agricultural production and faces the two long-standing problems of smallholder plots, as well as the fragmentation and scattering of land by each farmer which are mainly influenced by these factors: Family-social factors such as benefits of awareness, participation, bias, family disputes and cultural-communication factors such as communication centers, the interests of group work, communication with agricultural service centers, traditional beliefs and educational-technical factors such as access to technical instructions, the presence of specialists, the availability of machines, the holding of workshops and Juridical-legal acts such as dedication, the law of inheritance, the law of participation in partnership with the owner, the way of sharing the land between the partners and economic-financial factors such as price difference between lands, bad economic conditions, machinery and equipment costs, banking facilities and etc. These are nowadays considered as obstacles to the development of agricultural mechanization in the country. This leads to a reduction in productivity, increased costs, inefficient farm management and inefficient use of new technologies, reduced agricultural investment and intensified land use changes and the elimination of small land from the production cycle, inadequate access to finance, a decrease in revenue, rural migration, and hidden unemployment, inadequate use of agricultural mechanization, inadequate use of water resources, and waste of production resources leading to a decline in agricultural output as indicators of underdevelopment (Secretariat of the Fourth Program Headquarters, 2005).

Understanding these issues and developing appropriate programs to solve or mitigate them will have implications for the agricultural sector, optimizing the potential of the agricultural sector, increasing production, increasing farmer's income, stabilizing the rural population and agricultural development (NajibiKheirabadi and Maghsoudi, 2010).

In this study, an attempt is made to take an effective step towards the development of agriculture in Jiroft by identifying the prioritization of the factors affecting the lack of development of agricultural mechanization due to the fragmentation of land using the viewpoint of the exploiters of Jiroft city. For this purpose, Hierarchical Analysis Process (AHP) technique has been used. This technique provides appropriate ways to organize information and make judgments and use them in decision-making based on ability, emotion, logic, and subject matter, then the judgments are combined into results that are consistent with internal expectations. The above process to solve complex problems by hierarchical criteria helps us to draw conclusions by extracting judgments to advance priorities (Saati, 1998)

A study conducted in Greece to study land consolidation as one of the ways to develop agriculture in Macedonia. The results showed that soil dispersion is one of the main obstacles to Macedonian agricultural development and the establishment of rural cooperatives and technical funding of the government (Grygewski, 2005). A descriptive-analytical study conducted with a survey approach to evaluate the effects of land consolidation on rural agricultural development, showed that the implementation of the integrated land consolidation plan led to a reduction in the number of agricultural plots, reduced production costs and savings in consumption. It also follows the application of agricultural mechanization in farms, increasing production and improving farmers' incomes (Falsliman and Moradi, 2011). Study to identify and analyze the factors affecting the development of agricultural mechanization in the city of Borujen showed that 45% of farmers are engaged in agriculture on lands with an area of less than 5 hectares and the biggest problem of farmers in using agricultural mechanization is the price of tools. There is a codified policy and careful planning to accelerate the development process of mechanization and land distribution and subsistence farming (Turki Boldaji and Ghanbari, 2013). A study

based on the library's study method and the study of scientific documents, as well as extensive internet searches in databases to study the history of agricultural mechanization in Iran and its policies in development programs, showed the main challenge facing the development of agricultural mechanization in Iran. The lack of a codified program is large-scale and operational, and the need to develop codified policies in the field of agricultural mechanization has been emphasized (Rezvani Alvarand Rachel, 2014). Comprehensive review of theoretical literature and library resources on the effects of land consolidation on agricultural economics with an emphasis on agricultural development, showed that one of the obstacles to rural development and transition from one stage to another is the distribution of agricultural land. In general classification, its causes include socio-cultural, economic, physical and user factors. On the other hand, agricultural development itself requires two groups of physical production factors (land, seeds, etc.) and non-physical (management). Optimum production requires the presence of physical and non-physical factors of production together (Mohammadzadeh and Amin Fenck, 2015). A study in China examined the estimated effect of land fragmentation on the use of machinery and crop production. The results showed that the integration of agricultural land consumption increases agricultural machinery and increases crop production (Lai and Roe, 2015). To investigate the effect of land size relationship on agricultural mechanization indicators in Qazvin, Iran, the three factors of inheritance, population growth and literacy had a greater impact on the distribution of agricultural land in Qazvin (Hashemipour and Mohammad Zamani, 2016). Examination of the barriers to agricultural land consolidation, showing that farmers are less inclined to integrate and prefer to engage with familiar individuals and families under the condition of temporary consolidation (Mahdavi and Kiani, 2017). In Finland a study on the effects of agriculture and the profitability of land consolidation showed that land consolidation is an effective and viable management tool to improve asset structure and, if implemented, reduce production costs by an average of 15 percent (Hyeronin and Rickenin, 2017).

In this study, the effect of fragmentation of exploitation levels on the development of agricultural mechanization with aim of finding the most important factor on the underdevelopment of Jiroft and providing appropriate solutions is discussed.

Materials and Methods

The field data were collected using a questionnaire. Jiroft city was the spatial territory of this research. Jiroft has a population of 380823 people with 4 sections, 14 rural and 1264 villages, with 762 villages having populations and 502 villages are empty. The statistical population of this research was 154867 farmers of agricultural sector that based on Cochran's formula (Equation 1), 384 farmers were selected by simple sampling method.

$$n = \frac{\frac{z^2 pq}{d^2}}{1+\frac{1}{N}\left(\frac{z^2 pq}{d^2}-1\right)} \quad (1)$$

n: Sample size.
N: The statistical population volume (population volume of the city, province, etc.).
z: The value of the normal variable of the standard unit.
p: The value of the attribute ratio in society. If it is not available, it can be considered 0.5. In this case, the amount of variance reaches its maximum value.
q: The percentage of people who do not have that attribute in society (q = 1-p).
d: The desired degree of certainty or possible accuracy or the amount of error allowed (Sobhani Fard, 2017).

We usually consider p and q equal to0.5. The value of z at the 95% confidence level is 1.96. d can be 0.01 or 0.05.

$$n = \frac{\frac{(1.96)^2\times 0.5\times 0.5}{(0.05)^2}}{1+\frac{1}{154867}\left(\frac{(1.96)^2\times 0.5\times 0.5}{(0.05)^2}-1\right)} = 384$$

In order to increase the accuracy and correctness of the results, the sample size was increased to 420. The collected data were evaluated and processed using a hierarchical technique, which is a group decision making method in complex environments. The basis of this method is the formation of a hierarchical decision tree. Each decision problem can be designed in the form of a tree. The first level of this tree represents the decision maker's purpose. Prioritizing competing options is to achieve this goal. Intermediate levels represent planners' preferred criteria for achieving the goal at the first level. The last level shows the options available to achieve the goal.

In this study, structure of the hierarchical decision tree was designed based on what is shown in Figure 1. The first level consists of the main objective of prioritizing the factors contributing to the underdevelopment of agricultural mechanization through the fragmentation of lands. The second level involves the basic criteria that influence the research goal, such as the benefits of knowledge, participation, prejudice, and so on. The final level includes the important options derived from the classification of criteria at the second level, including socio-family, cultural-communicational, educational-technical, juridical-legal, and economics-financial factors. In this research, it has been attempted to prioritize among the mentioned factors so that the planners and executives of agricultural mechanization development plan, while identifying the factors preventing agricultural mechanization development due to fragmentation of the land, attempt to eliminate it.

Comparative Tables were prepared based on the above hierarchical structure and paired comparison was performed using a scale that was designed from the same preference to the completely better one. This scale is shown in the Table 1. To calculate the numerical mean after completing the questionnaires by farmers, we will have different views on each of the options. To solve this problem, comparative tables should be combined. After preparing the hierarchical tree of geometric mean calculation, mathematical operations were performed by the Expert Choice 11 software in order to prioritize the effective factors in the underdevelopment of agricultural mechanization due to the fragmentation of the lands. Initially, relative weight of each criterion was estimated according to the purpose of comparison, and in the next step, the relative weight of each option was calculated according to paired comparison criteria.

$$a_{ij} = \left(\pi_{k=1}^{n} a_{ij}^{(k)}\right)^{\frac{1}{n}} \quad (2)$$

a_{ij}: Average geometric criterion a
a: A criterion that is compared to options
ij: Two options that compare
k: The code of the person who answered the questionnaire questions
n: Number of people who have compared criterion options (Samet, 2003).

In the real world, there is often an inconsistency. These inconsistencies may come into the model. When the incompatibility rate is zero, it means that full compatibility has occurred. As the rate rises, the inconsistency in the target also increases. Generally, if the incompatibility rate is less than 0.1, the incompatibility is relatively acceptable, otherwise a revision in judgment would be necessary.

After comparing the relative weights of the criteria of the options, it is necessary to calculate the final weight of each option. To do this, the integration process was used. In this way, the final answers to the problem were obtained.

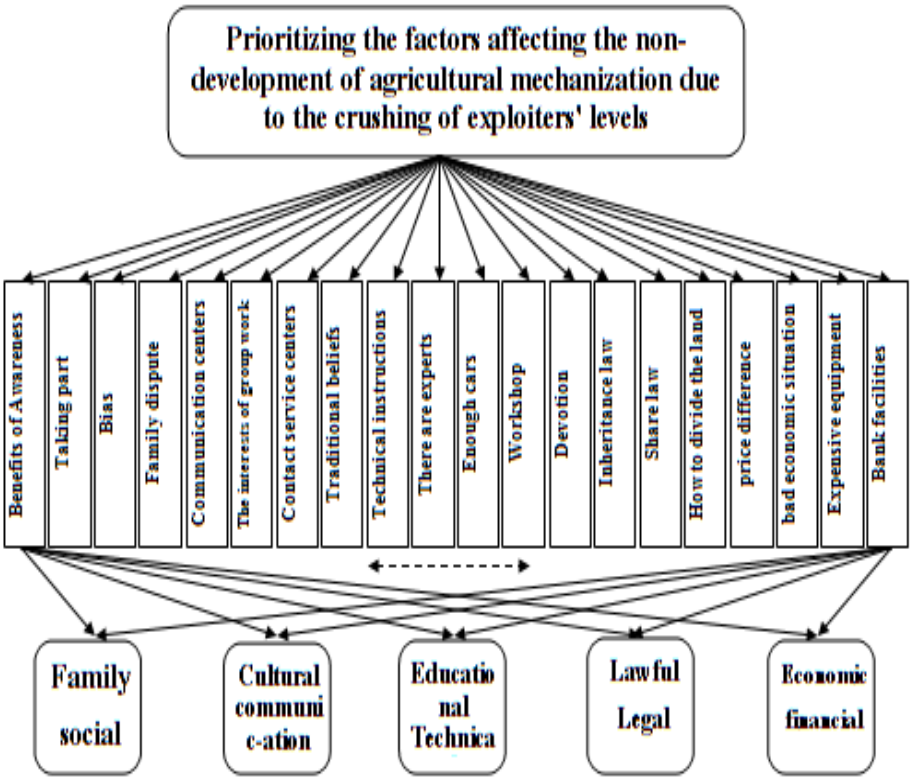

Fig.1. General structure of the tree hierarchy

Table1-Comparison of Paired Scales

1	**The same preference**	**Both options have the same effect on the target.**
3	Slightly better	The preference of one option over another (the comparative option) is small.
5	Better	The preferences of one option over another (the comparative option) is strong.
7	Much better	The preference of one option over another (the comparison option) is very strong.
9	Quite better	The choice of one option over another (the option to compare) is at its maximum.
2,4,6,8		The average scores represent the average states of each of the above comparison modes.

Results and Discussion

Comparison of criteria with respect to the purpose

In the first stage, the criteria were compared in pairs with respect to purpose of the study (prioritizing the factors affecting the non-development of agricultural mechanization due to the fragmentation of lands). According to Figure 2, which shows the pairwise comparison of criteria with respect to the purpose of the research, the criterion of knowledge and technical guidance advantages with the ratio of 0.071 and banking facilities with a ratio of 0.021 has the highest to lowest priority, respectively. The calculated incompatibility rate is 0.07, therefore, the compatibility of the criteria with the objective of the research is acceptable.

Paired comparison of options

In the second step, the options were compared in terms of criteria. Figure 3 shows the pairwise comparisons of criteria according to the benefits of knowledge. According to Figure 3, the family-social factor with the ratio of 0.356 and the economic-financial factor with the ratio of 0.041 have the highest and lowest shares respectively. The calculated incompatibility rate is equal to 0.09. Therefore, the compatibility of the criteria of the benefits of knowledge with the options is acceptable.

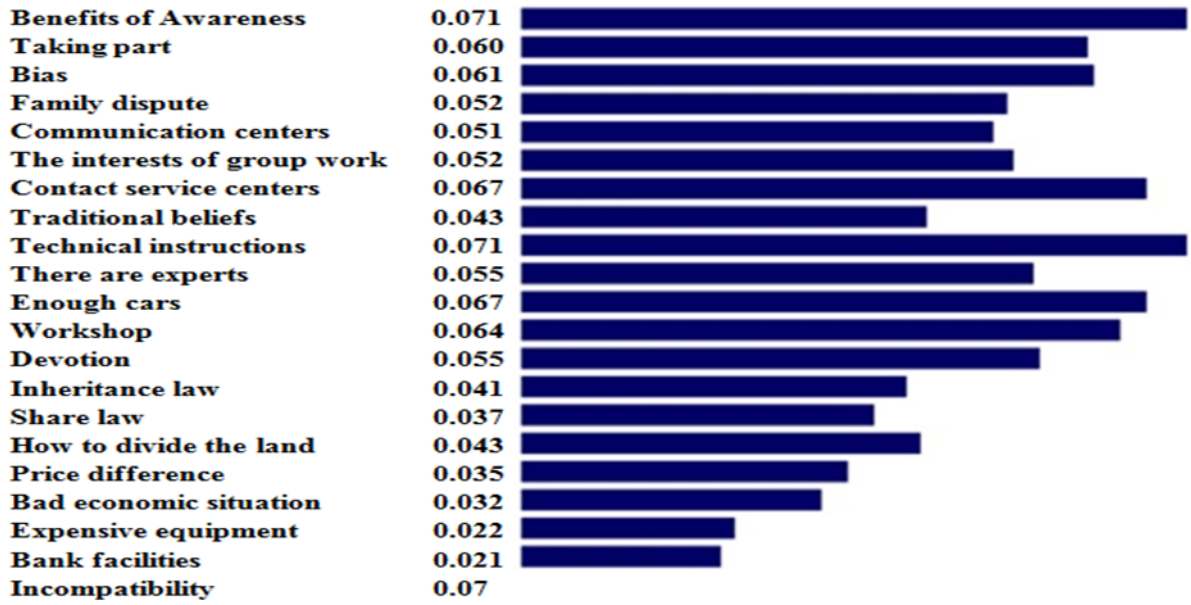

Fig.2. Comparison of the criteria in a paired relation to the purpose of the research

According to Figure 4, which shows a pairwise comparison of criteria with respect to participation criterion, the family-social factor with the ratio of 0.368 and the economic-financial factor with the ratio of 0.098 has the highest and lowest shares respectively. The calculated incompatibility rate is 0.07. Therefore, the compatibility of the participation criterion with the options is acceptable. Figure 5, shows a pairwise comparison of criteria with respect to bias criterion, and shows that the family-social factor with a ratio of 0.368 and the economic-financial factor with the ratio of 0.077 have the highest and lowest shares respectively. The calculated incompatibility rate is 0.08, so the compatibility of the bias criterion with the options is acceptable. A pairwise comparison of criteria with respect to family dispute criterion shows (Figure 6) that the family-social factor with the ratio of 0.544 and economic-financial factor with the ratio of 0.052 have the highest and lowest shares respectively. The calculated incompatibility rate is equal to 0.1, so the compatibility of the family difference criterion with the options is acceptable. According to Figure 7, which shows a pairwise comparison of criteria with respect to the criteria of communication centers, the family-social factor with the ratio of 0.479 and economic-financial factor with the ratio of 0.056 has the highest and lowest shares respectively. The calculated incompatibility rate is 0.08. Therefore, the compatibility of the centers of communication with the options is acceptable. A pairwise comparison of criteria with respect to the criteria of teamwork benefits shows (Figure 8) the family-social factor with a ratio of 0.490 and the economic-financial factor with the ratio of 0.048, has the highest and lowest shares respectively. The calculated incompatibility rate is equal to 0.09. Therefore, the compatibility of the criterion of the benefit of teamwork with options is acceptable. According to Figure 9, which shows a paired comparison of criteria according to the criteria of communication with service centers, the family-social factor with the ratio of 0.474 and economic-financial factor with the ratio of 0.047 has the highest and lowest share respectively. The calculated incompatibility rate is 0.05. Therefore, the compatibility of the criterion of communication with the service centers with the options is acceptable.

The family-social factor with a ratio of 0.526 and economic-financial factor with the ratio of 0.049 have the highest and lowest shares respectively (Figure 10). The calculated

incompatibility rate is 0.07 and since it is less than 0.1, the compatibility of the criterion of traditional beliefs with options is acceptable. Figure 11 shows a paired comparison of the criteria according to the criteria of technical guidelines, cultural-communication factor with the ratio of 0.404 and economic-financial factor with the ratio of 0.034 have the highest and lowest shares respectively. The calculated incompatibility rate is 0.07 and since it is less than 0.1, the compatibility of the criterion of technical guidelines with the options is acceptable. However, Figure 12, shows a paired comparison of the criteria according to the criterion of the existence of specialists with the family-social factor with the ratio of 0.503 and economic-financial factor with the ratio of 0.027, which is the highest and the lowest share respectively. The calculated incompatibility rate is 0.09 and since it is less than 0.1, the compatibility of the criterion of the availability of experts with options is acceptable. With respect to the adequacy of the machines (Figure 13), the family-social factor with a ratio of 0.447 and economic-financial factor with the ratio of 0.031 has the highest and lowest share respectively. The calculated incompatibility rate is 0.09 so the compatibility of the criterion of the adequacy of the machines with the options is acceptable. Figure 14 shows a paired comparison of the criteria according to the criteria of the workshop, the family-social factor with a ratio of 0.474 and economic-financial factor with the ratio of 0.033 have the highest and lowest shares respectively. The calculated incompatibility rate is equal to 0.09. Therefore, the compatibility of the workshop criteria with acceptable options is acceptable. Using a paired comparison of criteria with respect to the dedication criterion (Figure 15), the family-social factor with a ratio of 0.412 and the economic-financial factor with the ratio of 0.028, has the highest and lowest shares respectively. The calculated incompatibility rate is 0.08 so the compatibility of the endowment criterion with the options is acceptable. According to Figure 16, which shows a paired comparison of the criteria according to the law of inheritance, the family-social factor with the ratio of 0.455 and the economic-financial factor with the ratio of 0.030, has the highest and the lowest share respectively. The calculated incompatibility rate is 0.07. Therefore, the compatibility of the criterion of the inheritance law with acceptable options is acceptable. However, a paired comparison of the criteria according to the participatory law (Figure 17), the cultural factor is related to the ratio of 0.360 and the economic-financial factor with the ratio of 0.040, has the highest and lowest shares respectively. The calculated incompatibility rate is 0.09 so the compatibility of the criterion of the participatory law with the options is acceptable. A paired comparison of the criteria according to the criteria of the division of land (Figure 18), the family-social factor with a ratio of 0.316 and the economic-financial factor with the ratio of 0.073 has the highest and lowest shares respectively. The calculated incompatibility rate is 0.07. Therefore, the compatibility of the criteria for the division of land with options is acceptable. According to Figure 19, which shows a paired comparison of the criteria according to the price difference criterion, the educational-technical factor with the ratio of 0.340 and the economic-financial factor with the ratio of 0.033 have the highest and lowest shares respectively. The calculated incompatibility rate is equal to 0.06. Therefore, the compatibility of the price difference criterion with the options is acceptable. Based on Figure 20, which shows a paired comparison of criteria according to the criteria of bad economic conditions, the family-social factor with the ratio of 0.417 and the economic-financial factor with the ratio of 0.030 has the highest and lowest shares respectively. The calculated incompatibility rate is 0.08 so that the compatibility of the bad economic conditions with acceptable options is acceptable. Paired comparison of criteria according to the criteria of equipment cost (Figure 21), the cultural-communication factor with the ratio of 0.400 and the economic-financial factor with the ratio of 0.028, has the highest and lowest shares respectively.

Fig.3. Comparison of criteria in the form of a pair of criteria for awareness benefits

Fig.4. Comparison of criteria in terms of participation rate

Fig.5. Comparison of the criteria in a pairwise way to the bias criterion

Fig.6. Comparison of criteria in relation to family differences

Fig.7. Comparison of criteria in two ways compared to the criteria of communication centers

Fig.8. Comparison of benchmark criteria in comparison to the benchmark of group work benefits

Fig.9. Comparison of criteria in terms of the ratio of service centers to criteria

Fig.10. Comparison of criteria in the form of a pair of traditional beliefs

Fig.11. Comparison of criteria in a pair to the standard of technical instruction

Fig.12. Comparison of criteria in the form of a pair of experts

Fig.13. Comparison of criteria in a pairwise manner with respect to the adequacy of machines

Fig.14. Comparison of the criteria in terms of the criteria of the workshop

Fig.15. Comparison of criteria in the form of a pair of deductive criteria

Fig.16. Comparison of criteria in the form of a pair of criteria of the inheritance law

Fig.17. Comparison of benchmarks in terms of the law of participation

Fig.18. Comparison of criteria in a pairwise way to the land parcel standard

Fig.19. Comparison of criteria in a pairwise way to the price difference criterion

Fig.20. Comparison of benchmarks in terms of economic criteria

Fig.21. Comparison of criteria in terms of equipment costs

Fig.22. Comparison of benchmarks in terms of banking facility criteria

The calculated incompatibility rate is equal to 0.1 so the compatibility of the equipment cost criterion with the options is acceptable. According to Figure 22, which shows a paired comparison of the criteria according to the criteria of bank facilities, the family-social factor with a ratio of 0.434 and the economic-financial factor with the ratio of 0.032 has the highest and lowest shares respectively. The calculated incompatibility rate is 0.09. Therefore, the compatibility of the bank facilities criterion with options is acceptable.

Integration

Based on the results of the integration of options and criteria according to the purpose of the study (Figure 23) it can be concluded that among the barriers to implementation of the agricultural mechanization development project in Jiroft city, family-social factor was the most deterrent factor. The economic-financial factor is of the least importance. Finally, it can be said that the factors preventing the development of agricultural mechanization in Jiroft city due to fragmentation of lands are social-family, cultural-communication, educational-technical, lawful- legal, economic-financial.

Factors influencing the lack of development of agricultural mechanization in each region are different according to its conditions. For example, the study of Hashemipour and Zamani (2016), in Qazvin-Iran showed that the most important factors are inheritance, population growth and literacy, and in Azna-Iran, according to Mahdavi and Kiani (2017), individual-social and economic factors; and in Jiroft, family- social factors play a significant role in agricultural development.

Fig.23. The final weight of the options

Conclusions

Given the existing theoretical scope, present findings and limitations, and the results obtained from the Analytical Hierarchical Process technique model, the most important cause of land fragmentation is the family-social factor in Jiroft whereas family disputes have a strong role that village elders can play in mediation and problem solving. This process is done by involving all supply chain actors, analyzing problems and providing solutions. Applying mechanisms for organizing family farms, investing in infrastructure, adapting world technologies to country conditions in the scale of small farms (localization), marketing and branding are some of the most experienced strategies in the world for developing small farms. Familiarizing farmers with the benefits of mechanization development through promotional activities and through awareness raising will encourage them to expand the mechanization coefficient in their land. Farmers, for cultural reasons and not merely for economic reasons, have little risk-taking potential and therefore do not readily accept any new proposal simply because it is new. However, if leading farmers and local leaders who are largely trusted by farmers voluntarily implement mechanized development plans on their land, there will be considerable scope for acceptance by farmers, especially when the positive results of the plan are well known. Progressive farmers, if they accept themselves as innovators and implementers of the project on their land, will certainly help to boost the confidence of other farmers. Another influential factor was the technical skills of farmers. Undoubtedly, one of the obstacles to the acceptance of technology by farmers is the lack of skills in the use of equipment, which tend to be employed by participating in training classes and improving the technical skills of using different machines mechanization increases at the farm level.

References

1. Bagheri, N. 2016. Strategies for the development of agricultural mechanization in micro systems. Promoters (154): 43-47. (In Farsi).
2. Fall Solomon, M., and M. Moradi. 2011. Evaluation of the effects of land consolidation on rural development in rural areas. Geographical studies of arid regions. 2 (6): 85-67. (In Farsi).
3. Gergievsk, K. 2005. Land Consolidation as one of the modes for the enlargement of agricultural land in Macedonia. Journal Central European Agriculture 6 (4): 562-574.
4. Hashemipour, P., and D. Mohammad Zamani.2016. Investigating the Effect of Land Size Relationship on Agricultural Mechanization Indices by Regression Method in Qazvin. Vineyard Biomedical Engineering Journal 5 (2): 1-15. (In Farsi).
5. Hiironen, J., and K. Riekkinen. 2014. Agricultural impacts and profitability of land consolidations. Land Use Policy Volume 55. September 2016. Pages 309-317.
6. Lai, W., and B. Roe. 2015. Estimating the Effect of Land Fragmentation on Machinery Use and Crop Production. Association and Western Agricultural Economics Association Annual Meeting, San Francisco.
7. Lak, M. B., and A. M. Borghaee. 2011. Multi-Criteria Decision Making Based in Choosing an Appropriate Tractor (A Case Study for Hamedan Province). Journal of Agricultural Machinery Engineering 1 (1): 41-47. (In Farsi).
8. Mahdavi, I., and M. Kiani. 2017. Evaluation of barriers to agricultural land integration (case study: villages of Azna city). Iranian Economic Research and Development 48 (2): 342-333. (In Farsi).
9. Mohammad Zadeh, L., and D. A. Fenech. 2015. Analysis and evaluation of the effects of land consolidation in agricultural economy with an emphasis on agricultural development. The 3rd National Conference of Academic Students in Agriculture and Natural Resources. Karaj. Campus of Agriculture and Natural Resources of Tehran University. (In Farsi).
10. Nijibkhirabadi, H., and T. Maghsoudi.2010. Agricultural land degradation Challenges for agricultural development (factors and solutions). National Conference on Agricultural and Natural Resources Contribution to the Development of the Islamic Republic of Iran in Horizon 2025. Rasht. Islamic Azad University of Rasht Branch. (In Farsi).
11. Rezvani Alvar, M., and H. Rachel. 2014. History of Agricultural Mechanization in Iran and Its Policies in Development Plans. Second National Conference on Agriculture and Sustainable Natural Resources. Tehran. Educational institute of Mehr Arvand. Advocacy group for environmental lovers and the Iranian Nature Conservation Association. (In Farsi).
12. Saiedirad, M. H., and S. A. Parhizgar. 2011. Study on Agricultural Mechanization Indexes of Small Farms in Khorasan Razavi Province and Suggesting Possible Improvement. Journal of Agricultural Machinery Engineering 1 (1): 48-53. (In Farsi).
13. Saati, T. L. 1998. Decision making for manager. Translated by Ali Asghar Tofighi. Organization of industrial management. Publication: Tehran. (In Farsi).
14. Samati, M., and M. Asghari. 2003. Priority of development in industrial sector in Isfahan Province based on AHP method. Journal Commodity Research 4 (10). p27. (In Farsi).
15. Secretariat of the Fourth Program Headquarters. 2005. National Document for Development of Agriculture and Natural Resources in the Fourth Development Plan. Editor: Bahram Khazin. Tehran. Publisher: Agricultural Planning and Economics Research Institute, Process Management and Research Findings. (In Farsi).
16. Sobhani Fard, Y. 2017. Statistical Analysis. Tehran. University of Science and Industry. (In Farsi).
17. TurkiBoldaji, B., and Y. Ghanbari. 2013. Identifying and Analyzing the Factors Affecting the Development of Agricultural Mechanization Case Study: Borujen County. The 2nd National Conference on Sustainable Agriculture and Sustainable Environment. Hamedan. Tomorrow's environmental think tank. (In Farsi).

نشریه ماشین‌های کشاورزی
جلد ۱۱، شماره ۱، نیمسال اول ۱۴۰۰، ص ۵۳-۴۳

Journal of Agricultural Machinery
Vol. 11, No. 1, Spring- Summer 2021, p. 43-53

مقاله علمی-پژوهشی

بررسی اثر خردشدن سطوح بهره‌برداران بر توسعه مکانیزاسیون کشاورزی با استفاده از تکنیک AHP

مهدی ثباتی گاوگانی[۱]، داود محمدزمانی[۲*]، محمد غلامی پرشکوهی[۲]

تاریخ دریافت: ۱۳۹۸/۰۸/۱۸
تاریخ پذیرش: ۱۳۹۹/۰۴/۳۰

چکیده

بخش کشاورزی برای تأمین امنیت غذایی برای جامعه و ایفای نقش مؤثر در تقویت استقلال ملی نیاز به انتقال سریع از معیشت‌های سنتی و معیشتی به مرحله تولید و تجاری‌سازی پیشرفته دارد. مکانیزاسیون رویکردی است که دستیابی بخش کشاورزی به مرحلهٔ تولید تجاری را ممکن می‌سازد. بدون مکانیزاسیون، چشم‌انداز روشنی از کشاورزی پویا و پایدار که بتواند نیازهای غذایی را معقولانه برطرف سازد، متصور نیست. توسعهٔ مکانیزاسیون در جوامع کشاورزی و به‌ویژه در نواحی روستایی کشور با مشکلاتی همراه بوده است که شناخت عوامل مؤثر بر آن می‌تواند به برنامه‌ریزی برای رفع آن‌ها کمک کند. از این رو در تحقیق حاضر به بررسی اثر خردشدن سطوح بهره‌بردران بر توسعه مکانیزاسیون کشاورزی در دهستان‌های شهرستان جیرفت پرداخته شده است. نوع تحقیق کاربردی است و از نوع توصیفی- تحلیلی است، از روش پیمایشی استفاده شده است و اطلاعات از طریق پرسشنامه از ۴۲۰ کاربر در شهر جیرفت جمع‌آوری شده است. تجزیه و تحلیل اطلاعات با استفاده از تکنیک فرآیند تحلیلی سلسله مراتبی با استفاده از نرم‌افزار اکسپرت چویس ۱۱ انجام شده‌است. یافته‌های تحقیق نشان داد که عامل اجتماعی- خانوادگی در شهر جیرفت عامل اصلی بازدارنده عدم توسعه مکانیزاسیون و فرهنگ-ارتباطی، آموزشی-فنی، حقوقی و قانونی است و عوامل اقتصادی-مالی در اولویت‌های بعدی قرار گرفتند. پیشنهاد شده است که توسعه مکانیزاسیون، نوسازی فناوری نوین، آموزش و ارتقاء، ایجاد اعتماد، اعتبار و تسهیلات مالی برای نوسازی ادوات کشاورزی اجرا شود.

واژه‌های کلیدی: توسعهٔ مکانیزاسیون کشاورزی، خرد شدن اراضی، فرآیند تحلیلی سلسله مراتبی

۱- دانشجوی دکتری، گروه مهندسی بیوسیستم، دانشگاه آزاد اسلامی واحد تاکستان، تاکستان، ایران
۲- گروه مهندسی بیوسیستم، دانشگاه آزاد اسلامی واحد تاکستان، تاکستان، ایران
(*- نویسنده مسئول: Email: Dr.dmzamani@gmail.com)

DOI: 10.22067/jam.v11i1.82910

Journal of Agricultural Machinery
Vol. 11, No. 1, Spring- Summer 2021, p. 55-70

نشریه ماشین‌های کشاورزی
جلد ۱۱، شماره ۱، نیمسال اول ۱۴۰۰، ص ۷۰-۵۵

Full Research Paper

Effect of Pomegranate Seed Oil Encapsulated in Chitosan-capric Acid Nanogels Incorporating Thyme Essential Oil on Physicomechanical and Structural Properties of Jelly Candy

H. Mirzaee Moghaddam[1*], A. Rajaei[1]

Received: 01-01-2020
Accepted: 23-05-2020

Abstract

Pomegranate seed oil (PSO) is a well-known source of valuable compounds. The aim of this study was to investigate physicomechanical and structural properties of jelly candy enriched with PSO encapsulated in chitosan (CS)-capric acid (CA) nanogel incorporating thyme essentioal oil (TEO). For this purpose, initially the CS-CA nanogels were produced by creating amide bondes between CS and CA, which Scanning Electron Microscope (SEM) image showed the spherical form of CS-CA nanogels. Then, PSO-in-water Pickering emulsions were stabilized with the CS-CA nanogels as well as the CS-CA nanogels incorporating TEO. The results showed that the presence of TEO in the nanogel structure caused smaller oil droplets. Then, Pickering emulsions were used in the formulation of jelly candy and subsequently the microscopic structure, texture profile analysis (TPA) and color indexes of jelly candies were studied. The use of PSO in the encapsulated form reduced the separation of the PSO from the texture of the jelly candy. The results of TPA showed that although the samples containing PSO in the encapsulated form had lower hardness (156.6-173.4 N), gumminess (202.2-262.1 N), cohesiveness (1.3-1.5%), resilience (40.2-54.7 N.s) and adhesiveness (0.29-0.4 N.s) than the control (250.3 N, 627.9 N, 2.14%, 160.7 N.s, 0.63 N.s), their springiness (0.92-0.93%) was higher than the control (0.79%). Moreover, the color indexes showed that the samples containing PSO in the encapsulated form changed the color indexes more than the control, which was more in the presence of TEO.

Keywords: Encapsulated, Jelly candy, Nanogel, Physicomechanical and structural properties, Pomegranate seed oil, Thyme essential oil

Introduction

In recent years, food consumers are interested in foods that, in addition to having essential nutrients, can improve health, and prevent illnesses as well. Therefore, in Europe and the US, the rate of growth in the production and consumption of fortified foods is increasing (Dias *et al*., 2015). Pomegranate, scientifically named *Punica granatum*, is a fruit with a high concentration of polyphenols compared to other fruits. In addition, pomegranate seed oil (PSO) is one of six known vegetable oils rich in conjugated linolenic fatty acid (CLnA) isomers, which are recommended for preventing from cancer, obesity, diabetes and heart disease. It should be noted that the addition of valuable oils such as pomegranate seed oil to foods has many challenges including their poor dispersion because of low water solubility of these oils as well as their oxidation and creating unfavorable flavors due to their high susceptibility to oxidation in processing and storage conditions (Soleimanian *et al*., 2018; Yekdane and Goli, 2019). Encapsulation and the use of natural or synthetic antioxidants are considered as effective ways to overcome the former and the latter challenges, respectively (Balasubramani *et al.*, 2013). One of the most common methods for encapsulating and delivering bioactive compounds such as pomegranate seed oil in the food and pharmaceutical industries is the use of emulsions (Lamba *et al.*, 2015). Pickering emulsion is an emulsion of any kind, oil-in-water (O/W) or water-in-oil (W/O), or even is multiple that stabilized by solid particles

1- Assistant Professor, School of Agricultural Engineering, Shahrood University of Technology, Shahrood, Iran
(*- Corresponding Author Email: hosseinsg@yahoo.com)
DOI: 10.22067/jam.v11i1.84882

(Jiang *et al.*, 2019). In Pickering emulsions, the particles tend to be irreversibly absorbed at the droplet surface, which creates a physical barrier against prooxidant. Other benefit of Pickering is high resistance to coagulation (McClements and Li, 2010). Nanotechnology has introduced a major revolution in industry, agriculture and other sciences, and draws a very broad perspective to future for the advancement of science. This technology has created many capabilities in postharvest processes of agriculture products (Mirzaee Moghaddam *et al*., 2014). In the past decade, a wide range of polysaccharide nanoparticles have been investigated for the encapsulation of bioactive compounds. Among the different polysaccharides, chitosan (CS), which is produced by deacetylation of chitin, has been used frequently in recent years due to its high biocompatibility. Much research has been done in recent years on Pickering emulsions stabilized by CS (Mwangi *et al.*, 2016; Wang *et al*., 2015). Previous studies have reported that modifying the structure of CS with fatty acids can increase the emulsifier property of CS (Atarian *et al.*, 2019; Hosseini *et al.*, 2019). Thyme with scientific name *Thymus vulgaris* is an aromatic plant of Lamiaceae family and has been considered as a medicinal plant worldwide. According to researchers, the main pharmacological effects of thyme essential oil (TEO) are due to thymol and carvacrol that are the most important bioactive constituents of this plant (Pesavento *et al*., 2015). Essential oils often have antibacterial, antifungal, antiviral and antioxidant properties (Rodríguez *et al*., 2011). However, previous studies have shown that the essential oils, in addition to the properties mentioned, can contribute to the emulsifying activity. Chen *et al.* showed that the combination of cinnamaldehyde, which is a hydrophobic aromatic aldehyde, with CS can increase the emulsifier properties of CS (Chen *et al*., 2017). Developing new foods enriched with bioactive compounds is an interesting marketing strategy for the industry, especially for products such as jelly candy that need to be merged with health revisions. This product is consumed by a large and heterogeneous group of people from children to adults. For this reason, jelly candy can be a good means of delivering bioactive compounds such as PSO to the diet of people (Moura *et al*., 2019).

Previous studies on the production of Pickering emulsions using CS as well as characterization of manufactured emulsions have been performed. However, there has been no study on the encapsulation of PSO using CS nanoparticles containing TEO as well as the effect of the encapsulated PSO on the physicomechanical and structural properties of jelly candy. It should be noted that a proper understanding of the physicochemical and textural properties of new formulations can lead to better design of the devices required for the process of these new formulations on an industrial scale. Therefore, the aim of this study was to investigate the effect of encapsulated PSO by CS-CA nanogel incoporating TEO on the physicomechanical and textural properties of jelly candy.

Materials and Methods

Materials

PSO with 54% punicic acid from "Oil Seed" Company (Iran-Karaj), TEO from "Barijan Essence" (Iran-Kashan), the major constituents of which were included: Thymol (38.5%), Carvacrol (35.1%), Para-cement (8.8%), Gamma-terpene (2.5%) and Beta-caryophyllene (2.2%), CS (90% deacetylated, 50-190 KDa), CA, 1- Ethyl-3- (3-dimethylamino propyl) carbodiimide, acetic acid, sodium hydroxide, ethanol, Nile red and fluorescein isothiocyanate (FITC) from Sigma-Aldrich (Germany), gelatin from "Ghazvin Gelatin Halal" company (Iran-Ghazvin), and liquid glucose from "Orumiyeh Chi Chest Glucose" (Iran- Orumiyeh) were obtained.

Preparation of CS-CA nanogels

CS-CA nanogels were prepared by creating amide bonds between amine groups of CS and carboxylic acid groups of CA with an EDC-mediated reaction (Atarian *et al*., 2019). In brief, 1 g of CS was first dissolved in 100 ml of 1% (v/v) aqueous acetic acid. Then 100 mg EDC was mixed with 500 mg CA and dissolved in 5 ml ethanol subsequently the

mixture of EDC and CA dropwise added to the CS solution and shaked for 24 h at a dark place. In continue, pH of the solution was adjusted on 8.5-9.5 with 1M NaOH and centrifuged for 5 min at 4000 rpm to precipitate the CS-CA gels. After that, to remove unreacted substances and EDC, the precipitated CS-CA gels were washed three times with ethanol and distilled water. Finally, the CS-CA gels were dissolved in aqueous acetic acid 1% (v/v) and sonicated (5 min, 20 kHz) using a probe type ultrasound (Behin Tamin Ahura, Iran) to obtain the CS-CA nanogels and subsequently filtered through a 0.2 µm filter to uniform the CS-CA nanogels in terms of particle size.

Physicochemical and structural characterization of CS-CA nanogels

Fourier transformation infrared (FTIR) spectrometry analysis

To confirm the created amide bonde between CS and CA, an FT/IR-430 Fourier transform infrared spectrometer was used at 20 °C in the range of 500 to 4000 cm^{-1}. Before the analysis, the dried CS-CA nanogels along with the pure CS and CA were mixed with KBr powder subsequently prepared compressed tablets from them (Atarian *et al.*, 2019). In addition, place of testing was in Iran Polymer and Petrochemical Institute.

Scanning electron microscopy (SEM) analysis

The SEM was used to study the morphology of CS-CA nanogels. For this purpose, one droplet of the nanogel solution was first poured on the glassy lam and dried at ambient temperature. In the following, the samples were coated with gold and analyzied using the SEM (model KYKY-EM 3200, Made in China) (Hosseini *et al.*, 2019).

Preparation of PSO-in-water Pickering emulsions

PSO-in-water Pickering emulsions were prepared according to the method of Atarian *et al.* (2019) with some modification. Overall, 20 g PSO was first added dropwise to the CS-CA nanogel solution (2% w/v) and the solution of encapsulated TEO in the CS-CA nanogels (TEO: CS-CA nanogel ratio of 1:4), latter was prepared by the method of Hadian *et al.* (2017), under agitation (600 rppm) with a magnetic stirrer. Then, for better homogeneity of the emulsion, the initial emulsions were homogenized at 8000 rpm (IKA T10 basic, IKA Werke GmbH and Co., Germany) for 2 min. Finally, the solution was sonicated using a probe ultrasound (Behin Tamin Ahura, Iran) for 2 min (on- and off-time pulse durations of 10 and 5 s, respectively), with the power of 600 W, and frequency of 20 kHz.

Average size of droplets

To measure the size of the oil droplets, after 30 minutes of emulsion preparation, one drop of emulsion samples was first taken and gently poured on a glassy lam. Then the image of oil droplets was taken using a GX optical microscope (Australia) equipped with a CCD camera (CM TCAM3). Finally, ImageJ 1.52a software was used to measure the mean of droplets size (Xiao *et al.*, 2016).

Confocal Laser Scanning Microscope (CLSM)

Confocal laser scanning microscope (Heidelberg, Germany) was used to better visualize the interface structure of oil droplets. Prior to emulsion preparation, the CS-CA nanogels were first reacted with FITC (Hosseini *et al.*, 2019). Subsequently, Pickering emulsion was prepared according the method mentioned in section of 2.4 using the CS-CA nanogels bonded to FITC and PSO stained with Nile red. In the following, one droplet of the stained emulsion was poured on a glassy lam. Finally, to obtain photos the laser argon fluorescents at 532 nm for Nile red and 488 nm for FITC were used (Place of testing in Sharif University of Technology).

Preparation of jelly candies

For preparing the different jelly candies, a candy-based mixture formulation consisted of 20% gelatin, 50% distilled water, 10% sugar, and 20% liquid glucose was first perpared in a laboratory water bath at 70 °C. Then, according to Table 1, the certain amount of PSO, TEO, CS-CA nanogel and encapsulated PSO were added to the specified candy-based mixture and blended for 2 min to prepare a unifom mixture. After that, imidiately, the mixtures were moulded into a silicone mould (80×20×50 mm) and kept for 1h in a fridge at 4°C. The jelly candies were then unmoulded

and kept for two days at ambient temperature in a desiccator containing saturated potassium carbonate solution (Mohsenabadi *et al.*, 2018). Finally, the jelly candies were placed in plastic bags and stored at +4°C.

Table 1- Different compounds of the jelly candies

Sample	TEO (%)	Distilled water (%)	CS-CA nanogel (%)	PSO (%)	Blended* (%)
Control	0	10	0	0	90
2% PSO	0	8	0	2	90
2% PSO + 0.1% nanogel	0	7.9	0.1	2	90
2% PSO + 0.1% nanogel+0.05% TEO	0.05	7.85	0.1	2	90
0.1% nanogel	0	9.9	0.1	0	90
0.05% TEO	0.05	9.95	0	0	90

* Glucose (20%) + Gelatin (20%) + Sugar (10%) + Distilled water (50%)

Physicomechanical and structural properties of jelly candies

Microscopic structure

To study the effect of storage on the microstructure of different jelly candies, firstly, 3 and 48 h after preparing the samples, a thin layer from each sample was prepared and, then, analyzed with a GX optical microscope (Australia) equipped with a CCD camera (CM TCAM3).

Physicomechanical properties

Texture Profile Analysis (TPA)

In this study, the texture profile analysis (TPA) of jelly candies was carried out using a Material testing machine (Universal Test Machine, model STM-20, santam Company, Iran). For this purpose, first, from each sample a piece with the dimensions of 20×10×10 mm was prepared. Then, the samples were analyzed with two cycles of loading and unloading, using a cylindrical probe with diameter of 60 mm, speed of 60 mm min^{-1} and displacement length's 80% of the initial height. Finally, the time-force curves for each sample was plotted, and by using these curves (Figure 1), the texture properties namely hardness, cohesiveness, springiness, resilience, adhesiveness, and gumminess determined (Caine *et al.*, 2003). It should note that six replications were considered for each treatment.

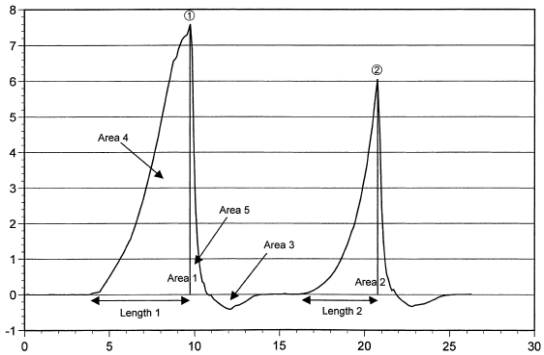

Fig.1. Typical force-by-time plot through two cycles of penetration to determin texture profile analysis parameters. Peak force is hardness; cohesiveness= Area2/Area1; springiness=Length2/Length1; resilience= (Area1-Area2)/2; gumminess= Hardness×cohesiveness; adhesiveness= Area 3 (Caine *et al.*, 2003).

Color evaluation

In order to measure the color indices of difftent jelly candies, three pieces were first selected from each treatment randomly and each piece separately analyzed using a colorimeter (Minoltachroma meter CR-400 KON, Japan, illuminant D_{65}, observer angle 0°). The colorimeter was calibrated with a

white standard plate. The color indices obtained from the colorimeter were L*, a* and b* that respectively represent brightness, redness and yellowness. Finally according to the equations (1), (2) and (3), chroma (color concentration), hue angle (color intensity) and total color difference (ΔE) were calculated for each sample, respectively (Mirzaee Moghaddam *et al*., 2014).

$$C^* = \sqrt{(a^*)^2 + (b^*)^2} \quad (1)$$

$$H^o = ArcTan(\frac{b^*}{a^*}) \quad (2)$$

$$\Delta E = \sqrt{(L_0 - L^*)^2 + (a_0 - a^*)^2 + (b_0 - b^*)^2} \quad (3)$$

Statistical analysis

All experiments except for SEM, CLSM and FTIR were performed in at least three replications. Mean and standard deviation (SD) were calculated using Microsoft Excel 2016 software. One-way ANOVA and Duncan's Multiple Range Test were used to compare differences at the 5% level with SPSS 21 software.

Results and Discussion

Characterization of CS-CA nanogels

FTIR analysis

In the first step of this study, the nanogels were prepared by self-assemble method using modified CS with CA. In order to modify of the CS, some of the free amine groups of CS were attached to the carboxylic acid groups of capric acid by using the EDC intermediate. The spectrums obtained by the FT-IR spectrometer were used to confirm the connection between the CS and CA. Figure 2 shows the FT-IR spectrums of CS, CA and CS-CA nanogel. From Figure 2-a related to CS, a peak in the 3400-3500 cm^{-1} range, which related to the hydroxyl groups of CS, is observed. In addition, at 2875 cm^{-1}, the peak is related to the stretching vibration of the CH_2 bands. At 2137 and 11656 cm^{-1}, the peaks corresponding to the stretching vibrations of the N-C and N-H groups of CS amide (non-acetylated amine groups) are observed, respectively. Moreover, the peak at 1454 cm^{-1} is related to the C-H vibrations in the sugar rings (Hadian *et al.*, 2017; Sabaa *et al.*, 2015). Figure 2-b displays the spectrum of CA that the peaks at 2918 and 2849 cm^{-1} are related to the C-H stretching vibrations of the CH_2 groups. In addition, the peak at 1704 cm^{-1} is related to the C=O stretching vibration of the carboxylic acid group. Moreover, the peak at 1476 cm^{-1} is related to the C-H bending vibration of the CH_2 and CH_3 groups. The peaks at 936 and 687 cm^{-1} are also related to the O-H and C-H bending vibration of the carboxylic acid groups, respectively (Larkin, 2011). Figure 2-c shows the spectrum of CS-CA nanogel. The peak at region 1629 cm^{-1} is due to the vibrations of the amide groups of the acetylated amines (Rao *et al.*, 2012) as well as the new amide bonds formed by the coupling between CS and CA. The peak at region 1527 cm^{-1} is related to the N-H vibration of the second type amide group (Wang *et al.*, 2003), which may be due to the formation of amide bonds between CS and CA. In the nanogel spectrum, a peak is seen in region 1704, which also is seen in the CA spectrum (related to C=O stretching vibration). This peak indicates that a number of carboxylic acid groups of CA have been bonded to the CS chain by electrostatic interactions. These findings are in agreement with the results reported in previous studies (Atarian *et al*., 2019; Hosseini *et al*., 2019).

SEM analysis

Figure 3-a shows the SEM image of CS-CA nanogels. As can be seen in Figure 3-a, the CS-CA filaments had been able to create the particles of about 100 nm by the aggregation. The formation of relatively spherical particles by the CS-CA filaments was probably due to the increasing of hydrophobic property of the CS chains, which caused the hydrophobic parts toward center, and hydrophilic parts toward outside have been arranged and aggregated. These results are consistent with the findings of the other researchers (Atarian *et al*., 2019; Hadian *et al*., 2017; Hosseini *et al*., 2019; Rajaei *et al.*, 2017).

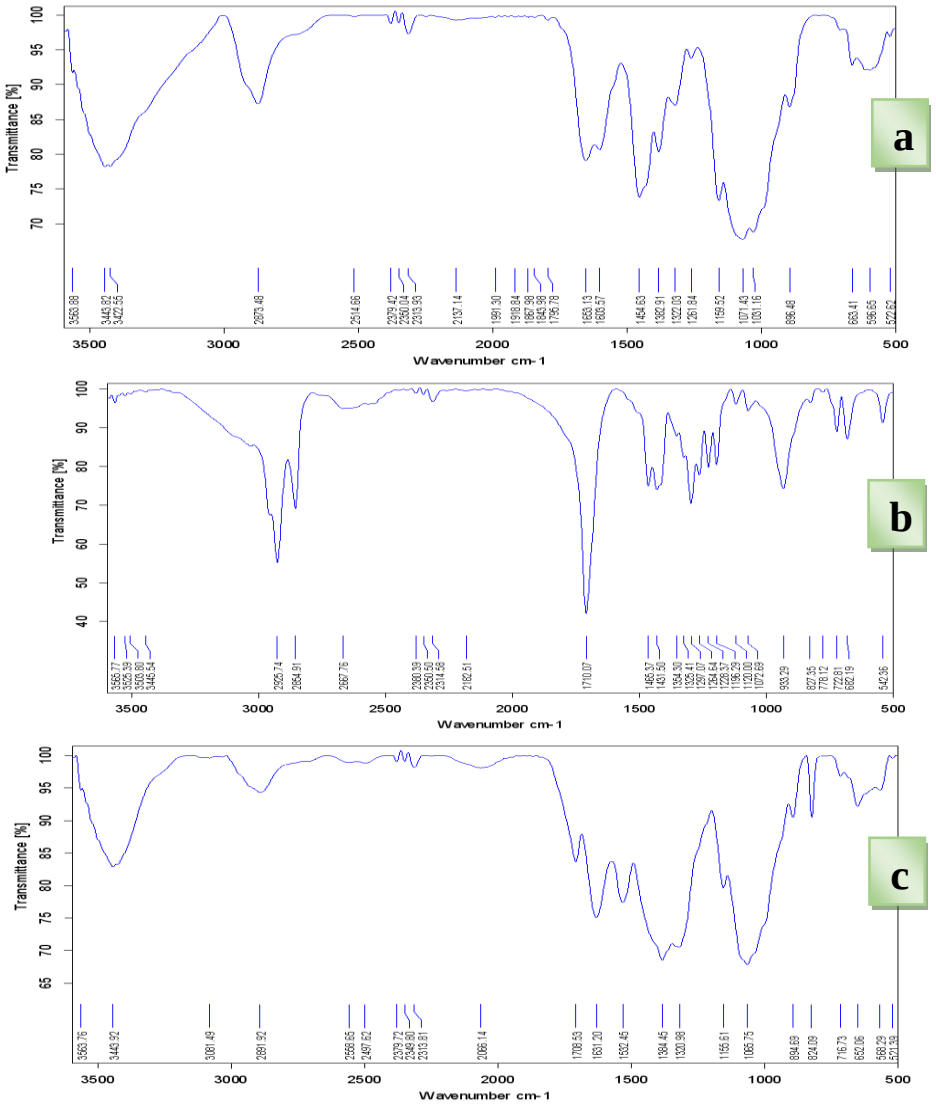

Fig.2. Fourier transform infrared spectroscopy (FTIR) analysis obtained for CS (a), CA (b) and CS-CA nanogel (c)

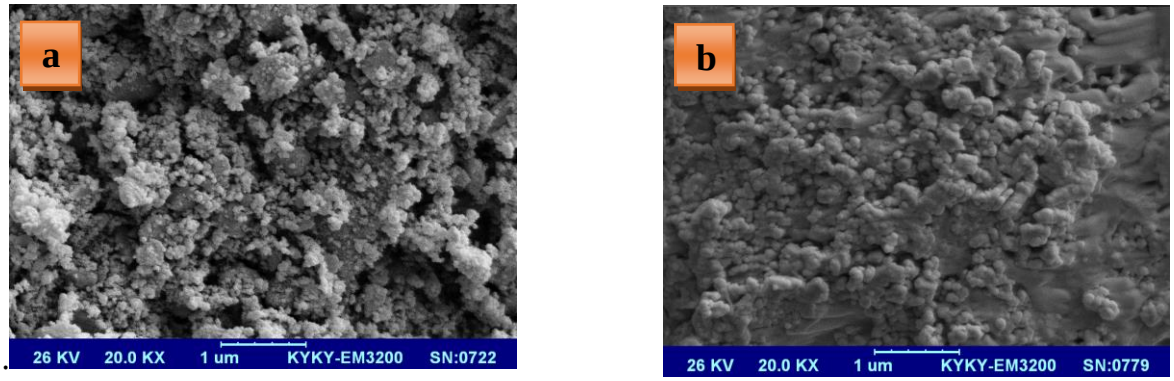

Fig.3. Scanning electron microscopy (SEM) images of CS-CA nanogel (a), and CS-CA nanogel incorporating TEO (b)

To investigate the effect of TEO on the particle size and the shape of CS-CA nanogels, the SEM image was taken from TEO encapsulated with the CS-CA nanogels (Figure 3-b). By comparing the images of CS-CA nanogels and the TEO encapsulated with the nanogels, it can be seen that although the particles are in the range of 100 nm in both figures, the uniformity of particle size distribution is less in the case of TEO encapsulated in the nanogels. Also in the case of the encapsulated TEO, the particles became more interconnected and slightly larger. These results indicate that the encapsulation of TEO in the CS-CA nanogels can change the shape of the particles. This restructuring is probably due to the change in the hydrophilic and the hydrophobic property of the nanogels. Ziaee, *et al.* (2014) investigated the effect of cumin essential oil (2 and 6%) on the size of nanogels. Their results indicated that an increase in the proportion of essential oil loaded in the nanogels maked to create particles of 30 to 250 nm size. In fact, the particle size of nanogels increased with increasing cumin essential oil that was in line with the present results.

Emulsion droplet size

Given that the size of oil droplets can affect the physical properties of jelly candies. In the next step, the CS-CA nanogels alone as well as with TEO was used for stabilizing of PSO-in-water Pickering emulsion, and subsequently the droplet size of emulsions determined. Fig. 4 illustrates the average droplet size as well as the optical microscopic image of Pickering emulsions stabilized with the CS-CA nanogels and the CS-CA nanogels incorporating TEO.

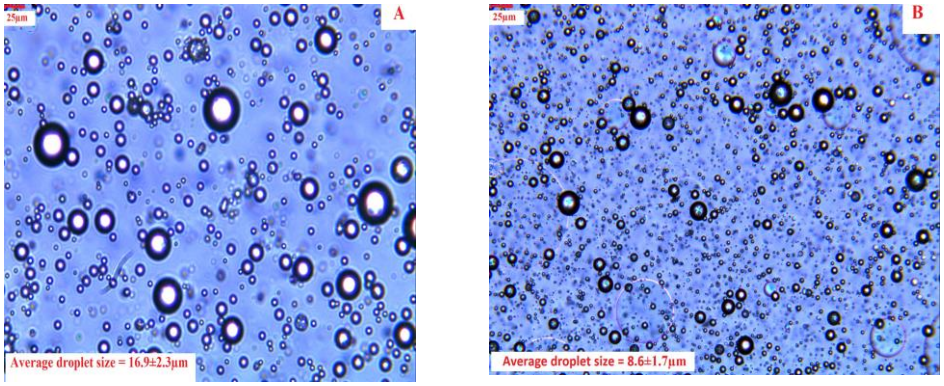

Fig.4. Average droplets size and optical microscopic images of the PSO-in-water Pickering emulsions stabilized by CS-CA nanogel (A), and CS-CA nanogel incorporating TEO (B)

It can be seen from Figure 4 that the average droplet size of emulsion stabilized with the CS-CA nanogels incorporating TEO (Figure 4-B) was smaller than the droplet size of emulsion stabilized with the CS-CA nanogels (Figure 4-A). Due to the hydrophobic nature of TEO, it can be deduced that TEO increased the hydrophobic property of CS-CA nanogels and thus smaller droplets was achieved. These results indicate that the use of TEO incorporating polysaccharides such as CS, whose hydrophilic nature is more than their hydrophobicity, can increase the hydrophobic nature and consequently their emulsifying property. These results are in line with the findings of Chen *et al.* (2017) who reported that cinnamaldehyde in combination with CS could improve the CS emulsifier property.

Interfacial structure

Because the morphological structure of Pickering emulsions including interfacial properties (composition and thickness) affect physical stability, CLSM was used to show the interfacial structure of Pickering emulsion prepared with the CS-CA nanogels that the obtained photos are shown in Figure 5. The CS-CA nanogels and the oil phase were stained by FITC and Nile red, respectively; Thus in Figure 5 the green (A) and red (B) colors represent the nanogels and the oil phase, respectively. Figure 5-C is the combined

fluorescence images of A and B. As shown in Figure 5, the oil phase is located inside the droplets. In addition, the CS-CA nanogels have formed a layer on the surface of droplets, which can create a barrier against coalescence. Moreover, it can be seen that the CS-CA nanogels have formed a dense and continuous network between the oil droplets. Hence, it can be said that in this type of Pickering emulsion, the steric barrier is not a single layer, but rather a network of particles adsorbed on the surface between the oil and the water that causes the steric barrier. The findings of this study, are consistent with those of others (Wang *et al*., 2015; Wongkongkatep *et al*., 2012).

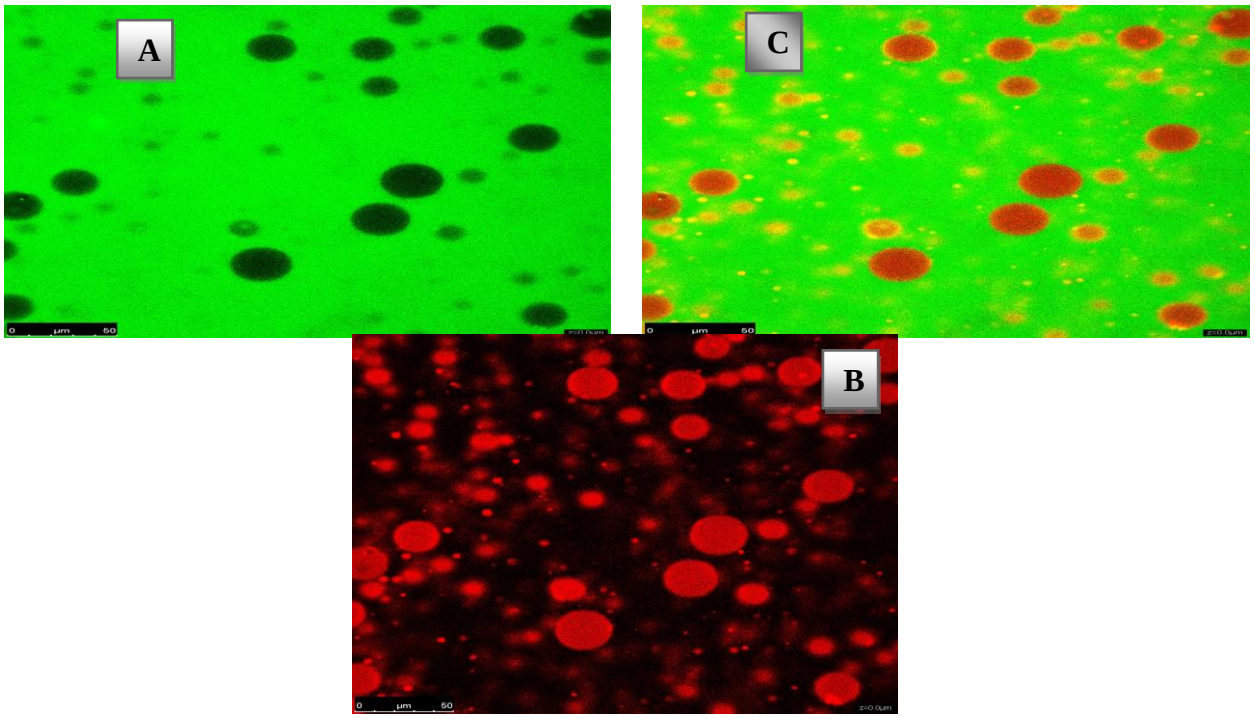

Fig.5. CLSM images of the CS-CA nanogels-stabilized Pickering emulsions: CS-CA nanogels was stained by FITC (green) excited at 488 nm (A); PSO was stained with Nile Red (red) excited at 488 nm (B); combined image of A and B (C)

Physical and mechanical properties of jelly candies enriched with PSO

Microscopic structure of jelly candies

In order to investigate the distribution of PSO droplets, the photo from the surface of samples was taken by the optical microscope. Figure 6 shows the optical microscope images obtained from the surface of different samples after 3 and 48 h of storage. According to Figure 6, it can be seen that among the control, the jelly candy containing 2% nanogel as well as the jelly candy incoporating 2% nanogel+ 0.05% TEO was not observed any significant difference in their structure after 48 h of storage. About the samples containing 2% PSO+0.1% nanogel and 2% PSO+0.1% nanogel+0.05% TEO after 48 h, was observed slightly larger droplets and drops accumulation in some spots. In addition, in the case of the sample containing 2% PSO+0.1% nanogel+0.05% TEO, the oil droplets were slightly smaller than the sample containing 2% PSO+0.1% nanogel. From Figure 6, the highest change in texture was observed in the samples containing 2% PSO compared to the other samples. About jelly candy with 2% PSO, the large droplets of PSO were observed in the matrix of sample after 3 h of storage. However, after 48 h of storage, the PSO droplets were completely separated from the jelly candy matrix and accumulated on its surface (Figure 6). The reason for the

separation of oil from the sample matrix with 2% PSO can be attributed to the lack of using of stabilizer. This result clearly showed that the use of PSO in the form of emulsion stabilized by the CS-CA nanogels was able to contribute to better dispersion and physical stability of oil droplets during storage.

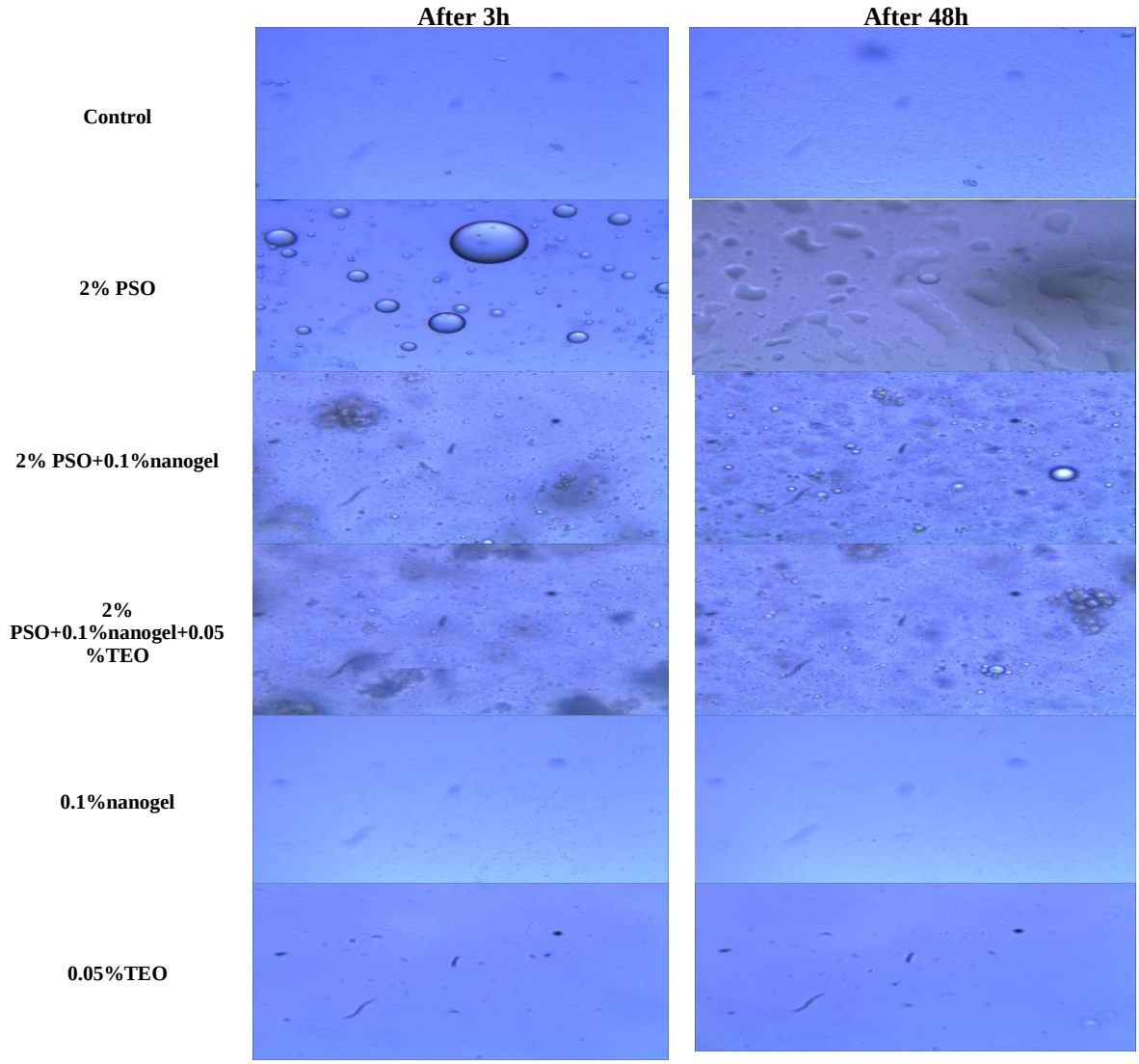

Fig.6. Surface microscopic images of different jelly candy samples

Texture profile analysis (TPA)

Figure 7 displays the results of TPA (hardness, cohesiveness, springiness, resilience, adhesiveness and gumminess) for the different jelly candy samples. As shown in Figure 7-a, it can be seen that the hardness of the control was higher than of all. Whereas the hardness of the jelly candies decreased by adding of PSO and TEO. In the case of jelly candies containing only 0.1% nanogel, the hardness results showed that the effect of the nanogel alone did not have a significant ($p>0.05$) effect on the hardness. From Figure 7-b, the results showed that the cohesiveness property of the control was higher than the rest of the samples, with a significant difference at 5% level. It should be noted that the cohesiveness property reflects the strength of intermolecular interactions. These results showed that the PSO, CS-CA nanogels, and TEO could attenuate the intermolecular forces of the candy structure. Concerning the results

of springiness, it can be seen that the adding of CS-CA nanogel, TEO and PSO to the jelly candy structure significantly ($p\leq0.05$) increased the springiness compared to the control sample. Moreover, the CS-CA nanogels had the most effect on increasing the springiness property (Figure 7-c). Regarding the resilience, the highest resilience was observed in the control sample, which was significantly different ($p\leq0.05$) from the other samples (Figure 7-d). The results of adhesiveness property showed that the use of PSO as well as nanogels reduced the adhesiveness of the samples compared to the control sample (Figure 7-e). Regarding the gumminess property, the highest gumminess belonged to the control sample, which had a significant difference at 5% level with the other samples. Results of gumminess property showed that the use of nanogel, PSO and TEO reduced this property (Figure 7-f). The observed trend in gumminess property was approximately similar to the hardness and resilience properties. The trend similarity of these properties is probably due to their high correlation. Various works have been done on the enrichment of jelly candy and the effect of enriching compounds on the mechanical properties of jelly candy. For example, Hani *et al.* (2015) reported that the red pitaya fruit puree in the formulation of gummy candy decresed the hardness and gumminess of gummy candy. Amjadi *et al.* (2018) also stated that increasing the amount of betanin in the gummy candy structure reduced its hardness and gumminess properties. In addition, Mogaddas Kia *et al.* (2020) showed that the red beet extract in the gummy candy formulation reduced the gumminess property. They interpreted that this gumminess reduction due the presence of red beet extract may be related to induce heterogeneity to network structure. Most research has focused on the effect of CS and gelatin on the mechanical properties of edible films, and no specification research was observed for mechanical properties of jelly candies. For this reason, the researches on edible films that are almost as close to the texture of jelly candy was used to interpret the results. Among these investigations, Benbettaïeb *et al.* (2014) reported that gelatin film had more hardness and less resilience than CS film. The addition of CS to the gelatin film also reduced their hardness and increased their resilience. These researchers reported that more hardness and less resilience of the gelatin films related the denser gelatin-created network. Thus, when the CS was combined with gelatin, due to the interaction between the two polymers, the hydrogen bonds between the gelatin polymers reduced and in fact, CS acted as a plasticizer, which made it more flexible (Benbettaïeb *et al*., 2014). These results are in agreement with the findings regarding the hardness and resilience of the present study. Various studies have been performed on the effect of oil on the texture properties of edible films. For example, Valenzuela *et al*. (2013) reported that the sunflower oil could reduced the strength of CS and protein blend films. These researchers have attributed the decrease of film strength due to the effect of oil on increasing structural heterogeneity and decreasing structure adhesion forces.

Color analysis

The results of color analysis for the different jelly candy samples are shown in Table 2. The results of the brightness index (L*) showed that the use of unencapsulated PSO reduced this index. Nevertheless, using encapsulated PSO (2% PSO+0.1 nanogel and 2% PSO+0.1 nanogel+0.05% TEO) increased the brightness index, which had a significant difference ($p\leq0.05$) with the control sample. A similar trend was observed for the redness index (a*) such as the brightness index. It should be noted that the positive values of a* index are red equivalent and the negative values are green equivalent. These results showed that the PSO in the emulsified form increased the green color of the samples. In the case of b* index, it was observed that the PSO in the form of emulsion, compared to the control sample, reduced this index significantly. In addition, the b* index of jelly candy containing 2% PSO+0.1 nanogel+0.05% TEO was lower than that of

jelly candy containing 2% PSO+0.1 nanogel. The results of total color difference (ΔE) showed that the least ΔE was related to the sample containing 0.1% nanogel and the highest color difference was for the samples containing PSO in emulsified form (2% PSO+0.1 nanogel and 2% PSO+0.1 nanogel+0.05% TEO). It should be noted that the total color differences of less than 3-4, are not detectable by the human eye (Benbettaïeb *et al.*, 2014). The results of color intensity (Hue angle) and color concentration (chroma) also showed that the PSO in the form of emulsion (2% PSO+0.1% nanogel and 2% PSO+0.1% nanogel+0.05% TEO) reduced the both indices. The overall results of color indices showed that the most color changes were in the samples containing PSO in the emulsified form.

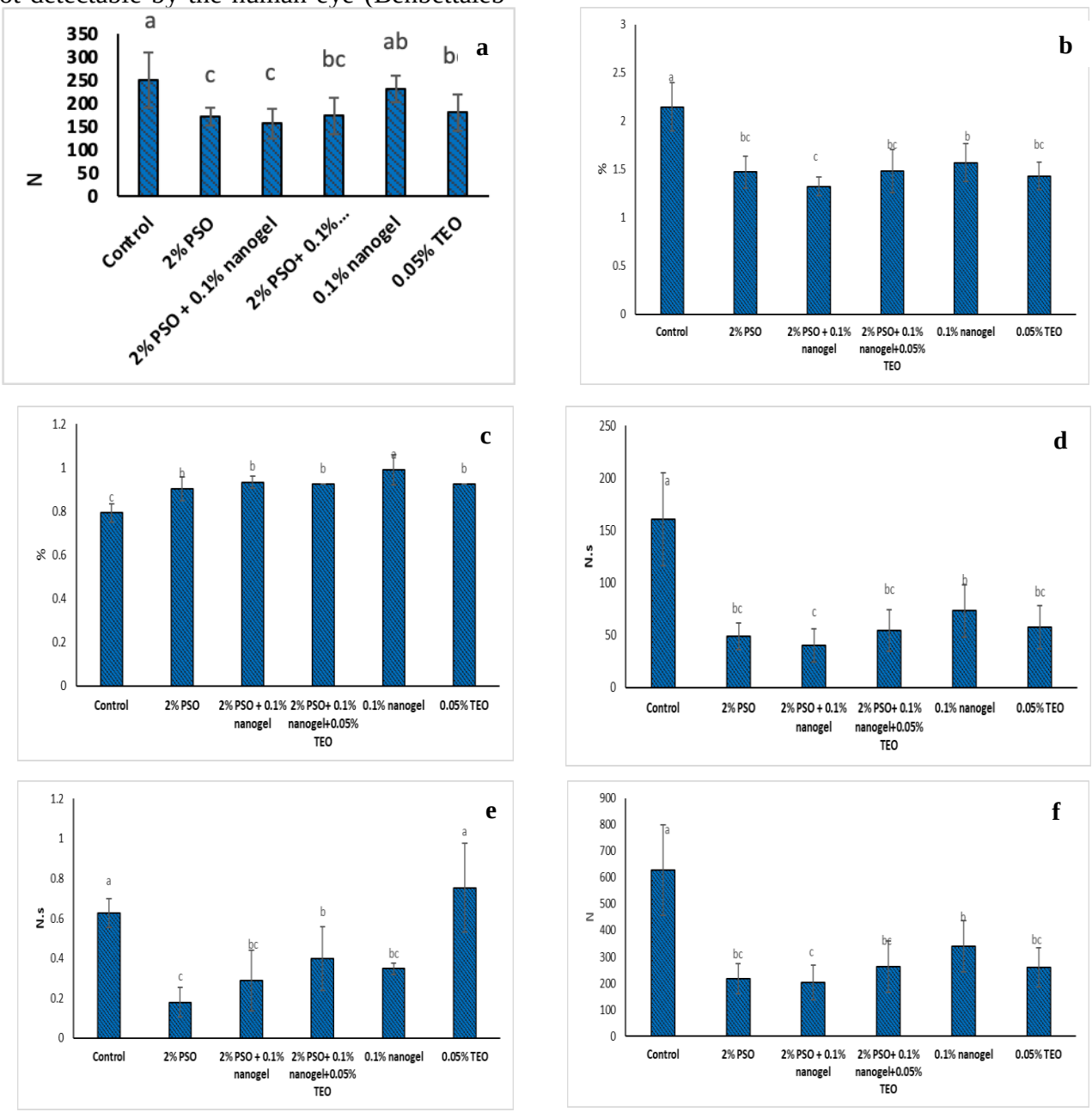

Fig.7. Hardness (a), Cohesiveness (b), Springiness (c), Resilience (d), Adhesiveness (e) and Gumminess (f) of jelly candy samples

Table 2- Color parameters of jelly candies

Treatment	L^*	a^*	b^*	ΔE	Hue Angle	Chroma
Control	52.53±0.76^{cd}	-1.20±0.35^{b}	53.93±0.50^{a}	-	267.48±1.57^{a}	54.00±0.44^{a}
2%PSO	48.07±1.40^{e}	1.40±0.20^{a}	49.53±0.50^{b}	12.52±1.10^{c}	268.38±0.21^{a}	49.55±0.51^{b}
2% PSO + 0.1% nanogel	56.47±1.92^{b}	-7.60±0.92^{d}	33.20±1.22^{b}	19.97±1.02^{b}	102.86±1.08^{c}	34.06±1.38^{c}
2% PSO + 0.1% nanogel+0.05% TEO	60.66±1.96^{a}	-8.47±0.50^{d}	31.40±1.40^{c}	21.93±1.19^{a}	105.08±0.29^{b}	32.52±1.48^{c}
0.1% nanogel	53.53±1.50^{c}	-3.1±0.30^{c}	54.0±0.40^{a}	5.92±1.23^{e}	92.19±1.93^{d}	54.06±0.36^{a}
0.05%TEO	50.40±0.40^{de}	-1.60±0.35^{b}	52.93±0.61^{a}	8.55±0.24^{d}	91.73±0.39^{d}	52.95±0.60^{a}

Values with different letters (a-e) in same column are significantly different, p<0.05.

Figure 8 displays the surface photo of different samples of jelly candy. In Figure 8, the color difference of the samples containing the PSO in emulsified form (2% PSO+0.1% nanogel and 2% PSO+0.1% nanogel+0.05% TEO) with the other samples is clearly seen. The samples containing the PSO in emulsified form had a lighter color than the other samples. The obvious difference between the samples containing PSO in the emulsified form, in terms of color indices, is probably due to the presence of oil droplets in the jelly candies texture. These oil droplets can change the transparency of the samples. The interaction between oil and water molecules also changes the refractive index of hydrocolloid compounds, which can change the color indices (Pereda *et al.*, 2012).

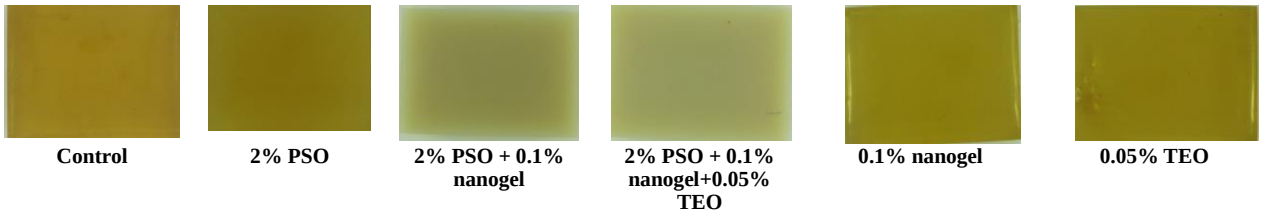

Fig.8. Appearance of different jelly candy samples

Conclusions

In this study, Pickering emulsion method using CS-CA nanogel incorporating TEO as a stabilizer was used to encapsulate PSO and subsequently to enrich jelly candy. The results showed that the use of PSO in the emulsified form improved the dispersion and physical stability of PSO in the jelly candy structure; nevertheless it reduced some of the textural properties such as hardness of jelly candy as well as changed the color characteristics of jelly candy. Physicomechanical results of jelly candy enriched with encapsulated PSO in this study can lead to better design of the devices required for the process of this new formulation on an industrial scale.

References

1. Amjadi, S., M. Ghorbani, H. Hamishehkar, and L. Roufegarinejad. 2018. Improvement in the stability of betanin by liposomal nanocarriers: Its application in gummy candy as a food model. Food Chemistry 256: 156-162.
2. Atarian, M., A. Rajaei, M. Tabatabaei, A. Mohsenifar, and H. Bodaghi. 2019. Formulation of Pickering sunflower oil-in-water emulsion stabilized by chitosan-stearic acid nanogel and studying its oxidative stability. Carbohydrate Polymers 210: 47-55.
3. Aveyard, R., B. P. Binks, and J. H. Clint. 2003. Emulsions stabilised solely by colloidal particles. Advances in Colloid and Interface Science 100: 503-546.
4. Balasubramani, P., R. Viswanathan, and M. Vairamani. 2013. Response surface optimisation of process variables for microencapsulation of garlic (*Allium sativum* L.) oleoresin by spray drying. Biosystems Engineering 114 (3): 205-213.

5. Benbettaieb, N., M. Kurek, S. Bornaz, and F. Debeaufort. 2014. Barrier, structural and mechanical properties of bovine gelatin-chitosan blend films related to biopolymer interactions. Journal of the Science of Food and Agriculture 94 (12): 2409-2419.
6. Beyki, M., S. Zhaveh, S. T. Khalili, T. Rahmani-Cherati, A. Abollahi, M. Bayat, and A. Mohsenifar. 2014. Encapsulation of Mentha piperita essential oils in chitosan–cinnamic acid nanogel with enhanced antimicrobial activity against Aspergillus flavus. Industrial Crops and Products 54: 310-319. https://doi.org/http://dx.doi.org/10.1016/j.indcrop.2014.01.033
7. Caine, W. R., J. L. Aalhus, D. R. Best, M. E. R. Dugan, and L. E. Jeremiah. 2003. Relationship of texture profile analysis and Warner-Bratzler shear force with sensory characteristics of beef rib steaks. Meat Science 64 (4): 333-339.
8. Chen, H., D. J. McClements, E. Chen, S. Liu, B. Li, and Y. Li. 2017. In situ interfacial conjugation of chitosan with cinnamaldehyde during homogenization improves the formation and stability of chitosan-stabilized emulsions. Langmuir 33 (51): 14608-14617.
9. de Moura, S. C. S. R., C. L. Berling, A. O. Garcia, M. B. Queiroz, I. D. Alvim, and M. D. Hubinger. 2019. Release of anthocyanins from the hibiscus extract encapsulated by ionic gelation and application of microparticles in jelly candy. Food Research International 121: 542-552.
10. Dias, M. I., I. C. F. R. Ferreira, and M. F. Barreiro. 2015. Microencapsulation of bioactives for food applications. Food & Function 6 (4): 1035-1052.
11. Golmakani, M. T., and K. Rezaei. 2008. Comparison of microwave-assisted hydrodistillation withthe traditional hydrodistillation method in the extractionof essential oils from *Thymus vulgaris* L. Food Chemistry 109 (4): 925-930.
12. Hadian, M., A. Rajaei, A. Mohsenifar, and M. Tabatabaei. 2017. Encapsulation of Rosmarinus officinalis essential oils in chitosan-benzoic acid nanogel with enhanced antibacterial activity in beef cutlet against Salmonella typhimurium during refrigerated storage. LWT-Food Science and Technology 84: 394-401.
13. Hani, N. M., S. R. Romli, and M. Ahmad. 2015. Influences of red pitaya fruit puree and gelling agents on the physico-mechanical properties and quality changes of gummy confections. International Journal of Food Science & Technology 50 (2): 331-339.
14. Hosseini, E., A. Rajaei, M. Tabatabaei, A. Mohsenifar, and K. Jahanbin. 2019. Preparation of Pickering Flaxseed Oil-in-Water Emulsion Stabilized by Chitosan-Myristic Acid Nanogels and Investigation of Its Oxidative Stability in Presence of Clove Essential Oil as Antioxidant. Food Biophysics 1-13.
15. Jiang, Y., F. Li, D. Li, D. Sun-Waterhouse, and Q. Huang. 2019. Zein/Pectin Nanoparticle-Stabilized Sesame Oil Pickering Emulsions: Sustainable Bioactive Carriers and Healthy Alternatives to Sesame Paste. Food and Bioprocess Technology 1-11.
16. Kakran, M., and M. N. Antipina. 2014. Emulsion-based techniques for encapsulation in biomedicine, food and personal care. Current Opinion in Pharmacology 18: 47-55.
17. Lamba, H., K. Sathish, and L. Sabikhi. 2015. Double emulsions: emerging delivery system for plant bioactives. Food and Bioprocess Technology 8 (4): 709-728.
18. Larkin, P. 2011. Infrared and Raman spectroscopy: principles and spectral interpretation. Elsevier.
19. McClements, D. J. 2010. Emulsion design to improve the delivery of functional lipophilic components. Annual Review of Food Science and Technology 1: 241-269.
20. McClements, D. J., and Y. Li. 2010. Structured emulsion-based delivery systems: Controlling the digestion and release of lipophilic food components. Advances in Colloid and Interface Science 159 (2): 213-228.
21. Moghaddas Kia, E., S. Ghaderzadeh, A. M. Langroodi, Z. Ghasempour, and A. Ehsani. 2020. Red beet extract usage in gelatin/gellan based gummy candy formulation introducing Salix

aegyptiaca distillate as a flavouring agent. Journal of Food Science and Technology https://doi.org/10.1007/s13197-020-04368-8
22. Mohsenabadi, N., A. Rajaei, M. Tabatabaei, and A. Mohsenifar. 2018. Physical and antimicrobial properties of starch-carboxy methyl cellulose film containing rosemary essential oils encapsulated in chitosan nanogel. International Journal of Biological Macromolecules 112: 148-155.
23. Mwangi, W. W., K. W. Ho, B. T. Tey, and E. S. Chan. 2016. Effects of environmental factors on the physical stability of pickering-emulsions stabilized by chitosan particles. Food Hydrocolloids 60: 543-550. https://doi.org/10.1016/j.foodhyd.2016.04.023.
24. Pereda, M., G. Amica, and N. E. Marcovich. 2012. Development and characterization of edible chitosan/olive oil emulsion films. Carbohydrate Polymers 87 (2): 1318-1325.
25. Pesavento, G., C. Calonico, A. R. Bilia, M. Barnabei, F. Calesini, R. Addona, and A. Lo Nostro. 2015. Antibacterial activity of Oregano, Rosmarinus and Thymus essential oils against Staphylococcus aureus and Listeria monocytogenes in beef meatballs. Food Control 54: 188-199. https://doi.org/http://dx.doi.org/10.1016/j.foodcont.2015.01.045.
26. Pu, J., J. D. Bankston, S. Sathivel. 2011. Developing microencapsulated flaxseed oil containing shrimp (*Litopenaeus setiferus*) astaxanthin using a pilot scale spray dryer. Biosystems Engineering 108 (2): 121-132.
27. Rajaei, A., M. Hadian, A. Mohsenifar, T. Rahmani-Cherati, M. Tabatabaei. 2017. A coating based on clove essential oils encapsulated by chitosan-myristic acid nanogel efficiently enhanced the shelf-life of beef cutlets. Food Packaging and Shelf Life 14: 137-145.
28. Rao, K. S. V. K., P. R. Reddy, Y. I. Lee, and C. Kim. 2012. Synthesis and characterization of chitosan--PEG--Ag nanocomposites for antimicrobial application. Carbohydrate Polymers 87 (1): 920-925.
29. Rodríguez, F. P., D. Campos, E. T. Ryser, A. L. Buchholz, G. D. Posada-Izquierdo, B. P. Marks, and E. Todd. 2011. A mathematical risk model for Escherichia coli O157: H7 cross-contamination of lettuce during processing. Food Microbiology 28 (4): 694-701.
30. Rota, M. C., A. Herrera, R. M. Mart\'\inez, J. A. Sotomayor, and M. J. Jordán. 2008. Antimicrobial activity and chemical composition of Thymus vulgaris, Thymus zygis and Thymus hyemalis essential oils. Food Control 19 (7): 681-687.
31. Sabaa, M. W., H. M. Abdallah, N. A. Mohamed, and R. R. Mohamed. 2015. Synthesis , Characterization and Application of Biodegradable Crosslinked Carboxymethyl Chitosan / Poly Vinyl. Materials Science & Engineering 56: 363-373. https://doi.org/10.1016/j.msec.2015.06.043.
32. Soleimanian, Y., S. A. H. Goli, J. Varshosaz, and S. M. Sahafi. 2018. Formulation and characterization of novel nanostructured lipid carriers made from beeswax, propolis wax and pomegranate seed oil. Food Chemistry 244: 83-92. https://doi.org/10.1016/j.foodchem.2017.10.010
33. Valenzuela, C., L. Abugoch, and C. Tapia. 2013. Quinoa protein-chitosan-sunflower oil edible film: Mechanical, barrier and structural properties. LWT-Food Science and Technology 50 (2): 531-537.
34. Wang, L. J., Y. Q. Hu, S. W. Yin, X. Q. Yang, F. R. Lai, and S. Q. Wang. 2015. Fabrication and characterization of antioxidant pickering emulsions stabilized by zein/chitosan complex particles (ZCPs). Journal of Agricultural and Food Chemistry 63 (9): 2514-2524. https://doi.org/10.1021/jf505227a.
35. Wang, X. H., D. P. Li, W. J. Wang, Q. L. Feng, F. Z. Cui, Y. X. Xu, M. van der Werf. 2003. Crosslinked collagen/chitosan matrix for artificial livers. Biomaterials 24 (19): 3213-3220.
36. Wei, Z., C. Wang, S. Zou, H. Liu, Z. Tong. 2012. Chitosan nanoparticles as particular emulsifier for preparation of novel pH-responsive Pickering emulsions and PLGA

microcapsules. Polymer 53 (6): 1229-1235. https://doi.org/10.1016/j.polymer.2012.02.015.
37. Wongkongkatep, P., K. Manopwisedjaroen, P. Tiposoth, S. Archakunakorn, T. Pongtharangkul, M. Suphantharika, J. Wongkongkatep. 2012. Bacteria Interface Pickering Emulsions Stabilized by Self-assembled Bacteria–Chitosan Network. Langmuir 28 (13): 5729-5736. https://doi.org/10.1021/la300660x.
38. Xiao, J., X. Wang, A. J. Perez Gonzalez, and Q. Huang. 2016. Kafirin nanoparticles-stabilized Pickering emulsions: Microstructure and rheological behavior. Food Hydrocolloids 54: 30-39. https://doi.org/10.1016/j.foodhyd.2015.09.008.
39. Yekdane, N., and S. A. H. Goli. 2019. Effect of Pomegranate Juice on Characteristics and Oxidative Stability of Microencapsulated Pomegranate Seed Oil Using Spray Drying. Food and Bioprocess Technology 12 (9): 1614-1625.
40. Zhang, S., Y. Zhou, C. Yang. 2015. Pickering emulsions stabilized by the complex of polystyrene particles and chitosan. Colloids and Surfaces A: Physicochemical and Engineering Aspects 482: 338-344.
41. Zhang, Y., L. Yang, Y. Zu, X. Chen, F. Wang, and F. Liu. 2010. Oxidative stability of sunflower oil supplemented with carnosic acid compared with synthetic antioxidants during accelerated storage. Food Chemistry 118 (3): 656-662.
42. Zhaveh, S., A. Mohsenifar, M. Beiki, S. T. Khalili, A. Abdollahi, T. Rahmani-Cherati, and M. Tabatabaei. 2015. Encapsulation of Cuminum cyminum essential oils in chitosan-caffeic acid nanogel with enhanced antimicrobial activity against Aspergillus flavus. Industrial Crops and Products 69: 251-256. https://doi.org/http://dx.doi.org/10.1016/j.indcrop.2015.02.028.
43. Ziaee, M., S. Moharramipour, and A. Mohsenifar. 2014. Toxicity of Carum copticum essential oil-loaded nanogel against Sitophilus granarius and Tribolium confusum. Journal of Applied Entomology 138 (10): 763-771.

نشریه ماشین‌های کشاورزی
جلد ۱۱، شماره ۱، نیمسال اول ۱۴۰۰، ص ۷۰-۵۵

Journal of Agricultural Machinery
Vol. 11, No. 1, Spring- Summer 2021, p. 55-70

مقاله علمی- پژوهشی

تأثیر روغن هسته انار کپسوله شده در نانوژل‌های کیتوزان-کاپریک اسید حاوی اسانس آویشن بر خواص فیزیکومکانیکی و ساختاری آبنبات ژله‌ای

حسین میرزائی مقدم[1*]، احمد رجائی[1]

تاریخ دریافت: ۱۳۹۸/۱۰/۱۱
تاریخ پذیرش: ۱۳۹۹/۰۳/۰۳

چکیده

روغن هسته انار (PSO) منبع شناخته شده‌ای از ترکیبات با ارزش است. بنابراین هدف از این مطالعه بررسی خواص فیزیکومکانیکی و ساختاری آبنبات ژله‌ای غنی شده با روغن هسته انار درون‌پوشانی شده در نانوژل‌های کیتوزان (CS)-کاپریک اسید (CA) حاوی اسانس آویشن (TEO) است. بدین منظور، در ابتدا نانوژل‌های کیتوزان-کاپریک اسید، با ایجاد پیوند آمید بین کیتوزان و کاپریک اسید تولید شدند که تصویر میکروسکوپ الکترونی روبشی (SEM) شکل کروی نانوژل‌های کیتوزان-کاپریک اسید را نشان داد. سپس امولسیون پیکرینگ روغن هسته انار با نانوژل کیتوزان-کاپریک اسید و اسانس آویشن درون‌پوشانی شده در نانوژل کیتوزان-کاپریک اسید پایدار شدند. نتایج نشان داد که حضور اسانس آویشن در ساختار نانوژل باعث ایجاد قطرات روغن کوچک‌تر شد. در ادامه از امولسیون‌های پیکرینگ در فرمولاسیون آبنبات ژله‌ای استفاده شد و متعاقباً ساختار میکروسکوپی، آنالیز بافت (TPA) و شاخص‌های رنگ آبنبات‌های ژله‌ای مورد بررسی قرار گرفت. استفاده از روغن هسته انار به‌صورت درون کپسوله شده، باعث کاهش جدا شدن روغن هسته انار از بافت آبنبات ژله‌ای شد. نتایج آزمون پروفایل بافت نشان داد که اگرچه نمونه‌های حاوی امولسیون روغن هسته انار، سختی (N۱۷۳/۴-۱۵۶/۶)، صمغی بودن (N۲۶۲/۱-۲۰۲/۲)، انسجام (۱/۳-۱/۵٪)، خاصیت ارتجاعی (N.s ۵۴/۷-۴۰/۲) و چسبندگی (N.s ۰/۴-۰/۲۹) کمتری نسبت به نمونه شاهد (N۲۵۰/۳، N۶۲۷/۹، N.s۱۶۰/۷، N.s۰/۶۳) داشتند، خاصیت فنریت آن‌ها (۰/۹۲-۰/۹۳٪) بیشتر از نمونه شاهد (۰/۷۹٪) بود. علاوه بر این، نتایج شاخص‌های رنگی نشان داد که نمونه‌های حاوی روغن هسته انار کپسوله شده باعث تغییر شاخص‌های رنگی نسبت به نمونه شاهد شد که این تغییر در حضور اسانس آویشن بیشتر بود.

واژه‌های کلیدی: آبنبات ژله‌ای، اسانس آویشن، خواص فیزیکومکانیکی و ساختاری، روغن هسته انار، کپسوله شده، نانوژل

۱- استادیار دانشکده کشاورزی، دانشگاه صنعتی شاهرود
(*- نویسنده مسئول: Email: hosseinsg@yahoo.com)

DOI: 10.22067/jam.v11i1.84882

Journal of Agricultural Machinery
Vol. 11, No. 1, Spring- Summer 2021, p. 71-81

نشریه ماشین‌های کشاورزی
جلد ۱۱، شماره ۱، نیمسال اول ۱۴۰۰، ص ۸۱-۷۱

Full Research Paper

Investigating the Effects of Qualitative Properties on Pears Dielectric Coefficient

M. J. Mahmoodi[1], M. Azadbakht[2*]

Received: 14-02-2020
Accepted: 23-05-2020

Abstract

Nowadays, the dielectric properties of food and biological products have become a valuable parameter in foodstuff engineering and coating technology, covering a remarkable spectral domain from 10^{-6} to 10^{12}. In the present study, 27 completely healthy pears were selected and subjected to quasi-static and dynamic loading. The storage period was ten days. In this study, the qualitative characteristics and their relationship with changes in dielectric coefficient were investigated. At the end of the storage period, the fruits' dielectric coefficient values and their qualitative characteristics were measured. The measurements were carried out for a capacitor plates' distance interval of 11 cm, 10 V input voltage and 60 kHz input voltage frequency. According to the results, in the dynamic loading mode of 400 N, the highest dielectric coefficient with a value of 5.2989 was obtained. In dynamic loading mode of 400 N, the qualitative property had the minimum value. The antioxidant, phenol content, Vitamin C content and firmness were 33.925%, 14.523 mg/100g, 5.7 mg/100g and 5.5333 g, respectively. The results of the study indicated that increasing the loading force on the pear reduces all qualitative indicators for all loading modes and an increase in dielectric coefficients of the products was observed.

Keywords: Dielectric, Nondestructive test, Pears, Quality, Qualitative properties

Introduction

Destructive methods are currently being applied for the evaluation of the internal quality attributes as well as the unique contents existent in fruits. However, the method is time-consuming, needful of specialized preparation of the specimens and non-applicable to the classification and sorting of fruits in commercial packages. Moreover, both the internal and external properties of fruits might be considerably different due to the differences in varieties, gardens, waste management methods, fruit maturation, and region. Thus, the large deal of changes in the quality attributes of the fruits from various varieties or even similar varieties has led to the development of nondestructive methods for the identification, [quality] prediction, and categorization of fruits in laboratories and rating them based on their qualities. These methods can usually predict and measure both the internal and external structure of fruits (Arendse *et al*., 2016).

The dielectric properties of food and biological products have become a valuable parameter in food engineering and technology. Dielectric spectrometry is an old instrument that is presently covering a remarkable spectral domain from 10^{-6} to 10^{12}. Dielectric spectrometry is a technique used for the study of the interaction between a matter of a type and the exerted electric field and it is extensively employed as an instrument for the recognition of the materials' senescence and error recognition for the insulation systems and it has consequently turned into a popular and powerful method. The method works based on polarity and electric conductance in materials and describes the interaction between a matter of a sort and the electromagnetic field. It examines the structural and physicochemical characteristics of such materials as water and soluble solids or the aqueous activities of a matter (Khaled *et*

1- MSc Graduated, Department of Bio-System Mechanical Engineering, Gorgan University of Agricultural Sciences and Natural Resources, Gorgan, Iran
2- Associate Professor of Department of Bio-System Mechanical Engineering, Gorgan University of Agricultural Sciences and Natural Resources, Gorgan, Iran
(*- Corresponding Author Email: azadbakht@gau.ac.ir)
DOI: 10.22067/jam.v11i1.85595

al., 2015). In an experiment on tomatoes, with increasing soluble solids, organic acids and parameters of tomato flavor determination, the amount of electrical conductivity increased. As the strength of the fruit tissue decreased, the amount of this factor increased. The results of regression analysis in this experiment showed that there was a significant correlation between the level of electrical conductivity and dependent variables including the weight of a fruit, soluble solids, absorbable acids and antioxidant capacity and phenols (Krauss *et al*., 2006). In a study on grape fruit, weight and moisture content parameters were measured during storage. The results showed that with increasing storage period from 0 to 10 days and temperature at 4 and 25 °C, weight and moisture content of grape samples decreased significantly in all cases (Khodamoradi and Ahmadi, 2019). Sipahioglu and Barringer (2003) measured the dielectric properties of 15 types of vegetables and fruits in 2450 MHz frequency and under the temperature range between 5 and 130°C. Equations were obtained as functions of temperature, moisture and water activity. Finally, it was concluded that the fruit moisture content was inversely related to the dielectric coefficient (Sipahioglu and Barringer, 2003). In another study, dielectric measurements were carried out during apples' maturity for finding the interrelationships of qualitative and dielectric properties. All the dielectric measurements were undertaken at 30°C from 500 MHz to 20 GHz. These experiments were carried out to make use of dielectric spectrometry for determining the maturity of the fruits. The results highlighted the good correlation between the intended index and dielectric index and it was pointed out as a nondestructive control method for forecasting the maturity of aquatic fruits like apples, bananas, mangoes and tomatoes (Fito *et al*., 2010). Guo *et al.* (2007) measured the dielectric properties of three fresh apple varieties in 24°C for 10 weeks and at 4°C in storage. The constant numerical correlation of the dielectric of fruits in a range of 10 MHz to 1800 MHz was calculated at 51 frequencies. Although there was a strong correlation between the dielectric coefficient and the soluble solids content and the dielectric coefficient of this relationship could be well predicted, no clear relationship was observed between the dielectric properties and the soluble solids content (Guo *et al*., 2007). Considering the time consuming and unusable in the subsequent stages for classification in order to commercialize and the need for specialized product in the evaluation of malware, the importance of the non-destructive evaluation of fruits was felt. By conducting this research and further research on this study, a comprehensive and non-destructive approach can be found to evaluate the qualitative properties of the fruit using their dielectric properties.

The objective of the present study is the investigation of the effect of pears' qualitative properties on their dielectric coefficient following the exertion of quasi-static and dynamic loading in various amounts. The dielectric coefficient was measured after applying quasi-static and dynamic loading and storage period for ten days using capacitive technique. The distance between the capacitor plates, input voltage, frequency and the orientation of the fruit were specified. Then, methods pertinent to qualitative properties measurement were utilized to obtain the antioxidant percentage, phenol and vitamin C contents and firmness of the pears, Spadana variety.

Materials and Methods

Sample preparation

Pears from Spadana variety were obtained from markets in Golestan-Gorgan province, Iran. The samples were then transferred to the laboratory of Gorgan University of Agricultural Sciences and Natural Resources. It was also placed in the oven to measure the amount of moisture content. According to Equation (1), 40 g of samples were placed in an oven at 105°C for 5 hours and then their moisture content was measured (Jahanbakhshi *et al.*, 2019). The moisture content of pears was measured as 77.92%**.** Environmental conditions for testing were conducted at a

temperature of 18°C and relative humidity of 72%.

$$MC = \frac{M_W - M_D}{M_W} \times 100 \quad (1)$$

Where, M_W=Initial mass of fruit (g), M_D=Mass of dried fruit (g), MC=Moisture content of the fruit, wet basis (%)

Quasi-static test

In order to perform the wide and thin-edge compression mechanical test, a pressure-deformation device (the Santam Indestrone-STM5- Made in Iran) with a load cell of 500 N was employed. Two circular plates were used for compression testing. This test was performed at a speed of 5 mm min^{-1} with three forces of 70, 100 and 130 N with three replications (Figure 1). For this experiment, the pear was placed horizontally between the two plates and pressed and the measurement time of this process was recorded. It was also designed to conduct a double-jaw thin edge test that a plastic object with a rectangular cross-section measuring 0.3 cm×1.5 cm at 5 mm min^{-1} with three forces of 15, 20 and 25 N was used in three replications. By moving the movable jaw, the pressure operation was carried out until the force reached the desired level (Razavi *et al*., 2018).

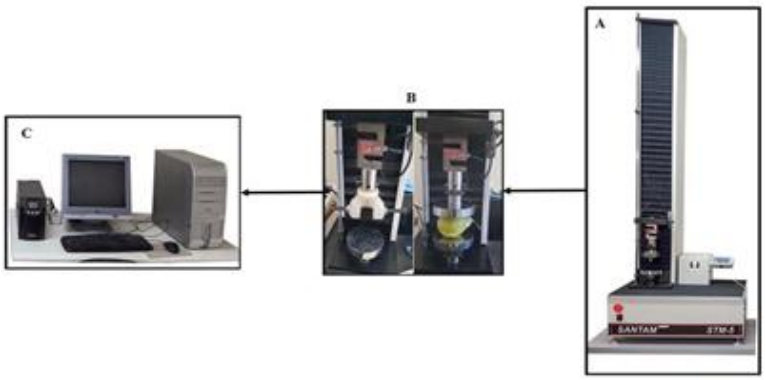

Fig.1. Static quasi-load diagram of pear
A: The force-deformation device (Indestrone); B: Jaw's wide-edges and thin-edges; C: Computer

Impact test

At first, the pendulum device and the required weights were made at the workshop of the Gorgan Biosystem engineering department (Figure 2). Then the fruits were placed in the desired place and the arm of the machine has been raised to the desired angle (90 degrees) and in the controlled state, the arm is dropped and the pear is hit. The pendulum had an arm of 200 g and three different connecting weights of 100, 150 and 200 g to hit. The air resistance and friction is ignored (Barriga-Téllez *et al*., 2011).

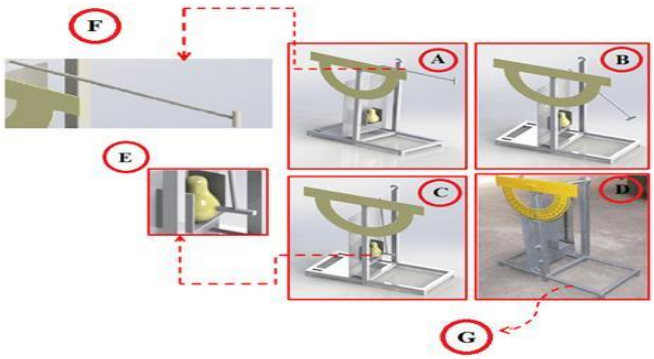

Fig.2. Schematic of the impact machine
A: Pendulum at a 90° angle; B: Walking along the path; C: Collapse pendulum to pear; D: Main device profile; E: Place the pear; F: Pendulum blow; G: the base of the device

Dielectric constant measurement mechanism

Two capacitive plates of aluminum were chosen because the metal is not oxidized in the vicinity of moisture and air, and is stable. For this reason, the measurement does not have an unpleasant effect. The capacitor plate was selected for a 10×10 cm^2 dimension so that the pears could be wholly placed therein. The capacitor body was designed and selected so as to allow adjustment of the distance between the capacitor plates. The device was made of plastic in its body so as not to influence the electric field. Experiments were conducted in 8.7°C and a relative humidity of 81% (Soltani *et al*., 2010).

Measuring circuit

Figure 3 shows the used circuit. The input power to the system was increased by a frequency of 50 Hz, up to 60 kHz, by increasing the frequency vibration. The input voltage was also 10 V, the distance between the capacitor plates was 11 cm. After placing the pears between the two capacitors, the two-head magnetic voltage was measured with a multi meter equipped with a Compact digital multi-meter ST-941 specification, and then related relationships were used.

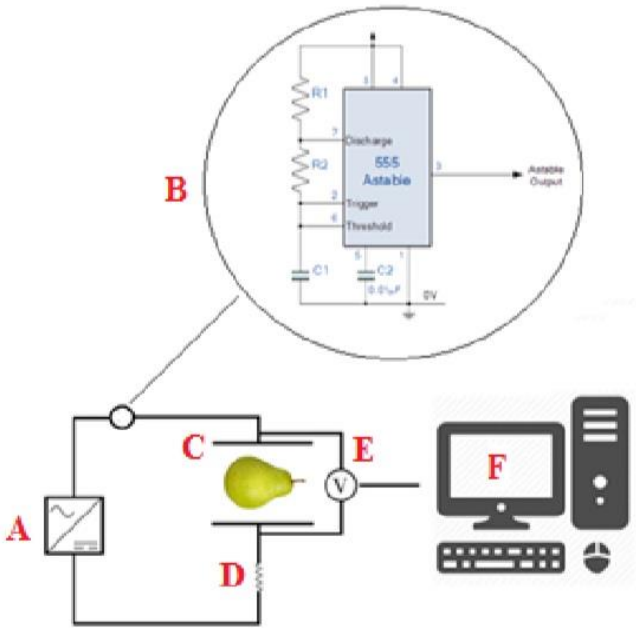

Fig.3. The circuit used in the experiment
A. Power supply; B. Conversion circuit; C. Capacitor plates; D. Resistance; E. Multi meter; F. Computer

The capacitive sensor's capacity was calculated using Equation (2) for this circuit (Soltani and Alimardani, 2011).

$$C = \frac{1}{2\pi Rf}\frac{V_0}{\sqrt{V_i^2 - V_0^2}} \quad (2)$$

Where, C= Capacitance (F), R= Resistance value (Ω), f= Frequency input voltage (Hz), V_i= Input voltage (v), V_0= Output voltage (v).

Equation (3) was applied to obtain the equivalent dielectric constant (Soltani and Alimardani, 2011).

$$K = \frac{C}{C_0} = \frac{V_0}{V_0'}\frac{\sqrt{V_i^2 - V_0'^2}}{\sqrt{V_i^2 - V_0^2}} \quad (3)$$

Where, K=Equivalent dielectric constant, C= Capacitor capacity with fruit (F), C_0= Capacitor capacity without fruit (F), V'_0= Sensor output voltage without fruit (v).

The values obtained in the above relations were subject to air presence between the plates and the Equation (4) was used to obtain the dielectric constant of the fruit sizes (Soltani and Alimardani, 2011).

$$e^{k_b} = e^{ka} + e^{kb} + e^{kv} \quad (4)$$

Where, K_b= Dielectric constant of fruit, K= Equivalent dielectric constant, a= Fruit volume ratio to capacitor volume, b= Fruit length ratio to capacitor length, v= Fruit thickness ratio to distance between capacitor plates.

Biochemical properties measurement

To measure the total phenol content and the percentage of free radicals' neutralization, specimens equal to 0.5 g of each sample's wet callus were ground and homogenized using 5 ml of methanol 80% (for a 1:10 ratio) in a cold mortar. The homogenized mixture was placed on a shaker device in a dark room for 24 hours and then subjected to the centrifugal force in 3000 rpm for 5 min. The upper part of the extract was used for measuring the biochemical characteristics.

Percentage of free radicals neutralization based on DPPH method

In this experiment, the percentage of DPPH free radical neutralization was measured based on the method proposed by Bandet *et al.* (1997). At first, 2 ml of DPPH with a concentration of 0.1 mmol (4 mg of DPPH in 100 ml of methanol) was admixed to the experiment tube and 2 ml of the prepared methanolic solution was next added thereto following which the experiment tubes were placed in a dark environment and the absorption rates were immediately read using spectrophotometer in 517 nm wavelength. The evidence specimen contained 2 ml of DPPH and 2 ml of methanol. Methanol was applied to calibrate the spectrophotometer. The figures outputted from Equation (5) substitutions were converted to neutralization percentages (Li *et al*., 2012).

$$DPPH = \frac{A_C - A_S}{A_C} \times 100 \quad (5)$$

As= specimens absorption rates

Ac= evidence specimen absorption rate

Total phenol

Folin-Ciocalteu (F-C) reaction was used to measure the total phenol content. To do so, 20 µl of methanolic extract (0.5 g in 5ml 80% methanol) was mixed with 100 µl of F-C and 1.16 ml of distilled water following which 300 µl of 1molar sodium carbonate (10.6 g in 100 ml of distilled water) was added thereto after 8 min resting time. The aforesaid solution was placed in a vapor bath, 40°C, in a dark room for 30 minutes. In the end, the specimens were read in 765 nm wavelength. The absorption number of the specimen was replaced for y in the line equation to obtain the phenol amount (x) in milligram Gallic acid per gram (Jaramillo-Flores *et al.*, 2003).

Vitamin C

Vitamin C was calculated using 2, 6-dichlorophenol indophenol titration method in such a manner that 5 g of sample was mixed and extracted using 40 ml of citric acid 8% in the first stage. Then, 10 ml of the filtered extract was picked up and mixed with 40 ml of citric acid 8% and subjected to titration using 2, 6-dichlorophenol indophenol reagent. The termination point of titration was the appearance of a pale purple that lasted for about 15 s. The vitamin C amount is expressed in milligram per 100 g of the sample weight. The vitamin C amount can be obtained by Equation (6) (Jaramillo-Flores *et al.*, 2003).

$$\text{Vitamin C} = \frac{sample\ weight \times standard\ volume\ of\ \ reagent\ consumed}{volume\ of\ extract\ obtained \times volume\ of\ reagent\ used \times 10 \times 2} \quad (6)$$

Firmness

A barometer device or penetrometer, Model EFFEGI, made in Italy, was used to measure the firmness of the flesh of pear specimens without having their skin peeled through the exertion of pressure in grams. According to the extant guidelines, the penetrometer probe was placed on the intended part of the pear which was next subjected to the required pressure, so that the probe could enter the fruit flesh and then the displayed value indicating the fruit firmness was read from the barometer gauge and recorded.

Statistical analysis

27 pears were selected without any bruising. The samples were exposed to three levels of quasi-static loads of wide-edge and thin-edge and impact dynamic load and in a storage room for 10 days. Then, dielectric coefficient measurement was carried out and the intended qualitative properties were measured immediately afterward.

Subsequently, the qualitative properties of pear samples, including antioxidants, phenol content, vitamin C, and firmness were measured.

The entire experiments were replicated thrice and the results were analyzed in SAS software using factorial test within a complete randomized block design.

Results and Discussions

Table 1 presents the results of variance analysis of the effect of the various amounts of the forces exerted on the dielectric coefficient of pear for wide-edge and thin-edge static compression and impact dynamic compression modes. According to Table 1, it can be concluded that the effect of the forces on the dielectric coefficient is indicative of significant differences in all three loading states in a 1% level.

Table 1-variance analysis of dielectric coefficient subject to various loading

		Variable	DF	Mean squares	F-value
Static loading	**Wide-edge pressure**	**Loading force**	2	0.0117	144876**
	Thin-edge pressure	**Loading force**	2	0.0327	185501**
Dynamic loading	**Impact mode**	**Loading force**	2	0.0089	292755**

** Significant difference at 1% level (p <0.01)

Quasi-static loading mode

Wide-edge compression

Figure 4 exhibits the effect of loading force on the amounts of qualitative properties and dielectric coefficients in wide-edge compression. According to the obtained results for the ten-day storage period, the increase in the force causes reductions in the Vitamin C, firmness, phenol, and antioxidant values.

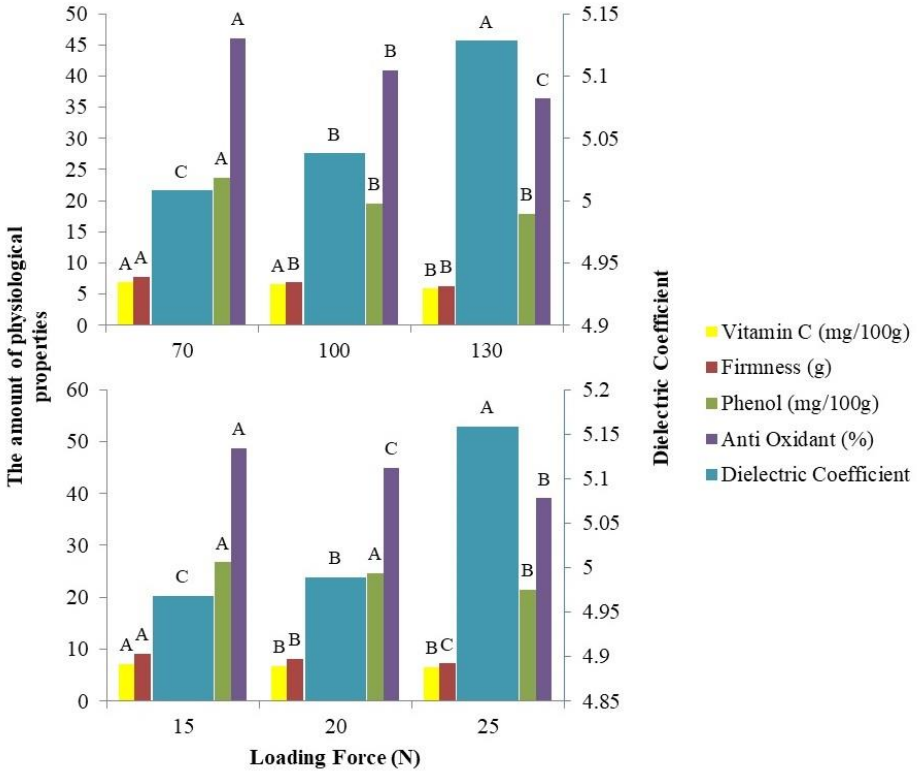

Fig.4. The effect of loading forces on the qualitative properties and the dielectric coefficient in wide-edge compression and thin-edge compression
Similar letters of every property indicate the absence of significant difference.

Vitamin C level did not decrease in 70 N and 100 N forces but it was significantly decreased in 130 N in contrast to the other two compressive forces exerted. The firmness of the pears was significantly decreased with the increase in the compressive force from 70 N to 100 N but no significant reduction was observed in 130 N compressive force. The increase in the exerted compressive force from 70 N to 100 N caused a significant reduction in the phenol content but an insignificant reduction in phenol content reduction was observed with the increase in the compressive force from 100 N to 130 N. As for the amount of existent antioxidant, a significant reduction was documented for all of the exerted compressive forces with the increase in the amount thereof.

Thin-edge compression

Vitamin C content significantly reduced as the compression force increased from 15 N to 20 N and an insignificant reduction was evidenced in 25 N compression force as compared to the two prior modes. Significant reduction in the fruit firmness was documented in thin-edge compression following the increase in the loading force for all of the three modes. No significant reduction was scored for the 15 N and 20 N compression forces in firmness but the increase in the force to 25 N caused a significant reduction in firmness; furthermore, the increase in the compression force was found reducing the antioxidant activities for all of the three loading modes.

Dynamic impact mode

Figure 5 demonstrates the significance of the loading forces on the qualitative properties in dynamic impact mode. According to the results obtained for the ten-day storage period, the increase in the loading force causes reductions in Vitamin C, phenol and antioxidant values.

Vitamin C amount is insignificantly reduced in 300 N and 350 N compression but the increase in the compression up to 400 N causes significant reductions in the fruit contents such as antioxidant activity percentage. The fruit firmness and phenol content significantly decreased in all the loading levels.

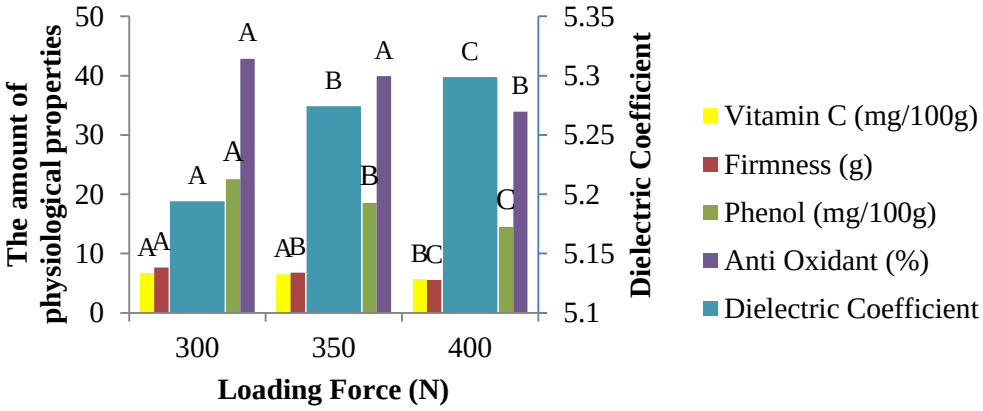

Fig.5. The effect of loading forces on the qualitative properties and the dielectric coefficient in dynamic impact mode

Similar letters of every property indicate the absence of significant difference.

Quasi-static loading mode

Wide-edge compression

In regard to the percentage of antioxidant existing in the fruits for all of the force levels exerted, the increase in the compressive force was found causing a significant reduction. Generally, the increase in the wide-edge compression brought about reductions in the Vitamin C, firmness, phenol, and antioxidant values. Such findings can be attributed to the increase in the rottenness for such a reason as the increase in the amount of exerted load and the resultant increase in the decaying of the fruit, destruction of the cells featuring food value and containing minerals (Altisent, 1991). Similar results were also found in experiments on cherries for which case it has been shown that a reduction in antioxidant capacity comes about with the pass of more time since storage date (Navgaran *et al.,* 2014). It was also observed that the increase in the compression force causes an increase in the dielectric coefficient for such a reason that the moisture content is more reduced in the higher loading forces and that there is an inverse relationship between the moisture content and the dielectric coefficient (Funebo and Ohlsson, 1999).

It can be discerned from the above-presented results that the increase in the amount of compression force causes a reduction in the qualitative properties followed by a significant increase in dielectric coefficient (Krauss *et al.*, 2006).

Thin-edge compression

Figure 4 displays the significance of the effect of loading forces on the qualitative properties in thin-edge compression. According to the results obtained for the ten-day storage period, the increase in the loading forces brings about reductions in Vitamin C, firmness, phenol and antioxidant values. It was observed in a similar study on tomatoes that the increase in the rot values causes a reduction in the Vitamin C content (Moretti *et al*., 1998). The reduction in Vitamin C content subject to loading can be attributed to the reduction in fruit moisture and the resultant oxidation and reduction of the Vitamin C content. Similar results have also been found in the studies by other researchers on Kiwi (Tavarini *et al*., 2008; Amodio *et al*., 2007).

Moreover, the figure illustrates the effect of loading force on the dielectric coefficient and it can be accordingly concluded that the increase in the thin-edge compression causes a significant increase in the dielectric coefficient. In addition, the increase in the dielectric coefficient following the increase in the compression force is due to the reduction in the moisture content in the loading forces (Funebo and Ohlsson, 1999).

Based on the abovementioned results, it can be understood that the increase in the loading force in the thin-edge static mode causes a reduction in the qualitative properties followed by an increase in the dielectric coefficient (Krauss *et al.*, 2006).

Dynamic impact mode

The reason for the obtained results regarding the reduction in phenol content can be attributed to the releasing of most of the phenolic ingredients as a result of the increase in the percentage of the damage subject to loading forces that has appeared in the form of fruit tissue browning and the subsequent reduction in the phenolic content of the fruit (Li *et al*., 2012). The figure is additionally reflective of the loading forces' effects on dielectric coefficient and it can be seen that the increase in the dynamic loading force causes reductions in the qualitative properties during the ten-day storage period.

According to the above-cited results pertaining to the dynamic loading, it can be concluded that the increase in the dynamic loading force causes a reduction in the qualitative properties' values following which the dielectric coefficient is significantly increased.

Conclusions

The present study investigated the effect of qualitative properties variations resulting from the exertion of various external loads on the dielectric coefficient value. The experiment results indicated that the qualitative properties variations are effective on the dielectric coefficient values in such a manner that the increase in the loads exerted onto the fruits

brings about reduction in all of the intended values of the qualitative properties including phenol, antioxidant, vitamin C and firmness following which dielectric coefficient was found increased in all of the cases. Generally, it can be concluded in an investigation of the obtained results under similar conditions that the qualitative properties' levels are reduced in thin-edge, wide-edge and impact loading, respectively, following which the dielectric coefficient is inversely increased. So, it can be concluded that the measurement of dielectric coefficient as a non-destructive test provides for the prediction of the increase or decrease in the qualitative properties of the pears. The higher the dielectric coefficient, the lower the qualitative properties. The proper nutritional quality of the pears can be figured out through devising an appropriate scale for the measurement of the changes in the future experiments.

References

1. Altisent, M. R. 1991. Damage Mechanisms in the Handling of Fruits. Progress in agricultural physics and engineering. John Matthew (Ed). Common Wealth Agricultural Bureaux (CAB) International, Willingford, UK. 231-257.
2. Amodio, M. L., G. Colelli, J. K. Hasey, and A. A. Kader. 2007. A comparative study of composition and postharvest performance of organically and conventionally grown kiwifruits. Journal of the Science of Food and Agriculture 8: 1228-1236. https://doi.org/10.1002/jsfa.
3. Arendse, E., O. A. Fawole, L. S. Magwaza, and U. L. Opara. 2016. Non-destructive characterization and volume estimation of pomegranate fruit external and internal morphological fractions using X-ray computed tomography. Journal of Food Engineering 186: 42-49. https://doi.org/10.1016/j.jfoodeng.2016.04.011.
4. Barriga-Téllez, L. M., M. G. Garnica-Romo, J. I. Aranda-Sánchez, G. A. Correa, M. C. Bartolomé-Camacho, and H. E. Martínez-Flores. 2011. Nondestructive tests for measuring the firmness of guava fruit stored and treated with methyl jasmonate and calcium chloride. International Journal of Food Science & Technology 46: 1310-1315. https://doi.org/10.1111/j.1365-2621.2011.02633.x
5. Fito, P., M. Castro-Giráldez, P. J. Fito, and C. Chenoll. 2010. Development of a dielectric spectroscopy technique for the determination of apple (Granny Smith) maturity. Innovative Food Science & Emerging Technologies 11: 749-754. https://doi.org/10.1016/j.ifset.2010.08.002.
6. Funebo, T., and T. Ohlsson. 1999. Dielectric properties of fruits and vegetables as a function of temperature and moisture content. Journal of Microwave Power and Electromagnetic Energy 34: 42-54.
7. Guo, W. chuan, S. O. Nelson, S. Trabelsi, and S. J. Kays. 2007. 10-1800-MHz dielectric properties of fresh apples during storage. Journal of Food Engineering 83: 562-569. https://doi.org/10.1016/j.jfoodeng.2007.04.009.
8. Jahanbakhshi, A., R. Yeganeh, G. Shahgoli. 2019. Determination of mechanical properties of banana fruit under quasi-static loading in pressure, bending, and shearing tests. International Journal of Fruit Science 1-9.
9. Jaramillo-Flores, M. E., L. González-Cruz, M. Cornejo-Mazón, L. Dorantes-álvarez, G. F. Gutiérrez-López, and H. Hernández-Sánchez. 2003. Effect of Thermal Treatment on the Antioxidant Activity and Content of Carotenoids and Phenolic Compounds of Cactus Pear Cladodes (Opuntia ficus-indica). Food Science and Technology International 9: 271-278. https://doi.org/10.1177/108201303036093.
10. Khaled, D. El, N. Novas, J. A. Gazquez, R. M. Garcia, and F. Manzano-Agugliaro. 2015. Fruit and vegetable quality assessment via dielectric sensing. Sensors. 15: 15363-15397.
11. Khodamoradi, S., and E. Ahmadi. 2019. Effect of Chitosan Coating on Physical, Mechanical and Chemical Properties of Grapes During Storage. Journal Agriculture Machinery 9: 347-364.

(In Farsi).
12. Krauss, S., W. H. Schnitzler, J. Grassmann, and M. Woitke. 2006. The influence of different electrical conductivity values in a simplified recirculating soilless system on inner and outer fruit quality characteristics of tomato. Journal of Agricultural and Food Chemistry 54: 441-448.
13. Li, W. L., X. H. Li, X. Fan, Y. Tang, and J. Yun. 2012. Response of antioxidant activity and sensory quality in fresh-cut pear as affected by high O2active packaging in comparison with low O2packaging. Food Science and Technology International 18: 197-205. https://doi.org/10.1177/1082013211415147.
14. Moretti, C. L., S. A. Sargent, D. J. Huber, A. G. Calbo, and R. Puschmann. 1998. Chemical composition and physical properties of pericarp, locule, and placental tissues of tomatoes with internal bruising. Journal of the American Society for Horticultural Science 123: 656-660.
15. Navgaran, K. Z., L. Naseri, and M. Esmaiili. 2014. Effect of packaging material containing nano-silver and silicate clay particles on postharvest. Journal of Food Researches 24: 89-102.
16. Razavi, M. S., A. Asghari, M. Azadbakh, and H. A. Shamsabadi. 2018. Analyzing the pear bruised volume after static loading by Magnetic Resonance Imaging (MRI). Scientia Horticulturae 229: 33-39. https://doi.org/10.1016/j.scienta.2017.10.011.
17. Sipahioglu, O., and S. A. Barringer. 2003. Dielectric properties of vegetables and fruits as a function of temperature, ash, and moisture content. Journal of Food Science 68: 234-239. https://doi.org/10.1111/j.1365-2621.2003.tb14145.x.
18. Soltani, M., R. Alimardani, and M. Omidi. 2010. Prediction of banana quality during ripening stage using capacitance sensing system. Australian Journal of Crop Science 4: 443-447.
19. Soltani, M., R. Alimardani, and M. Omidi. 2011. A Feasibility Study of Employing a Capacitance Based Method in Banana Ripeness Recognition. Iran Journal Biosystem Engineering
20. Tavarini, S., E. Degl'Innocenti, D. Remorini, R. Massai, and L. Guidi. 2008. Antioxidant capacity, ascorbic acid, total phenols and carotenoids changes during harvest and after storage of Hayward kiwifruit. Food Chemistry 107: 282-288. https://doi.org/10.1016/j.foodchem.2007.08.015.

نشریه ماشین‌های کشاورزی
جلد ۱۱، شماره ۱، نیمسال اول ۱۴۰۰، ص ۸۱-۷۱

Journal of Agricultural Machinery
Vol. 11, No. 1, Spring- Summer 2021, p. 71-81

مقاله علمی-پژوهشی

تاثیر خواص فیزیولوژیکی گلابی بر مقدار ضریب دی‌الکتریک میوه

محمدجواد محمودی[۱]، محسن آزادبخت[۲*]

تاریخ دریافت: ۱۳۹۸/۱۱/۲۵
تاریخ پذیرش: ۱۳۹۹/۰۳/۰۳

چکیده

امروزه خواص دی‌الکتریک محصولات غذایی و بیولوژیکی به پارامتری ارزشمند در مهندسی مواد غذایی و فناوری تبدیل شده است که محدوده طیفی فوق‌العاده‌ای از 10^{-6} تا 10^{12} هرتز را پوشش می‌دهد. در این تحقیق ابتدا تعداد ۲۷ گلابی کاملاً سالم به‌وسیله آزمون غیرمخرب سی‌تی اسکن انتخاب و سپس تحت بارگذاری شبه‌استاتیکی و دینامیکی قرار گرفتند و انبارداری ۱۰ روزه به‌منظور بررسی میزان خواص فیزیولوژیکی و ارتباط آن با تغییرات ضریب دی‌الکتریک انتخاب شد. در پایان دوره انبارداری مقدار ضریب دی‌الکتریک میوه‌ها و پس از آن مقدار خواص فیزیولوژیکی آن‌ها اندازه‌گیری شد. اندازه‌گیری‌ها در فاصله صفحات خازن ۱۱ سانتی‌متری، ولتاژ ورودی ۱۰ ولت، فرکانس ولتاژ ورودی ۶۰ کیلوهرتز انجام شد. طبق نتایج حاصل شده حالت بارگذاری دینامیکی ۴۰۰ نیوتنی دارای بیشترین ضریب‌دی‌الکتریک در بین همه حالت‌های بارگذاری با مقدار ۵/۲۹۸۹ و به دنبال آن این حالت بارگذاری دارای کمترین مقادیر خواص فیزیولوژیکی در بین تمام حالت‌های بارگذاری با مقادیر آنتی‌اکسیدان ۳۳/۹۲۵ درصد، محتوای فنلی ۱۴/۵۲۳ و ویتامین C 5.7 میلی‌گرم بر ۱۰۰ گرم و سفتی ۵/۵۳۳۳ گرم بود. نتایج آزمایش‌ها نشان دادند که با افزایش مقدار نیروی بارگذاری بر روی میوه گلابی، همه مقادیر خواص فیزیولوژیکی مورد نظر در تمام موارد بارگذاری کاهش یافته و در نهایت، مقدار ضریب دی‌الکتریک محصول افزایش می‌یابد.

واژه‌های کلیدی: آزمون غیرمخرب، خواص کیفی، دی‌الکتریک، کیفیت، گلابی

۱- دانش‌آموخته کارشناسی ارشد، گروه مهندسی مکانیک بیوسیستم، دانشگاه علوم کشاورزی و منابع طبیعی گرگان، گرگان، ایران
۲- دانشیار گروه مهندسی مکانیک بیوسیستم، دانشگاه علوم کشاورزی و منابع طبیعی گرگان، گرگان، ایران
(*- نویسنده مسئول: Email: azadbakht@gau.ac.ir)

DOI: 10.22067/jam.v11i1.85595

Journal of Agricultural Machinery
Vol. 11, No. 1, Spring- Summer 2021, p. 83-95

نشریه ماشین‌های کشاورزی
جلد ۱۱، شماره ۱، نیمسال اول ۱۴۰۰، ص ۹۵-۸۳

Full Research Paper

Degree-Day Index for Estimating the Thermal Requirements of a Greenhouse Equipped with an Air-Earth Heat Exchanger System

H. Faridi[1], A. Arabhosseini[2*], Gh. Zarei[3], M. Okos[4]

Received: 06-04-2020
Accepted: 20-07-2020

Abstract

In this research, an attempt was made to utilize an Earth-Air Heat Exchanger (EAHE) system as a source of shallow geothermal energy to provide thermal demands of a commercial greenhouse located in Alborz province, Iran. The degree-day index was applied to estimate the EAHE system's potential to meet the thermal requirements of the greenhouse including cooling and heating demands. The results indicated that this region needed more energy to reach to the relevant temperature inside the greenhouse for the heating demand comparing to the cooling one. The average potential of the EAHE system based on the degree-day index was 10.76ºC for increasing temperature in the cold and 17.96ºC for decreasing temperature in the warm season. This means that the EAHE system was capable of supplying the greenhouse thermal demands in this area according to the calculated values of Heating Degree-Day (HDD) and Cooling Degree-Day (CDD). This method would be beneficial in monitoring and optimizing plant growth conditions as the best crop type or cultivation selection which in turn can help in irrigation and fertigation management of the crop grown.

Keywords: Degree-Day, Heat exchanger, Geothermal, Greenhouse

Introduction

In 1973, the oil shocks increased the considerable importance of energy and forced the world toward other energy sources and their optimal consumption. Alternative policies, energy efficiency, and the achievement of sophisticated technologies were the strategies taken by different countries, especially developed countries, to address the energy resource shortage challenge (Franczak, 2017; Faridi *et al.*, 2019a). For this reason, the optimal use of energy resources in the process of economic development has always been considered as a vital objective in sustainable development. The renewable or environmentally friendly energies such as solar, wind, geothermal, etc. are suggested to prevent the more tremendous impact of these harms. Among all renewable energies, the geothermal one can offer a valuable source of thermal energy for a building because it is not limited to season, time, and conditions. At present, this renewable energy source is used to generate electricity at a significant scale as well as for direct applications like environmental heating, greenhouses and aquaculture (Dreidy *et al.*, 2017).

The closer to the depth of the earth, the fewer changes occur in the earth's temperature during the year, so that from a depth of 1.5 to 2 meters from the surface of the earth, temperature fluctuations throughout the year are negligible (Sehli *et al.*, 2012; Bisoniya 2015). This near-constant temperature at this depth is called Earth's Undisturbed Temperature (EUT). In fact, the earth capacity is considered as a passive method for the purpose of heating and cooling buildings. For the effective use of the thermal capacity of the earth, a heat exchanger system should be created which usually uses a various arrangement of buried pipes along the length

1- PhD, Department of Biosystems Engineering, College of Aburaihan, University of Tehran, Tehran, Iran
2- Associate Professor, Department of Agrotechnology, College of Aburaihan, University of Tehran, Tehran, Iran
3- Associate Professor, Agricultural Engineering Research Institute (AERI), Agricultural Research, Education and Extension Organization (AREEO), Karaj, Iran
4- Full Professor, Department of Agricultural & Biological Engineering, Purdue University, West Lafayette, USA
(*- Corresponding Author Email: ahosseini@ut.ac.ir)
DOI: 10.22067/jam.v11i1.86233

of a building, or vertically on the ground. The concept of Earth-Air Heat Exchanger (EAHE) is quite simple. As observed in Figure 1, in the summer, a rotating environment (water or air) is operated to extract heat from the building and transfer it to the ground and inversely in the winter from the same rotating medium to extract heat from the ground and transfer it to the building (Sehli *et al.*, 2012; Ciriaco *et al.*, 2020). Geothermal energy can be employed as an EAHE system for the inactive cooling in greenhouses exerting renewable energies (Abbaspour-Fard *et al.*, 2011; Faridi *et al.*, 2019b). In tropical and semi-tropical countries, the development of heat exchangers has been widely studied in greenhouses in different climates such as South Asia (Misra *et al.*, 2013).

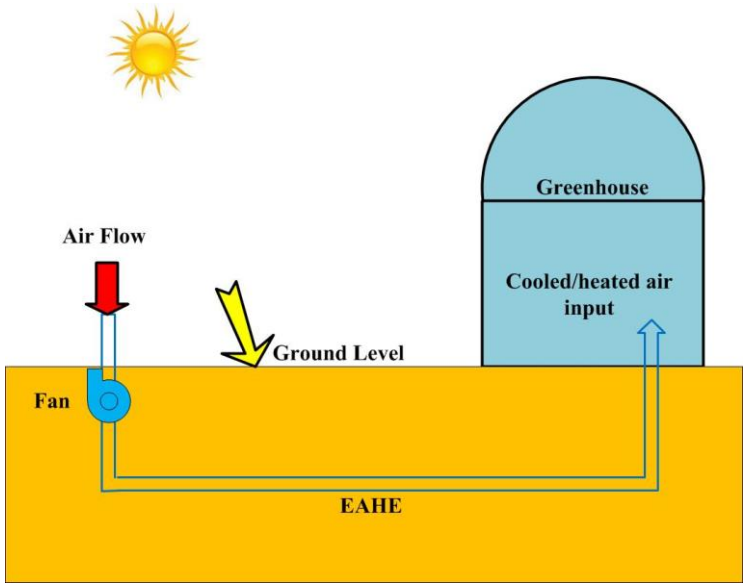

Fig.1. Simple concept of the EAHE system with the aim of heating and cooling a closed space

The arid climate of Iran, the shortage of rainfall, as well as high evapotranspiration rate, has struck the country with severe water scarcity (Amiri and Eslamian, 2012). As a result, greenhouse production can be a worthy choice for reducing water consumption compared to outdoor production (Kabeel and El-Said, 2015). However, energy consumption in greenhouses is higher than traditional ones to provide the necessary environmental conditions (heating, cooling, ventilation, etc.) and has made the energy consumption as a crucial challenge (Mongkon *et al.*, 2014). On the other hand, the energy essential management in greenhouses performs a critical role in the sustainable development of agriculture (Vadiee and Martin, 2014). Supplying the demands of heating, cooling and ventilation in greenhouses are dependent of external weather conditions. The use of climate information during the design or management of heating, cooling and ventilation systems for the greenhouse will be useful for easily obtaining more accurate and realistic results (Yucel *et al.*, 2014; López-Aguilar *et al.*, 2020).

Climate conditions are the primary factors influencing on the energy consumption in producing greenhouse crops in a region, so that it is possible to scientifically investigate the climate history (minimum/maximum biological temperature) of the region for certain periods and identify the conditions necessary for cultivating the desired crops regarding to the reduction of energy consumption. One of the factors used to check the weather history of a region is the degree-day index (Day, 2016; Zheng *et al.*, 2020). Changes in this index will carry out a substantial role in environmental issues, including the intensity of energy consumption for heating and cooling of the

environment (Roshan and Grab, 2012; Day, 2016). The sum of degree-days from an appropriate start date is expended for crop production plan, pest management, scheduling pest and energy consumption control and related objectives. A degree-day is calculated as a functional integral of time that changes in general with air temperature (Verbai *et al.*, 2014; Moreno *et al.*, 2014). This function reduces the deviations of temperature from the optimal temperature thresholds changed by components or the range for which the air conditioner is appropriate (Ciulla *et al.*, 2015; Goff, 2015; Way, Lewkowicz and Bonnaventure, 2017). In other words, measuring the average temperature of the air using the threshold temperature is called degree-day. These temperature thresholds for calculating the cooling and heating day depend on the specific objectives that can vary according to the type of research and location being studied (Romanovskaja and Baksiene, 2011; Mourshed, 2012). Identifying the areas susceptible to agriculture based on the recognition of natural potential can play a major role in environmental and land use planning, while providing suitable grounds for human activities (Romanovskaja and Baksiene, 2011). Climate is a determinant factor in the distribution of plants and their physiological and phonological processes (Mideksa and Kallbekken, 2010).

Significant increase in total energy consumption will more appreciably increase extention of the necessity of continuity and acceleration in energy efficiency measures in the energy supply and demand. The first step in this field is accurate calculations based on the region's climatic conditions.

The continuation of this process will lead to a dependence of the country on energy imports. In recent years, climate policy in the energy sector has been more extremely limited to reduce emissions (Ebinger and Vergara, 2011; Schaeffer *et al.*, 2012). However, knowing about the adaptation and vulnerability of the energy sector to climate and spatial changes can lead to an understanding of the energy management and efficiency (Marimon *et al.*, 2020). As the heat dissipation of the building is directly proportional to the difference between the internal and external air of the building, the energy consumption of a building over a period of time is related to the total temperature difference in this period. Therefore, it is necessary to obtain sufficient knowledge of the spatial variations of the heating and cooling needs in a region to better manage energy. The degree-day computing techniques depend on spatial data.

There are numerous studies reported about the application of degree-day index by researchers. Jiangsu district heating and cooling day trend were studied by Jiang *et al.* (2009). An alternative modelling presented to estimate the amount of energy needed for heating and cooling of greenhouse products (Papakostas *et al.*, 2009). Rehman *et al.* (2011) calculated the monthly and annual heating and cooling requirements of industries in five coastal cities of Saudi Arabia with temperature thresholds of 13, 18, 20 and 24ºC. Chai *et al.* (2011) compared the interpolated models in the zoning and temperature estimation of China's Xinjiang province. Marimon *et al.* (2020) studied a support system based on degree-day index to start fungicide spray programs for peach powdery mildew.

In most cases, the enormous expenses in greenhouse production belong to the energy consumption for cooling in summer and heating in winter (Ghasemi Mobtaker *et al.*, 2017). There is a possibility of break in fuel and electricity supply at the peak times of energy consumption. Plants in the greenhouse are sensitive to temperature shocks, so any disruption or shortage in energy supply causes severe problems and sometimes with consequential damages. The EAHE system could represent as an alternative for such cases to decrease the risks. The knowledge about the potential of EAHE system and the degree-day are useful for the grower to select an agricultural production, which fits better to energy balance during the production period.

The objective of this study is to investigate and determine the potential of EAHE system

for the purpose of energy consumption in the greenhouse based on the degree-day method.

Materials and Methods

A multi-span commercial greenhouse with North-South arrangement was selected for this research project with the area of 3840 m^2 located in Alborz province, Iran (with latitude and longitude of 35°52' N and 50°40' E, respectively, at 1300 m above sea level). The greenhouse is equipped with the EAHE system for each unit which employs an autonomous air-conditioning system based on the geothermal principle to supply the greenhouse cooling demands without any conventional cooling system (such as pad-fan, mist, fog, etc.). The EAHE system partly provides the greenhouse heating requirement by reducing the consumption of fossil fuels compared with the conventional greenhouses of the region (Figure. 2). It is worth noting that the shallow geothermal system as EAHE one used in this study is different from the conventional systems as illustrated in Figure 1. This system has two external air (ambient) inputs, 30 outputs along the greenhouse floor and one umbrella roof vent for each span. First, the temperature changes of the target area were investigated for 10 years ago (2007-2017) for surveying the EAHE potential in order to supply the energy demands of a tomato greenhouse. Then, the degree-day of heating and cooling for the given time period was calculated and analysed for the temperature of the greenhouse by the EAHE system.

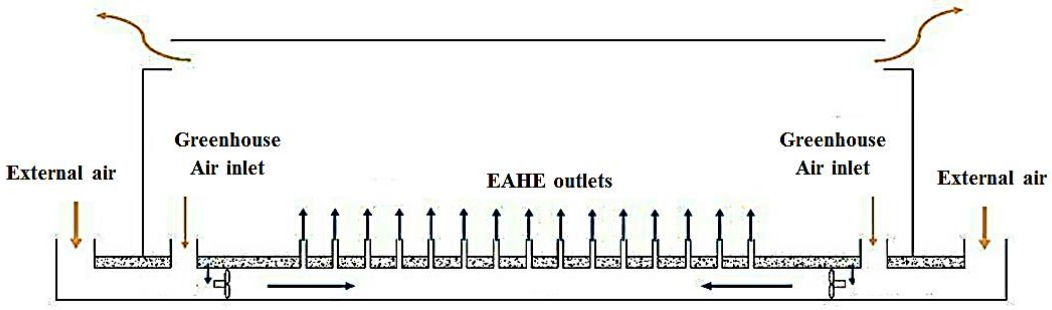

Fig.2. Geothermal model used in the greenhouse's unit

The cooling and heating requirements for a given period including N days are referred to Cooling Degree-Day (CDD) and Heating Degree-Day (HDD), respectively. The CDD and HDD are derived from Equations (1) and (2) according to the ASHRAE equation (ASHRAE, 2016):

$$CDD = \sum_{1}^{N} (T_{ave} - \theta_1)^+ \quad (1)$$

If $\theta_1 < T_{ave}$

$$HDD = \sum_{1}^{N} (\theta_2 - T_{ave})^+ \quad (2)$$

If $\theta_2 > T_{ave}$

In which:

θ_1: Cooling threshold temperature (ºC)

θ_2: Heating threshold temperature (ºC)

T_{ave}: Average daily temperature (ºC)

CDD: Cooling Degree-Day for a given period of N days

HDD: Heating Degree-Day for a given period of N days

The + sign means that the sole difference between positive numbers is considered. Threshold temperature for cooling and heating will be replaced by the tomato optimal temperature range of 16 to 23ºC (Adams, 2012). The degree-day values defined in this way endure in fact a kind of energy index. In other words, the degree-day is an indicator for energy consumption to heat or cool the protected environment (Day, 2016).

In this research, the average daily temperature of the Hashtgerd weather station in Alborz province (the most neighbouring station to Kouhsar district of the case-study greenhouse) was selected during the period of

2007-2017. Next CDD and HDD were calculated in the desired statistical period for cultivation tomato without considering the EAHE system effect on cooling and heating the greenhouse unit. After the calculation stage of CDD and HDD, two 12-channel data loggers were connected to 12 temperature sensors in numerous locations of the greenhouse with 960 m^2 area for monitoring the potential of the EAHE system (Figure 3). To check the heating potential of EAHE system from December 3, 2017, it was totalled for 30 days at the intervals of 10 minutes. The similar procedure was performed to check the cooling potential of EAHE system in July 2018. The key reason for choosing the specific time period prominently mentioned for the purpose of databases is having the peak values for the cooling and heating needs. The ambient temperature during the given period was measured by the ST-171 sensor. The steps in this study are in accordance with the flowchart of Figure 4.

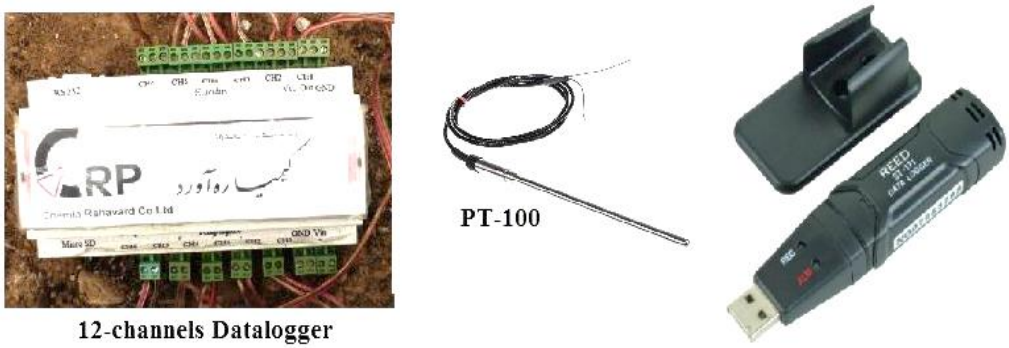

Fig.3. Measurement tools for recording the greenhouse outside and inside temperature

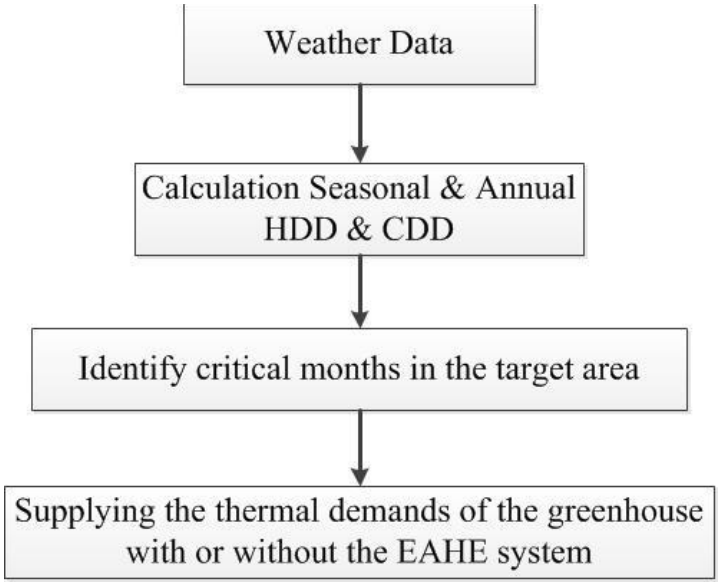

Fig.4. The flowchart of research's steps

Results and Discussion

The HDD and CDD levels

The CDD and HDD were calculated according to Equations (1) and (2) for the eleven years (2007-2017) based on meteorology data. Tomato cultivation is selected for this period in the greenhouse. Figure 5 shows the annual values of HDD and

CDD for each year during 2007-2017. According to the results demonstrated in Figure 5, the highest amount of HDD was 2444.31 degree-days for year 2017 as the coldest year in this period, while the lowest CDD was 315.29 degree-days for 2017. Furthermore, the lowest HDD was 1540.1 degree-days for 2009, while the highest CDD was 830.07 degree-days for 2011. According to the results, it can be declared that the Kouhsar area is one of the areas which need a higher heating requirement than the cooling one for the ambient temperature modification in Alborz province due to the geographical location. As a result, a degree-day index can be used to optimize and crop selection for protected agriculture. In this area a more resistant crop to cooler weather (for example lettuce or strawberry) should be selected during the winter (As shown in Figure 4). The results are in consistent with the results reported by other researchers despite utilizing the EAHE system for the greenhouse energy demands (Abdolhosseini *et al.*, 2013; Goff, 2015).

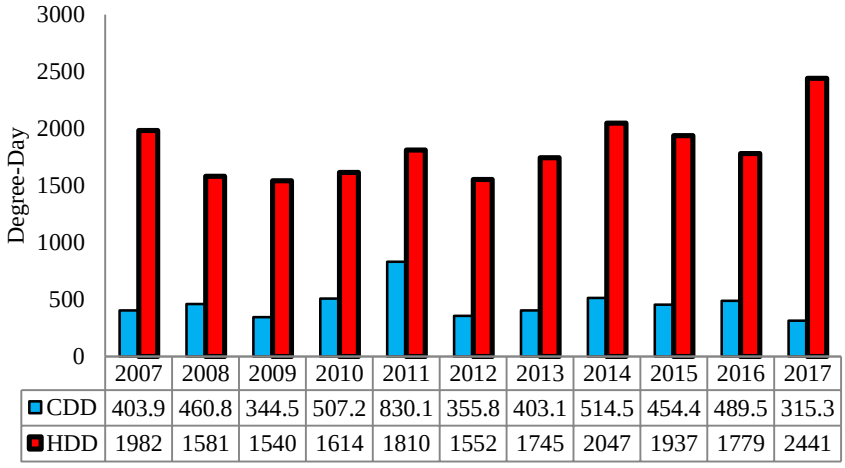

	2007	2008	2009	2010	2011	2012	2013	2014	2015	2016	2017
CDD	403.9	460.8	344.5	507.2	830.1	355.8	403.1	514.5	454.4	489.5	315.3
HDD	1982	1581	1540	1614	1810	1552	1745	2047	1937	1779	2441

Fig.5. The tomato annual cooling and heating degree-days for 2007-2017 meteorology periods.

The values of HDD (Figure 6) and CDD (Figure 7) were calculated for two critical seasons of each year separately including the cold season during December to March for heating and the warm season during June to September for cooling. The results obtained from degree-day calculations of each month in the meteorology period studied by the critical seasons. The highest HDD was equal to 611.92 degree-days for February (2007), and the lowest HDD was equal to 129.04 degree-days for March 2012. Figure 6 shows the trend of changes in HDD charts, which indicates that in recent years, the degree-day of heating for the studied region area has decreased progressively. The reason for this can be related to the exacerbation of the greenhouse effect caused by the human activities, climate change, global warming, and the changes in rainfall pattern from snow to rain (Borah *et al.*, 2015). It is expected that the degree-day of cooling will increase for ecosystem balance by reducing the amount of HDD, which indicates a gradual increase in temperature in the target area (De Rosa *et al.*, 2015; Borah *et al.*, 2015).

As shown in Figure 7, the lowest CDD is equal to 12.8 degree-days for September 2012 and the highest CDD is equal to 297.68 degree-days for July 2011. The trend of the changes in CDD charts in Fig. 7 shows that in recent years the degree of cooling day has increased for the study area (Abdolhosseini *et al.*, 2013; Borah *et al.*, 2015; Azimi and Narangifard, 2017). The obtained results from this study and the thermal energy requirement of this greenhouse constructed in Kouhsar, Alborz province can be used not only for planning outdoor agricultural production as well as managing and controlling pests, but can be also used for the purpose of energy consumption monitoring of the greenhouse by

selecting the proper type of crop in accordance with the characteristics of the desired area, as well as selecting the appropriate heating and cooling systems.

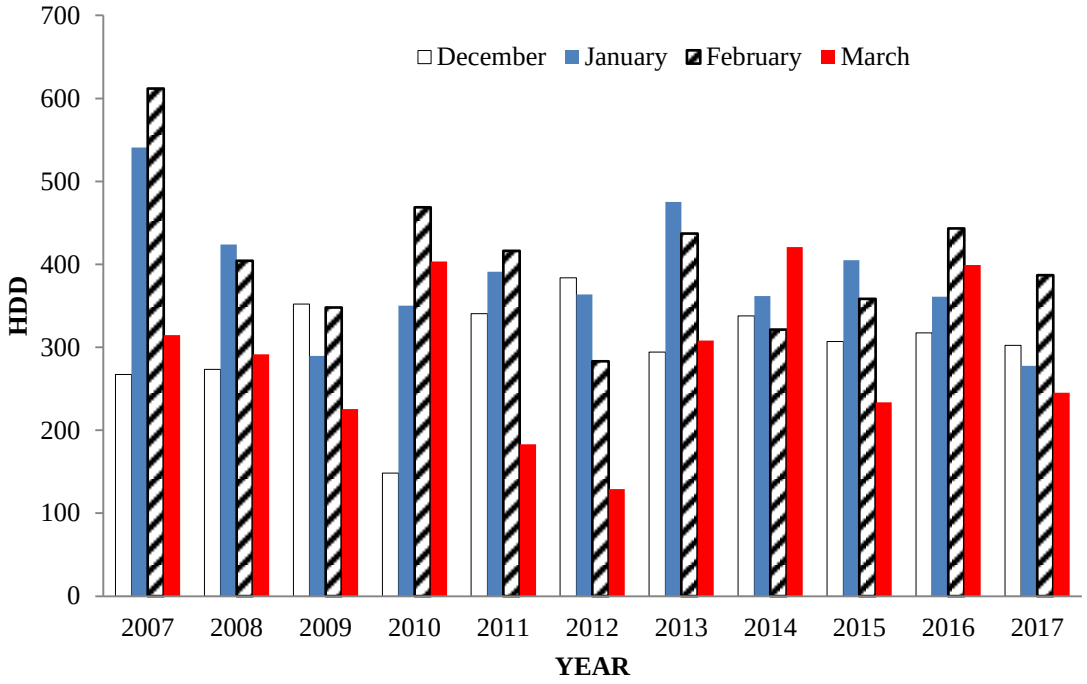

Fig.6. Heating Degree-Day (HDD) results of the cold months for 2007-2017 meteorology periods

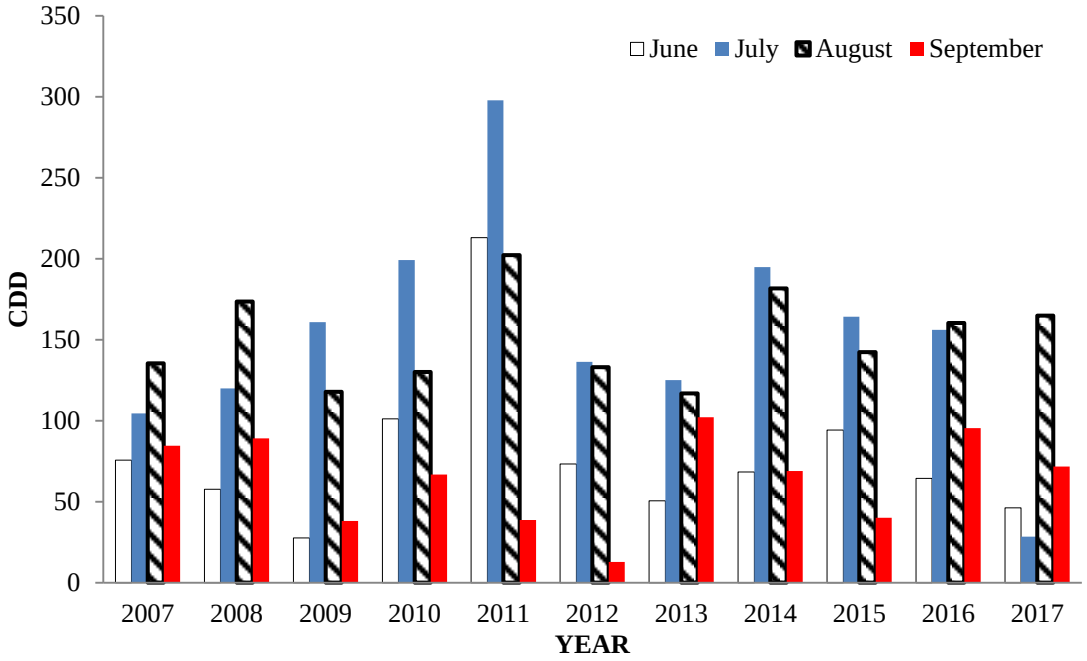

Fig.7. Cooling Degree-Day results of the hot months for 2007-2017 meteorology periods

The degree-day values stated by several researchers in the previous information of the seasonal and annual heating and cooling requirements of buildings such as greenhouses using weather data from the last years (Krese *et al.*, 2012; Atilgan *et al.*, 2016). This will be effective method for managing and optimizing energy consumption. Moreover, the EAHE system can considerably contribute to the supply of heating, cooling energy and air

ventilation in the greenhouse according to the results.

EAHE Potential for tomato HDD and CDD requirements

There is a significant difference between the ambient air temperature and the temperature measured in the greenhouse for tomato production according to the results presented in Figure 8. The temperature inside the greenhouse undergoes fewer fluctuations than the ambient air temperature using the EAHE system, which indicates a uniform distribution of temperature in the greenhouse. According to the calculations, the CDD value for July as the warmest month in the study area resulted in the highest cooling degree-days of 18, indicating that the system was capable to provide the cooling needs for the desired product less than the threshold temperature (23°C). It's worth noting that the energy of the system was provided only by geothermal energy without any kind of pad and fan system. As a result, this system can be considered in terms of energy saving and the use of geothermal energy as renewable and clean energy in the target area and for tomato crop. For this reason, the application of such EAHE system is advised to other conventional greenhouses as an energy-saving technology to adjust the temperature with an initial investment for this system.

Figure 8 also indicates the difference between the outside and inside temperature of the greenhouse ($T_{greenhouse}$-$T_{ambient}$) as occurred by the potential of the EAHE system. Since the monthly cooling requirement of the tomato is 468 degree-days and the monthly ability of the EAHE system is 538.7 degree-days, this system is quite capable of providing the cooling demands for the crop in July as the hottest month of the year in this area.

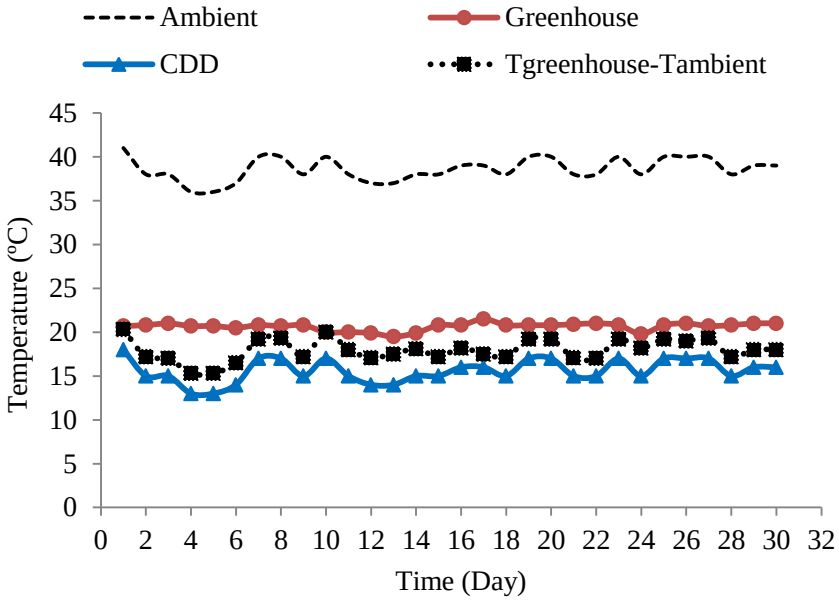

Fig.8. The EAHE potential to supply the cooling demands of the greenhouse using CDD index

The results of this study analogously indicate that there is a significant difference between the outside and inside temperatures in the cold season in order to evaluate the system's potential of providing the required greenhouse heating demands. As shown in Fig. 9, the sum of the monthly required HDDs for the tomato is 280.94 degree-days, and the monthly potential of the EAHE system for supplying the required greenhouse heating demands is 323.03 degree-days. Given that the average ambient air temperature for this period is approximately 7ºC (6.63ºC), and the required tomato temperature (at least 16ºC), it is necessary to increase the temperature by approximately 9ºC (9.37ºC), which easily

utilizes geothermal energy to satisfy this crop's thermal requirement.

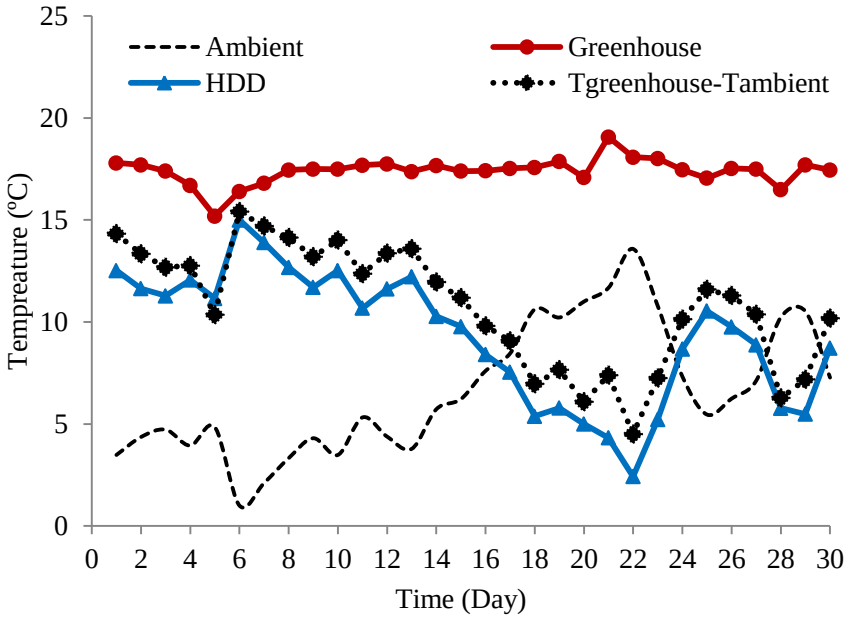

Fig.9. The evaluation of EAHE potential to supply the heating demands of the greenhouse using HDD index

Conclusions

Energy consumption in greenhouses is higher than outdoor traditional agriculture to provide the necessary environmental conditions (heating, cooling, ventilation and etc.). The degree-day is one of the most leading climatic indicators that indicates the intensity and duration of the ambient temperature. The aggregate number of degrees-days from an appropriate start date can be used to crop production planning as well as pest management and control disorder schedules. Weekly or monthly statistics also could be used for the energy consumption monitoring plan and related targets to typically determine the cost of cooling and heating systems and air conditioning for agricultural buildings like greenhouses while annual Figures can be properly employed to estimate future costs.

During the meteorology period from 2007 to 2017 in Kouhsar area of Alborz province, Iran, the annual cooling and heating degree-day was calculated for the purpose of the tomato cultivating. On that occasion, the potential of the EAHE system was investigated to satisfy the greenhouse heating and cooling requirements based on the degree-day index. The average potential of the EAHE system is 10.76ºC for increasing temperature in the cold and 17.96ºC for decreasing temperature in the warm season. The results showed degree-day index can be considered as one of the most significant fundamental information in estimating the amount of energy needed to warm up the greenhouse in the cold season and cool down it in the warm season. The degree-day index utilizes them to produce fruitful results in planning and decision making in the energy sector. According to the calculations and the results obtained, it can be declared that Kouhsar area in Alborz province is one of the areas with more heating requirements than that of the cooling ones. Consequently, this feature can be used to construct a greenhouse, as well as to select the appropriate crop, taking into account the geographical location and weather conditions.

Acknowledgments

The authors are grateful for the support provided to the project by university of Tehran as well as the Agriculture Engineering Research Institute (AERI) and specially the Greenhouse Engineering Department and

special thanks to Hamoon Cooperation for their great support.

References

1. Abbaspour-Fard, M. H., A. Gholami, and M. Khojastehpour. 2011. Evaluation of an earth-to-air heat exchanger for the north-east of Iran with semi-arid climate. International Journal of Green Energy 8: 499-510.
2. Abdolhosseini, M., S. Eslamian, and S. F. Mousavi. 2013. Effect of climate change on potential evapotranspiration: a case study on Gharehsoo sub-basin, Iran. International Journal of Hydrology Science and Technology 2 (4): 362-372.
3. Amiri, M. J., and S. S. Eslamian. 2010. Investigation of climate change in Iran. Journal of Environmental Science and Technology 3 (4): 208-216.
4. Atilgan, A., A. Yucel, O. Z. Hassan, and B. Saltuk. 2016. Determination of heating and cooling degree days for broiler breeding in the Tigris basin. Scientific Papers: Series D, Animal Science, The International Session of Scientific Communications of the Faculty of Animal Science 59.
5. Azimi, F., R. Ebrahimi, and M. Narangifard. 2017. Analysis and mapping of the HDD, CDD and temperatures for southern Caspian Sea (CS) Based Model EH5OM. International Journal of Urban Management and Energy Sustainability 1 (4): 28-38.
6. Bisoniya, T. S. 2015. Design of earth–air heat exchanger system. Geothermal Energy 3 (1): 18.
7. Borah, P., M. K. Singh, and S. Mahapatra. 2015. Estimation of degree-days for different climatic zones of North-East India. Sustainable Cities and Society 14: 70-81.
8. Chai, H., W. Cheng, C. Zhou, X. Chen, X. Ma, and S. Zhao. 2011. Analysis and comparison of spatial interpolation methods for temperature data in Xinjiang Uygur Autonomous Region, China. Natural Science 3 (12): 999-1010.
9. Ciriaco, A. E., S. J.Zarrouk, and G. Zakeri. 2020. Geothermal resource and reserve assessment methodology: Overview, analysis and future directions. Renewable and Sustainable Energy Reviews 119: 109515.
10. Ciulla, G., V. Lo Brano, and E. Moreci. 2015. Degree days and building energy demand. 3rd Southern African Solar Energy Conference, South Africa, 11-13 May, 2015.
11. Day, T. 2016. Degree-days: Theory and Application (TM41). The Chartered Institution of Building Services Engineers, CIBSE, London, UK.
12. De Rosa, M., V. Bianco, F. Scarpa, and L. A. Tagliafico. 2015. Historical trends and current state of heating and cooling degree days in Italy. Energy Conversion and Management 90: 323-335.
13. Dreidy, M., H. Mokhlis, and S. Mekhilef. 2017. Inertia response and frequency control techniques for renewable energy sources: A review. Renewable & Sustainable Energy Reviews 69: 144-155.
14. Ebinger, J., and W. Vergara. 2011. Climate impacts on energy systems: key issues for energy sector adaptation. Washington, DC: World Bank.
15. Franczak, M. 2017. Oil Shock: The 1973 Crisis and Its Economic Legacy. Edited by Elisabetta Bini, Giuliano Garavini, and Federico Romero. London: IB Tauris, 2016. 336 pp. Illustrations, notes. Cloth, $110.00. ISBN: 978-1-78453-556-8. Business History Review 91 (3): 595-598.
16. Faridi, H., A. Arabhosseini, G. Zarei, and M. Okos. 2019a. Design parameters of an earth-air heat exchanger with a square cross section- case study: greenhouse. Agricultural Mechanization and Systems Research, DOI: 10.22092/erams.2019.126401.1313. (in press).
17. Faridi, H., A. Arabhosseini, G. Zarei, and M. Okos. 2019b. Utilization of Soil Temperature Modeling to Check the Possibility of Earth-Air Heat Exchanger for Agricultural Building. Iranian (Iranica) Journal of Energy and Environment 10 (4): 260-268.

18. Ghasemi Mobtaker, H., Y., Ajabshirchi, S. F., Ranjbar, and M. Matloobi. 2017. Investigating the Effect of a North Wall on Energy Consumption of an East-West Oriented Single Span Greenhouse. Journal of Agricultural Machinery 7 (2): 350-363. (In Farsi).
19. Goff, J. M. 2015. A Value-Added Approach in Degree Day Calculation, National Weather Service: Burlington, VT.
20. Jiang, F., X. Li, B. Wei, R. Hu, and Z. Li. 2009. Observed trends of heating and cooling degree-days in Xinjiang Province, China. Theoretical and Applied Climatology 97 (3-4): 349-360.
21. Kabeel, A. E., and E. M. El-Said. 2015. Water production for irrigation and drinking needs in remote arid communities using closed-system greenhouse: A review. Engineering Science and Technology, an International Journal 18 (2): 294-301.
22. Krese, G., M. Prek, and V. Butala. 2012. Analysis of building electric energy consumption data using an improved cooling degree day method. Strojniški vestnik-Journal of Mechanical Engineering 58 (2): 107-114.
23. López-Aguilar, K., A. Benavides-Mendoza, S. González-Morales, A. Juárez-Maldonado, P. Chiñas-Sánchez, and A. Morelos-Moreno. 2020. Artificial Neural Network Modelling of Greenhouse Tomato Yield and Aerial Dry Matter. Agriculture 10 (4): 97.
24. Marimon, N., I. Eduardo, J. Martínez-Minaya, A. Vicente, and J. Luque. 2020. A decision support system based on degree-days to initiate fungicide spray programs for peach powdery mildew in Catalonia, Spain. Plant Disease, (ja).
25. Mideksa, T. K., and S. Kallbekken. 2010. The impact of climate change on the electricity market: A review. Energy Policy 38 (7): 3579-3585.
26. Misra, R., V. Bansal, G. D. Agrawal, J. Mathur, and T. Aseri. 2013. Transient analysis based determination of derating factor for earth air tunnel heat exchanger in summer. Energy and Buildings 58: 103-110.
27. Mongkon, S., S. Thepa, P. Namprakai, and N. Pratinthong. 2014. Cooling performance assessment of horizontal earth tube system and effect on planting in tropical greenhouse. Energy Conversion and Management 78: 225-236.
28. Moreno, L. S., C. G. Pedreira, K. J. Boote, and R. R. Alves. 2014. Base temperature determination of tropical Panicum spp. grasses and its effects on degree-day-based models. Agricultural and Forest Meteorology 186: 26-33.
29. Mourshed, M. 2012. Relationship between annual mean temperature and degree-days. Energy and Buildings 54: 418-425.
30. Papakostas, K. T., A. K. Michopoulos, and N. A. Kyriakis. 2009. Equivalent full-load hours for estimating heating and cooling energy requirements in buildings: Greece case study. Applied Energy 86 (5): 757-761.
31. Rehman, S., L. M. Al-Hadhrami, and S. Khan. 2011. Annual and seasonal trends of cooling, heating, and industrial degree-days in coastal regions of Saudi Arabia. Theoretical and Applied Climatology 104 (3-4): 479-488.
32. Romanovskaja, D., and E. Baksiene. 2011. The influence of climate change on the beginning of spring season and prediction of apple tree flowering in Lithuania. Sodininkystė ir Daržininkystė 30 (3/4): 29-39.
33. Roshan, G. R., and S. W. Grab. 2012. Regional climate change scenarios and their impacts on water requirements for wheat production in Iran. International Journal of Plant Production 6 (2): 239-266.
34. Schaeffer, R., A. S. Szklo, A. F. P. de Lucena, B. S. M. C. Borba, L. P. P. Nogueira, F. P. Fleming, A. Troccoli, M. Harrison, and M. S. Boulahya. 2012. Energy sector vulnerability to climate change: a review. Energy 38 (1): 1-12.

35. Sehli, A., A. Hasni, and M. Tamali. 2012. The potential of earth-air heat exchangers for low energy cooling of buildings in South Algeria. Energy Procedia 18: 496-506.
36. Shen, X., and B. Liu. 2016. Changes in the timing, length and heating degree days of the heating season in central heating zone of China. Scientific reports 6: 33384.
37. Vadiee, A., and V. Martin. 2014. Energy management strategies for commercial greenhouses. Applied Energy 114: 880-888.
38. Verbai, Z., A. Lakatos, and F. Kalmár. 2014. Prediction of energy demand for heating of residential buildings using variable degree day. Energy 76: 780-787.
39. Way, R. G., A. G. Lewkowicz, and P. P. Bonnaventure 2017. Development of moderate-resolution gridded monthly air temperature and degree-day maps for the Labrador-Ungava region of northern Canada. International Journal of Climatology 37 (1): 493-508.
40. Yucel, A., A. Atilgan, H. Oz, and B. Saltuk. 2014. The determination of heating and cooling day values using degree-day method: Tomato plant example. Infrastruktura i Ekologia Terenów Wiejskich (IV/1): 1049-1061.
41. Zheng, S., G. Huang, X. Zhou, and X. Zhu. 2020. Climate-change impacts on electricity demands at a metropolitan scale: A case study of Guangzhou, China. Applied Energy 261: 114295.

نشریه ماشین‌های کشاورزی
جلد ۱۱، شماره ۱، نیمسال اول ۱۴۰۰، ص ۹۵-۸۳

Journal of Agricultural Machinery
Vol. 11, No. 1, Spring- Summer 2021, p. 83-95

مقاله علمی-پژوهشی

پیش‌بینی نیازهای حرارتی یک گلخانه مجهز به مبدل حرارتی هوا-زمین به کمک شاخص درجه-روز

حمیده فریدی[۱]، اکبر عرب حسینی[۲*]، قاسم زارعی[۳]، مارتین اوکوس[۴]

تاریخ دریافت: ۱۳۹۹/۰۱/۱۸
تاریخ پذیرش: ۱۳۹۹/۰۴/۳۰

چکیده

در این تحقیق، استفاده از مبدل حرارتی زمین-هوا (EAHE) به‌عنوان منبع انرژی زمین گرمایی کم عمق برای تأمین نیازهای حرارتی یک گلخانه تجاری واقع در استان البرز، مورد بررسی قرار گرفت. از شاخص درجه-روز برای برآورد پتانسیل سیستم EAHE به‌منظور تامین نیازهای حرارتی گلخانه از جمله سرمایش و گرمایش استفاده شد. نتایج نشان داد که این منطقه برای رسیدن به دمای مناسب در داخل گلخانه برای تامین گرمایش نسبت به نیاز سرمایشی، نیاز به انرژی بیشتری دارد. متوسط پتانسیل سیستم EAHE بر اساس شاخص درجه-روز برای افزایش دما در فصل سرد ۱۰/۷۶°C و برای کاهش دما در فصل گرم ۱۷/۹۶°C است. این بدان معنی است که سیستم EAHE قادر به تأمین نیازهای حرارتی گلخانه در این منطقه با توجه به مقادیر محاسبه شده درجه-روز گرمایش (HDD) و درجه-روز سرمایش (CDD) است. این روش می‌تواند در نظارت و بهینه‌سازی شرایط رشد گیاه به‌عنوان انتخاب بهترین نوع محصول یا نوع کشت و همچنین در آبیاری و مدیریت باروری محصولات زراعی مفید باشد.

واژه‌های کلیدی: درجه-روز، زمین گرمایی، گلخانه، مبدل حرارتی

۱- دانش‌آموخته مقطع دکتری تخصصی، گروه مهندسی مکانیک بیوسیستم، پردیس ابوریحان، دانشگاه تهران، تهران، ایران
۲- دانشیار، گروه مهندسی مکانیک بیوسیستم، پردیس ابوریحان، دانشگاه تهران، تهران، ایران
۳- دانشیار، موسسه تحقیقات فنی و مهندسی کشاورزی، سازمان تحقیقات، آموزش و ترویج کشاورزی، کرج، ایران
۴- استاد، دانشکده مهندسی کشاورزی و بیولوژی، دانشگاه پوردو، لفایت، ایالات متحده امریکا
(*- نویسنده مسئول: Email: ahosseini@ut.ac.ir)

DOI: 10.22067/jam.v11i1.86233

Journal of Agricultural Machinery
Vol. 11, No. 1, Spring- Summer 2021, p. 97-110

نشریه ماشین‌های کشاورزی
جلد ۱۱، شماره ۱، نیمسال اول ۱۴۰۰، ص ۱۱۰-۹۷

Full Research Paper

Investigating the Energy Consumption and Economic Indices for Sweet-Cherry and Sour-Cherry Production in Northeastern Iran

R. Vahid-Berimanlou[1], F. Nadi[2*]

Received: 02-10-2019
Accepted: 15-01-2020

Abstract

The aim of this study was to investigate the energy consumption and production costs of sweet-cherry and sour-cherry in Northeastern Iran. Required data were collected from 75 sweet-cherry and 42 sour-cherry producers. The total energy inputs in sweet-cherry and sour-cherry production were estimated as 37.76 and 31.03 GJha^{-1}, respectively. The energy efficiency of sweet-cherry production was greater than sour-cherry production. Chemical fertilizers and diesel fuel were the most highly consumed energies in both crops. The higher share of non-renewable energies consumed to produce sweet-cherry than sour-cherry revealed that sweet-cherry production was more dependent on non-renewable sources compared with the sour-cherry production. The economic analysis revealed that production costs for sweet-cherry were higher than sour-cherry but sweet-cherry was more profitable than sour-cherry because of premium prices for sweet-cherry. The modeling results showed that the human labor input had the most impact on costs of both crops. As a consequence, the main practical solutions could be saving in diesel fuel and fertilizer management, which could more properly overcome economic and energy problems in the two crops.

Keywords: Cherry, Cobb-Douglas, Energy modeling, Income, Production costs

Introduction

According to the Food and Agriculture Organization (FAO) annualy reports, around 2.4 tons of sweet-cherries and 1.2 tons of sour-cherries were produced in the world in 2017 (FAO, 2019). Additionally, based on the Iranian Agriculture Ministry (IAM), the allocated area of orchards for Sour-cherry and Sweet-cherry production is about 21181 and 38703 hectares, respectively in 2017. Iran with over 316 thousand tons of sweet-cherry and 116 thousand tons of sour-cherry is recognized as the third-largest sweet-cherry producers and the fifth-largest sour-cherry producers in the world. The average yield of sour-cherry and sweet-cherry was 6457 and 9497 kg ha^{-1}, respectively (Ministry of Agriculture, 2019).

For the agricultural sector, there are two important factors, which should be taken into account seriously: ensuring the food security, intensifying the foreign exchanges and attaining political and economic independence as well as contributing to the gross domestic product of the country. This is because maximizing income and production are the main objectives of the agricultural sector (Mahallati *et al.*, 2015). Modifying common agricultural practices and the optimization strategies related to land use and increasing production are inevitable (Chapagain and Riseman, 2014).

Over the past years, numerous studies have been conducted to evaluate and optimize energy flow and the economic analysis of producing orchard crops, with the aim of controlling the critical inputs and reduceing the environmental impacts at national and international levels. For instance, Tables 1 and 2 show the synopsis of the research findings reported on energetic and economic analysis for different orchard products in Iran and around the world.

1- MSc of Agriculture Mechanization Engineering, Azadshahr Branch, Islamic Azad University, Azadshahr, Iran
2- Department of Agricultural Machinery Mechanics, Azadshahr Branch, Islamic Azad University, Azadshahr, Iran
(*- Corresponding Author Email: F.nadi@iauaz.ac.ir)
DOI: 10.22067/jam.v11i1.83466

Considering the literature review, the significance of the energy and economic issues in the agricultural sector, and the paucity of comprehensive research on the analysis of input and output energy in the production of sweet-cherry and sour-cherry, this study investigates the aspects of econometrics and energetic of sweet-cherry and sour-cherry production in the North-Khorasan province, located in northeastern Iran.

Table 1- Synopsis of the research findings reported on energetic and economic analysis for different orchard products in Iran

Crop	Province	Analysis method	Result (hotspot in energy consumption)	Reference
Sour-cherry & Sweet-cherry	Alborz	Energetic	Fertilizer, Fuel, Electricity	(Haddadi *et al.*, 2015)
Pistachio	Kerman		Fertilizer, Fuel	(Mirzaei Khalilabadi *et al.*, 2014)
Walnut	Hamadan	Energetic & Economic	Fertilizers	(Banaeian and Zangeneh 2011)
Apple	West Azerbaijan		Packaging, Irrigation	(Fadavi *et al.*, 2011)
Apple	West Azarbayjan	Energetic	Irrigation, Fuel	(Taghavifar and Mardani, 2015)
Peach	Chaharmahal va Bakhtiari		Fertilizers, Electricity	(Ghatrehsamani *et al.*, 2016)
Peach	Golestan		Fuel	(Royan *et al.*, 2012)
Peach	Chaharmahal va Bakhtiari		Fuel, Electricity, Fertilizers	(Ghasemi-Varnamkhasti *et al.*, 2015)
Kiwifruit	Mazandaran	Energetic & Economic	Fertilizers, Fuel	(Mohammadi *et al.*, 210)
Kiwifruit	Gilan	Energetic	Fertilizers	(Nabavi-Pelesaraei *et al.*, 2016)
Kiwifruit	Gilan		Electricity, Fertilizers, Irrigation	(Soltanali *et al.*, 2017)
Citrus	Mazandaran	Energetic & Economic	Fertilizers, Fuel, Pesticides	(Aghkhani *et al.*, 2018)
Citrus	Mazandaran	Energetic	Fertilizers, Pesticides	(Loghmanpour *et al.*, 2013)
Citrus	Mazandaran		Fertilizers	(Zarini et al., 2013)
Nectarine	Mazandaran		Fertilizers	(Qasemi-Kordkheili *et al.*, 2013)
Grape	Hamadan		Fertilizers, Electricity	(Rasouli *et al.*, 2014)
Grape	Markazi		Fertilizers, Human labour, Electrical, Irrigation, Irrigation	(Mohseni *et al.*, 2019)
Prune	Tehran			(Tabatabaie *et al*., 2013)
Hazelnut	Guilan		Electricity	(Nabavi-Pelesaraei *et al.*, 2013)
Pear	Tehran	Energetic & Economic	Fertilizers, Fuel	(Tabatabaie *et al.*, 2013)

Table 2- Synopsis of the research findings reported on energetic and economic analysis for different orchard products in the world

Crop	Country	Analysis method	Result (hotspot in energy consumption)	Reference
Organic mulberry	Turkey	Energetic	Irrigation	(Gokdogan *et al.*, 2017)
Lemon, Orange and mandarin	Turkey	Energetic	Fertilizer, Fuel	(Ozkan *et al.*, 2004)
Peach & Cherry	Turkey	Energetic & Economic	Machinery, Fuel, Fertilizers	(Aydın, and Aktürk, 2018)
Peach	Turkey	Energetic	Machinery	(Gündoğmuş, 2014)
Sweet-cherry	Turkey	Energetic &	Fertilizer, Electricity, Fuel	(Kizilaslan, 2009)
Apricot	Turkey	Economic	Fertilizer, Chemicals	(Esengun *et al.*, 2007)
Walnut	Turkey	Econometric	Fertilizers, Fuel, Chemicals	(Gundogmus, 2013)
Sweet cherry	Turkey	Energetic	Fertilizers, Fuel	(Demircan *et al.*, 2006)
Fig	Turkey	Energetic	Fertilizers	(Cobanoglu, 2010)
Banana	Turkey	Energetic	Electricity	(Akcaoz, 2011)
Pomegranate	Turkey	Energetic	Fertilizer, Chemicals	(Akcaoz *et al.*, 2009)
Open-field grape	Turkey	Energetic &	Fuel, Electricity, Chemicals	(Ozkan et al. 2007)
Greenhouse grape	Turkey	Economic	Electricity, Chemicals	(Ozkan *et al.*, 2007)
Sour-cherry and Sweet-cherry	USA	Energetic	Irrigation, Fertilizer	(Proebsting, 1980)
Mango	India	Energetic	Chemicals, Fuel, Electricity	(Verma *et al.*, 2018)
Apple	Greece	Energetic	Fuel, Machinery, Fertilizers	(Strapatsa *et al.*, 2006)
Pear	China	Energetic	Manure, Machinery	(Liu *et al.*, 2010)

Materials and Methods

Details of the studied area

The present study was conducted in the North-Khorasan province (37°09′42″N, 57°03′20.30″E). The province covers 1.72 percent of the total area of Iran, with an area of 28434 square kilometers. The statistical population in this study was all sweet-cherry and sour-cherry producers in the North-Khorasan province during 2016-2017. The random sampling method was used due to the large statistical population. Cochran has provided Equation 1 for calculating the number of samples required in the random sampling technique (Snedecor and Cochran, 1980).

$$n = \frac{N(t.s)^2}{Nd^2 + (t.s)^2} \quad (1)$$

Where N is the number of producers, t is reliability coefficient at 95% reliability, S^2 is the population variance, d is the desired probability and n is the sample size.

The data were collected through a questionnaire method and face-to-face interviews with 42 sour-cherry and 75 sweet-cherry producers. The content validity method was used to assess the validity of the questionnaire. Cronbach's alpha coefficient was used to assess the reliability of the scale. At first, the variance of scores of each questionnaire question and the total variance of the test for each sweet-cherry and sour-cherry questionnaire were determined and then its coefficient was obtained. The reliability of the test was 0.86 for sour-cherry and 0.85 for sweet-cherry questionnaires.

Energy analysis

In this study, seven inputs including human labor, agricultural machinery, diesel fuel, chemical fertilizers, chemical pesticides, water for irrigation, and electricity were considered as inputs. The output of this study was sweet-cherry and sour-cherry yields. Table 3 presents the energy equivalents for various inputs.

Table 3- Energy equivalent for energy inputs and outputs

Energy source	Unit	Energy equivalent (MJ unit^{-1})	Source
Human labor	h	1.96	(Yaldiz *et al.*, 1993)
Machinery	h	62.7	(Yaldiz *et al.*, 1993)
Diesel	L	47.8	(Cervinka, 1980)
Chemicals			
a) Insecticide		199	(Yaldiz *et al.*, 1990a,b)
b) Fungicides	kg	216	(Pathak and Bining, 1985)
c) Herbicide		238	(Helsel, 1992)
Fertilizer			
a) N		78.1	(Mudahar *et al.*, 1987)
b) P_2O_5	kg	17.4	(Mudahar *et al.*, 1987)
c) K_2O		13.7	(Mudahar *et al.*, 1987)
Water	m^3	1.02	(Acaroglu, 1998)
Electricity	kWh	12	(Cervinka, 1980)
Sour-Cherry	kg	2.93	(Proebsting, 1980)
Sweet-Cherry	kg	2.93	(Proebsting, 1980)

To compare the energy flow of sweet-cherry and sour-cherry productions, energy indicators such as energy efficiency, energy productivity, specific energy and net energy were calculated according to the following equations:

$$\text{Energy Efficiency} = \frac{\text{Energy Output (MJ ha}^{-1})}{\text{Energy Input (MJ ha}^{-1})} \quad (2)$$

$$\text{Energy productivity} = \frac{\text{Yield (kg ha}^{-1})}{\text{Energy Input (MJ ha}^{-1})} \quad (3)$$

$$\text{Specific energy} = \frac{\text{Energy Input (MJ ha}^{-1})}{\text{Yield}\left(\text{kg ha}^{-1}\right)} \quad (4)$$

$$\text{Net energy} = \text{Output energy(MJ ha}^{-1}) - \text{Input energy(MJ ha}^{-1}) \quad (5)$$

Economic analysis

To have an economic evaluation of the sweet-cherry and sour-cherry production in

North-Khorasan province, economic indicators, such as total production value, gross income, net income, benefit-cost ratio and economic productivity were calculated according to Equations (6) to (10).

$$\text{Total production value= Crop yield (kg ha}^{-1}\text{)}\times \text{ Crop price (\$ kg}^{-1}\text{)} \quad (6)$$

$$\text{Gross income = Total production value } (\$\ \text{ha}^{-1}) \text{ - Variable production cost (\$ ha}^{-1}\text{)} \quad (7)$$

$$\text{Net income = Total production value } (\$\ \text{ha}^{-1}) \text{ - Total production cost (\$ ha}^{-1}\text{)} \quad (8)$$

$$\textit{B}\text{enefit -cost ratio} = \frac{\text{Total production value } (\$\ \text{ha}^{-1})}{\text{Total production cost } (\$\ \text{ha}^{-1})} \quad (9)$$

$$\textit{E}\text{conomic productivity} = \frac{\text{Crop yield } (\text{kg ha}^{-1})}{\text{Total production cost } (\$\ \text{ha}^{-1})} \quad (10)$$

Energy modeling

Cobb-Douglas function was used to estimate the relationships between input energies and the yield, input costs and income (Tabatabaie *et al*., 2013; Nikkhah *et al*., 2016; Gundogmus, 2013). The Cobb-Douglas function is expressed in Equation (11) (Cobb and Douglas, 1928):

$$Y=f(x)\exp(u) \quad (11)$$

which can be further written as

$$\ln Y_i=a+\sum_{i=1}^{n}\alpha_j \ln(X_{ij}) + e_i \quad i=1,2,\ldots,n \quad (12)$$

Where Y_i is the yield of the i_{th} farmer, X_{ij} is the vector of inputs used in the production process, a is a constant, e_i is the error term, and a_j is coefficients of inputs which are estimated from the model. With the assumption that the yield is the function of inputs, Equation (12) can be written as:

$$\ln Y_i=a_0+\alpha_1 \ln X_1+\alpha_2 \ln X_2+\alpha_3 \ln X_3+\ldots+\alpha_8 \ln X_8+e_i \quad (13)$$

Where $x_1, x_2, x_3, x_4, x_5, x_6$ and x_7 are human labor, agricultural machinery, diesel fuel, fertilizers, chemicals, irrigation water, electricity, respectively.

Moreover, the impacts of direct (DE), indirect (IDE), renewable (RE) and non-renewable (NRE) energies on sweet-cherry and sour-cherry yields were examined by Equations (9) and (10).

$$\ln Y_i=a_0+\beta_1 \ln DE+\beta_2 \ln IDE+e_i \quad (14)$$

$$\ln Y_i=a_0+\gamma_1 \ln RE+\gamma_2 \ln NRE+e_i \quad (15)$$

Where β_i and γ_i are the regression coefficients.

Returns to scale was used to determine the proportional change in output due to proportional increase in all inputs by the same factor. It was calculated by summing the regression coefficients of models of Equations (13)-(15). If the sum of the coefficients is greater than, equal to, or less than 1, it indicates that the return to scale is increasing, constant or decreasing, respectively.

The marginal physical productivity (MPP)

The MPP shows the rate of change induced in the performance, assuming that the other factors of production remained unchanged, by increasing one unit in one of the energy inputs. The MPP positive value indicates that any increase in the input will increase the yield output. The MPP negative value indicates that each additional input unit reduces performance. The MPP was calculated by Equation (16):

$$MPP_{Xj}=\frac{GM(Y)}{GM(X_j)}\times \alpha_j \quad (16)$$

Where MPP_{xj} is marginal physical productivity of j^{th} input; GM(Y) is the geometric mean of yield; $GM(X_j)$ is geometric mean of j^{th} input energy on per hectare.

Data analysis was performed in Minitab17 and JMP8 statistical software programs. Regression relationships between the inputs and yield were established through a linear regression method. Figures were prepared by Origin 2018.

Results and Discussion

Distribution of energy inputs

The consumed inputs in sour-cherry and sweet-cherry production and their energy equivalents are summarized in Table 4. The results indicated that the total energy consumed in sour-cherry production was less than sweet-cherry production. The total output energy of sweet-cherry was higher than sour-cherry because more sweet-cherry is yielded in comparison with sour-cherry. The total input energy for producing sweet-cherry was 29.20 GJ ha^{-1} in Isparta province (Demircan *et al*., 2006), 33.60 GJ ha^{-1} in Çanakkale province (Aydın and Aktürk, 2018) 18 GJ ha^{-1} and 17.53 GJ ha^{-1} for sour-cherry and sweet-cherry in Alborz province (Haddadi *et al.*, 2015), which showed that energy used for producing sweet-cherry in the North-Khorasan province was much higher than the Alborz province and Turkey.

Table 4- Amounts of inputs and output with their equivalent energy in sour-cherry and sweet-cherry production

Energy source	Sour-cherry		Sweet-cherry	
	Quantity used per unit area (ha)	Energy equivalent (MJ ha^{-1})	Quantity used per unit area (ha)	Energy equivalent (MJ ha^{-1})
Human labor (h)	2106.74	4129.20	2232.5	4374.83
Machinery (h)	56.05	3514.53	83.98	5265.81
Diesel (L)	113.54	6528.58	144.23	8293.10
Chemicals		679.98		725.03
a) Insecticide	1.40	278.60	1.45	288.55
b) Fungicides	1.12	241.92	1.58	341.28
c) Herbicide	0.67	159.46	0.40	95.2
Fertilizer		13179.65		15414.78
a) Nitrogen (kg)	149.13	11647.05	174.97	13665.16
b) Phosphorus (kg)	50.50	878.70	55.91	972.83
c) Potassium (kg)	47.73	653.90	56.70	776.79
Irrigation Water (m^3)	514.65	524.95	724.06	738.54
Electricity (kWh)	205.79	2469.48	245.54	2946.49
Total energy input (MJ ha^{-1})		31026.37		37758.57
Total energy output (MJ ha^{-1})	4287.55	12562.53	5472.39	16034.09

As Figure 1 shows, the chemical fertilizers have the largest share of energy consumption in the production of sour-cherry (41%) and sweet-cherry (39%). Nitrogen is the most used energy in both products when is compared to the other fertilizers. Similar results were observed in producing Pistachio (Mirzaei Khalilabadi *et al*., 2014), Walnut (Banaeian and Zangeneh, 2011), Kiwifruit (Mohammadi *et al*., 210), Sweet-cherry (Kizilaslan, 2009; Demircan *et al*., 2006), Citrus (Zarini *et al.*, 2013) and Plum (Tabatabaie *et al.*, 2012).

The second most energy-intensive input was diesel fuel for both crops, despite the lack of diesel fuel consumption at the harvesting operation, relatively large amounts of fuel were consumed at the stages of tillage and spraying. The reason for the high consumption of this source could be due to the old machines, lack of gas regulation and proper use of gear by most farmers.

The agricultural machinery input was the third most energy consumed input in sweet-cherry production and it was the fourth energy consumed input in sour-cherry production. Tillage and transportation operations had the highest and lowest energy consumption, respectively. Meanwhile Akcaoz (2011) found that the agricultural machinery input in banana in Turkey was the third most used input and transportation operation had the most share in the agricultural machinery input. Besides, the share of agricultural machinery input was reported around 7-8% in the Alborz province for sweet-cherry and sour-cherry (Haddadi *et al.*, 2015). In the North Khorasan due to high

consumption of the input in tillage and spraying operation, and despite the absence of this input at the harvesting operation, this input was considered as one of the most energy-consuming inputs in the production of both crops.

The human labor input in the sour-cherry production and the sweet-cherry production was the lowest consumed inputs, respectively. Harvesting operation had the highest share of energy consumption in this input. A similar result was observed in producing sweet-cherry in Turkey, in which the human labor input with 13% of the share of total energy consumed was reported as the third most consumed input. Notwithstanding these results, the share of energy consumed by human labor was 4% for pomegranate (Akcaoz *et al.*, 2009), 6% for peach (Royan *et al.*, 2012) and 7% apple (Rafiee *et al.*, 2010). Sweet-cherry and sour-cherry are small fruits, and consequently, harvesting them is of difficulty and it needs more human labor. However, timely pruning trees has also a significant contribution to the deceasing of human labor in a harvesting operation.

Inputs of chemicals and water for irrigation and electricity had the lowest energy consumption in both crops. Fungicides were the most energy consumed input in comparison with other pesticides. Similar results in using chemicals in producing nectarine in the Sari region (Qasemi-Kordkheili *et al.*, 2013), apple in Turkey (AkdemİR *et al.*, 2012) were reported. The irrigation water energy was also one of the lowest energy consumed inputs in producing sweet-cherry and sour-cherry productions in the Alborz province (Haddadi *et al.*, 2015), peach in the Golestan province (Royan *et al.*, 2012) and apple in the Isfahan province (Sami *et al.*, 2011).

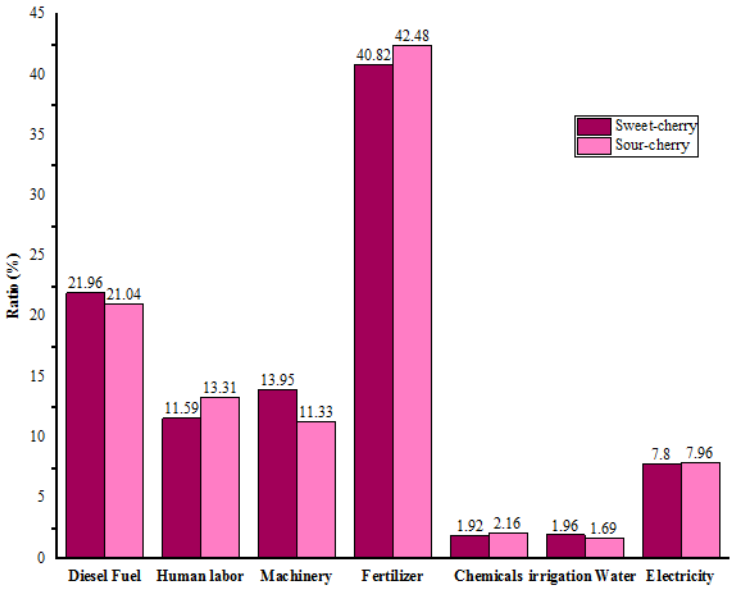

Fig.1. The anthropogenic energy input ratios in energy in sour-cherry and sweet-cherry production

Assessment of energy indicators

Table 5 presents the energy indicators in the sweet-cherry and sour-cherry production. The energy efficiency and energy productivity of sour-cherry were not greater than sweet-cherry, suggesting that the sweet-cherry production was more efficient than sour-cherry production in terms of energy consumption.

The other studies showed that energy efficiency was 1.48 for sour-cherry, 1.25 for sweet-cherry in the Alborz province (Haddadi *et al.*, 2015), 1.23 for sweet-cherry in the Isparta province (Demircan *et al.*, 2006), 0.78 for sweet-cherry in Çanakkale province (Aydın and Aktürk, 2018). Energy productivity was 1.45 for sweet-cherry and

1.83 for sour cherry in Alborz (Haddadi *et al.*, 2015), 0.32 for sweet-cherry in the Isparta province (Demircan *et al.*, 2006), 0.32 for sweet-cherry in the Çanakkale province (Aydın and Aktürk, 2018), 0.51 for sweet-cherry and 0.20 for sour-cherry in the US (Proebsting, 1980). The comparison of the results of this study with other studies shows that sweet-cherry and sour-cherry production elsewhere were more efficient than both crops production in the North-Khorasan province. The main reasons for low energy efficiency and productivity in the North Khorasan province are the inefficient use of energy inputs and the low yield of sour-cherry and sweet-cherry than elsewhere.

Reducing fertilizer and fuel consumption not only prevents environmental pollution (water, soil and air) but also reduces energy consumption in production. Providing proper training in the regulation and the proper use of machineries as well as soil testing can help farmers use inputs more appropriately. Thus allow to achieve more sustainable and profitable agriculture, energy efficiency and improved productivity. It also suggests that pruning and using higher productive varieties help farmers boost energy use efficiency and income.

Table 5- Total energy consumption distributed by energy sources in sweet-cherry and sour-cherry production

Indicators	Unit	Sour-cherry	Sweet-cherry
Energy efficiency	-	0.41	0.43
Energy productivity	kg MJ^{-1}	0.14	0.15
Specific energy	MJ kg^{-1}	7.24	6.92
Net energy	MJ ha^{-1}	-20732.55	-21634.60
Direct energy	MJ ha^{-1}	13652.21	16352.96
Indirect energy	MJ ha^{-1}	17374.16	21405.62
Renewable energy	MJ ha^{-1}	4654.15	5113.37
Non-renewable energy	MJ ha^{-1}	26372.23	32645.20
Total energy input	MJ ha^{-1}	31026.37	37758.57
Total energy output	MJ ha^{-1}	12562.53	16034.09

The share of direct, indirect, renewable, and non-renewable energies in the production of sweet-cherry and sour-cherry are shown in Figure 2. For both crops, the share of indirect and non-renewable energy was higher than direct and renewable energy. In sweet-cherry production, the use of diesel fuel, agricultural machinery, chemical fertilizers and chemical pesticides were higher than those of in sour-cherry production. For this reason, the share of indirect energy in sweet-cherry production was more than sour-cherry production. According to Figure 2, the share of non-renewable energy in sweet-cherry production was higher than sour-cherry, so sweet-cherry production was more dependent on non-renewable energy than sour-cherry. Aydın and Aktürk (2018) that reported the share of non-renewable energy in sweet-cherry production was 96.41% in the Çanakkale province, while this share was 73.05% in sweet-cherry production in the Isparta province, which shows sweet-cherry production in the North- Khorasan province was more dependent on non-renewable energy than the Çanakkale province and sweet-cherry production in the Isparta province was more sustainable.

Association of inputs and the yield

Table 6 shows the results of applying Cobb Douglas function to determine the relationship between the inputs and yield for both crops. The return to the scale implies that increasing 1% in the energy of all inputs can increase the yield in the sour-cherry when compared with sweet-cherry. Regression coefficients in Table 4 shows the influence of diesel fuel, and human labor and water were more significant than other inputs on the yield of both crops.

According to the results of sensitivity analysis by increasing 1 MJ in the energy of water for irrigation, chemical pesticides, human labor, diesel fuel and chemical

fertilizers, the sour-cherry yield was increased to 1.241, 0.766, 0.237, 0.152, and 0.042, respectively, while by increasing 1 MJ in the energy of water for irrigation, human labor, diesel fuel, agricultural machinery and chemical fertilizers, the sweet-yield was increased to 0.941, 0.290, 0.127, 0.086 and 0.021 kg, respectively.

Fig.2. The share of total mean energy inputs as direct, indirect renewable and non-renewable forms in sweet-cherry and sour-cherry production

Table 6- Energetic estimation results of energy inputs with yield

Energy source	Sour-cherry				Sweet-cherry			
	Coefficient	t-ratio	P-value	MPP	Coefficient	t-ratio	P-value	MPP
Model: $Lny_i = a_0 + \alpha_1 lnx_1 + \alpha_2 lnx_2 + \alpha_3 lnx_3 + \cdots + \alpha_8 lnx_8 + e_i$								
Diesel fuel	0.227	4.09**	0.001	0.152	0.188	3.26*	0.000	0.127
Human labor	0.228	4.33**	0.001	0.237	0.232	3.87**	0.001	0.290
Machinery	-0.008	-1.11ns	0.899	-0.010	0.083	2.02*	0.000	0.086
Fertilizer	0.108	2.27*	0.000	0.042	0.049	1.06*	0.000	0.021
Chemicals	0.097	2.41*	0.000	0.766	-.063	-1.42ns	0.397	-0.591
Irrigation water	0.152	3.81**	0.001	1.241	0.127	2.39*	0.000	0.941
Electricity	-0.018	-1.35ns	0.249	-0.104	-0.009	-0.98ns	0.716	-0.056
R^2	0.92				0.89			
Durbin-Watson	2.01				2.06			
Return to scale	0.786				0.607			

*Significant at 1% level, **Significant at 10% level and ns non-significant

The results of using Cobb Douglas function were shown in Table 7 to determine the relationship between types of input energies and the yield of sweet-cherry and sour-cherry. The Durbin-Watson statistics indicated no auto-correlation at the 5% significance level and the effect of both energy types on the yield was positive.

Indirect energies had a greater impact than direct energies. Similar results were obtained in various studies in Iran (Mohammadi *et al.*, 2010; Tabatabaie *et al.*, 2013; Royan *et al.*, 2012).

Findings highlighted that the impact of both renewable and non-renewable energies on the yield was positive. The amount of non-

renewable energy consumed during the production of sweet-cherry and sour-cherry was about six times higher than renewable energy. The use of non-renewable energy as a resource-depletion can affect the environment. Carbon dioxide emissions from the energy required to produce fertilizers and pesticides as well as fuel can have adverse effects on the environment. Therefore, using biodiesel as fuel or by-products as fertilizers can reduce the need for non-renewable resources and increase energy efficiency.

Table 7- Estimation of impacts of direct energy vs. indirect energy and renewable energy vs. non-renewable energy on yield

Energy source	Sour-cherry			Sweet-cherry		
	Coefficient	t-ratio	P-value	Coefficient	t-ratio	P-value
$\ln Y_i = \beta_1 \ln DE + \beta_2 \ln IDE + e_i$						
Direct energy	0.358	3.78**	0.001	0.317	3.54**	0.001
Indirect energy	0.324	3.79**	0.001	0.369	4.12*	0.001
R^2	0.72			0.81		
Durbin-Watson	1.90			1.78		
Return to scale	0.682			0.686		
$\ln Y_i = \gamma_1 \ln RE + \gamma_2 \ln NRE + e_i$						
Renewable energy	0.456	7.22**	0.001	0.419	5.09**	0.001
Nonrenewable energy	0.365	6.69**	0.001	0.89	3.49**	0.001
R^2	0.83			0.74		
Durbin-Watson	1.77			1.86		
Return to scale	0.821			0.708		

*Significant at 1% level, **Significant at 10% level and ns non-significant

Production costs and economic indicators

It is very important to reduce the production cost in agricultural sector while increasing yield. For this purpose, economic analysis should be done. Table 8 shows the econometric analysis in the production of sour-cherry and sweet-cherry products. The costs of the total production for sweet-cherry were more than those of sour-cherry. Also, the gross value of sweet-cherry was more than sour cherry because the price of sweet-cherry was more than sour-cherry in the market.

The economic productivity in sour-cherry production was found to be more than sour-cherry production which means that with each dollar expense we can produce more weight of sour-cherry than sweet-cherry. While the benefit-cost ratio of sweet-cherry was more than sour-cherry, indicating a higher profitability of sweet-cherry production compared to sour-cherry.

The human labor input had the highest expense in the production of both crops. This was due to lack of mechanization in the horticulture sector, pruning, and fertilization, and harvesting operations are carried out by human labor, thus, human labor expense had the highest share from total cost.

The agricultural machinery was the second most expensive input in the production of both crops. Water irrigation was ranked third in the production costs of both crops. According to Table 6, the total contribution of the other inputs was less than 3%. Improvement in management practices (e.g. the efficient use of fertilizers and fuel) reduces the production costs. A compromise should be made between the economic interests of the farmers and the sustainability of local environmental systems is the key to achieve new and sustainable farming techniques and management systems.

Association of inputs and the income

Table 9 illustrates the econometric estimation results of input costs and the income using Cobb-Douglas production function. The return to the scale for sour-cherry and sweet-cherry was determined to be 0.698 and 0.592, respectively. Therefore, there is an increasing rate of return to the scale for both products. In the production of sour-cherry and sweet-cherry, the human labor cost the had the highest effect on the income at 1% probability level.

Table 8- Economic analysis of sour-cherry and sweet-cherry production

Inputs (unit)	Sour-Cherry		Sweet-cherry	
	Cost	Ratio (%)	Cost	Ratio (%)
Human labor ($ ha^{-1})	2508.0	76.96	2657.2	72.05
Machinery ($ ha^{-1})	293.6	9.01	439.9	11.93
Fertilizers ($ ha^{-1})	78.7	2.42	92.1	2.50
Chemicals ($ ha^{-1})	49.44	1.52	53.1	1.44
Diesel fuel ($ ha^{-1})	8.1	0.25	10.3	0.28
Irrigation water ($ ha^{-1})	242.7	7.44	341.4	9.26
Electricity ($ ha^{-1})	78.4	2.40	93.5	2.54
Variable production cost ($ ha^{-1})	3259.0	100	3687.64	100
Fix production cost ($ ha^{-1})	423.7		479.4	
Total production costs ($ ha^{-1})	3682.7		4167.1	
Crop price ($ kg^{-1})	1.42		2.26	
Gross production value ($ ha^{-1})	6696.7		12378.0	
Economic indicators				
Benefit-cost ratio (-)	1.82		2.97	
Economic productivity (kg S^{-1})	1.16		1.03	
Gross income ($ ha^{-1})	3437.7		8690.4	
Net income ($ ha^{-1})	3014.1		8210.0	

Table 9- Econometric estimation results of energy inputs

Energy source	Sour-cherry			Sweet-cherry		
	Coefficient	t-ratio	P-value	Coefficient	t-ratio	P-value
Model: $Lny_i = a_0 + \alpha_1 lnx_1 + \alpha_2 lnx_2 + \alpha_3 lnx_3 + \cdots + \alpha_8 lnx_8 + e_i$						
Diesel fuel	0.193	3.84**	0.001	0.138	2.58*	0.001
Human labor	0.223	4.15**	0.001	0.214	3.67**	0.000
Machinery	-0.021	-1.17ns	0.889	0.081	1.26*	0.000
Fertilizer	0.094	2.11*	0.000	0.109	1.43ns	0.350
Chemicals	0.119	2.67ns	0.010	-0.041	-1.68*	0.000
Irrigation water	0.138	3.61*	0.000	0.038	1.02*	0.000
Electricity	-0.048	-1.71ns	0.290	0.053	1.19ns	0.359
R^2	0.84			0.79		
Durbin-Watson	2.11			1.82		
Return to scale	0.698			0.592		

*Significant at 1% level, **Significant at 10% level and ns non-significant

Conclusions

The purpose of this study was to compare the energy consumption and income of sour-cherry and sweet-cherry production. The results of this research would be very productive for any construction of orchard of sweet-cherry and sour-cherry. According to the analysis, the following results were obtained:

1. Total energy consumption for sweet-cherry production was 1.22 times higher than sour-cherry production. Furthermore, the yield of sweet-cherry production was more than the sour-cherry production. It was concluded that the use of inputs in production was accompanied by the same results in the yield.
2. In the production of both crops, fertilizers were the energy-intensive input whereas human labor and agricultural machinery were the costliest inputs.
3. The economic analysis revealed that the production costs for sweet-cherry were higher than sour-cherry but sweet-cherry was more profitable than sour-cherry due to the premium prices for sweet-cherry.
4. Accurate fertilizer management (especially nitrogen) and saving fuel by the proper tractor selection and management, precise and timely pruning, using high yield varieties were suggested to decrease energy consumption and increase income.

References

1. Acaroglu, M. 1998. Energy from biomass, and applications. University of Selçuk, Turkey.
2. Aghakhani, M. H., H. Soltanali, S. Ahmadipour, and A. Rohani. 2018. Investigation of greenhouse gas emissions, energy consumption and costs of citrus production: a case study of Mazandaran province. Journal of Energy Planning and Policy Research 12: 181-229.
3. Akcaoz, H. 2011. Analysis of energy use for banana production: A case study from Turkey. African Journal of Agricultural Research 6 (25): 5618-5624.
4. Akcaoz, H., O. Ozcatalbas, and H. Kizilay. 2009. Analysis of energy use for pomegranate production in Turkey. Journal of Food, Agriculture and Environment 7 (2): 475-480.
5. Akdemİr, S., H. Akcaoz, and H. Kİzİlay. 2012. An analysis of energy use and input costs for apple production in Turkey. Journal of Food, Agriculture & Environment 10 (2): 473-479.
6. Aydın, B., and D. Aktürk. 2018. Energy Use Efficiency and Economic Analysis of Peach and Cherry Production Regarding Good Agricultural Practices in Turkey: A Case Study in Çanakkale Province. Energy 158: 967-974.
7. Banaeian, N., and N. Zangeneh. 2011. Modeling Energy Flow and Economic Analysis for Walnut Production in Iran. Research Journal of Applied Sciences, Engineering and Technology 3 (3): 194-201.
8. Cervinka, V. 1980. Fuel and energy efficiency. PP. 15-21 in: D. Pimentel ed. Handbook of Energy Utilization in Agriculture. CRC Press Inc., Boca Raton.
9. Chapagain, T., and A. Riseman. 2014. Barley–pea intercropping: Effects on land productivity, carbon and nitrogen transformations. Field Crops Research 166: 18-25.
10. Cobanoglu, F. 2010. Analysis of energy use for fig production in Turkey. Journal of Food, Agriculture and Environment 8: 842-847.
11. Cobb, C. W., and P. H. Douglas. 1928. A Theory of Production. American Economic Review 18: 139-165.
12. Demircan, V. K., H. M. Ekinci, D. Keener, C. Akbolat, and A. Ekinci. 2006. Energy and economic analysis of sweet cherry production in Turkey: A case study from Isparta province. Energy Conversion and Management 47: 1761-1769.
13. Esengun, K., O. Gündüz, and G. Erdal. 2007. Input-output energy analysis in dry apricot production of Turkey. Energy Conversion and Management 48: 592-598.
14. Fadavi, R., A. Keyhani, and S. S. Mohtasebi. 2011. An analysis of energy use, input costs and relation between energy inputs and yield of apple orchard. Research in Agricultural Engineering 57 (3): 88-96.
15. FAO. 2019. Food and Agriculture Organization. Available at: http://www.fao.org/faostat/en/#data/QC. Accessed 29 December 2019.
16. Ghasemi-Varnamkhasti, M., S. M. Hashemi-Garmdareh, and S. A. Hashemi-Garmdareh. 2015. Evaluation and optimization of energy consumption in the production of peaches CASE STUDY: Saman Region in Chahar Mahal va Bakhtiari Province. Journal of Agricultural Machinery 5 (1): 206-216. (In Farsi).
17. Ghatrehsamani, S., R. Ebrahimi, S. N. Kazi, A. B. Badry, and E. Sadeghinezhad. 2016. Optimization model of peach production relevant to input energies-Yield function in Chaharmahal va Bakhtiari province, Iran. Energy 99: 315-321.
18. Gokdogan, O., H. I. Oguz, and M. F. Baran. 2017. Energy input-output analysis in organic mulberry (Morus spp.) production in Turkey: a case study Adiyaman-Tut Region. Erwerbs-Obstbau 59 (4): 325-330.
19. Gujarati, D. N. 1995. Basic econometrics. McGraw-Hill. New York.
20. Gündoğmuş, E. 2013. Modeling and sensitivity analysis of energy inputs for walnut production. Actual Problems of Economics 140 (2): 188-197.

21. Gündoğmuş, E. 2014. Does energy efficiency increase with orchard size? A case study from peach production. Energy Efficiency 7 (5): 833-839.
22. Haddadi, H., M. P. Gholami, and M. Ghahdorijan. 2015. Determination of economic and energy indicators for the production of horticultural products (with an area of less than 4000 square meters). International Conference of Applied Research in Agriculture. Tehran, Iran. . (In Farsi).
23. Helsel, Z. R. 1992. Energy and alternatives for fertilizer and pesticide use. PP 177–210 in R.C. Fluck ed. Energy in World Agriculture. Elsevier. Amsterdam.
24. Kizilaslan, H. 2009. Input-output analysis of cherries production in Tokat province of Turkey. Applied Energy 86 (7&8): 1354-1358.
25. Liu, Y., V. Langer, H. H. Jensen, and H. Egelyng. 2010. Energy use in organic, green and conventional pear producing systems-cases from China. Journal of Sustainable Agriculture 34: 630-646.
26. Loghmanpour Zarini, R., H., Yaghoubi, and A. Akram. 2013. Energy use in citrus production of Mzandaran province in Iran. African Crop Science Journal 21 (1): 61-65.
27. Mahallati, M. N., A. Koocheki, F. Mondani, H. Feizi, and S. Amirmoradi. 2015. Determination of optimal strip width in strip intercropping of maize (*Zea mays* L.) and bean (*Phaseolus vulgaris* L.) in Northeast Iran. Journal of Cleaner Production 106: 343-350.
28. Ministry of Agricultural Jahad of Iran. 2019. Iran Agriculture Statistics. Avaliable from: https://www.maj.ir/Dorsapax/userfiles/Sub65/Amarnamehj3-1396-site.pdf. Accessed 29 December 2019. (In Farsi).
29. Mirzaei Khalilabadi, H. R., A. H. Chizari, and M. Dahajipour Heidarabadi. 2014. Effects of Increasing Price of Energy Carriers on Energy Consumption in Pistachio Production: Case Study in Rafsanjan, Iran. Journal of Agricultural Science & Technology 16 (4): 697-704.
30. Mohammadi, A., Sh. Rafiee, S. S. Mohtasebi, and H. Rafiee. 2010. Energy inputs–yield relationship and cost analysis of kiwifruit production in Iran. Renewable Energy 35 (5): 1071-1075.
31. Mohseni, P., S. A. Borghaee, and M. Khanali. 2019. Energy Consumption Analysis and Environmental Impact Assessment of Grape Production in Hasawa Region, Arak. Journal of Agricultural Machinery 9 (1): 177-193. (In Farsi).
32. Mudahar, M. S., and T. P. Hignett. 1987. Energy requirements, technology and resources in fertilizer sector. PP 25-61 in Z. R. Helsel ed. Energy in Plant Nutrition and Pest Control. Energy in World Agriculture. Elsevier. Amsterdam.
33. Nabavi-Pelesaraei, A., A. Sadeghzadeh, M. H. Payman, and H. Ghasemi Mobtaker. 2013. An analysis of energy use, CO_2 emissions and relation between energy inputs and yield of hazelnut production in Guilan province of Iran. International Journal of Advanced Biological and Biomedical Research 1 (12): 1601-1613.
34. Nabavi-Pelesaraei, A., Sh. Rafiee, H. Hosseinzadeh-Bandbafha, and S. Shamshirband. 2016. Modeling energy consumption and greenhouse gas emissions for kiwifruit production using artificial neural networks. Journal of Cleaner Production 133: 924-931.
35. Nikkhah, A., B. Emadi, H. Soltanali, S. Firouzi, K. A. Rosentrater, and M. S. Allahyari. 2016. Integration of life cycle assessment and Cobb-Douglas modeling for the environmental assessment of kiwifruit in Iran. Journal of Cleaner Production 137: 843-849.
36. Ozkan, B., C. Fert, and C. F. Karadeniz. 2007. Energy and cost analysis for greenhouse and open field grape production. Energy 32: 1500-1504.
37. Ozkan, B., H. Akcaoz, and F. Karadeniz. 2004. Energy requirement and economic analysis of citrus production in Turkey. Energy Conversion and Management 45: 1821-1830.
38. Proebsting, E. L. 1980. Energy inputs in cherry production. PP 251-4 in D. Pimentel ed. Handbook of energy utilization in agriculture. CRC Press Inc., Boca Raton.

39. Qasemi-Kordkheili, P., N. Kazemi, A. Hemati, and M. Taki. 2013. Energy consumption, input-output relationship and economic analysis for nectarine production in Sari region, Iran. International Journal of Agriculture and Crop Sciences 5 (2): 125-131.
40. Rafiee, Sh., S. H. Musavi Avval, and A. Mohammadi. 2010. Modeling and sensitivity analysis of energy inputs for apple production in Iran. Energy 35 (8): 3301-3306.
41. Rasouli, M., M. Namdari, and S. H. Mousavi Avval. 2014. Modeling and analysis of energy efficiency in grape production of Iran. International Journal of Agricultural Technology 10 (3): 517-532.
42. Royan, M., M. Khojastehpour, B. Emadi, and H. G. Mobtaker. 2012. Investigation of energy inputs for peach production using sensitivity analysis in Iran. Energy Conversion and Management 64 :441-446.
43. Sami, M., M. J. Shiekhdavoodi, and A. Asakereh. 2011. Energy use in apple production in the Esfahan province of Iran. African Crop Science Journal 19 (2):125-130.
44. Snedecor, G. W., and W. G. Cochran. 1980. Statistical methods. Iowa State University Press. Iowa.
45. Soltanali, H., A. Nikkhah, and A. Rohani. 2017. Energy Audit of Iranian Kiwifruit Production Using Intelligent Systems. Energy 139: 646-654.
46. Strapatsa, A. V., G. D. Nanos, and C. A. Tsatsarelis. 2006. Energy flow for integrated apple production in Greece. Agriculture, Ecosystem and Environment 116: 176-180.
47. Tabatabaie, S. M. H., Sh. Rafiee, A. Keyhani, and A. Ebrahimi. 2013. Energy and economic assessment of prune production in Tehran province of Iran. Journal of Cleaner Production 39: 280-284.
48. Tabatabaie, S. M. H., Sh. Rafiee, A. Keyhani, and M. D. Heidari. 2013. Energy use pattern and sensitivity analysis of energy inputs and input costs for pear production in Iran. Renewable Energy 51: 7-12.
49. Tabatabaie, S. M. H., Sh. Rafiee, and A. Keyhani. 2012. Energy consumption flow and econometric models of two plum cultivars productions in Tehran province of Iran. Energy 44 (1): 211-216.
50. Taghavifar, H., and A. Mardani. 2015. Prognostication of energy consumption and greenhouse gas (GHG) emissions analysis of apple production in West Azarbayjan of Iran using Artificial Neural Network. Journal of Cleaner Production 87: 159-167.
51. Verma, A. K., A. K. A., Lawrence, A. Tripathi, and S. Pal, 2018. Energy Use Pattern in Mango Production at Mall-Malihabad Mango Belt of Utter Pradesh. International Journal of Pure & Applied Bioscience 6 (6): 64-71.
52. Yaldiz, O., H. Ozturk, Y. Zeren, and A. Baoçetinçelik. 1993. Energy usage in production of field crops in Turkey. 5th International Congress on Mechanization and Energy Use in Agriculture. Kusadasi, Turkey.
53. Yaldiz, O., H. H. Ozturk, and A. Baoçetinçelik, 1990a. The determination of energy out-puts/inputs rates at some products of the Çukurova region. International Conference on Agricultural Engineering. Berlin. Germany.
54. Yaldiz, O., H. H. Ozturk, Y. Zeren, and A. Baoçetinçelik, 1990b. Energy use in fieldcrop production in Turkey. Journal of Agriculture Faculty, University of Akdeniz 3 (1-2): 51-62 (In Turkish).

نشریه ماشین‌های کشاورزی
جلد ۱۱، شماره ۱، نیمسال اول ۱۴۰۰، ص ۱۱۰-۹۷

Journal of Agricultural Machinery
Vol. 11, No. 1, Spring- Summer 2021, p. 97-110

مقاله علمی-پژوهشی

بررسی مصرف انرژی و شاخص‌های اقتصادی تولید آلبالو و گیلاس در شمال شرق ایران

رضا وحید بریمانلو[۱]، فاطمه نادی[۲*]

تاریخ دریافت: ۱۳۹۸/۰۷/۱۰
تاریخ پذیرش: ۱۳۹۸/۱۰/۲۵

چکیده

هدف این تحقیق بررسی مصرف انرژی و هزینه‌های تولید آلبالو و گیلاس در شمال شرق ایران بود. اطلاعات از طریق ۷۵ تولیدکننده گیلاس و ۴۲ تولیدکننده آلبالو جمع‌آوری شدند. انرژی کل نهاده‌ها برای تولید گیلاس و آلبالو به‌ترتیب ۳۷/۷۶ و ۳۱/۰۳ $GJha^{-1}$ تخمین زده شد. در حالی‌که بازده انرژی گیلاس بیشتر از آلبالو بود. در هر دو محصول کود شیمیایی و سوخت دیزل بیشترین مصرف انرژی را داشتند. سهم انرژی‌های تجدیدپذیر در تولید گیلاس بیشتر از آلبالو بود که نشان می‌دهد تولید گیلاس در این منطقه به منابع تجدیدناپذیر وابسته‌تر است. تحلیل اقتصادی نشان داد که هزینه تولید گیلاس بیشتر از آلبالو بود اما به‌دلیل قیمت بالاتر گیلاس، سود گیلاس بیشتر بود. نتایج مدل‌سازی نشان داد که نیروی انسانی بیشترین تاثیر را روی هزینه تولید هر دو محصول داشت. در نهایت، صرفه‌جویی در مصرف سوخت دیزل و مدیریت کوددهی به‌عنوان راه‌حل‌های اصلی برای حل مسایل اقتصادی و انرژی هر دو محصول توصیه شد.

واژه‌های کلیدی: آلبالو، درآمد، کاب داگلاس، گیلاس، مدل‌سازی انرژی، هزینه تولید

۱- دانش‌آموخته کارشناسی ارشد انرژی- مکانیزاسیون، واحد آزادشهر، دانشگاه آزاد اسلامی، آزادشهر، ایران
۲- گروه مهندسی مکانیک ماشین‌های کشاورزی، واحد آزادشهر، دانشگاه آزاد اسلامی، آزادشهر، ایران
(*- نویسنده مسئول: Email: f.nadi@iauaz.ac.ir)

DOI: 10.22067/jam.v11i1.83466

Journal of Agricultural Machinery
Vol. 11, No. 1, Spring- Summer 2021, p. 111-122

نشریه ماشین‌های کشاورزی
جلد ۱۱، شماره ۱، نیمسال اول ۱۴۰۰، ص ۱۲۲-۱۱۱

Full Research Paper

Economical Assessment of Replacing and Refining Methods of Hydraulic Oil of Sugarcane Harvesters in Sugarcane Cultivation Industry of Khuzestan

H. Nematpour Malek Abad[1], M. J. Sheikhdavoodi[2*], I. Hazbavi[3], A. Marzban[4]

Received: 11-11-2018
Accepted: 06-03-2019

Abstract

Contamination due to hydraulic fluids exerts deleterious effects after a long time, however this factor is often ignored or its consecutive breakdowns and system failures are considered due to other factors. Therefore, in order to prevent the likelihood of occurring such problems, the following two strategies are presented: using oil change method to replace all of the hydraulic fluids from the discharge system with the new oil and using offline hydraulic oil filtration system for the removal of contaminated oil particles. In this regard, the present study aimed to investigate the economic status of cane sugar harvesting machines with an emphasis on hydraulic oil filtration process in seven units of sugarcane developmental company and affiliated industries in Khuzestan province, Iran. To perform this study, all statistics and data of the sugarcane and affiliated industries in seven companies during the crop year 2011-2016 were collected and classified. The results indicated that the application of the hydraulic filtration method led to the oil consumption saving (per liter) and in price (Iranian Rial) during the three crop-years of 2014-2016, as following: Imam Khomeini: 25500 L and 2882154363 Rials, Amir Kabir: 49000 L and 5847389466 Rials, Hakim Farabi: 82000 L and 9534396744 Rials, Dabal Khazaee: 73400 L and 6808230362 Rials, Dehkhoda: 31680 L and 3421979639 Rials, Salman Farsi: 73500 L and 7606675370 Rials and Mirza Koochak Khan: 75934 L and 8083068395 Rials.

Keywords: Economical assessment, Hydraulic oil, Oil replacing, Refining, Sugarcane harvester

Introduction

Maintenance costs related to farm machinery are those expenditures necessary to restore or maintain technical soundness and reliability of the machines (Ashtiani Iraqi *et al.*, 2005). The prediction of maintenance costs for mechanized agricultural units is of particular importance in several aspects: firstly, the machine is regarded as one of the main commodities in the agricultural industry that makes it possible to accurately measure the profitability by including the cost items. Secondly, to determine the break-even point for replacing the machine with a new one, it is necessary to estimate the useful lifespan of machines by analyzing the trend of changes in these costs; and thirdly, the possible undesirable causes of cost overruns become possible (Lazarus, 2002). Maintenance is usually described as activities that upgrade the system reliability and guarantee the operational performance of the equipment. Nowadays, maintenance is identified as one of the major issues in the machinery use. Thus, there has always been an attempt to select and run more effective ways to reduce maintenance costs, increase efficiency, and improve safety and timely performance (Bartholomew, 1981). The maintenance and inspection approaches and tools, which have been gradually introduced in the industry since the 1970s, include a wide variety of different methods such as vibration analysis, sound analysis, ultrasonic analysis, thermography, performance analysis, oil tribology analysis, engine circuit analysis and others (Dahunsi, 2008). These methods are mostly focused on the individual indicators for machinery system

1- PhD Graduate of Agricultural Mechanization, Department of Biosystems Engineering, Shahid Chamran University of Ahvaz, Iran
2- Professor, Department of Biosystems Engineering, Shahid Chamran University of Ahvaz, Iran
3- Assistant Professor, Department of Biosystems Engineering, Lorestan University, Khorramabad, Iran
4- Associate Professor, Agricultural Sciences and Natural Resources University of Khuzestan, Mollasani, Iran
(Corresponding Author Email: javad1950@gmail.com)
DOI: 10.22067/jam.v11i1.76542

assessment and used to determine the health conditions of various components and parts of the machine. An effective lubrication program with oil analysis can provide longer equipment life, detect early signs of contamination and degradation, reduce equipment downtime and ultimately save you money. In addition, the erosion control and corrosion, wear related deteriorating factors, and optimum oil consumption are also of the benefits of oil analysis in the preventive maintenance (Macinan *et al.,* 2006). In oil analysis technique, oil sampling and testing should be investigated on a regular basis to increase the efficiency and accuracy of the oil analysis program. Thus, it is recommended to perform machine care oil analysis for hydraulic systems every 250 hours. However, depending on the equipment condition in special circumstances, the time can be changed and arranged. In mechanical systems, oil contamination leads to major and numerous problems such as machine failure, repairs, reduced shelf life of oil and so on. Furthermore, it directly effects on the equipment and production effectiveness and consequently imposes the significant unexpected costs. On the other hand, considering the oil contamination control schedule and clean oils, eliminating and controlling contaminated oil would achieve many benefits including minimizing the equipment failure, reducing the operational and maintenance costs, improving the operational efficiency of the equipment and increasing the oil shelf life. Oil contaminations are divided into two basic groups: physical and chemical. Physical contaminations refer to solid particles along with oil whose main consequence is the mechanical wear. On the other hand, chemical contaminations generally include water, some metals such as copper, and materials produced from oil usage. Therefore, in order to prevent the likelihood of problems occurring, the following strategies could be applied: Replace all of the hydraulic fluids from the discharge system with the new oil and use of offline hydraulic oil filtration system for removing the contaminated oil particles (Massoudi, 2011, Ranjbar *et al.*, 2003 and Saghafi, 2008). Prior to the emergence of maintenance and repairing systems, it was assumed that the machines and equipment were used until they were in service, and the maintenance and repairing teams were only involved in the repairing the machines once they had failed to resume their works (Bartelmous and Zimroz, 2009). Nowadays, the advancement of technology, as well as higher prices for agricultural machinery, preventive maintenance (PM) strategy, as a systematic and scheduled policy for identifying the maintenance tasks to prevent the abnormal wear and tear of machine components and lowering emergency machines breakdown, is planned and run based on the intermittent implementation procedures (Mirmoazi, 2004). Therefore, the main objective of the (PM) was to develop systematic conditions for monitoring the status of existing equipments and machines in order to achieve maximum efficiency and productivity and reducing the breakdown and failure with of the machines (Yeganeh Salehpour, 2002). It is obvious that the timeliness of harvesting process is limited based on climatic conditions and plant status, and the failure of harvesting machines during this period might cause to delayed harvest, which in turn increases loss and wastes (Scoma, 1990). The use of the offline filtration method has the following advantages over the oil change method: 1. Any future damages to the machine could be avoided which directly affects the expense reduction. 2. A large amount of oil would be recycled and reused, which is economically important. As a result, the offline oil filtration system plays a fundamental role in the smooth and continuous operation of hydraulic systems. The present study aimed to investigate the economic status of cane sugar harvesting machines with an emphasis on hydraulic oil filtration process in seven units of sugarcane developmental company and affiliated industries in Khuzestan province, Iran.

Materials and Methods

One of the most important sources of the sugar production is sugarcane. Sugar is among the eight human food sources (wheat, rice, corn, sugar, cattle, sorghum, millet and cassava). Also, sugarcane is mainly used for livestock feed, electricity generation, fiber and fertilizer and in many countries sugarcane is a renewable resource for the biofuel production (Haroni *et al.*, 2018). This study was focused on the performance of sugar cane harvesting machines known as the A7000 (Austoft) sugar cane harvester manufactured by Australia in seven sugarcane developmental companies and affiliated industries development company, which were taking care of sugar cane harvesting operations in Khuzestan province. The purpose of this study was to compare the economic efficiency of two offline replacements and filtration techniques for hydraulic oil with an emphasis on the hydraulic oil filtration process. The quantity of hydraulic oil used in each harvester was 480 (L) and the working temperature of hydraulic oil of the sugarcane harvesters in sugarcane development corporations is adjusted from 80 to 100 degrees Celsius, which is replaced each 1000 (h). The offline refinery device of hydraulic oil (filtration) has been formed by two separated pumps and a filter with a debit of 300 L min^{-1} (see Figure 1). This device, which is performed in the offline mode, is similar to a dialysis machine. The machine is connected to a hydraulic oil tank (reservoir) and then, its electric motors start working. While the oil is passing through the pump, the filters are blocked by the oil particles. By allowing the oil to pass the machine's filters by repeating the process, the device will reach to National Aerospace Standard (NAS) (the number of particles is in one milliliter of oil, and the higher its amount, the higher the level of contamination in the oil will be.) which, regarding the hydraulic oil of sugarcane harvester, the number of particles in 5-15 µm sizes available in the oil should not be more than 256000, fitting the pumps and hydro-motors (because moving and disposing the components of hydraulic systems can easily pass these particles). The device filtration components include one magnetic filter made of metal in 100 µm size, one filter made of paper in 10 µm size, two fiberglass filter in 10 µm size that are used for absorbing the tank water to reduce the water boiling point that the available water starts evaporating in lower temperature and one filter in 5 µm size is installed in device output route.

Fig.1. Representation of offline refinery device of hydraulic oil (filtration)

In order to collect data on the criteria such as the oil consumption (demand) price for sugar cane harvesting machines during the cropping years of 2011-2013 (oil replacement

technique) and 2014-2016 (offline oil filtration technique), the researcher directly visited the sugarcane developmental companies and affiliated industries development companies operating in Khuzestan province. In this study, fixed costs included purchase costs of equipment required for offline oil filtration, building and facilities. The annual depreciation cost (D) of offline refinery device of hydraulic oil (filtration) was computed by using the formula (1):

$$D = {}^{P-S}/_{L} \quad (1)$$

Where P is the list price of the equipment (rial)
S= 0.1*P (is the salvage value) (rial)
M=10 (is the estimated life of the equipment in years)
The usance cost (I) of offline refinery device of hydraulic oil (filtration) was computed as:

$$I = {}^{(P+S)}/_{2} * i \quad (2)$$

Where P is the list price of the equipment (rial)
S= 0.1*P (is the salvage value) (rial)
And i: is the interest rate.

Due to lack of availability to the working life and dilapidated price of the machine in this study, they were considered to be 10 years and 10% of a new machine price, respectively (Almasi, 2008). Moreover, variable costs include labor and transportation in the offline filtration cycle or oil replacement. Oil consumption costs involved expenses related to ordering, supplying, purification, replacement and hydraulic oil analysis (Determination of the Exact Amount of Water in the Oil (water contamination), Determination of the Uncleanness Level of Oil, Determination of the Si Amount, Viscosity Measurement of oil and Measurement of the Total acid number (TAN)). These data were extracted and calculated from different types of warehouses and purchase orders of subsidiaries supervised by Sugarcane developmental Company. Then the amount of hydraulic oil consumption for each company was received from the technical offices of the company and affiliated service centers. To remove the effects of inflation on the prices of various years, all prices were calculated based on the prices of 2016 fiscal years. Finally, oil consumption level, oil savings due to the use of hydraulic oil filtration technique, Rial savings, the cost-benefit and the break-even point analysis of offline hydraulic oil filtration have been calculated and evaluated.

Results and Discussion

According to previous studies, it was expected that applying offline hydraulic oil filtration in preventive maintenance programs would lead to the removal of suspended contaminants in oil to protect and extend equipment life. It was also estimated that it would increase as well as increases the oil shelf life and consequently would reduce oil consumption and costs. Therefore, this section investigated the economic comparison of two offline replacements and filtration techniques for hydraulic oil in sugarcane developmental companies and analyzed their results.

Economic evaluation of two offline replacements and filtration techniques

Based on the results obtained from the seven sugarcane developmental companies and affiliated industries development companies in Khuzestan province including Imam Khomeini, Amir Kabir, Hakim Farabi, Dabal Khazaee, Dehkhoda, Salman Farsi and Mirza Koochak Khan, the offline hydraulic oil filtration program was implemented and planned on a regular basis from the 2014 cropping year. Data on oil consumption and harvester status in all seven companies have been shown in Table 1. As can be seen from data in Table 1, the use of offline hydraulic oil filtration technique during the studied years, reduced the amount of oil consumed per hour from 0.95, 1.99, 3.47, 3.73, 1.35, 2.46 and 4.20 (L h^{-1}) in 2014 to 0.88, 1.88, 3.06, 3, 1.25, 2.33 and 4 in 2016 in seven studied companies. In addition, the amount of oil usage per hectare was declined from 2.07, 3.97, 7.33, 8.45, 3.01, 5.36 and 9.21 (L ha^{-1}) in 2014 to 2, 3.85, 6.7, 6.45, 2.9, 5.2 and 6 in 2016. In addition, the amount of oil usage per ton was declined from 0.027, 0.06, 0.095, 0.095, 0.037, 0.06 and 0.1 (L ton^{-1}) in 2014 to 0.023, 0.045, 0.075, 0.071,

0.034, 0.056 and 0.064 in 2016. In addition, the amount of sugarcane yield (ton ha^{-1}) was increased from 76.67, 66.17, 77.16, 88.95, 81.35, 89.33 and 92.1 in 2014 to 86.96, 85.56, 89.33, 90.85, 85.29, 92.86 and 93.75 in 2016.

Table 1- Hydraulic oil consumption of sugarcane harvester in sugarcane developmental companies

Sugarcane development company	Year description	2011	2012	2013	2014	2015	2016
Imam Khomeini	Oil consumed (L h^{-1})	1.23	1.05	1.07	0.95	0.92	0.88
	Oil consumed (L ha^{-1})	2.51	1.77	2.28	2.07	2.02	2
	Oil consumed (L ton^{-1})	0.033	0.027	0.030	0.027	0.024	0.023
	Sugarcane yield (ton ha^{-1})	76.1	65.56	76	76.67	84.17	86.96
Amir Kabir	Oil consumed (L h^{-1})	2.15	1.93	2.24	1.99	1.92	1.88
	Oil consumed (L ha^{-1})	4.54	4	4.48	3.97	3.9	3.85
	Oil consumed (L ton^{-1})	0.082	0.07	0.078	0.06	0.05	0.045
	Sugarcane yield (ton ha^{-1})	55.37	57.14	57.44	66.17	78	85.56
Hakim Farabi	Oil consumed (L h^{-1})	3.5	3.45	3.08	3.47	3.08	3.06
	Oil consumed (L ha^{-1})	8.96	7.23	6.78	7.33	6.74	6.7
	Oil consumed (L ton^{-1})	0.12	0.095	0.095	0.095	0.078	0.075
	Sugarcane yield (ton ha^{-1})	75	76.11	71.37	77.16	86.41	89.33
Dabal Khazaee	Oil consumed (L h^{-1})	3.41	3.88	3.50	3.73	3.65	3
	Oil consumed (L ha^{-1})	7.94	7.84	7.90	8.45	8.35	6.45
	Oil consumed (L ton^{-1})	0.095	0.095	0.095	0.095	0.093	0.071
	Sugarcane yield (ton ha^{-1})	83.58	82.53	83.16	88.95	89.78	90.85
Dehkhoda	Oil consumed (L h^{-1})	1.5	1.46	1.2	1.35	1.3	1.25
	Oil consumed (L ha^{-1})	3.62	3.03	2.62	3.01	2.95	2.9
	Oil consumed (L ton^{-1})	0.048	0.038	0.037	0.037	0.035	0.034
	Sugarcane yield (ton ha^{-1})	75.42	79.74	70.81	81.35	84.29	85.29
Salman Farsi	Oil consumed (L h^{-1})	2.93	3.03	1.84	2.46	2.4	2.33
	Oil consumed (L ha^{-1})	5.9	6.4	4.20	5.36	5.3	5.2
	Oil consumed (L ton^{-1})	0.072	0.1	0.06	0.06	0.058	0.056
	Sugarcane yield (ton ha^{-1})	81.94	64	70	89.33	91.38	92.86
Mirza Koochak Khan	Oil consumed (L h^{-1})	4.64	4.7	4.11	4.20	4.15	4
	Oil consumed (L ha^{-1})	7.9	7.4	7.3	9.21	6.3	6
	Oil consumed (L ton^{-1})	0.12	0.15	0.1	0.1	0.068	0.064
	Sugarcane yield (ton ha^{-1})	65.83	49.33	73	92.1	92.65	93.75

Statistical analysis

According to Table 2, because P <0.05, the hypothesis of the equal consumption of hydraulic oil (L ha^{-1}) in the harvesters before and after the hydraulic oil refining method with the confidently of 99% is rejected and with 99% confidence, the use of hydraulic oil refining method has been effective in reducing the consumption of hydraulic oil (L ha^{-1}) in harvesters.

Table 2- The t-test results to compare the oil consumption (L ha^{-1}) before and after using the hydraulic oil refining of harvesters in sugarcane developmental companies

Variable	Stage	Average	The standard deviation	Degrees of freedom	t	p-value
Oil consumption (L ha^{-1})	Before oil refining (oil replacing)	5	2	6	3	0.01
	After oil refining	5	2			

Figure 2 shows a comparison of oil consumption (L ha^{-1}) in seven Imam Khomeini, Amir Kabir, Hakim Farabi, Dabal Khazaee, Dehkhoda, Salman Farsi and Mirza Koochak Khan companies, which used offline hydraulic oil filtration technique for operating sugarcane harvester. Further, the downward oil consumption trend observed in all these seven sugar cane companies indicated that the use of offline hydraulic oil filtration technique had a greater impact on reducing oil consumption in harvester machines. As evident from Figure 2, Mirza Koochak Khan company was in a sufficiently favorable situation compared to other studied companies in terms of reduced oil consumption. This can be attributed to different reasons including: 1) Proper overhaul of sugarcane harvesters, checking and replacing hydraulic hoses correctly, pressing the hoses connections properly, using a suitable hose according to the standards of the manufacturer company and considering the quality of the parts. In addition, when a pump is uninstalled (opened) during machine's service, the inputs are blocked using the blinders to stop the oil leak in the hose. 2) Controlling the oil intake and exhaust by the maintenance group and creating sensitivity of the mechanics regarding oil frugality. 3) Encouragement and promotion of every personnel whose machine would consume the minimum amount of oil. 4) Expert and experienced staff. 5) Efficient management. 6) Training courses for offline hydraulic oil filtration technique. 7) Timely delivery of services for sugar cane harvesting machines in this unit.

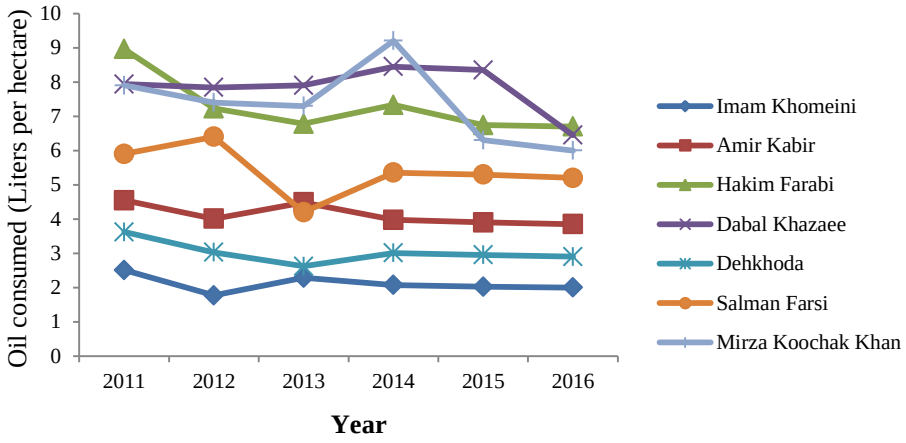

Fig.2. Comparison of oil consumption (L ha^{-1}) in sugarcane developmental companies

According to Figure 3, by using offline hydraulic oil filtration technique during 2014-2016, the average fixed costs (AFC) and average variable costs (Rials per hectare) in seven studied companies based on the hydraulic oil replacement technique has been declined from 216903, 422946.5, 736774.5, 762278.62, 307923.1, 538000.6 and 727454.17 (Rials per hectare) during 2011-2013 to 130272, 246678.1, 433977.2, 488947.72, 188042.64, 331748.82 and 452123.17 (Rials per hectare). Offline hydraulic oil filtration technique during 2014-2016 and Figure 3 represents a comparison of the situation of average fixed costs (AFC) and average variable costs (Rials per hectare) in two offline replacement and filtration techniques. Dabal Khazaee Company, with a total average fixed costs and total variable costs of (762279) (Rials per hectare) in the hydraulic oil replacement during 2011-2013 and 488948 (Rials per hectare) in the hydraulic oil filtration during 2014-2016, achieved the highest total average fixed costs and total variable costs among the companies, respectively (Figure 3). In addition, Imam Khomeini company, having a total average fixed costs and total variable costs of 216903 (Rials per hectare) in the hydraulic oil replacement during 2011-2013 and 130272

(Rials per hectare) in the hydraulic oil filtration during 2014-2016 achieved the lowest total average fixed costs and total variable costs among the seven companies.

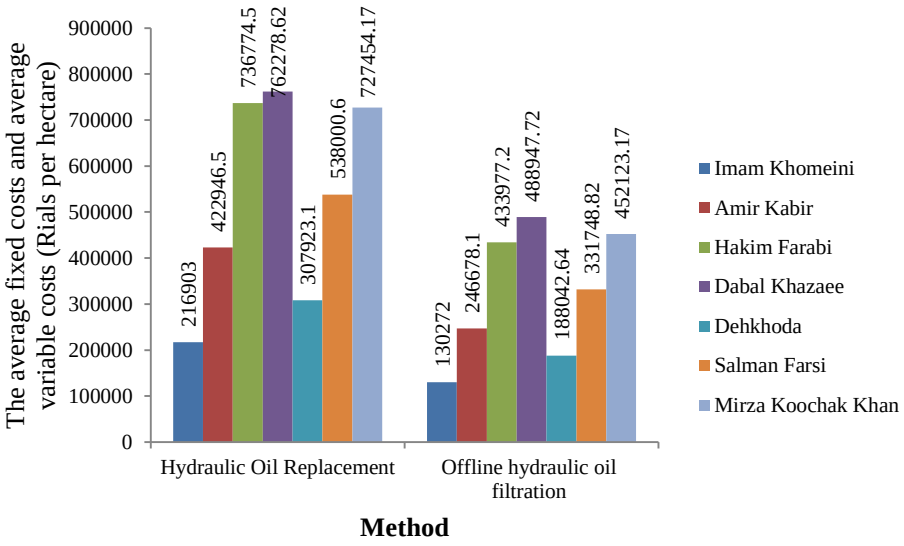

Fig.3. Comparison of the average fixed costs (AFC) and average variable costs (Rials per hectare) for hydraulic oil based on two offline replacements and filtration techniques used in sugarcane developmental companies

Table 3 displays the total amount of savings built up using the offline hydraulic oil filtration in hydraulic oil units within three years. As mentioned before, cost saving on the consumable items including oil was one of the benefits of offline hydraulic oil filtration. Therefore, the establishment of maintenance and repairing program based on the condition analysis could significantly reduce the cost of purchasing consumables items including hydraulic oil. According to Table 3, the total amount of savings built up using offline hydraulic oil filtration in the sugarcane developmental companies was 411014 liters and 44183894339 Rials.

Table 3- Savings in sugarcane developmental companies using offline hydraulic oil filtration during the studied years

Company		2014	2015	2016	Total
Imam Khomeini	Oil (liter)	7000	8800	9700	25500
	Cost saving (rial)	806570607	991745429	1083838328	2882154363
Amir Kabir	Oil (liter)	12000	14200	22800	49000
	Cost saving (rial)	1469961972	1677475065	2699952429	5847389466
Hakim Farabi	Oil (liter)	21000	21000	40000	82000
	Cost saving (rial)	2261508914	2509577337	4763310493	9534396744
Dabal Khazaee	Oil (liter)	23300	28000	22100	73400
	Cost saving (rial)	1803570533	1977212822	3027447007	6808230362
Dehkhoda	Oil (liter)	10560	10560	10560	31680
	Cost saving (rial)	1174264947	1110212619	1137502073	3421979639
Salman Farsi	Oil (liter)	15000	22000	36500	73500
	Cost saving (rial)	1603907811	2188273898	3814493661	7606675370
Mirza Koochak Khan	Oil (liter)	28321	10971	36642	75934
	Cost saving (rial)	1259237207	1504405731	5319425457	8083068395

Figure 4 compares the total amount of Rial savings in seven Imam Khomeini, Amir Kabir, Hakim Farabi, Dabal Khazaee, Dehkhoda, Salman Farsi and Mirza Koochak Khan Companies. As can be seen from data in Figure 4, the total amount of savings built up in Hakim Farabi Company was 9534396744 Rials and the total amount of oil consumption was 82000 liters, indicating higher amount of savings in oil consumption compared to other companies.

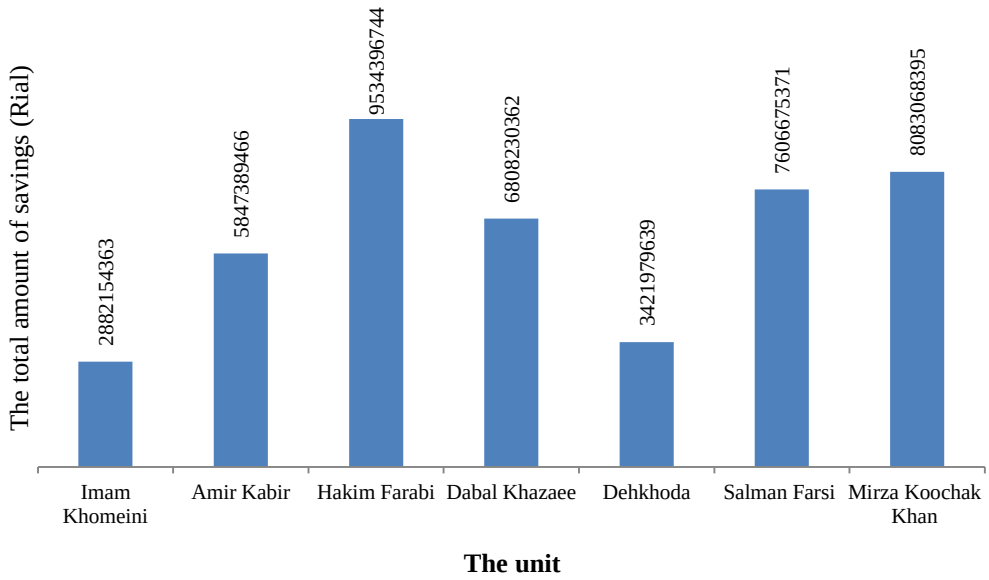

Fig.4. Comparison of the total amount of Rial savings in seven sugarcane developmental companies during 2014-2016

According to Figure 5, the cost-benefit ratio for using offline hydraulic oil filtration in six companies of Imam Khomeini, Amir Kabir, Hakim Farabi, Dabal Khazaee, Salman Farsi and Mirza Koochak Khan companies has been increased from 4.66, 8.5, 13.16, 10.49, 9.33 and 7.33 during 2014 to 6.27, 15.62, 27.71, 17.61, 22.19 and 30.94 in 2016, respectively and Dehkhoda Company experienced a decline of cost benefit ratio from 6.83 in 2014 to 6.62 in 2016. This could be attributed to the lower operational capacity of the company relative to oil consumption and Figure 5 shows a comparison of cost benefit analysis using offline hydraulic oil filtration in sugarcane developmental companies during 2014-2016. As evident in this figure**,** the highest and lowest benefit-cost ratios were observed in Hakim Farabi and Imam Khomeini Companies (2014), Hakim Farabi and Imam Khomeini (2015) and Mirza Koochak Khan and Imam Khomeini (2016), respectively. Finally, the lowest benefit-cost ratio during the crop years 2014-2016 was related to the Imam Khomeini sugarcane developmental company with a profit/cost ratio of 4.66, 5.74 and 6.27.

According to Figure 6, the break-even point (ha) for using offline hydraulic oil filtration in seven companies of Imam Khomeini, Amir Kabir, Hakim Farabi, Dabal Khazaee, Dehkhoda, Salman Farsi and Mirza Koochak Khan companies has been decreased from 2151.15, 1046.84, 647.08, 781.45, 1529.77, 894.92 and 1249.08 during 2014 to 1742.02, 857.98, 485.21, 439.48, 1246.44, 713.83 and 447 in 2016, respectively. Figure 6 shows a comparison of break-even point (ha) analysis using offline hydraulic oil filtration in sugarcane developmental companies during 2014-2016. The highest and lowest break-even point (ha) were observed in Imam Khomein and Hakim Farabi Companies (2014), Imam Khomein and Mirza Koochak Khan (2015), and Imam Khomein and Mirza Koochak Khan

(2016), respectively. Finally, the highest break-even point (ha) during the crop years 2014-2016 was related to the Imam Khomeini sugarcane developmental company with a break-even point (ha) of 2151.15, 2154.13 and 1742.02.

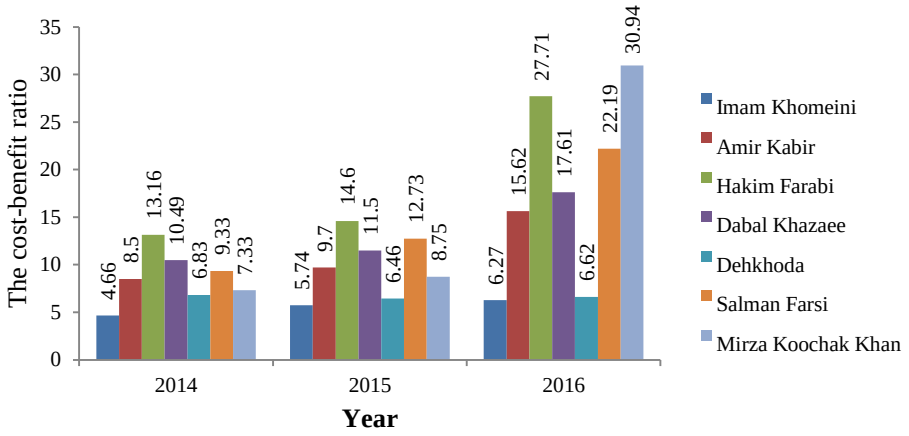

Fig.5. The comparison of cost-benefit ratio based on the using offline hydraulic oil filtration in sugarcane developmental companies

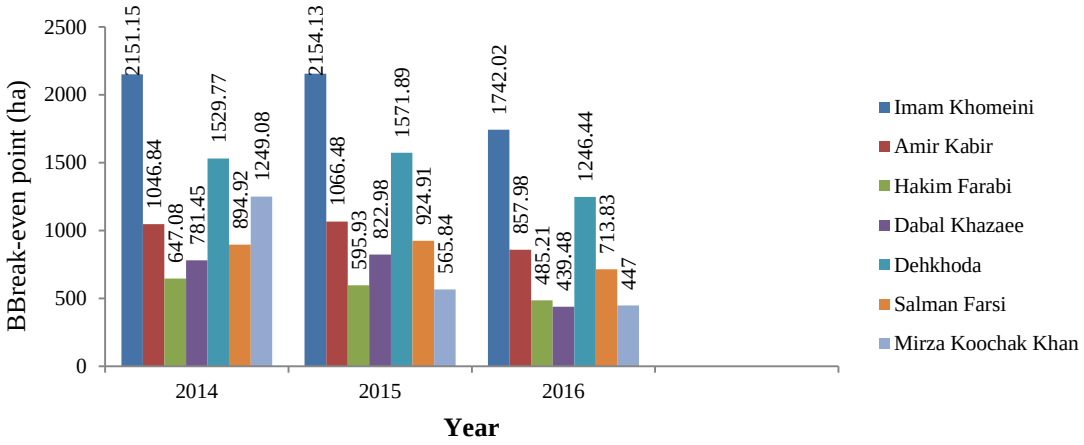

Fig.6. The comparison of break-even point (ha) based on the using offline hydraulic oil filtration in sugarcane developmental companies

Consistent with this study results, Masoudi (2001) stated that the maintenance group of locomotive condition of Iran railways had reported 123 cases of oil change in the first ten months of 2000 which were due to diagnosing unfavorable condition like water contamination, excessive increase or decrease of viscosity and unusual increase of rusting elements. Hence, the damages to 67 cylinders, 58 pistons, 281 rings and 40 sets of bearings have been prevented which can result in saving more than 309,000 dollars. Also, by increasing the oil function from 65000 km to 96000 km and preventing the unnecessary oil change, this unit has been able to save 734,000,000 rials in oil consumption. Furthermore, Masoudi (2001) stated that during the implementation of a BaseLine aiming to determine rusting effect of erosive particles for a steam turbine of Arak petrochemical complex with a volume of 18000 liters, the unusual amount (17 ppm) of Silica element was identified. The amount of Tin and Aluminum was risen simultaneously which implies an uncommon erosion of the device. The following graph returns back to a normal situation after eliminating the contamination, and the device continues to function normally. Thus, identifying and controlling the amplifier erosion elements of

an expensive petrochemical and power plant equipment, by means of the maintenance condition of the machines lead to enormous economic savings. It should be mentioned that the financial loss due to the unplanned stoppage of the mentioned turbine was 200 million rials per hour and its major maintenance is estimated hundreds of thousands of dollars.

Conclusions and suggestions

Since the contamination caused by hydraulic fluids spilling exerts its deleterious effects in the long term, this factor is often ignored or consecutive breakdowns and system failures caused by it are attributed to other factors. The studies have shown that at least 75 percent of all hydraulic systems fail due to contaminated or aging hydraulic fluid and neglecting the issue. Therefore, in order to prevent the likelihood of problems occurring, the following strategies should be applied: replacing all of the hydraulic fluids from the discharge system with the new oil and use of offline hydraulic oil filtration system for removal of contaminated oil particles. The application of the offline filtration method has the following advantages over the replacement method: 1) Avoiding any future damage to the machine that directly affects the expense reduction. 2) Recycling and reusing a large amount of oil, which has a tremendous economic importance. As a result, the offline oil filtration system plays a fundamental role in the smooth and continuous operation of hydraulic systems. The results of this study on the improvement of maintenance and repair operations in sugarcane harvest machines based on the offline hydraulic oil filtration method have been summarized as follows:

1- In terms of reduced oil consumption, Mirza Koochak Khan Company was in a sufficiently favorable condition compared to other studied companies (Imam Khomeini, Amir Kabir, Hakim Farabi, Dabal Khazaee, Dehkhoda and Salman Farsi).

2- Dabal Khazaee Company, with a total average fixed costs and total variable costs of (762279) (Rials per hectare) in the hydraulic oil replacement during 2011-2013 and having 488948 (Rials per hectare) in the hydraulic oil filtration during 2014-2016, showed the highest total average fixed costs and total variable costs among the seven sugarcane developmental companies.

3- Imam Khomeini company, with a total average fixed costs and total variable costs of 216903 (Rials per hectare) in the hydraulic oil replacement during 2011-2013 and having 130272 (Rials per hectare) in the hydraulic oil filtration during 2014-2016, achieved the lowest total average fixed costs and total variable costs among the seven sugarcane developmental companies.

4- The total amount of savings built up using offline hydraulic oil filtration in the sugarcane developmental companies was 411014 liters and 44183894339 Rials.

5- The total amount of savings built up in Hakim Farabi Company was 9534396744 Rials. Meanwhile, the total amount of saving in oil consumption was 82000 liters, indicating higher amount of savings compared with other companies.

6- The lowest benefit-cost ratio during the crop years of 2014-2016 was related to the Imam Khomeini sugarcane developmental company with a profit/cost ratio of 4.66, 5.74 and 6.27.

7- The highest break-even point (ha) during the crop years of 2014-2016 was related to the Imam Khomeini sugarcane developmental company with a break-even point (ha) of 2151.15, 2154.13 and 1742.02.

8- The further analysis has shown that the hydraulic oil filtration operation prevented the early replacement of hydraulic oil and thus reduced the costs.

According to the results of this study and the sources studied, the following suggestions have some important implications for improving performance and increasing the efficiency of operating systems:

1- The successful implementation of this project dependens upon the regular sampling and trained personnel. Therefore, the managers need to pay close attention to offering

appropriate trainings and considering the proper application of the principles of oil analysis and offline filtration.

2- Since the purpose of this study was to investigate the general impacts of offline hydraulic oil filtration on the performance of sugarcane harvesting machines, the researcher made a decision to use the past oil consumption statistics and data for analyzing data. Considerably more work is needed to be done to determine the effects of these parameters on the oil consumption by separating existing data and even measuring new data in the form of research projects.

3- These findings suggest several courses of action for similar studies investments on offline oil filtration operation in sugarcane machines (such as the proposal presented in the previous paragraph), and an in-depth examination of the technical, environmental and managerial factors and, finally, the development of a comprehensive local or national standard and criteria for the operators of the technique.

References

1. Ashtiani Iraqi, A. R., I. Ranjbar, and M. Torchy. 2005. Optimum mathematical model for predicting randm costs of operating tractors in Mazandaran Dasht-e-Naz Farm Company. Journal of Agricultural Science (15) 4: 95-109.
2. Almasi, M., Sh. Kiani, and N. Loveimi. 2008. The Fundamental Principles of Agriculture Mechanization. Jungle Publication. 293 pages.
3. Bartelmous, W., and R. Zimroz. 2009. A New Feature for Monitoring the Condition of Gearboxes in Monstaionary Operating Conditions. Mechanical Systems and Signal Processing 23: 1528-1534.
4. Bartholomew, R. B. 1981. Farm Machinery Costing Under Inflation. Transaction of ASAE, 24 (1): 98-101.
5. Dahunsi, O. A. 2008. Spectrometric Oil Analysis-An Untapped Resource for Condition Monitoring. Mechanical Engineering Department, Federal University of Technology Akuer, Undo State, Nigeria.
6. Haroni, S., M. J. Sheykhdavodi, and M. Kiani Deh Kiani. 2018. Application of Artificial Neural Networks for Predicting the Yield and GHG Emissions of Sugarcane Production. Journal of Agricultural Machinery 8: 389-401. (In Farsi).
7. Lazarus, W. 2002. Farm Machinery Economic Cost for 2002. University of Minnesota Extension Service.
8. Masoudi, A. R. 2011. Introduction to Oil Analysis (translation), Technical and Engineering Company of Alborz Tadbirkaran, Tehran.
9. Macinan, V., B. Tormos, A. Sala, and L. Ramirez. 2006. Fuzzy Logic- Based Expert System for Diesel Engine Oil Analysis Diagnosis. 462-470. The Britsh Institute of Non- Destructive Testing. Spencer, Northampton. NN1 5AA, England.
10. Mirmoazi, H. 2004. Opportunity cost of capital in Islamic economic framework. Islamic Economics Magazine. No. 16. Page 78.
11. Ranjbar, I., H. R. Ghasemzadeh, and Sh. Davoudi. 2003. Engine power and tractor (translation). Tabriz University Press. Pages: 401-412.
12. Scoma, A. K. 1990. Major reliability and lubricant consumption saving. Lubricant and Particle Analysis, pp: 1-6.
13. Saqafi, M. 2008. Tractors and its mechanism (translation).Center for Academic Publication, Ministry of Culture and Islamic Guidance. Tehran. Pages: 184-196.
14. Yeganeh Salehpoor, H. R. 2002. Determining the appropriate mathematical model for predicting maintenance costs of agricultural tractors used in Karun sugarcane cultivation and industry. Iranian Agricultural Science Institute 4: 707-716.

نشریه ماشین‌های کشاورزی
جلد ۱۱، شماره ۱، نیمسال اول ۱۴۰۰، ص ۱۲۲-۱۱۱

Journal of Agricultural Machinery
Vol. 11, No. 1, Spring- Summer 2021, p. 111-122

مقاله علمی- پژوهشی

ارزیابی اقتصادی روش‌های تعویض و تصفیه روغن هیدرولیک دروگرهای نیشکر در کشت و صنعت‌های نیشکری خوزستان

حدیث نعمت‌پور ملک‌آباد[۱]، محمد جواد شیخ‌داودی[۲*]، عیسی حزباوی[۳]، افشین مرزبان[۴]

تاریخ دریافت: ۱۳۹۷/۰۸/۲۰
تاریخ پذیرش: ۱۳۹۷/۱۲/۱۵

چکیده

از آنجا که آلودگی روغن هیدرولیک اثرات زیان‌بار خود را در درازمدت نمایان می‌سازد اغلب مورد بی‌توجهی قرار می‌گیرد یا آن‌که علت توقفات پی در پی و خرابی سیستم به عوامل دیگری نسبت داده می‌شود. بنابراین برای جلوگیری از به‌وجود آمدن چنین مشکلاتی دو استراتژی زیر ارائه شده است: با روش تعویض تمامی روغن از سیستم تخلیه و روغن نو جایگزین گردد یا با روش پالایش آفلاین روغن هیدرولیک ذرات از روغن آلوده جدا گردد. در همین راستا، مطالعه حاضر با هدف بررسی وضعیت اقتصادی ماشین‌های برداشت نیشکر با تأکید بر فرآیند فیلتراسیون روغن هیدرولیک در هفت واحد از شرکت‌های توسعه نیشکر و صنایع جانبی استان خوزستان انجام شد. به این منظور، تمام آمار و اطلاعات مربوط به هفت واحد از شرکت‌های توسعه نیشکر و صنایع جانبی در طول سال‌های زراعی ۱۳۹۵-۱۳۹۰ جمع‌آوری و طبقه‌بندی شدند. نتایج نشان می‌دهد صرفه‌جویی انجام شده بر حسب لیتر و همچنین صرفه‌جویی ریالی به‌کارگیری روش پالایش آفلاین روغن هیدرولیک برای کشت و صنعت‌های نیشکر در طی سه سال زراعی ۱۳۹۵-۱۳۹۳ که از این روش استفاده گردیده، به‌ترتیب برای واحد امام خمینی: ۲۵۵۰۰ لیتر و ۲۸۸۲۱۵۴۳۶۳ ریال، امیرکبیر: ۴۹۰۰۰ لیتر و ۵۸۴۷۳۸۹۴۶۶ ریال، حکیم فارابی: ۸۲۰۰۰ لیتر و ۹۵۳۴۳۹۶۷۴۴ ریال، دعبل خزاعی: ۷۳۴۰۰ لیتر و ۶۸۰۸۲۳۰۳۶۲ ریال، دهخدا: ۳۱۶۸۰ لیتر و ۳۴۲۱۹۷۹۶۳۹ ریال، سلمان فارسی: ۷۳۵۰۰ لیتر و ۷۶۰۶۶۷۵۳۷۰ ریال و میرزا کوچک خان: ۷۵۹۳۴ لیتر و ۸۰۸۳۰۶۸۳۹۵ ریال می‌باشد.

واژه‌های کلیدی: ارزیابی اقتصادی، تصفیه، تعویض، دروگر نیشکر، روغن هیدرولیک

۱- دانش‌آموخته دکتری مکانیزاسیون کشاورزی، گروه مهندسی بیوسیستم، دانشگاه شهید چمران اهواز
۲- استاد گروه مهندسی بیوسیستم، دانشگاه شهید چمران اهواز
۳- استادیار گروه مهندسی بیوسیستم، دانشگاه لرستان
۴- دانشیار گروه ماشین‌های کشاورزی و مکانیزاسیون، دانشگاه علوم کشاورزی و منابع طبیعی خوزستان
(*- نویسنده مسئول: Email: javad1950@gmail.com)

DOI: 10.22067/jam.v11i1.76542

Journal of Agricultural Machinery
Vol. 11, No. 1, Spring- Summer 2021, p. 123-130

نشریه ماشین‌های کشاورزی
جلد ۱۱، شماره ۱، نیمسال اول ۱۴۰۰، ص ۱۳۰-۱۲۳

Short Paper

Application of MS Excel to Estimate Power Needs of Tillage Tools

I. Ahmadi[1*]

Received: 13-01-2019
Accepted: 11-05-2019

Abstract

This study deals with the application of the Microsoft Excel for the estimation of the power requirements of some tillage implements. The mathematical formulas embedded in the spreadsheet file have been developed in the previously published papers; however, those formulas were augmented herein in order to contain some agricultural mechanization issues. Another feature of this article is the ability of the spreadsheet to generate trend curves automatically. The comparison of the power expenditure aspects of different tillage implements as well as the inspection of the effect of an arbitrary selected input parameter on the spreadsheet outputs were effectively performed. Numerically, the specific work of the rotary tiller was estimated two times to five times higher than the specific work of drawing implements. Furthermore, as an example of trend curves derived in this article, the increase in disc angle in the range of 25° to 70° reduced the draft and power needs of the disc plow by 66% and 54%, respectively. However, it increased the disc plow specific draft and power by 34% and21%, respectively.

Keywords: Draft force, Excel software, Mechanical power, Tillage implements

Introduction

Spreadsheets are a scientific tool which eliminates the boring and repetitive computational tasks that may be carried out manually (Oke, 2004). It becomes increasingly popular in engineering because of their instinctive cell-based structure and simply applied capabilities. For example, Excel facilitates the user with numerous number of cells which intentionally can be linked and cooperated together. These cells along with built-in robust programming environment, i.e., Visual Basic for Applications or VBA, can be desirably customized to implement the models required for solving engineering problems. Getting involved to solve the problem using Excel helps the students discover the exact procedure working behind the solver programs. Graphical features of Excel also permit obtaining various plots which are appropriate for educational purposes (Niazkar and Afzali, 2015).

On the other hand, various advantages will be achieved if the mechanical power required for the operation of tillage implements is available. For example, proper matching of a machine with its prime mover as well as designing a new tillage implement depends on the availability of the power requirement of the machine. While the majority of researchers focused on the power prediction of a single tillage implement (Ahmadi and Beigi, 2018; Bentaher *et al.*, 2008; Okayasu *et al.*, 2012; Karmakar and Kushwaha, 2006; Shmulevich, 2010), very few of them examined the possibility of combining power prediction models of some tillage implements (Anpat and Raheman, 2017; Godwin and O'Dogherty, 2007).

Regarding the application of spreadsheets in Biosystems engineering, a pioneer study was conducted by Jones and Grisso (1992). They used a spreadsheet to maximize tractive efficiency of a two-wheel drive tractor as a function of wheel slip, and to determine the failure force exerted on a tillage tool as a function of the rupture angle of the soil. In another study, Zoz and Grisso (2003) have demonstrated that the use of spreadsheet templates is more efficient than the original iterative procedure used to predict the

1- Assistant Professor of Biosystems Engineering, Department of Plant Production and Genetics Engineering, Isfahan (Khorasgan) Branch, Islamic Azad University, Isfahan, Iran
(*- Corresponding Author Email: i_ahmadi_m@yahoo.com)
DOI: 10.22067/jam.v11i1.78519

performance of 2WD and 4WD/MFWD tractors based on the Brixius model. Furthermore, Grisso *et al.* (2007) have demonstrated the use of a spreadsheet for matching tractors and implements. The spreadsheet was based on the ASABE Standard D497.5 and the Brixius Model to predict implement draft and tractor performance, respectively. The results showed that the spreadsheet can be used effectively to match implements with tractors.

The aim of this article is the presentation of an Excel spreadsheet file having the power estimation capability for some tillage implements. The mathematical formulas used here have been developed in the previously published papers. Therefore, this paper does not deal with the details of the development of the formulas; however, the utilization of the developed models is examined herein. Other features of this paper are as follows:

- The previous formulas were augmented herein in order to contain some agricultural mechanization issues (i.e. the estimation of the machine field capacity and the time required for a machine to till a field having a known area).
- The ability of the spreadsheet to generate trend curves automatically. A trend curve is a chart that shows the effect of an independent parameter of the model on the spreadsheet outputs. The trend curves can be used to determine optimum working conditions of a machine; therefore, the results derived from them can be interesting for a machine designer as well as a farmer.

The considered tillage implements contain: a chisel plow (Ahmadi, 2017b), a disc harrow (Ahmadi, 2018), a disc plow (Ahmadi, 2016a), a moldboard plow (Ahmadi, 2016b), a rotary tiller (Ahmadi, 2017a), and a subsoiler (Ahmadi, 2017c). The power estimator of each machine receives the values of its inputs and produces its outputs based on the dedicated mathematical formulas of that machine.

Materials and Methods

Excel spreadsheet file

Input parameters of the spreadsheet are classified into two groups: 1- Common parameters among all machines, that contain soil specifications and field conditions (soil cohesion, coefficient of soil internal friction, soil bulk density, field area and field efficiency of the machine), 2- Machine dedicated parameters which contain machine specifications and working conditions. Figure 1 depicts the working environment of the file. The examined Excel file has been attached to this paper as a supplementary material for inspection and utilization (please change the file name to "Augmented Excel file" in order to work correctly). After the file is executed, the operator faces the common parameters worksheet, where he/she can specify values for the soil properties and state parameters. Then, regarding the examined tillage implement, one of the bottom worksheets (highlighted in different colors) is selected and values of the machine and working condition parameters are specified. Finally, output parameters will be generated.

Tillage implements are also divided into two groups: 1- Drawn machines, also known as passive implements, which receive drawbar power, 2- Active implements, which receive rotary power. The file outputs for drawn machines are: draft force, drawbar power, specific draft and specific drawbar power (obtained from the ratio of draft force/drawbar power to the cross-sectional area of the affected soil), field capacity of the machine, and the time required for the machine to finish work. The file outputs for the active implement are: torque requirement, rotary power (specific rotary power), specific work (obtained from the ratio of work carried out by the machine to the volume of the affected soil), field capacity of the machine, and the time required for the operation. Because some Macros are embedded in the developed spreadsheet, the Macros should be enabled after the file was executed. This can be carried out using the “Security Warning” dialog box located below the ribbon of the Excel file (Figure 1).

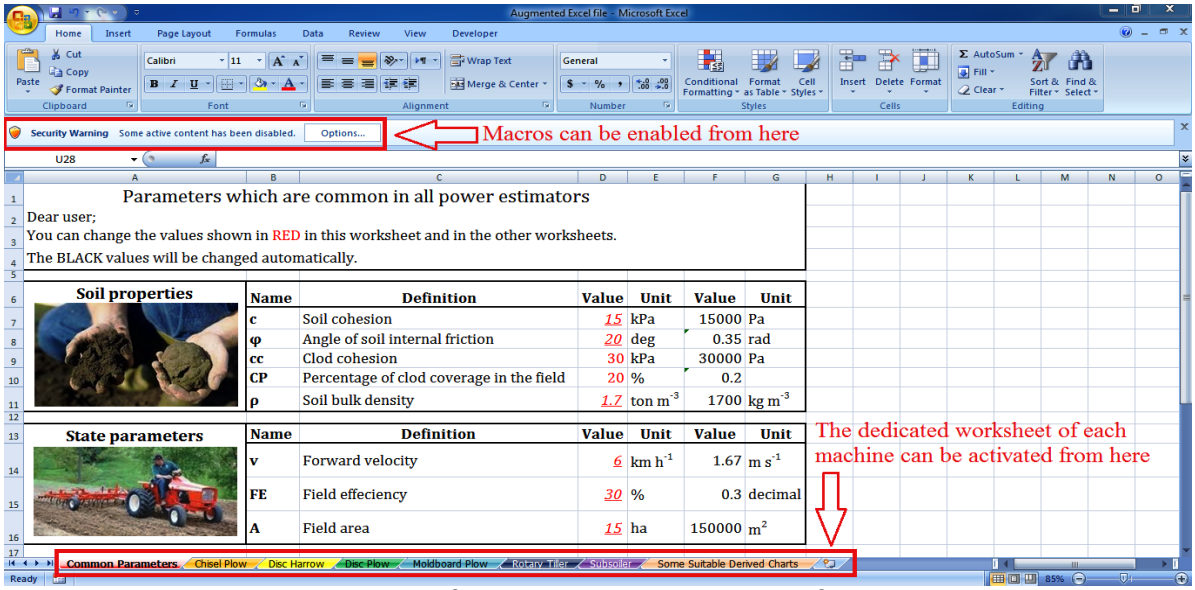

Fig.1. General view of the working environment of the spreadsheet

The spreadsheet offers two modes of operation: 1- To compare different tillage implements regarding their power needs. In order to cancel the effect of the cross-sectional area of the affected soil on a machine's power need, the file outputs having the prefix of "specific" should be utilized, 2- To inspect the effect of an input parameter on the estimator outputs. The optimum working conditions of the machine will be achieved, if the output curves showing the effect of each input parameter on the estimator outputs are generated. The instruction for obtaining trend curves is as follows:

- The name of the target parameter and its value should be introduced in the blue-bordered table.
- The Macro code that corresponds to the target parameter should be executed. The Macro name is available in the blue-bordered table when the parameter name is introduced. Pressing the ALT and F8 keys simultaneously, opens the Macro dialog box where you can select the appropriate Macro name. Clicking on the Run button is the last step to reach the trend curves.
- When the trend curves are generated, the value of the examined parameter in the black-bordered table should be converted to a new value manually, to avoid automatic re-altering of it.

Results and Discussion

Tables 1, 2 and 3 specify show the values of input parameters that are common in all power estimators, input parameters of drawn implements, and input parameters of the rotary tiller, respectively. Table 4 compares the examined tillage implements about the generated outputs.

Table 1- Input parameters shared among all power estimators

	Name	Definition (unit)	Value
Soil properties	c	Soil cohesion (kPa)	15
	cc	Clod cohesion (kPa)	30
	CP	Percentage of clod coverage in the field (%)	20
	ρ	Soil bulk density (g cm^{-3})	1.7
	φ	Angle of soil internal friction (°)	20
State parameters	A	Field area (ha)	15
	FE	Field efficiency (%)	30
	v	Forward velocity (km h^{-1})	6

Table 2- Input parameters of drawn implements

Name	Definition (unit)	Value
Δh	Soil vertical swell created by a subsoiler (cm)	3
An	Surface area of a subsoiler wing (cm^2)	150
b	Working width of a plow bottom (cm)	30
Dp	Depth of primary tillage before disc harrowing (cm)	25
h	Working depth of different implements (cm)	10, 20, 30, 80
M	The mass of soil engaging tool of an implement (kg)	10, 45, 150
N	Number of the chisel plow or subsoiler shanks	3, 5
Nb	Number of disc blades per gang	10
OPb	Overlap percentage of disc blades (width-ways) (%)	0, 30
OPs	Overlap percentage of the disturbed soil (%)	0, 30
R	Radius of a disc blade (cm)	15, 30
t	Thickness of a subsoiler shank (cm)	6
Ws	Width of the chisel plow or subsoiler shank (cm)	3, 10
Ww	Width of a subsoiler wing (cm)	30
α	Rake angle (°)	0, 15
δ	Angle of soil-metal friction (°)	20
η	Angle of soil displacement in horizontal plane (°)	48, 75
θ	Moldboard tail angle (°)	30
θd	Disc angle (°)	45, 70
θg	Disc gang angle (°)	20

Table 3- Input parameters of the rotary tiller

Name	Definition (unit)	Value
BL	Blade length (cm)	7
BW	Blade width (cm)	5
Nb	Number of blades per flange	3
Nf	Number of flanges of the rotary tiller	7
R	Radius of the rotor (cm)	24
ω	Angular velocity of the rotor (rad s^{-1})	30

Table 4- Comparison of the examined tillage implements based on the spreadsheet outputs (a: Chisel plow, b: Disc harrow, c: Disc plow, d: Moldboard plow, e: Rotary tiller, f: Subsoiler)

Name	Definition (unit)	a	b	c	d	e	f
DPR	Drawbar power requirement (kW)	49.6	13.69	18.45	28.05	-2.32	107.16
DPs	Specific power (W cm^{-2})	6.79	7.06	10.56	9.35	61.31	5.03
FC	Field capacity of the machine (ha h^{-1})	1.02	0.82	0.4	0.63	0.41	1.12
P	Draft force (kN)	29.73	8.2	11.05	16.78	-1.39	64.18
Ps	Specific draft (N cm^{-2})	4.07	4.23	6.32	5.59	-2.84	3.01
RP	Rotary power requirement (kW)	0	0	0	0	30.04	0
RT	The time required for the operation (h)	14.7	18.3	37.5	23.8	36.6	13.4
SW	Specific work (kJ m^{-3})	24.4	43.4	63.3	56	114.67	30.1
T	Required torque (Nm)	0	0	0	0	1001.28	0

The specific work of rotary tiller, which is two times to five times higher than the specific work of drawn implements, is the main point derived from Table 4. This result is in accordance with reports of other researchers (Srivastava *et al.,* 2006) including the negative draft produced by the active implement. The specific draft forces of drawn implements obtained herein are comparable to the corresponding outputs of the estimating formulas given in the ASAE standard (ASAE Standard D497.4) regarding the operation of the examined machine in an average textured soil.

Figure 2 shows the example trend curves derived from the spreadsheet file. Some suitable charts have been also gathered in the last worksheet of the supplementary material file.

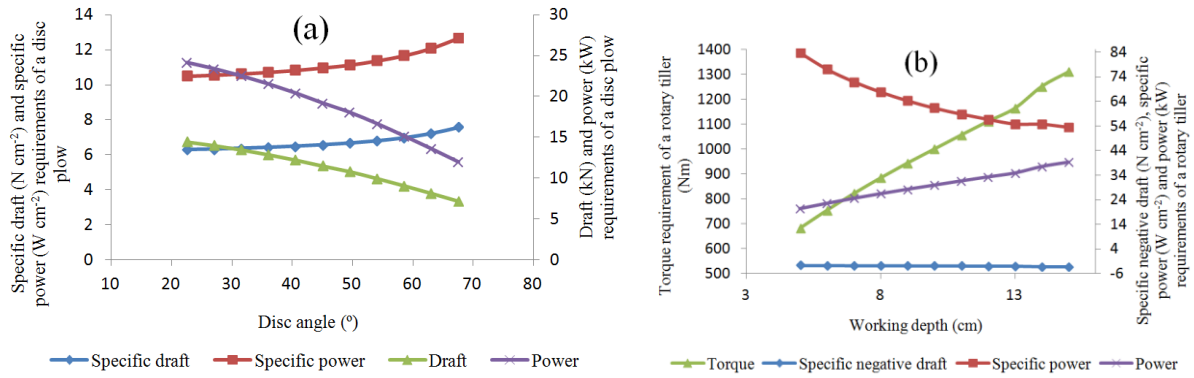

Fig.2. Example trend curves obtained from the developed spreadsheet

Figure 2a shows the variation of the disc plow draft and power, as well as specific draft and power as a function of disc angle. The increase in disc angle between 25° to 70° reduces the draft and power needs of the disc plow by 66% and 54%, respectively. However, it increases the specific draft and power by 34% and 21%, respectively. Therefore, if the available mechanical power is the restricting criterion to design a disc plow, the machine must have a higher disc angle; otherwise, it is better to design the machine with a lower disc angle. Figure 2b depicts the variation of the rotary tiller torque and power, as well as specific negative draft and power as a function of the machine working depth. Increasing the working depth of the rotary tiller between 5 cm to 15 cm, increases the torque and rotary power requirements of the machine by 64% and 50%, respectively. However, it decreases the specific power of the machine by 43%. Therefore, at the expense of the increase in torque and power requirements of a rotary tiller, it is advisable to increase the working depth of the machine as much as possible.

As another example of the application of the spreadsheet for the comparison of similar tillage implements with regard to their power needs, the trend curves of a disc plow and a disc harrow is shown in Figure 3a and 3b, respectively.

To have a fair comparison, the radius of disc blade is considered 20 *cm* in both machines. Table 5 shows the results of this.

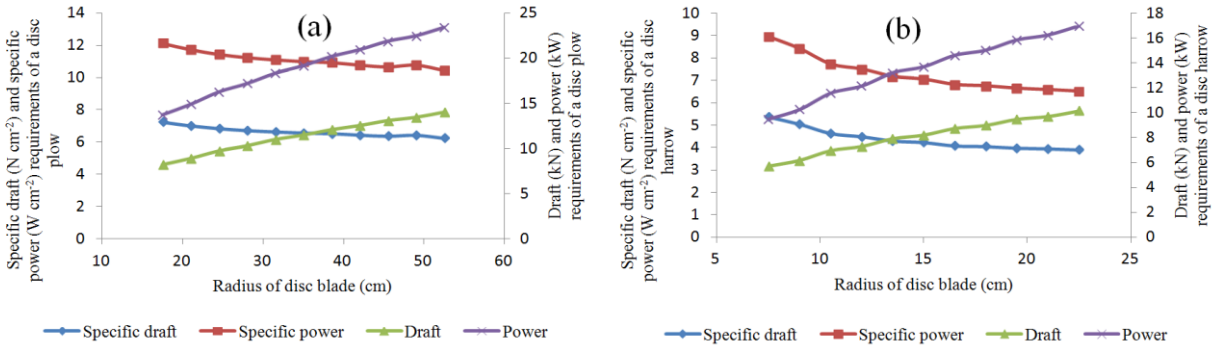

Fig.3. Effect of radius of disc blade on the power needs of a disc plow and a disc harrow

Table 5- Comparison of a disc plow and a disc harrow regarding their power needs (radius of disc blade is 20 cm)

	Disc plow	**Disc harrow**
Draft (kN)	8	9
Power (kW)	16	17
Specific draft (N cm^{-2})	7	4
Specific power (W cm^{-2})	13	7

Table 5 demonstrates that although the examined disc plow and harrow almost have the same draft and power requirements, the specific draft and power of the disc harrow is almost half of the disc plow i.e. the disc harrow affects the soil cross-sectional area twice in comparison with the disc plow. This result is expected due to the value of the disc gang of a disc harrow (20°) in comparison with the disc angle of a disc plow (45°)

Conclusions

1. The spreadsheet developed based on the mathematical formulas given in the previously published papers could effectively predict power needs of some tillage implements.
2. The comparison of power expenditure aspects of different tillage implements as well as the inspection of the effect of an arbitrary selected input parameter on the estimator outputs were effectively performed using the spreadsheet developed herein.
3. The spreadsheet effectively estimated field capacity of the examined machines, too.

References

1. Ahmadi, I. 2016a. Development and assessment of a draft force calculator for disk plow using the laws of classical mechanics. Soil and Tillage Research 163: 32-40.
2. Ahmadi, I. 2016b. Development and evaluation of a draft force calculator for moldboard plow using the laws of classical mechanics. Soil and Tillage Research 161: 129-134.
3. Ahmadi, I. 2017a. A torque calculator for rotary tiller using the laws of classical mechanics. Soil and Tillage Research 165: 137-143.
4. Ahmadi, I. 2017b. Development of the chisel plow draft force and power calculator based on some mechanical laws. Iranian Journal of Biosystems Engineering 47 (4): 625-632. (In Farsi).
5. Ahmadi, I. 2017c. Effect of soil, machine, and working state parameters on the required draft force of a subsoiler using a theoretical draft-calculating model. Soil Research 55: 389-400.
6. Ahmadi, I. 2018. A draught force estimator for disc harrow using the laws of classical soil mechanics. Biosystems Engineering 171: 52-62.
7. Ahmadi, I., and M. Beigi. 2018. An estimator for torque and draft force requirements of a new up-cut rotary tiller. Journal of Agricultural Machinery. https://doi.org/10.22067/jam.v10i1. 71744. (In Farsi).
8. Anpat, R. M., and H. Raheman. 2017. Investigations on power requirement of active-passive combination tillage implement. Engineering in Agriculture, Environment and Food 10: 4-13.
9. ASAE Standards. 2000. D497.4, Agricultural machinery management data. ASAE, St. Joseph, MI.
10. Bentaher, H., E. Hamza, G. Kantchev, A. Maalej, and W. Arnold. 2008. Three-point hitch-mechanism instrumentation for tillage power optimization. Biosystems Engineering 100: 24-30.
11. Godwin, R. J., and M. J. O'Dogherty. 2007. Integrated soil tillage force prediction models. Journal of Terramechanics 44: 3-14.
12. Grisso, R. D., J. V. Perumpral, and F. M. Zoz. 2007. Spreadsheet for Matching Tractors and Drawn Implements. Applied Engineering in Agriculture 23 (3): 259-265.
13. Jones, D., and R. D. Grisso. 1992. Golden section search as an optimization tool for spreadsheets. Computers and Electronics in Agriculture 7 (4): 323-335.
14. Karmakar, S., and R. L. Kushwaha. 2006. Dynamic modeling of soil–tool interaction: an overview from a fluid flow perspective. Journal of Terramechanics 43: 411-425.
15. Niazkar, M., and S. H. Afzali. 2015. Application of Excel spreadsheet in engineering education. First International and Fourth National Conference on Engineering Education, Shiraz University, 10-12 November 2015.

16. Okayasu, T., K. Morishita, H. Terao, M. Mitsuoka, E. Inoue, and K. O. Fukami. 2012. Modeling and prediction of soil cutting behavior by a plow. In: CIGR-Ag Eng, Int. Conf. Agricult. Eng., "Agriculture and Engineering for a Healthier Life", pp. 23, Valencia, July 8-12. ISBN-10: 84-615-9928-4.
17. Oke, S. A. 2004. Spreadsheets applications in engineering education – A review. International Journal of Engineering Education 20 (6): 893-901.
18. Shmulevich, I. 2010. State of the art modeling of soil–tillage interaction using discrete element method. Soil and Tillage Research 111: 41-53.
19. Srivastava, A. K., C. E. Goering, R. P. Rohrbach, and D. R. Buckmaster. 2006. Engineering Principles of Agricultural Machines, second ed. ASAE Publication, USA.
20. Zoz, F. M., and R. D. Grisso. 2003. Traction and tractor performance. ASAE Distinguished Lecture Series #27. St. Joseph, MI: ASAE.

نشریه ماشین‌های کشاورزی
جلد ۱۱، شماره ۱، نیمسال اول ۱۴۰۰، ص ۱۳۰-۱۲۳

Journal of Agricultural Machinery
Vol. 11, No. 1, Spring- Summer 2021, p. 123-130

مقاله کوتاه پژوهشی

کاربرد نرم‌افزار اکسل برای تخمین نیاز توان مکانیکی ادوات خاک‌ورزی

ایمان احمدی[1*]

تاریخ دریافت: ۱۳۹۷/۱۰/۲۳
تاریخ پذیرش: ۱۳۹۸/۰۲/۲۱

چکیده

این مطالعه راجع به کاربرد نرم‌افزار مایکروسافت اکسل در تخمین نیازهای توانی برخی از ادوات خاک‌ورزی است. فرمول‌های ریاضی به‌کار رفته در فایل صفحه گسترده، در مقالات منتشر شده قبلی توسعه یافته بودند؛ به هر حال آن فرمول‌ها در این مقاله در جهت شمول برخی موضوعات مکانیزاسیون کشاورزی تکمیل شدند. ویژگی دیگر این مقاله توانایی صفحه گسترده در تولید خودکار نمودارهای روندنما است. مقایسه ادوات خاک‌ورزی مختلف از نقطه نظر نیازهای توانی، همچنین مطالعه اثر یک پارامتر ورودی دلخواه روی خروجی‌های صفحه گسترده به‌طور مؤثری در این مقاله صورت پذیرفت. از نظر عددی تخمین زده شد که مقدار کار ویژه گاوآهن دوار ۲ تا ۵ برابر کار ویژه ادوات خاک‌ورزی کشیدنی است. به علاوه، به‌عنوان مثالی از نمودارهای روند نمای به‌دست آمده از این مقاله، افزایش زاویه بشقاب در بازه ۲۵ تا ۷۰ درجه، نیازهای مقاومت و توان کششی گاوآهن بشقابی را به‌ترتیب ۶۶ و ۵۴ درصد کاهش داد؛ هر چند این کار به افزایش ۳۴ و ۲۱ درصدی به‌ترتیب مقاومت کششی ویژه و توان کششی ویژه این گاوآهن منجر شد.

واژه‌های کلیدی: ادوات خاک‌ورزی، توان مکانیکی، مقاومت کششی، نرم‌افزار اکسل

۱- استادیار مکانیک بیوسیستم، گروه مهندسی تولید و ژنتیک گیاهی، دانشگاه آزاد اسلامی، واحد اصفهان (خوراسگان)، اصفهان، ایران
(*- نویسنده مسئول: Email: i_ahmadi_m@yahoo.com)

DOI: 10.22067/jam.v11i1.78519

FORMAT OF MANUSCRIPT PREPARATION FOR JOURNAL OF AGRICULTURAL MACHINERY

It is important that the manuscript be written according to the Journal format. Submission to this journal proceeds totally online and you will be guided stepwise through the creation and uploading of your files through the web site of the Journal as: http://jame.um.ac.ir

Essential title page information

The title page MUST be prepared and uploaded separately from the main text with the following information:

• Title. Concise and informative and not more than 15 words.

• Author names and affiliations. Present the authors' affiliation addresses (where the work was actually done) below the names. Indicate all affiliations with a superscript number immediately after the author's name and also in front of the appropriate address. Provide the full postal address of each affiliation and if available, the e-mail address of each author.

• Corresponding author. Clearly indicate who will handle correspondence at all stages of refereeing and publication, also post-publication. Ensure that phone numbers (with country and area code) are provided in addition to the e-mail address and the complete postal address. Contact details must be kept up to date by the corresponding author.

• Present/permanent address. If an author has moved since the work described in the article was done, or was visiting at the time, a 'Present address' (or 'Permanent address') may be indicated as a footnote to that author's name. The address at which the author actually did the work must be retained as the main, affiliation address. Superscript numerals are used for such footnotes.

Paper configuration

Each paper should have the following distinct sections: Title, Abstract and up to five Keywords, Introduction, Material and methods, Results and discussion, Conclusion, and References. The Acknowledgment (briefly), Recommendations and Nomenclature can also be added. Each section should be prepared as follow:

Abstract: A concise and factual abstract is required. The abstract should state briefly the purpose of the research, the principal results and major conclusions. It should not exceed 250 words. The abstract is presented separately from the article in a single paragraph, so it must be able to stand alone. For this reason, References should be avoided. Also, non-standard or uncommon abbreviations should be avoided, but if essential they must be defined at their first mention in the abstract itself.

Keywords: Up to five keywords appear immediately after the abstract with alphabetical order.

Introduction: Clearly state the research problem and the necessity of research, the objectives of the work and provide an adequate background, avoiding a detailed literature survey or a summary of the results.

Material and methods: Provide sufficient detail to allow the work to be reproduced. Methods already published should be indicated by a reference: only relevant modifications should be described. For the analytical and modeling works a section may be added as "Theory".

Results and discussion: Results should be clear and concise. The discussion should explore the significance of the results of the work, not repeat them. A combined Results and Discussion section is often appropriate. Avoid extensive citations and discussion of published literature.

Conclusions: The main conclusions of the study is presented in a short Conclusions section, which should be stand alone.

Paper layout

The main text should be prepared in A4 paper size, with 1.5 line spacing and all margins of 3 cm. All pages should be numbered sequentially and not more than 15 pages. All lines should be numbered continuously by applying the "Line numbering" command of MS Word.

Fonts

- All writings should be written using Times New Roman font. Both American and British English format are accepted, but not their mixture!
- The font size for title is 14 point and for the main text is 12 point.
- The subtitles should be written in Bold and font size of 12 point.

Units

Please use SI units only. It is not necessary to give the SI unit and (say) its Imperial equivalent. Engineering Notation, where units are in multiples of 1,000, should be used. Thus, we wish to see the use of mm and m and not cm. Use exponent form instead of conventional format (e.g. m s^{-1} and NOT m/s).

Math formulae

Present simple formulae in the line of normal text where possible. In principle, variables are to be presented in italics. Number consecutively any equations that have to be displayed separately from the text in the right margin (if referred to explicitly in the text).

Tables

Number tables consecutively in accordance with their appearance in the text. Place footnotes to tables below the table body and indicate them with superscript lowercase letters. Avoid vertical rules. Be sparing in the use of tables and ensure that the data presented in tables do not duplicate results described elsewhere in the article. The Table caption appears above the Table with font size of 10. Use no border for the Tables.

Figures

Ensure that each illustration has a caption. Supply captions separately, not attached to the figure. A caption should comprise a brief title (not on the figure itself) and a description of the illustration. Keep text in the illustrations themselves to a minimum but explain all symbols and abbreviations used (preferably in the caption). The caption should allow the reader to understand the main elements of what is being shown without needing to refer to the main text. The Figure caption appears below the Figure and written with font size of 10 points. Use no border for the Figures. The font size within the Figure should not smaller than 8 point and bigger than 10 point. Try to present the Figures in gray scale instead of color illustration. The followings are a sample of Table and Figure.

Table 1- Consumption of inputs during the first year of saffron cultivation

Type of inputs	Consumption (kg ha^{-1})
Consumed corms	3000
Urea	100
Ammonium phosphate	100
Animal manure	32000
Consumed irrigation water	3000 (m^3)*

* The annual water consumption for saffron cultivation was considered equal to 3000 m^3 (Mahdavi, 1999).

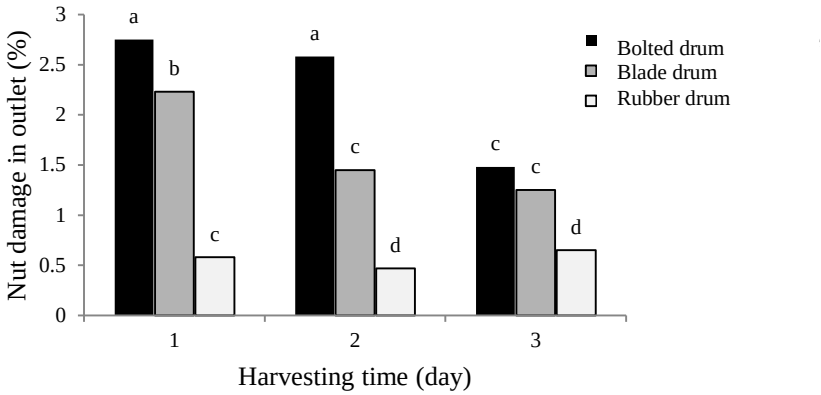

Fig. 3. The effects of harvesting time and machine type on the percentage of cracked shells in the outlet

References

Citation in text

Please ensure that every reference cited in the text is also present in the reference list (and vice versa). Unpublished results and personal communications are not recommended in the reference list, but may be mentioned in the text. If these references are included in the reference list they should follow the standard reference style of the journal and should include a substitution of the publication date with either 'Unpublished results' or 'Personal communication'. Avoid anonymous references. Citation of a reference as 'in press' implies that the item has been accepted for publication.

Reference style

Use "Author, Date" style for list of references and citations all in English language using Times New Roman font size of 10 point as follow:

Citations

Single author: (Loghavi, 2008).

Two authors: (Aghkhani and Abbaspour-Fard, 2009).

Three authors and more: (Abbaspour-Fard *et al.*, 2008).

Multiple citations: (Smith, 1999; Samuel *et al*., 2008; Smith and Samuel, 2009)

Use the complete name of the journals instead of their abbreviations. For those authors using EndNote software for list of References and citations, please use the following style which can be downloaded from Journal of Agricultural Machinery:

Style Name: Jame Endnote Style

List of References

Journal article

Aghkhani, M. H., and M. H. Abbaspour-Fard. 2009. Automatic off-road vehicle steering system with a surface laid cable: Concept and preliminary tests. Biosystems Engineering 103: 265-270.

Special issue

Rice, K. 1992. Theory and conceptual issues. In: Gall, G.A.E., Staton, M. (Eds.), Integrating Conservation Biology and Agricultural Production. Agricultural Ecosystems Environment: 9-26.

Reference to a Book

Gaugh, H. G. 1992. Statistical Analysis of Regional Yield Trials. Elsevier. Amsterdam.

Reference to a chapter in an edited book

Mettam, G. R., and L. B. Adams. 1999. How to prepare an electronic version of your article. PP 281-304 in B. S. Jones and R. Z. Smith eds. Introduction to the Electronic Age. E-Publishing Inc., New York.

Reference to a thesis or dissertation (if you can, avoid this type of reference)

Abbaspour-Fard, M. H. 2001. The dynamic behavior of particulate biomaterials using discrete element method (DEM). Faculty of Agriculture. Newcastle University, Newcastle upon Tyne.

Reference to a conference proceeding

Hemmat, A., V. I. Adamchuk, and P. Jasa. 2007. On-the-go soil strength sensing using an instrumented disc coulter. International Agricultural Engineering Conference (IAEC). Asian Association for Agricultural Engineering, Bangkok, Thailand.

Web references

As a minimum, the full URL should be given and the date when the reference was last accessed. Any further information, if known (DOI, author names, dates, reference to a source publication, etc.), should also be given. Web references can be included in the reference list e.g.:

Brittion, A. 2006. How much and how often should we drink British Medical Journal, 332: 1224-1225. Available from: http://bmj.bjjournals.com/cgi/content/full/332/7552/1224. Accessed 2 June 2006.

Miscellaneous

- All submitted papers will be peer reviewed by some accredited referees under the supervision of the editorial board and if accepted will be put in queue for publication based on the date of acceptance and other journal's rules and regulations.
- The editorial board of the Journal keeps their right to accept or reject any of the submitted papers.
- No change can be made on a paper which has been proof read by the authors.

Persian abstract

The title, abstract, and Persian keywords should be at the bottom of the article.

مندرجات

نشریه ماشین های کشاورزی

با شماره پروانه 89/12639 و درجه علمی – پژوهشی شماره 3/11/3781 از وزارت علوم، تحقیقات و فناوری
89/6/13 89/3/17

"بر اساس مصوبه وزارت عتف از سال 1398، کلیه نشریات دارای درجه "علمی-پژوهشی" به نشریه "علمی" تغییر نام یافتند."

جلد 11 شماره 1 نیمسال اول 1400

صاحب امتیاز: دانشگاه فردوسی مشهد

مدیر مسئول: سید محمدرضا مدرس رضوی — استاد- گروه مکانیک دانشکده مهندسی (دانشگاه فردوسی مشهد)

سردبیر: محمدحسین عباسپور فرد — استاد- گروه مهندسی مکانیک بیوسیستم (دانشگاه فردوسی مشهد)

ناشر: انتشارات دانشگاه فردوسی مشهد

نشانی: مشهد- کد پستی 91775 صندوق پستی 1163
دانشکده کشاورزی- دبیرخانه نشریات علمی - نشریه ماشین‌های کشاورزی - نمابر:05138787430

این نشریه در پایگاه‌های زیر نمایه شده است:
پایگاه استنادی جهان اسلام (ISC)
پایگاه اطلاعات علمی جهاد دانشگاهی (SID)
بانک اطلاعات نشریات کشور (MAGIRAN)

پست الکترونیک: Jame@um.ac.ir

مقالات این شماره در سایت http://jame.um.ac.ir **به‌صورت مقاله کامل نمایه شده است.**

این نشریه به تعداد 2 شماره در سال منتشر می‌شود.

Ferdowsi University of Mashhad

Journal of Agricultural Machinery

Iranian Society of Mechanical Engineers (ISME)

Vol. 11 No. 1

2021

ISSN: 2228-6829

Contents